I PERFLUOROVINYL COMPLEXES OF PT(II)

II BRIDGE SUBSTITUTION IN B_5H_9

III THE CRYSTAL STRUCTURE OF $[(C_2H_5)_2NBS]_2$

BY

GARRY ARTHUR RIVETT

B.A. (Honours), University of Saskatchewan, 1967

M.Sc., University of Saskatchewan, 1969

B.Ed., University of Saskatchewan, 1972

A THESIS SUBMITTED IN PARTIAL FULFILLMENT

OF THE REQUIREMENTS FOR THE DEGREE OF

DOCTOR OF PHILOSOPHY

in the Department

of

Chemistry

ACCEPTED

FACU[illegible]

DATE

We accept this thesis as conforming
to the required standard

....

....

....

....

University of Victoria

October 1974

Supervisor: Dr. K.R. Dixon

ABSTRACT

I A series of complexes of the form

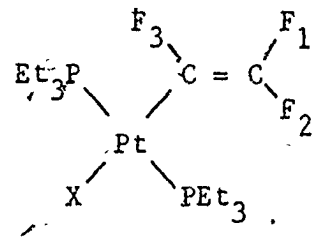

were prepared and characterized for a series of fourteen X ligands. The values of $^{2}J_{Pt-F_3}$, $^{3}J_{Pt-F_1}$ and $^{3}J_{Pt-F_2}$ were obtained in order to examine the correlation of these couplings with other measures of the trans-influence. It was found that $^{2}J_{Pt-F_3}$ correlated in a linear fashion with other measures of the trans-influence, but $^{3}J_{Pt-F_1}$ and $^{3}J_{Pt-F_2}$ did not. The lack of a linear correlation for the three bond couplings is ascribed to a varying through space contribution to these couplings. The magnitude of the through space coupling depends not only on the distance between the platinum and fluorine nuclei, but also on the orientation of the plane of the perfluorovinyl ligand with respect to the square plane of ligands about platinum.

Supervisor: Dr. S.G. Gibbins

II The compound lithium octahydropentaborate(1-) was prepared and shown to decompose upon removal of solvent. Dimethylboron bromide

was reacted with lithium octahydropentaborate(1-) in ether to form μ-dimethylborylpentaborane(9), but the corresponding reactions of the lithium borate(1-) salt with diethylaluminum chloride and dimethylthallium bromide were unsuccessful. This lack of success was ascribed, for the aluminum compound, to the rapid formation of the etherate of diethylaluminum bromide and, for the thallium compound, to the two phase reaction system.

Attempts were made to prepare the bridged compounds by the direct reaction of pentaborane(9) with i) trimethylaluminum and ii) trimethylborane. The only volatile borane reaction products were terminally alkylated. The reaction of pentaborane(9) with trimethylaluminum gave a hydrogen rich reaction residue of empirical formula $AlC_{2.3}B_{3.8}H_{13.7}$. The chemical nature of this residue was not elucidated.

Supervisor: Dr. G.W. Bushnell

III The crystal structure of bis(diethylamino)dithiaboretane $[(C_2H_5)_2NBS]_2$ has been determined by means of x-ray diffraction. The crystals belonged to the tetragonal system, space group $P_{4_1 2_1 2}$ (No. 92). The unit cell dimensions were established initially by photographic work and finally by diffractometer measurements. The intensities of 373 reflections were measured on a four circle manual diffractometer and the structure refined to an R value of 0.093. The molecular symmetry is approximately 222 (D_2).

The existence of a four membered alternating boron-sulfur ring has been established. The ring is planar and bond angles indicate it is strained. Bond lengths show the boron-sulfur bond lacks multiple bond character. The boron-nitrogen bond is a multiple bond. Thus the C-N-C plane of the molecule is forced to be approximately planar to the boron-sulfur atom plane.

The physical properties of $[(C_2H_5)_2NBS]_2$ correlate well with the observed intermolecular distances.

TABLE OF CONTENTS

LIST OF TABLES

LIST OF FIGURES

CHAPTER I

INTRODUCTION

Perfluorovinylbis(triethylphosphine)platinum(II) Complexes

A Note on Formulae

For the purposes of this work the formulae of bis(triethylphosphine)platinum(II) complexes can be considered to be of two types;

1) Those in which the third and fourth ligands are anionic (X and Y) are given the formula $[PtXY(PEt_3)_2]$ and,

2) Those in which the third ligand is anionic (X) and the fourth neutral (L) are given the formula $[PtXL(PEt_3)_2]^+$.

Thus the series of perfluorovinylbis(triethylphosphine)platinum(II) complexes in which the fourth ligand is anionic have the formula trans-$[PtX(C_2F_3)(PEt_3)_2]$ while if the fourth ligand is neutral the formula is trans-$[Pt(C_2F_3)L(PEt_3)_2]^+$.

To avoid repetition when both series are being considered together the general formula trans-$[PtL(C_2F_3)(PEt_3)_2]$ will be used. The formulae trans-$[PtL(CH_3)(PEt_3)_2]$ or trans-$[PtLCl(PEt_3)_2]$ should be read as indicating that L could be either an anionic or neutral ligand. When either series is discussed specifically the standard formula will be used.

It should also be noted that the symbols Et and Ph will be used for C_2H_5 and C_6H_5 respectively throughout this work.

1.1. General

Transition elements have been defined as elements which have partly filled d or f shells in any of their commonly occurring oxidation states.[1] The ground state for unbound transition metal atoms or ions corresponds to that state in which all five d orbitals are energetically degenerate.

When a transition metal atom or ion is surrounded by ligands, the energies of the d orbitals on the metal are increased due to interaction with the electron clouds on the ligands. The degeneracy of the d orbitals is also partially removed. To examine this, consider a transition metal in an octahedral environment. If the ligands are presumed to be located on the Cartesian axes, it can be seen that the metal d_{z^2} and $d_{x^2-y^2}$ orbitals point directly at the ligands, while the d_{xy}, d_{yz} and d_{xz} orbitals are directed between the ligands. Thus the interelectronic repulsions are strongest for an electron in the d_{z^2} and $d_{x^2-y^2}$ orbitals, and these orbitals are higher in energy than the d_{xy}, d_{yz} and d_{xz} orbitals, Figure I. The d_{z^2} and $d_{x^2-y^2}$ orbitals are now referred to as the e_g orbitals and the d_{xy}, d_{yz} and d_{xz} orbitals are referred to as the t_{2g} orbitals. These designations have their origin in group theory.

If an octahedrally complexed transition metal possessed eight d electrons six of these electrons would occupy the t_{2g} orbitals while the remaining pair occupied the e_g orbitals with parallel spins. But if the complex were to distort in a tetragonal manner, ie., the

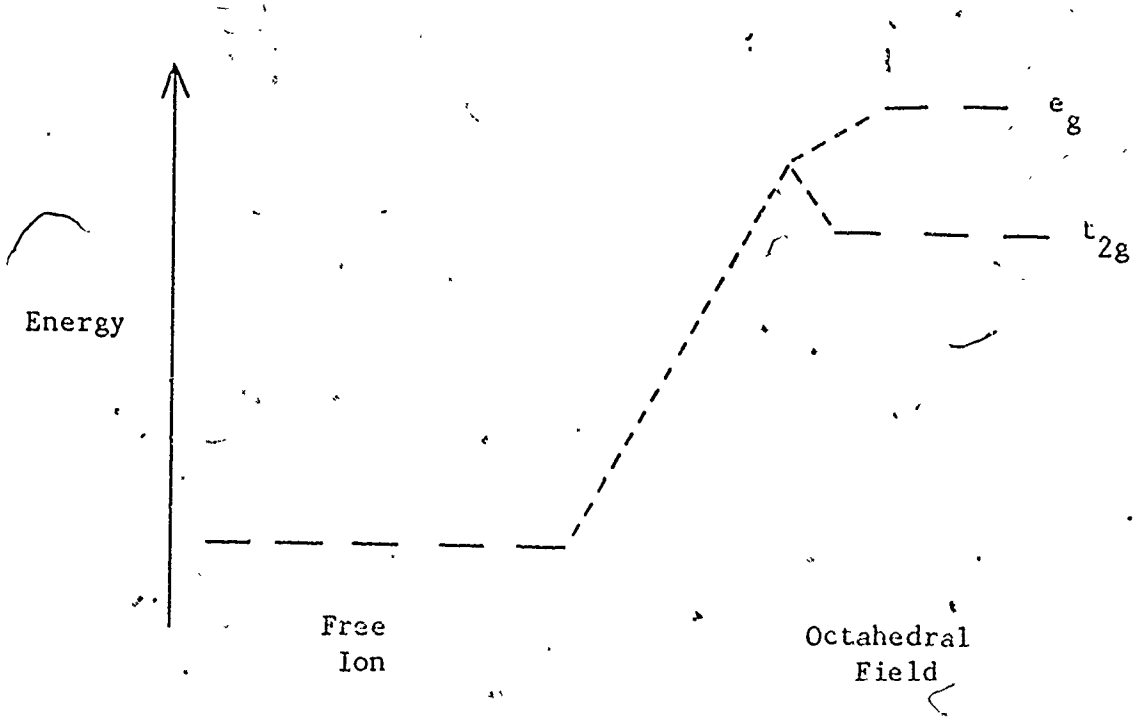

Figure I

d Orbital Splittings in an Octahedral Field

ligands on the z axis moved farther from the metal, the energy of the d_z2 would drop as shown in Figure II. If the tetragonal distortion was great enough the electrons which had occupied the e_g orbitals with parallel spins would now occupy the lower energy d_z2 orbital with paired spins. It has been found that for very large tetragonal distortions, or the limiting case of square planar coordination, the energy of the d_z2 orbital drops below that of the d_{xy} orbital.

The transition metal ions which are commonly found to have square planar coordination are Rh(I), Ir(I), Pd(II) and Au(III), all of which are d^8 species. Of these Pd(II) and Pt(II) have received the most attention.

Square planar complexes participate in three main types of

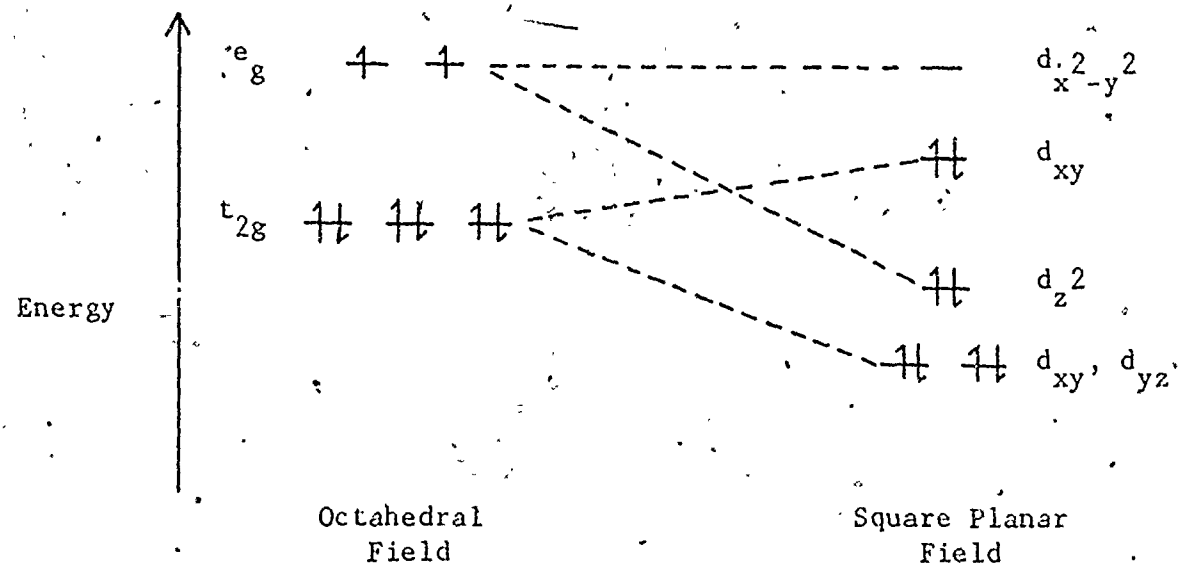

Figure II

Orbital Splitting for d^8 Ions in Octahedral and Square Planar Fields

reaction. These are:

1) Oxidative addition. This reaction can be schematically represented as

$$M^{n+} + X\text{-}Y \longrightarrow X\text{-}M^{n+2}\text{-}Y$$

and examples are

a) $\underline{\text{trans}}\text{-}[PtI(CH_3)(PEt_3)_2] + CH_3I \longrightarrow [PtI_2(CH_3)_2(PEt_3)_2]$

b) $\underline{\text{trans}}\text{-}[IrCl(CO)(PPh_3)_2] + H_2 \longrightarrow [IrH_2Cl(CO)(PPh_3)_2]$

2) Insertion into metal-hydrogen or metal-carbon bonds.

Olefins will insert into metal-hydrogen bonds as in

$$\underline{\text{trans}}\text{-}[PtHCl(PEt_3)_2] + C_2H_4 \longrightarrow \underline{\text{trans}}\text{-}[PtCl(C_2H_5)(PEt_3)_2]$$

and carbon monoxide will insert into metal-carbon bonds as in

$$\underline{\text{trans}}\text{-}[PtCl(CH_3)(PEt_3)_2] + CO \longrightarrow \underline{\text{trans}}\text{-}[PtCl(COCH_3)(PEt_3)_2]$$

3) Substitution reactions. Schematically these reactions can be represented as

$$L\text{-}\overset{\overset{X}{|}}{M}\text{-}A + :E \longrightarrow L\text{-}\overset{\overset{X}{|}}{M}\text{-}E + A \quad \ldots\ldots\ldots (1.1)$$

Of the above reaction types substitution reactions have been studied most. Kineticists have examined substitution at square coordinate Pt(II) in great detail. It has been demonstrated that the normal mode of substitution is associative, i.e., a five coordinate intermediate is formed.[2] A number of factors appear to have an effect on the substitutive reactivity of a complex. These are:

1) The nature of the entering group.

2) The nature of the other ligands in the complex.

3) The nature of the leaving group.

4) The nature of the reaction center.

The factors are listed in order of dominant effect. In equation 1.1 we can relate point 1) to the nature of E, 2) to the nature of L and X, 3) to the nature of A, and 4) to M. In this work M (Pt(II)) is unchanged, as are the X ligands ($(C_2H_5)_3P$). The factor 2) can be further subdivided into the cis-effect dealing with the effect of X on the reaction rate, and the trans-effect dealing with the effect of L. Compared with the trans-effect the cis-effect is quite small; it is of importance only in those cases in which the ligand trans to the substitution site has a very small trans-effect.

In discussing the trans-effect separation into two parts is useful. These are ground state effects and transition state effects,

and can be described diagramatically as in Figure III.

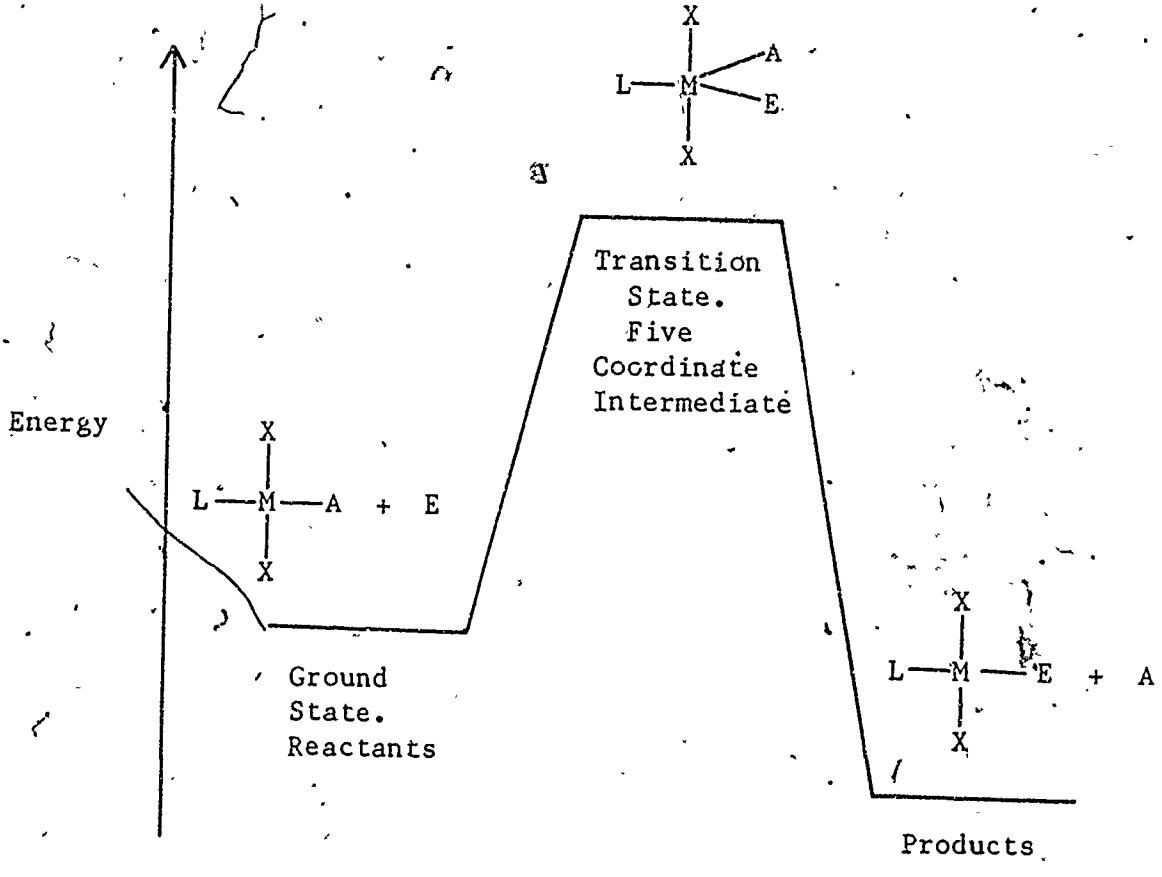

Figure III

Energy Pathway for Substitution Reactions in Square Planar Complexes

To study the overall trans-effect kinetic data is necessary, but a study of the ground state can be conducted by non-kinetic methods. In the years since 1966, when the division between ground state and activated state effects was first suggested, considerable data have been collected relating to the effect of the ligand L on the strength of the bond trans- to itself in the ground state of the molecule. This

body of data has been classified under the heading of trans-influence. The work described in this thesis is solely concerned with the measurement of the trans-influence for a series of Pt(II) complexes.

1.2. The Trans-influence

1.2.1. Theories of the Trans-influence

The major part of the following material is from Appleton et al[3] and Hartley[4]. Specific references are given to other sources.

The trans-influence of a ligand has been defined as the extent to which that ligand weakens a bond trans- to itself in the equilibrium state of a complex[5] whereas the trans-effect of the ligand is the effect the ligand has on the rate of substitution reactions at a site trans- to itself. The trans-influence is thus thermodynamic in nature, whereas the trans-effect is a kinetic phenomenon.

Grinberg[6] advanced the earliest theory of the forces leading to the trans-influence. He postulated that the metal, M, induced a dipole in the trans-influence ligand, L. L in turn induced a dipole in M, displacing electronic charge toward A, thereby weakening the M-A bond, Figure IV. However, this theory is generally discounted since it is based on electrostatics, but the bonding in

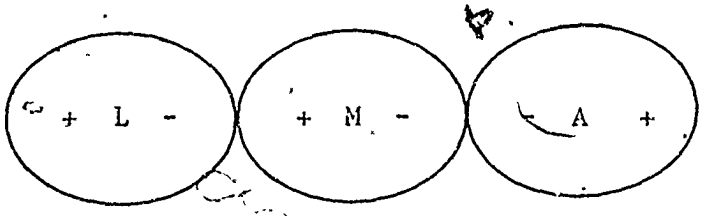

Figure IV

Grinberg's Polarization Theory

those complexes for which the trans-influence is most pronounced (Pt(II)) is believed to be mainly covalent.

Syrkin[7] postulated a theory of the trans-influence based on the hybridization of metal s and d orbitals as shown in Figure V. The L-M-A axis can be considered to be along either the x axis (s+d) or y axis (s-d). If L forms a strong covalent bond with M it will decrease the availability of the hybrid orbital to A, weakening the M-A bond.

More recently, theoretical calculations have been carried out with differing results. Zumdahl and Drago[8] carried out molecular orbital calculations on a series of complexes of Pt(II) and their results support Syrkin, i.e., weakening of the M-A bond is due

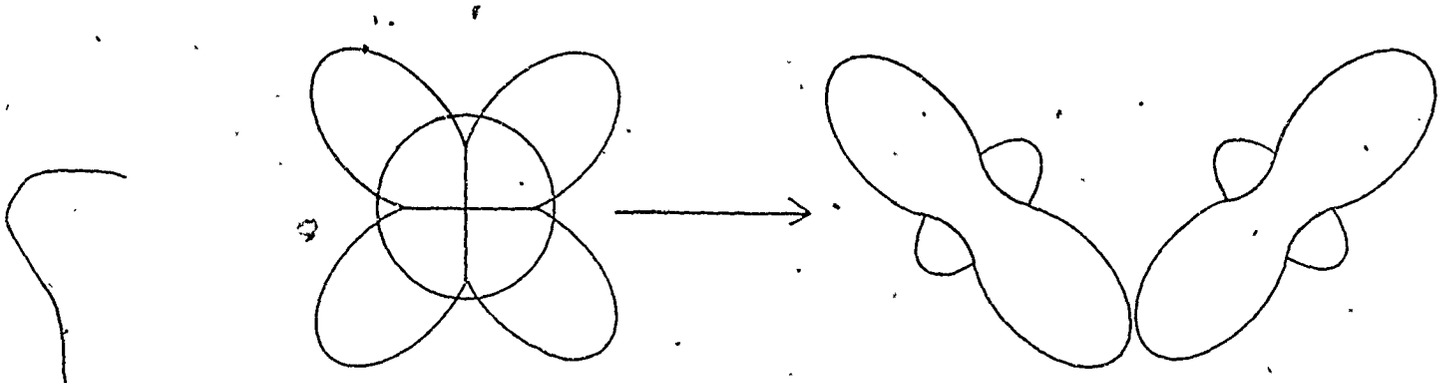

s, $d_{x^2-y^2}$ $\quad$ $s + d_{x^2-y^2}$ $\quad$ $s - d_{x^2-y^2}$

Figure V

Syrkin's Hybrid Orbitals

primarily to the weakening of $Pt_{(6s)}$-A and $Pt_{(d_{x^2-y^2})}$-A interactions. However Langford and Gray[9] ascribe the high trans-influence of ligands as H^-, CH_3^- and PR_3 to the large overlap of these ligands with the $Pt_{(6p)}$ orbital, reducing the availability of this orbital to A.

There has been some controversy regarding the role of π-bonding with respect to the trans-influence. For example the high trans-effect of phosphines was ascribed to the ability of the phosphine

to remove electronic charge from the dxz, dyz and dxy orbitals. Thus π-bonding ligands trans- to the phosphine would be less strongly bound. However, it was pointed out that a strong σ effect could quite adequately describe the effect of the phosphine ligand on ligands trans- to itself.[5] It is now felt that π-bonding is of importance in understanding the trans-influence only in cases where synergic π-bonding is necessary to the formation of the σ bond, i.e., complexes containing carbon monoxide or olefins. With synergic bonding the contribution from metal dxz, dyz and dxy orbitals to vacant ligand orbitals has an effect on the strength of the metal-ligand σ bond.

1.2.2. Measurement of the Trans-influence

The trans-influence has been measured by a variety of techniques of which the most important are x-ray crystallography, vibrational spectroscopy and nuclear magnetic resonance spectroscopy.

1.2.2.1. X-ray Crystallography

X-ray crystallography appears to be an ideal way to measure the trans-influence. As the trans-influence of the ligand L is changed for a series of trans-$[MLAX_2]$ species the M-A bond distance should change. There are, however, a number of difficulties inherent in the method.

1) A crystal structure analysis is rather more time consuming and expensive than say, obtaining an infrared or nuclear magnetic

resonance (n.m.r.) spectrum of the same compound.

2) Differences in the M-A bond lengths for a series of compounds with changing L are quite small and may be of the order of magnitude of the experimental error.

3) Crystal interactions can cause significant changes in bond length, i.e., changing the counter ion can cause slight differences in bond length or different crystalline modifications of the same compound can show different bond lengths.

4) The quality of the crystal employed in the determination and the particular method by which the data is collected and the structure refined can cause small changes in the structural parameters obtained.

No complete data have yet been gathered on the changes in the M-A bond length on changing the ligand L in a series of complexes trans- $MLAX_2$. However, it is possible to construct an order of crystallographic trans-influence from related compounds. This yields the order of structural trans-influence $0 < NH_3 \simeq Cl^- \simeq C{=}C \simeq RNC \simeq CO < AsR_3 \leqslant PR_3 \simeq$ carbenes $H^- \simeq \sigma\text{-}C \simeq R_3Si$.

1.2.2.2. Vibrational Spectroscopy

The vibrational stretching motion of a diatomic molecule A-B can be approximated by a harmonic oscillator. The frequency of vibration is given by

$$\nu = \frac{1}{2\pi c}\sqrt{\frac{f}{\mu}} \qquad (1.2)$$

where ν is the vibrational frequency, f is the force constant of A-B bond and μ is the reduced mass given by

$$\mu = \frac{M_A M_B}{M_A + M_B} \qquad (1.3)$$

The assumption is made that for a series of complexes trans-$[MLAX_2]$ μ remains unchanged with changes in L and that the force constant of the M-A bond is proportional to the stretching frequency ν. A decrease in the stretching frequency denotes a weakening of the M-A bond.

The assumption that μ remains unchanged does not strictly hold. For example, μ for the Pt-C stretch in trans-$[Pt(C_2F_3)(CO)(PEt_3)_2]$ is 69.2 a.m.u., whereas μ for trans-$[Pt(C_2F_3)\{P(OPh)_3\}(PEt_3)_2]$ is 73.2 a.m.u. The increase in reduced mass indicates that the frequency of the Pt-C stretch will decrease from L = CO to L = $P(OPh)_3$, irrespective of any changes in trans-influence.

A further complication arises in that there is a possibility of the M-A vibration coupling with other vibrational modes of the molecule. Vibrational couplings are normally ignored if ν_{M-A} is well separated from other vibrational modes which might couple.

Also, differences between spectra obtained from samples in solution and in the solid state are sometimes noted. As is found with crystallography, counter ion changes can also cause slight shifts in M-A stretching frequencies.

Complexes of the type trans-$[PtLClX_2]$ have been examined in detail with regard to metal-chloride stretching frequency. It has been found that this frequency is virtually independent of X, and appears as a single band at about $300cm^{-1}$. The value of ν_{Pt-Cl} changes from a high of $.344cm^{-1}$ for L = CO to a low of $235cm^{-1}$ for L = $GeMe_3^-$ with X as either PEt_3 or PMe_2Ph. A trans-influence series for some thirty-five ligands has been compiled; those of interest to this work in order of increasing trans-influence are $CO < Cl < py < P(OPh)_3 \simeq P(OMe)_3 < PPh_3 < PEt_3 < CH_3^- < C_6H_5^- \lesssim H^-$.

The series of complexes trans-$[PtHLX_2]$ have also been examined in some detail and a trans-influence series assembled for some thirty ligands. Appropriate members of this series are $NO_3^- < N_3^- < Cl^- < Br^- < N_3^- < py < I^- < NO_2^- < CO < P(Ph)_3 < P(OPh)_3 \simeq PEt_3 \lesssim P(OMe)_3 < CN^-$. Once again changing the groups cis- to the hydrogen atom has little effect on ν_{Pt-H}. Difficulties can arise in that ν_{Pt-H} appears to be somewhat solvent dependent, and the magnitude of the solvent effect changes with L. Vibrational coupling occurs for hydride trans- to ligands such as CN^-, CO and RNC, but corrected values can be obtained by observing the difference between ν_{Pt-H} and ν_{Pt-D} in analogous complexes.

The complexes trans-$[PtL(CH_3)X_2]$ have not been studied in as much detail as the chloro and hydrido complexes, but again at least two trans-influence series based on ν_{Pt-C} can be constructed. These series are $CN^- < I^- < NO_2^- < Br^- < Cl^- < SCN^- < NO_3^-$ for trans-$[PtX(CH_3)(PEt_3)_2]$ complexes and $py < C_2H_4 < CO <$ phosphine $<$ carbene for trans-$[Pt(CH_3)L(PMe_2Ph)_2]^+$

complexes. The ν_{Pt-C} band is normally very weak and possibilities for vibrational coupling can occur with species such as CN^- and NO_2^-.

Internal ligand vibrations such as ν_{CO} or ν_{CN} have also been correlated with trans-influence but the situation is much more complex. The complexity is due to the fact that the effect of the ligand L on the back donation to the vacant π orbitals of A must be considered, as well as the direct trans-influence on the M-A σ bond. Systems such as trans-$[PtCl_2L(amine)]$ have been investigated and it was found that ν_{N-H} could be correlated with ν_{Pt-H} for a series of L.

1.2.2.3. Nuclear Magnetic Resonance Spectroscopy

Chemical shifts have not been much employed as a measure of the trans-influence. The overall shielding constant for a nucleus is composed of diamagnetic and paramagnetic contributions,

$$\sigma = \sigma_d + \sigma_p \qquad (1.4)$$

The diamagnetic contribution is considered to be small when the chemical shifts are quite large, as is the case with the compounds in question. The paramagnetic contribution to the chemical shift of an atom bonded to, for example, platinum arises from shielding of the substituent by the d orbitals on platinum. Therefore, if the atom is far from the metal there should be less shielding and consequently a smaller chemical shift. But other effects at the platinum nucleus,

associated with changing L, could change the d orbital cloud on the metal, thus changing the paramagnetic contribution, without any change in the M-A bond.

There is evidence that the chemical shift of a hydrogen atom bonded to platinum in the series $[PtHL(PR_3)_2]$ does correlate roughly with other parameters such as J_{Pt-H},[10] but it is felt that, at this time, there are more direct methods of measuring the trans-influence, such as metal-ligand stretching vibrations or nuclear magnetic resonance coupling constants.

The spin-spin couplings in nuclear magnetic resonance experiments are thought to be transmitted from nucleus to nucleus by three mechanisms. The first mechanism involves transmission of spin alignment via the bonding electrons. This is the Fermi contact term and it is frequently considered to be the dominant term. The second mechanism involves the induction of orbital electronic currents by the nuclear moment producing magnetic fields at the sites of other nuclei. This process is termed the orbital contribution. The third, the dipole-dipole-mechanism, involves the transmission of nuclear spins via polarization of the valence electron spin. Usually only the Fermi contact term is considered when calculating coupling constants. The inclusion of orbital and dipole-dipole contributions will be discussed in 3.2.2. The term through space coupling will be applied to these latter contributions. This term has also been applied to couplings between nuclei separated by many bonds but spatially proximate. The latter usage is not intended here.

The magnitude of the coupling constant between two directly bound nuclei, A and B, considering only the Fermi contact term, is given in the trans-influence literature by the proportionality

$$J_{AB} \propto \left[\gamma_A \gamma_B S_A^2(0) S_B^2(0) \left|\psi_{A(ns)}^{(0)}\right|^2 \left|\psi_{B(ns)}^{(0)}\right|^2 {}^3\Delta E^{-1}\right] \quad (1.5)$$

where J_{AB} is the value of the coupling constant, γ_A and γ_B are the gyromagnetic ratios of A and B, $S_A^2(0)$ and $S_B^2(0)$ represent the s character used by each of the A and B atoms in their bonding hybrid orbitals, $\left|\psi_{A(ns)}^{(0)}\right|^2$, $\left|\psi_{B(ns)}^{(0)}\right|^2$, are the electron densities of the ns valence orbitals at their respective nuclei and ${}^3\Delta E$ is a mean triplet-singlet excitation energy.

Obviously the above equation will not allow the direct computation of the coupling constant but will allow comparison of the ratios of coupling constants for related types of compounds.

In a closely related series of compounds, e.g., trans-$[PtLAX_2]$, where only the A ligand is being changed it is normally considered that ${}^3\Delta E$, $S_L^2(0)$, and $\left|\psi_{L(ns)}^{(0)}\right|^2$, change very little. Only the $S_{Pt}^2(0)$ and $\left|\psi_{Pt(6s)}^{(0)}\right|^2$ terms are thought to change, and the change in the $S_{Pt}^2(0)$ term is thought to be dominant. For example for the compound cis-$[PtCl(CH_3)(PEt_3)_2]$ J_{Pt-P} for phosphorus trans- to the methyl group is 1719 Hz while J_{Pt-P} for phosphorus trans- to the chloride is 4179 Hz. The large difference in coupling constant must originate with a difference in $S_{Pt}^2(0)$, the platinum s character available for use

in the two Pt-P bonds, since $|\psi_{Pt(6s)}^{(0)}|^2$ would, of necessity, be the same for both Pt-P bonds.

Over more than one bond the coupling constant $J_{A...N}$ is given by

$$J_{A...N} \propto \left[\gamma_A \gamma_N S_A^2(0) S_B^2(0) f(A...N) |\psi_{A(ns)}^{(0)}|^2 |\psi_{N(ns)}^{(0)}|^2 {}^3\Delta E^{-1}\right] \quad (1.$$

where all symbols have the meanings given above with the exception of f(A...N) which represents all the electronic and stereochemical factors concerned in the transmission of the coupling from A to N.

Therefore, the current theories hold that in a series of compounds trans-$[PtLAX_2]$ where A is being changed, the magnitude of J_{Pt-L} should depend on the amount of Pt_{6s} orbital available for the Pt-L bond. Ligands A with a high trans-influence would concentrate Pt_{6s} electron density in the Pt-A bond, thus decreasing the availability of the Pt_{6s} orbital for bonding to L. This weakening of the Pt-L bond would be shown by a decrease in the value of J_{Pt-L}.

Trans-influence series based on coupling over one bond have been compiled employing $^1J_{Pt-H}$ for complexes trans-A-Pt-H or $^1J_{Pt-P}$ for complexes trans-A-Pt-P. Similar series with coupling over two bonds based on $^2J_{Pt-H}$ for complexes trans-A-Pt-CH_3 or $^2J_{Pt-F}$ for complexes trans-A-Pt-CF_3 have also been compiled. These series are quite similar. For example, that for compounds of the type trans-$[PtHAX_2]$ where X=PEt_3 or $PMePh_2$ in order of increasing trans-influence (order

of decreasing J_{Pt-H}) is $I^- < NO_3^- < Br^- < Cl^- < SCN^- < py < NO_2^- < CO < C_2H_4 < PPh_3 < P(OPh)_3 < PEt_3 < CN^-$.

It is a normal practice in the literature to attempt to correlate trans-influence series measured for different complexes or by different methods. The coupling constants J_{Pt-L} are often plotted against J_{Pt-H}. If the result is a straight line it is considered that J_{Pt-L} does indeed measure the trans-influence. Further, J_{Pt-H} has been plotted against ν_{Pt-H} from vibrational spectra, once again yielding a straight line plot. This indicates that the two spectroscopic techniques are measuring the same phenomenon.

Recently Mather, Pidcock and Rapsey[11] described a correlation between $^1J_{Pt-p}$ and the Pt-P bond lengths in a series of complexes in which the phosphorus atom was trans- to various ligands. Although the correlation was not linear there appears to be a definite relationship. The plots are very similar in shape to Cotton's bond length-bond strength graphs.[1]

1.3 Objects of Research

The object of the research was to prepare series of complexes of the types trans-$[PtX(C_2F_3)(PEt_3)_2]$ and trans-$[Pt(C_2F_3)L(PEt_3)_2][ClO_4]$ and to determine if the n.m.r. coupling between platinum and each of the three fluorine nuclei in the perfluorovinyl ligand could be correlated with existing measures of the n.m.r. trans-influence.

CHAPTER II

EXPERIMENTAL

Perfluorovinylbis(triethylphosphine)platinum(II) Complexes

2.1. General

2.1.1. Chemicals

The tetrafluoroethylene employed in the preparation of trans-perfluorovinylchlorobis(triethylphosphine)platinum(II) was obtained from Columbia Organic Chemicals Co. It was used without purification after an infrared spectrum showed only absorptions due to tetrafluoroethylene. All other preparative chemicals employed were reagent grade. Solvents were spectral grade and were dried over molecular sieve, with the exception of n-pentane, which was distilled from phosphorous pentoxide and stored over sodium.

2.1.2. Instruments

Infrared spectra were obtained as Nujol mulls between cesium iodide plates on a Beckman I.R.20 double beam spectrometer. Cesium iodide reference plates were used. Spectra were run from 250 to 4000 cm^{-1}. Reproducibility was $\pm$ 3 cm^{-1}.

All melting points were obtained on a Reichert hot stage melting point apparatus. Melting points were not corrected. The perfluorovinyl compounds were analyzed on a Perkin-Elmer model 240 carbon-hydrogen-nitrogen analyzer by D.L. McGillivray of the Chemistry Department, University of Victoria. The proton spectra of the perfluorovinyl species were obtained at 35 ^{o}C in 0.5 cm thin wall n.m.r. tubes on a Perkin-Elmer model R12A spectrometer. The spectra

were run at 60 MHz. All spectra were run in chloroform except that of trans-perfluorovinylazidobis(triethylphosphine)platinum(II) which was insoluble in chloroform. Its spectrum was obtained in methanol. For those compounds which did not resonate near chloroform, this solvent was employed as internal reference. For those compounds displaying resonances near chloroform, i.e., those with phenyl groups, deuterochloroform was used as solvent and tetramethylsilane (T.M.S.) employed as internal reference. The use of T.M.S. was avoided as far as possible as it caused precipitation of the perfluorovinyl species.

The fluorine spectra were obtained on a Varian model HA-60 I.L. Spectrometer at 56.446 MHz. The solvents used were as those for proton spectra. The spectra were run at room temperature and in all cases trichlorofluoromethane was the external reference. Due to the low concentration of each fluorine nucleus, the spectra were compiled on a Northern Scientific Model NS-560, SAC series, time averaging computer. Total scans for each nucleus varied from 10 scans at 500 seconds per scan to 200 scans at 50 seconds per scan. In general, the best results were obtained with a large number of short scans.

Fluorine nuclei were assigned labels as indicated in Tables I, II and III. The spectrum for nucleus III was taken twice, once over 1000 Hz to measure Pt-F and F-F couplings and once over 250 Hz to measure P-F couplings.

2.2. Preparations

2.2.1. Trans-hydridochlorobis(triethylphosphine)platinum(II)

This compound was prepared by the method of Chatt and Shaw [12]. Cis-dichlorobis(triethylphosphine)platinum(II) was prepared by reacting 3.7 ml of triethylphosphine with 5.0 g of potassium tetrachloroplatinate(II) (12 mmol) in 100 ml water for forty-five minutes. To assist conversion to the cis isomer, the mixture was heated on a water bath, with stirring, until the first black particles indicating decomposition appeared. The mixture was cooled, filtered, washed with water and dried under vacuum. To complete conversion to the cis isomer, the filtered material was boiled in anyhdrous diethyl ether containing 0.5 ml triethylphosphine. The solution was boiled almost to dryness and the residual ether then removed under vacuum. Yield was 4.9 g (9.8 mmol) 81%. The cis-dichlorobis(triethylphosphine)platinum(II) was then reduced by treatment with 4.0 ml hydrazine hydrate in 100 ml water. This solution was heated on a water bath for thirty minutes. After cooling, dilute HCl was added until the mixture was acid to narrow range Litmus paper (pH 6 to 8.5). The precipitate of trans-hydridochlorobis(triethylphosphine)platinum(II) was collected and dried under vacuum, and recrystallized from pentane. Yield was 3.0 g (6.4 mmol), 53%, based on K_2PtCl_4. Melting point 82 ^{o}C, Pt-H stretching frequency 2222 cm^{-1} as nujol mull, cf. 2183 in hexane[12], 2209 in chloroform[13].

2.2.2. Preparation of trans-perfluorovinylchlorobis (triethylphosphine)platinum(II)

This compound was prepared by the method of Clark and Tsang[14]. Trans-hydridochlorobis(triethylphosphine)platinum(II) (500 mg, 1.07 mmol) was weighed into a dry 250 ml capacity pyrex carius tube. The tube was attached to a vacuum line and evacuated. 50 ml of spectral grade benzene was condensed into the carius tube, followed by 500 mg (5.0 mmol) tetrafluoroethylene. The tube was flame sealed and removed to a protective metal tube which was placed in an oven at 95 °C for twenty-nine hours. The carius tube was cooled to -196 °C and opened. Benzene, unreacted tetrafluoroethylene and gaseous reaction products were removed. The solid material remaining in the tube was extracted with warm cyclohexane. The cyclohexane was removed on a rotary evaporator and an infrared spectrum of the solid remaining was obtained as a nujol mull. The absence of absorption at 2220 cm^{-1} indicated the reaction had gone to completion. Two C=C double bond stretching bands were noted with frequencies at 1648 cm^{-1} due to trans-(1-difluoromethyl-2,2-difluorovinyl)chlorobis(triethylphosphine) platinum(II) and at 1725 cm^{-1} due to trans-perfluorovinylchlorobis (triethylphosphine)platinum(II), cf 1643 cm^{-1} and 1724 cm^{-1}[14]. These two compounds were separated on a florisil column, 100-200 mesh, 2.5 cm in diameter and 60 cm in length. Chloroform-pentane in a 2:1 ratio was used as eluent and the perfluorovinyl species was the first product off the column. Yield 181 mg (0.33 mmol) 32%. The yield of trans-

(1-difluoromethyl-2,2-difluorovinyl)chlorobis(triethylphosphine) platinum(II) was 114 mg (0.19 mmol) 18%.

Attempts were made to improve the yield of trans-perfluorovinylchlorobis(triethylphosphine)platinum(II). When the reaction solvent, benzene, was rigorously dried no reaction occurred and the parent hydride was recovered unchanged. When a seven fold excess of tetrafluoroethylene was employed at a reaction temperature of 110 °C for forty-eight hours in 50 ml of cyclohexane as a reaction solvent, the yield of trans-perfluorovinylchlorobis(triethylphosphine) platinum(II) increased to 54.8%.

When the above conditions were used in conjunction with a new carius tube yields rose to 80.8%.

Characterization was as follows. Melting point 58-59 °C, cf. 61 °C[14]. Analysis. Calculated for $C_{14}H_{30}ClF_3P_2Pt$: C, 30.69; H, 5.52. Found: C, 30.89; H, 5.52.

The infrared spectrum showed $\mu_{C=C}$ at 1725 cm^{-1} and μ_{Pt-Cl} at 285 and 305 cm^{-1}, cf. $\mu_{C=C}$ 1724 cm^{-1}[14]. The proton n.m.r. spectrum showed a quintet (relative area three) at 6.16 p.p.m. upfield from chloroform and a septet (relative area two) at 5.42 p.p.m. upfield from chloroform. Fluorine n.m.r. results are shown in Tables I, II and III.

2.2.3. The preparation of trans-perfluorovinylbromobis (triethylphosphine)platinum(II)

Trans-perfluorovinylchlorobis(triethylphosphine) platinum(II)(125.5 mg, 0.229 mmol) and lithium bromide (403.7 mg, 4.48 mmol) were stirred under nitrogen in 5 ml acetone for one hour.

The acetone was removed on a rotary evaporator and the red-colored residue extracted with methylene chloride. This purple colored solution was filtered to remove lithium chloride and unreacted lithium bromide. The methylene chloride was removed on a rotary evaporator. The residue was dissolved in methanol and crystallization from this purple solution was effected by the addition of about 25% by volume water and cooling to -20 °C. Overnight all traces of the purple color disappeared and did not reappear when the crystals were redissolved. The product was obtained as very pale yellow crystals, yield 110 mg (0.179 mmol) 78%. Melting point 83-84 °C, cf. 82-83 °C[15]. Analysis. Calculated for $C_{14}H_{30}BrF_3P_2Pt$: C, 28.29; H, 5.09, Found: C, 27.98; H, 4.99. $\nu_{C=C}$ was 1730 cm^{-1}. The proton n.m.r. spectrum showed a quintet (relative area three) at 6.17 p.p.m. upfield from chloroform and a septet (relative area two) at 5.29 p.p.m. upfield from chloroform. Fluorine n.m.r. results are shown in Tables I, II and I-I.

An ultraviolet-visible spectrum of the purple methylene chloride solution showed a strong asymmetric absorption at 238 mμ and a much weaker absorption at about 285 mμ. Molar extinction coefficients were not obtained.

2.2.4. The preparation of trans-perfluorovinyliodobis (triethylphosphine)platinum(II)

Trans-perfluorovinylchlorobis(triethylphosphine) platinum(II) (125.3 mg, 0.229 mmol) was dissolved in 5 ml of acetone. Sodium iodide (344.0 mg, 2.30 mmol) was added and the solution stirred under nitrogen for one hour. The sodium chloride reaction product was removed by filtration and the acetone removed on a rotary evaporator. The solid residue was dissolved in diethyl ether and the ether solution washed with water to remove traces of sodium chloride and unreacted sodium iodide, and dried over magnesium sulfate. The ether was removed on a rotary evaporator and the iodide compound recrystallized from methanol-water solution as pale yellow crystals. Yield: 125 mg (0.198 mmol), 87%. Melting point 104-106 °C. Analysis. Calculated for $C_{14}H_{30}IF_3P_2Pt$: C, 26.22; H, 4.72. Found: C, 25.64; H, 4.54. $\nu_{C=C}$ was 1730 cm^{-1}. The proton n.m.r. showed a quintet (relative area three) at 6.16 p.p.m. upfield from chloroform and a septet (relative area two) at 5.17 p.p.m. upfield from chloroform. Fluorine n.m.r. results are shown in Tables I, II and III.

2.2.5. The preparation of trans-perfluorovinylnitritobis (triethylphosphine)platinum(II)

Trans-perfluorovinylchlorobis(triethylphosphine)platinum(II) (124.8 mg, 0.228 mmol) was dissolved in 5 ml methanol. Sodium nitrite (18.1 mg, 0.262 mmol) was added and the solution stirred under nitrogen

for thirty minutes. As no precipitate of sodium chloride appeared 53.5 mg (0.275 mmol) silver tetrafluoroborate dissolved in 1 ml water and 1 ml methanol was added. An immediate precipitate of silver chloride was noted. The solution was stirred under nitrogen for one hour, the silver chloride was removed by filtration and the methanol removed on a rotary evaporator. The residue was dissolved in diethyl ether and washed with several portions of water to remove unreacted starting materials. The ether solution was dried with magnesium sulfate and filtered. The ether was removed on a rotary evaporator and the nitrito compound recrystallized from methanol-water at -20 °C. Yield 94 mg (0.171 mmol) 75%. Melting point 122-124 °C, ν_{NO_2} 1460, 1340, 1065, 820 and 586 cm^{-1}. $\nu_{C=C}$ 1723 cm^{-1}. Analysis. Calculated for $C_{14}H_{30}NO_2F_3P_2Pt$: C, 30.11; H, 5.42; N, 2.51. Found: C, 30.42; H, 5.39; N, 2.50. The proton n.m.r. showed a quintet (relative area three) at 6.13 p.p.m. upfield from chloroform and a septet (relative area two) at 5.51 p.p.m. upfield from chloroform. Fluorine n.m.r. spectral parameters are listed in Tables I, II and III.

2.2.6. The preparation of trans-perfluorovinylnitratobis (triethylphosphine)platinum(II)

Trans-perfluorovinylchlorobis(triethylphosphine)platinum(II) (123.4 mg, 0.224 mmol) was dissolved in 3 ml methanol. Silver nitrate, (44.6 mg, 0.262 mmol) dissolved in 1:1 methanol:water, was added dropwise. The solution was stirred under nitrogen for thirty minutes, then

the AgCl was removed by filtration and the methanol removed on a rotary evaporator. The residue was dissolved in diethyl ether and washed with water to remove unreacted silver nitrate. The solution was dried over magnesium sulfate and filtered. The ether was removed on a rotary evaporator and the residue recrystallized as colorless crystals from petroleum ether (60-90 °C). Yield 79 mg (0.137 mmol) 61%. Melting point 120-122 °C. Analysis. Calculated for $C_{14}H_{30}NO_3F_3P_2Pt$: C, 29.27; H, 5.26; N, 2.44. Found: C, 29.90; H, 5.32; N, 2.34. $\nu_{C=C}$ 1730 cm^{-1}, ν_{NO_3} 1485 and 1276 cm^{-1}. The proton n.m.r. showed a quintet (relative area three) at 6.14 p.p.m. upfield from chloroform and a septet (relative area two) at 5.48 p.p.m. upfield from chloroform. Fluorine n.m.r. spectral parameters are listed in Tables I, II and III.

2.2.7. The preparation of trans-perfluorovinylcyanobis (triethylphosphine)platinum(II)

Trans-perfluorovinylchlorobis(triethylphosphine)platinum(II) (126.0 mg, 0.228 mmol) was dissolved in 5 ml methanol, followed by the addition of sodium cyanide, (12.5 mg, 0.255 mmol). Silver tetrafluoroborate, (69.7 mg, 0.358 mmol) was dissolved in 2 ml of 1:1 water:methanol and pipetted into the solution. A white precipitate formed immediately. The solution was stirred for one hour under nitrogen, then filtered to remove the silver chloride. The methanol was removed on a rotary evaporator and the residue dissolved in diethyl ether.

The ether solution was washed with several portions of water and dried over magnesium sulfate. The solution was filtered and the ether removed on a rotary evaporator. The cyano compound was recrystallized at -20 °C from methanol-water as colorless crystals. Yield 81 mg (0.150 mmol) 68%. Melting point 105-107 °C. Analysis. Calculated for $C_{15}H_{30}NF_3P_2Pt$: C, 33.34; H, 5.60; N, 2.59. Found: C, 32.91; H, 5.40; N, 2.34. $\nu_{C=C}$ 1728 cm^{-1}, $\nu_{C\equiv N}$ 2148 cm^{-1}. The proton n.m.r. showed a quintet (relative area three) at 6.18 p.p.m. upfield from chloroform and a septet (relative area two) at 5.28 p.p.m. upfield from chloroform. Fluorine n.m.r. results are given in Tables I, II and III.

2.2.8. The preparation of trans-perfluorovinylazidobis (triethylphosphine)platinum(II)

Trans-perfluorovinylchlorobis(triethylphosphine)platinum(II) (126.6 mg, 0.231 mmol) was dissolved in 5 ml methanol. Silver tetrafluoroborate (52.3 mg, 0.269 mmol) was added, followed by sodium azide (15.7 mg, 0.242 mmol) dissolved in 3:1 methanol:water. The silver chloride reaction product was removed by filtration and the methanol solution passed down a short florisil column to remove ionic species, thereby precluding the formation of silver azide. The azide compound was recrystallized from methanol-water. Yield 75 mg (0.135 mmol) 58%. Melting point 70-71 °C. Analysis. Calculated for

$C_{14}H_{30}N_3F_3P_2Pt$: C, 30.22; H, 5.43; N, 7.55. Found: C, 30.10; H, 5.23; N, 7.50. $\nu_{C=C}$ 1731 cm^{-1}, $\nu_{N\equiv N}$ 2045 cm^{-1}. The azide compound proved to be different from the other compounds prepared in this series in that it was light sensitive and insoluble in all common organic solvents except methanol. For the latter reason the proton and fluorine n.m.r. spectra were recorded in methanol solution. The proton n.m.r. showed a quintet (relative area three) at 3.49 p.p.m. upfield from methanol, and a septet (relative area two) at 2.78 p.p.m. upfield from methanol. The fluorine n.m.r. spectral parameters are listed in Tables I, II and III.

2.2.9. The preparation of trans-perfluorovinylcarbonylbis (triethylphosphine)platinum(II)perchlorate

Trans-perfluorovinylchlorobis(triethylphosphine)platinum(II) (151.0 mg, 0.276 mmol) was dissolved in 5 ml acetone. Silver perchlorate (42.0 mg, 0.203 mmol) was added to the solution. Silver chloride precipitated. Carbon monoxide was bubbled through the solution for thirty minutes and the silver chloride was then removed by filtration.

The acetone was removed on a rotary evaporator and the residue treated with diethyl ether, to separate the ether soluble starting material from the ether insoluble product. The solution was filtered and the filtered material washed with several portions of water to remove any residual silver perchlorate. The solid was dried under vacuum and

recrystallized from chloroform by the addition of a few drops of diethyl ether. Yield of the white crystals was 97 mg (0.151 mmol) 74% on the basis of silver perchlorate, 55% on the basis of trans-perfluorovinylchlorobis(triethylphosphine)platinum(II). Melting point 134-136 °C. Analysis. Calculated for $C_{15}H_{30}ClO_5F_3P_2Pt$: C, 28.16; H, 4.73. Found: C, 28.27; H, 4.73. $\mu_{C=C}$ 1730 cm^{-1}, $\mu_{C\equiv O}$ 2105 cm^{-1}. In the proton n.m.r. a quintet (relative area three) at 6.02 p.p.m. upfield from chloroform and a septet (relative area two) at 5.05 p.p.m. upfield from chloroform were noted. Fluorine n.m.r. results are tabulated in Tables I, II and III.

2.2.10. The preparation of trans-perfluorovinylpyridylbis (triethylphosphine)platinum(II)perchlorate

Trans-perfluorovinylchlorobis(triethylphosphine)platinum(II) (150.4 mg, 0.275 mmol) and sodium perchlorate monohydrate (43.1 mg, 0.307 mmol) were dissolved in 7 ml acetone. 28 µl pyridine (density 0.982 g/ml; 27.4 mg; 0.347 mmol) were syringed into the solution which was then stirred under nitrogen for one hour. The sodium chloride reaction product was removed by filtration. The acetone was removed on a rotary evaporator and the residue treated with diethyl ether to remove unreacted pyridine and chlorocomplex. The pyridyl complex was separated from the remaining sodium perchlorate by treatment with methylene chloride. The methylene chloride was removed on a

rotary evaporator. The solid was dissolved in chloroform and trans-perfluorovinylpyridylbis(triethylphosphine)platinum(II) perchlorate was precipitated by the addition of diethyl ether. Yield. 95 mg (0.138 mmol) 50%. Melting point 152-153 °C. Analysis. Calculated for $C_{19}H_{35}NClO_4F_3P_2Pt$: C, 33.03; H, 5.11; N, 2.03. Found: C, 32.90; H, 5.11; N, 2.12. $\nu_{C=C}$ 1733 cm^{-1}. Vibrations identifiable as originating with the pyridine ring occurred at 1615, 1218, 1010, 704 and 682 cm^{-1}. In the proton n.m.r. a quintet (relative area three) was noted 1.12 p.p.m. downfield from T.M.S. while a septet (relative area two) was noted 1.59 p.p.m. downfield from T.M.S. Two absorptions were noted for pyridine, at 8.58 p.p.m. downfield from T.M.S. (relative area two), and at 7.81 p.p.m. downfield from T.M.S. (relative area three). The multiplets due to these groups were not well resolved. Fluorine n.m.r. results are tabulated in Tables I, II and III.

2.2.11. The preparation of trans-perfluorovinyltris(triethylphosphine) platinum(II)perchlorate

Trans-perfluorovinylchlorobis(triethylphosphine)platinum(II) (151.2 mg, 0.267 mmol) was dissolved in 0.5 ml of acetone. Sodium perchlorate monohydrate (49.1 mg, 0.348 mmol) was dissolved in 5 ml of acetone and this solution was added dropwise to the first solution under nitrogen. 51 μl triethylphosphine (density 0.801 g/ml; 40.8 mg;

0.346 mmol)were syringed into the flask and the mixture stirred under nitrogen for two hours. The sodium chloride formed in the reaction was then removed by filtration and the acetone removed on a rotary evaporator. The trans-perfluorovinyltris(triethylphosphine) platinum(II)perchlorate was extracted into methylene chloride. The methylene chloride was removed on a rotary evaporator and the product recrystallized from chloroform-ether solution at -20 °C. Yield 129 mg (0.177 mmol) 66%.

This product proved to be one of the least stable of the complexes formed, melting with decomposition at 127-129 °C. It decomposed partially over four days in chloroform in an n.m.r. tube, yielding a brown precipitate. Analysis. Calculated for $C_{20}H_{45}ClO_4F_3P_3Pt$: C, 32.89; H, 6.20. Found: C, 33.11; H, 6.27. $\mu_{C=C}$ 1730 cm^{-1}. In other respects the infrared spectrum appeared identical to that of the parent chloro complex with the exception of a strong absorbance at 1080 cm^{-1} due to the perchlorate anion, and the absence of Pt-Cl absorptions. The proton n.m.r. spectrum showed a quintet (relative area three) at 7.27 p.p.m. upfield from chloroform. But rather than the usual septet a poorly resolved multiplet (relative area two) centered 5.35 p.p.m. upfield from chloroform was noted. The relative intensities of the members of the multiplet appeared to be 1:3:4:4:3:1 and undoubtedly arose from the overlap of the resonances of the two chemically different methylene groups. Fluorine n.m.r. spectral results are shown in Tables I, II and III.

2.2.12. The preparation of trans-perfluorovinyltriphenylphosphinebis (triethylphosphine)platinum(II)perchlorate

Trans-perfluorovinylchlorobis(triethylphosphine)platinum(II) (150.4 mg, 0.274 mmol) was dissolved in 5 ml acetone. Sodium perchlorate (43.4 mg, 0.312 mmol) was added. Triphenylphosphine (78.7 mg, 0.300 mmol) was dissolved in acetone and added dropwise to the above solution which was then stirred under nitrogen for five hours. The solution was filtered and the acetone removed on a rotary evaporator. Unreacted phosphine and chloro complex were removed by extraction with ether. The solid residue was dried and the desired vinyl complex extracted from unreacted sodium perchlorate with methylene chloride. The methylene chloride was removed on a rotary evaporator and the triphenylphosphine complex recrystallized from chloroform-ether solution. Yield 106 mg (0.119 mmol) 44%. Melting point 163-164 °C. Analysis. Calculated for $C_{32}H_{45}ClO_4F_3P_3Pt$: C, 43.71; H, 5.19. Found: C, 43.96; H, 5.18. $\mu_{C=C}$ 1730 cm^{-1}. Absorptions due to the triphenylphosphine ligand occurred at 743, 700 and 500 cm^{-1}. The proton n.m.r. showed three absorptions. A peak (relative area five) due to the phenyl protons was noted at 7.60 p.p.m. downfield from T.M.S., the usual quintet (relative area six) at 0.97 p.p.m. downfield from T.M.S., and a poorly resolved septet (relative area four) at 1.44 p.p.m. downfield from T.M.S. The fluorine n.m.r. results are shown in Tables I, II and III.

2.2.13. The preparation of trans-perfluorovinyltrimethylphosphitebis (triethylphosphine)platinum(II)perchlorate

Trans-perfluorovinylchlorobis(triethylphosphine)platinum(II) (151.5 mg, 0.267 mmol) was dissolved in 3 ml of acetone. Sodium perchlorate monohydrate (48.8 mg, 0.348 mmol) was added. 36 µl trimethylphosphite (density 1.05 g/ml; 37.8 mg; 0.305 mmol) were syringed into the solution. An immediate white precipitate was noted. The solution was stirred under nitrogen for thirty minutes, the solid sodium chloride removed by filtration and the acetone removed on a rotary evaporator. The desired product was extracted into methylene chloride and filtered. The methylene chloride was removed on a rotary evaporator and the product obtained as white flocculent substance from acetone-ether. Yield 176 mg (0.249 mmol) 93%. Melting point 140-142 °C. Analysis. Calculated for $C_{17}H_{39}ClO_7F_3P_3Pt$: C, 27.74; H, 5.34. Found: C, 27.44; H, 5.15. $\nu_{C=C}$ 1738 cm^{-1}. Absorptions originating with the trimethylphosphite ligand occurred at 1099 and 840 cm^{-1}. The proton n.m.r. spectrum showed a quintet (relative area six) at 6.33 p.p.m. upfield from chloroform. The usual septet (relative area four) at 7.84 p.p.m. upfield from chloroform was poorly resolved. A doublet (relative area three) centered at 6.04 p.p.m. upfield from chloroform was noted. This absorption originated with the methoxy protons and the splitting arose from coupling with the phosphorous nucleus for which I=1/2. The results of the fluorine n.m.r. spectra are given in Tables I, II and III.

2.2.14. The preparation of trans-perfluorovinyltriethylphosphitebis (triethylphosphine)platinum(II)perchlorate

Trans-perfluorovinylchlorobis(triethylphosphine)platinum(II) (153.2 mg, 0.270 mmol) and sodium perchlorate monohydrate (49.1 mg, 0.349 mmol) were dissolved in 4 ml acetone. 53 μl triethylphosphite (density 0.969 g/ml; 51.4 mg; 0.309 mmol) were syringed into the solution, which was then stirred for one hour. The sodium chloride was removed by filtration and the acetone removed on a rotary evaporator. The residue was slurried in diethyl ether and the ether then removed by decantation. After drying, the triethyl phosphite complex was extracted with methylene chloride. This solvent was removed on a rotary evaporator and the complex recrystallized from chloroform-ether. Yield 195 mg (0.252 mmol) 93%. Melting point 136-137 ^{o}C. $\nu_{C=C}$ 1730 cm^{-1}. Analysis. Calculated for $C_{20}H_{45}ClO_4F_3P_3Pt$: C, 30.83; H, 5.83: Found: C, 30.87; H, 5.75. The proton n.m.r. spectrum was more complex than that of any other compound prepared in this series. The lowest field group was a quintet (relative area two) at 3.20 p.p.m. upfield from chloroform and was due to the methylene protons of the triethylphosphite ligand. The usual quintet (relative area four) due to the methylene protons of the triethylphosphine ligand appeared 5.34 p.p.m. upfield from chloroform. The highest field group was a multiplet (relative area nine) which appeared to be composed of (1) a quintet centered at 8.89 p.p.m. upfield from chloroform due to the methyl protons of

the triethylphosphine ligands and (2) a triplet centered at 8.58 p.p.m. upfield from chloroform due to the methyl protons of the triethylphosphite ligand. The fluorine spectra are reported in Tables I, II and III.

2.2.15. The preparation of trans-perfluorovinyltriphenylphosphitebis (triethylphosphine)platinum(II)perchlorate

Trans-perfluorovinylchlorobis(triethylphosphine)platinum(II) (151.0 mg, 0.268 mmol) and sodium perchlorate monohydrate (50.7 mg, 0.361 mmol) were dissolved in 4 ml of acetone. 51 µl triphenylphosphite (density 0.801 g/ml; 40.8 mg; 0.346 mmol) were syringed into the solution, which was then stirred for two hours. The sodium chloride was removed by filtration and the acetone on a rotary evaporator. Any unreacted starting material was removed by extraction with diethyl ether. The desired complex was extracted from the residue with methylene chloride which was then removed on a rotary evaporator. The complex was recrystallized from chloroform-ether. Yield 180 mg (0.195 mmol) 73%. Melting point 70-72 °C. $\nu_{C=C}$ 1730 cm^{-1}. Other absorptions identifiable with the triphenylphosphite ligand occurred at 1696, 1490, 1280, 925, 690 and 510 cm^{-1}. Analysis. Calculated for $C_{32}H_{45}ClO_4F_3P_3Pt$: C, 41.68; H, 4.72. Found: C, 41.23; H, 4.77. The proton n.m.r. showed a quintet (relative area six) at 1.09 p.p.m. downfield from T.M.S. and a septet (relative area four) at 2.07 p.p.m. downfield from T.M.S. due to the triethylphosphine ligand. The absorption due

to the triphenyl phosphite ligand (relative area five) occurred 7.19 p.p.m. downfield from T.M.S. The fluorine spectral parameters are shown in Tables I, II and III.

TABLE I

FLUORINE[19] NUCLEAR MAGNETIC RESONANCE SPECTRAL PARAMETERS

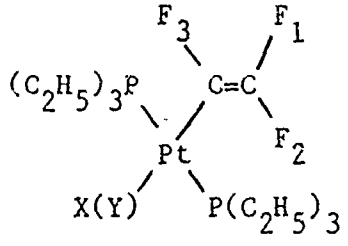

X	σ_1 p.p.m.	J_{12} Hz.	J_{13} Hz.	J_{Pt-F_1} Hz.	$J_{P_{cis}-F_1}$ Hz.	$J_{P_{trans}-F_1}$ Hz.
Cl^-	100.8	105.0	31.0	56.0	6.0	
Br^-	104.8	102.5	31.9	56.5	6.1	
I^-	102.3	102.3	33.2	56.6	6.0	
NO_2^-	95.3	100.6	31.1	37.5	6.0	
ONO_2^-	102.9	101.8	32.2	52.4	5.9	
CN^-	95.5	100.5	29.6	46.3	5.6	
N_3^-	102.0	105.1	30.9	56.4	5.4	
Y						
CO	96.7	89.0	32.6	64.7	6.6	
C_5H_5N	95.9	102.0	32.5	41.0	6.0	
Et_3P	92.1	95.1	33.5	22.0	6.2	12.5
Ph_3P	92.9	95.5	34.3	29.3	6.9	13.8
$(MeO)_3P$	90.9	96.4	32.6	35.3	5.8	22.0
$(EtO)_3P$	93.2	96.2	32.5	33.3	6.0	22.3
$(PhO)_3P$	91.5	94.1	33.7	38.3	6.7	21.8

Note: For Y the perfluorovinyl species are cationic in nature, and these compounds contain the perchlorate anion.

TABLE II

FLUORINE[19] NUCLEAR MAGNETIC RESONANCE SPECTRAL PARAMETERS

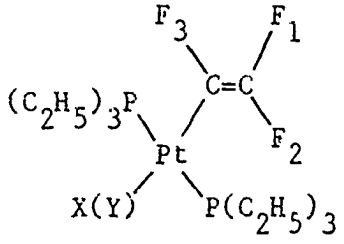

X	σ_2 p.p.m.	J_{12} Hz.	J_{23} Hz.	J_{Pt-F_2} Hz.	$J_{P_{cis}-F_1}$ Hz.	$J_{P_{trans}-F_1}$ Hz.
Cl^-	130.5	105.0	105.0	61.0	3.5	
Br^-	129.3	103.2	103.2	59.7	3.5	
I^-	128.9	102.8	102.8	58.6	4.2	
NO_2^-	128.4	99.8	104.0	61.3	4.2	
ONC_2^-	131.7	102.3	105.7	59.9	4.2	
CN^-	128.6	101.4	101.4	42.6	3.9	
N_3^-	131.7	104.6	104.6	58.5	3.6	
Y						
CO	122.7	91.2	105.7	30.8	3.5	
C_5H_5N	127.2	102.0	107.5	51.0	4.0	
Et_3P	123.5	95.4	98.7	44.8	3.2	3.2
Ph_3P	123.1	93.7	106.2	39.0	4.2	4.2
$(MeO)_3P$	124.7	97.8	103.3	37.4	4.2	4.2
$(EtO)_3P$	124.8	96.6	102.5	37.4	4.2	4.2
$(PhO)_3P$	123.0	94.6	104.2	35.4	17.5	5.0

Note: For Y the perfluorovinyl species are cationic in nature and these compounds contain the perchlorate anion.

TABLE III

FLUORINE[19] NUCLEAR MAGNETIC RESONANCE SPECTRAL PARAMETERS

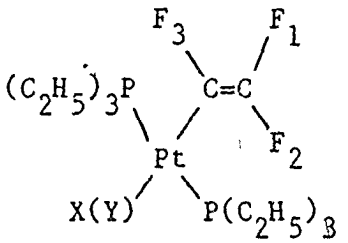

X	σ_{F_3} p.p.m.	J_{13} Hz.	J_{23} Hz.	J_{Pt-F_3} Hz.	$J_{P_{cis}-F_3}$ Hz.	$J_{P_{trans}-F_3}$ Hz.
Cl^-	147.9	31.0	104.5	512	1.5	
Br^-	146.7	32.9	105.3	519	0	
I^-	145.5	33.3	102.8	510	4.8	
NO_2^-	158.0	31.1	104.9	422	6.4	
ONO_2^-	151.5	31.6	105.0	538	2.3	
CN^-	160.1	30.2	103.2	350	4.9	
N_3^-	152.7	29.4	104.2	468	2.3	
Y						
CO	164.4	33.3	104.8	378	4.2	
C_5H_5N	157.2	32.5	107.0	454	4.0	
Et_3P	151.6	33.2	103.0	282	6.2	33.2
Ph_3P	152.7	34.7	103.8	320	6.2	34.7
$(MeO)_3P$	159.0	32.9	102.8	309	5.2	50.8
$(EtO)_3P$	158.8	32.8	102.2	306	5.2	49.9
$(PhO)_3P$	158.6	33.3	103.7	316	5.7	54.3

Note: For Y the perfluorovinyl species are cationic in nature, and these compounds contain the perchlorate anion.

CHAPTER III

DISCUSSION

Perfluorovinylbis(triethylphosphine)platinum(II) Complexes

3. Discussion: A Series of Perfluorovinylbis(triethylphosphine) platinum(II) Complexes and the Trans-influence

3.1. Preparations, Analyses and Stereochemistry

A series of neutral complexes of formula trans-$[PtX(C_2F_3)(PEt_3)_2]$ were prepared for $X = Cl^-$, Br^-, I^-, NO_2^-, ONO_2^-, CN^- and N_3^- and a series of cationic complexes of formula trans-$[Pt(C_2F_3)L(PEt_3)^+][ClO_4^-]$ were prepared for L = CO, C_5H_5N, PEt_3, PPh_3, $P(OMe)_3$, $P(OEt_3)$ and $P(OPh)_3$.

These complexes were prepared from the parent trans-$[PtCl(C_2F_3)(PEt_3)_2]$. The preparation of the parent from trans-$[PtHCl(PEt_3)_2]$ and C_2F_4 was first reported by Clark and Tsang[14]. A mechanism for the formation of the perfluorovinyl complex was suggested by Clark, Dixon and Jacobs[16]. The overall reaction in benzene at 120 °C in a glass vessel was found to be:

$$\text{trans-}[PtHCl(PEt_3)_2] + \text{excess } C_2F_4 \longrightarrow \text{trans-}[PtCl(CF{=}CF_2)(PEt_3)_2] \quad (A)$$

$$+ \text{trans-}[PtCl(C(CF_2H){=}CF_2)(PEt_3)_2] \quad (B)$$

$$+ \text{trans-}[PtCl(CO)(PEt_3)_2][BF_4/SiF_5] \quad (C)$$

The unusual generation of C was explained through reaction of A with H_2O and SiF_4. In a stainless steel autoclave the reaction above was found to produce only trans-$[PtCl(CF_2CF_2H)(PEt_3)_2]$. This is similar to the type of reaction in which an olefin will insert into a metal-hydrogen bond as mentioned in Section 1.1 above. The metal-alkyl formed from olefin insertion will dissociate into olefin and

metal-hydride on heating, but the perfluoroalkyl metal complexes will not undergo a similar dissociation.

Trans-$[PtCl(CF_2CF_2H)(PEt_3)_2]$ was shown to eliminate HF rather readily to form A. The elimination is a slow process in dry benzene in silica, but occurs readily in glass, or with traces of water and SiF_4. On the basis of this data, the following reaction sequence was suggested:

a) $PtH + C_2F_4 \longrightarrow PtCF_2CF_2H$ (1.8)

b) $PtCF_2CF_2H \xrightarrow[H_2O,\ SiF_4]{\text{traces}} HF + PtCF{=}CF_2$ (1.9)

c) $HF + \text{glass} \longrightarrow H_2O,\ BF_3,\ SiF_4,\ BF_4^-,\ SiF_6^{2-}$ (1.10)

d) $2PtCF{=}CF_2 + H_2O + SiF_4 \longrightarrow (PtC{\equiv}O)^+ + HF + SiF_5^- + PtC(CF_2H){=}CF_2$ (1.11)

It appears that reaction a) above is not as simple as indicated since it was found that when trans-$[PtHCl(PEt_3)_2]$ was heated with excess C_2F_4 at 110 °C in rigorously dried benzene no reaction occurred. The hydride was recovered quantitatively. Clark et al[14] employed reagent benzene, which contains about 0.05% water, in the autoclave reaction mentioned above. It seems likely, therefore, that the presence of traces of water are necessary not only for the elimination of HF as postulated in step b) of the reaction sequence, but also for the formation of trans-$[PtCl(CF_2CF_2H)(PEt_3)_2]$ from metal hydride and tetrafluoroethylene.

As it was desired to obtain the maximum yield of trans-

$[PtCl(CF=CF_2)(PEt_3)_2]$ for this work, some modifications to the previously published experimental conditions were made. These were: 1) to carry out the reactions in cyclohexane rather than benzene, as the yield of product C above was found to be lower in cyclohexane than in benzene[14], 2) to carry out the reactions in new Carius tubes as used tubes led to lower yields, undoubtedly due to surface effects since HF is produced in the reaction, and 3) to carry out the reactions at 110 °C even though the yield of C increases with temperature, because the yields of A and B also increase. With these modifications the yield of trans-$[PtCl(CF=CF_2)(PEt_3)_2]$ increased to 80%.

Work conducted by Dixon, Moss and Smith[17] indicates that the perfluorovinyl ligand has a reasonably strong trans-influence, thus it seems likely that this ligand would also have a moderately high trans-effect. The present research shows this to be so, as replacement of the chloride trans to the perfluorovinyl ligand is facile.

A direct metathetical reaction utilizing sodium or silver salts, as first employed by Chatt and Shaw[12], was used to replace chloride with bromide, iodide or nitrate in acetone. Presumably the formation of the acetone insoluble sodium or silver chloride provides the driving force for the substitutions. These simple metathetical reactions did not work for nitrite, azide and cyanide substitution. For these substitutions it was first necessary to remove the chloride, as silver chloride, with silver tetrafluoroborate. The weakly coordinating BF_4^- ligand was then replaced with NO_2^-, CN^- or N_3^-. This method

was first employed by Clark and Ruddick[18].

To prepare species in which anionic chloride was replaced by a neutral ligand the method of Church and Mays[19] was used. This method can be summarized as:

$$\underline{\text{trans}}\text{-}[PtCl(CF{=}CF_2)(PEt_3)_2] + L + NaClO_4 \xrightarrow{\text{acetone}} \underline{\text{trans}}\text{-}[Pt(CF{=}CF_2)L(PEt_3)_2][ClO_4] + NaCl$$

Once again the driving force of the reaction is presumably the formation of sodium chloride, with its low solubility in acetone. In the case where L = CO the best yields were obtained employing silver perchlorate rather than sodium perchlorate, as silver chloride has lower solubility in acetone than does sodium chloride.

Product identification was through a variety of techniques. In accordance with standard practice in the literature analyses were carried out only for carbon, hydrogen and nitrogen and platinum was not determined. The infrared spectra were all similar to that of the parent chloride, with the major changes being the disappearance of the band due to the Pt-Cl stretch at 305 cm^{-1} and the appearance of a variety of new bands originating with, and identifiable as due to the replacing ligand. The infrared spectra of $\underline{\text{trans}}$-$[PtCl(CF{=}CF_2)(PEt_3)_2]$ and $\underline{\text{trans}}$-$[Pt(CF{=}CF_2)(C_5H_5N)(PEt_3)_2][ClO_4]$ are reproduced in Appendix I as being representative of the infrared spectra obtained.

The stereochemistry of the perfluorovinyl species was established by the method of Jenkins and Shaw[20]. When the couplings $J_{PP'}$ are much larger than J_{PH} for phosphines $\underline{\text{trans}}$ to one another,

the proton magnetic resonance spectrum shows couplings of magnitude

$$J_{PH} = \tfrac{1}{2}\left[(J_{PH(true)} + J_{P'H(true)}\right]$$

This phenomenon is termed virtual coupling. When the phosphines are cis to one another the organic group will couple only to the phosphorus atom of its own phosphine group.

Clark and Tsang[21] have shown for complexes in which triethyl phosphine ligands are trans to one another the methyl proton resonance consists of a 1:4:6:4:1 quintet. This pattern arises from the coupling of the methyl protons with the methylene protons to give a triplet, followed by coupling of the methyl protons with each phosphorus atom in turn. All the complexes prepared for this study showed the 1:4:6:4:1 methyl proton resonance expected for trans isomers.

The splitting pattern of the methylene proton resonance can be complex. Couplings can occur between these protons and 1) the methyl protons, 2) the phosphorus nuclei and 3) the platinum nucleus. As mentioned in Section 2.2. the pattern observed usually took the form of a septet which was well resolved in some instances and poorly in others.

The proton magnetic resonance spectra of trans-$[PtCl(CF{=}CF_2)(PEt_3)_2]$ and trans-$[Pt(CF{=}CF_2)(C_5H_5N)(PEt_3)_2][ClO_4]$ are reproduced in Appendix I. These spectra are representative of all the proton n.m.r. spectra.

3.2. The Trans-influence

The trans-influence of a given ligand in a series of complexes can be determined by any or all of the three methods mentioned in 1.2.2. above. No attempt was made to determine the crystal structures of any of the complexes, but attempts were made to construct trans-influence series by means of both vibrational and nuclear magnetic resonance spectroscopies.

3.2.1. Vibrational Spectra and the Trans-influence

In compounds of the type trans-$[PtL(CF{=}CF_2)(PEt_3)_2]$ there are two possible vibrational indicators of the trans-influence. The first of these is the platinum-carbon stretching frequency and the second is the carbon-carbon double bond stretching frequency.

On the basis of the harmonic oscillator approach the platinum-carbon stretching frequency should decrease as the trans-influence of L increases. The observed platinum-carbon stretching bands were quite weak as can be seen from the spectra in Appendix 1; for trans-$[Pt(CF{=}CF_2)(PEt_3)_3][ClO_4]$ the μ_{Pt-C} band was not observed.

Table IV shows the measured value of μ_{Pt-C} compared with those from the literature for trans-$[PtX(CH_3)(PEt_3)_2]$[23].

The general features of the two series are similar. The positions of NO_2^- and CN^- in both series can be considered suspect due to the possibility of vibrational coupling of the Pt-C stretch with the $Pt-NO_2^-$ and $Pt-CN^-$ stretches, which are nearby in frequency, as indicated

TABLE IV

Observed		Literature	
X	ν_{Pt-C} (cm^{-1})	X	ν_{Pt-C} (cm^{-1})
NO_2^-	527	CN^-	516
I^-	538	I^-	540
ONO_2^-	543	NO_2^-	544
Br^-	544	Br^-	548
N_3^-	544	Cl^-	551
Cl^-	546	ONO_2^-	566
CN^-	551		

in Section 1.2.2.2.

Literature data on ν_{Pt-C} for compounds of the type trans-$[Pt(CH_3)L(PEt_3)_2][ClO_4]$ is scanty; data for complexes of the type trans-$[Pt(CH_3)L(PMe_2Ph)_2][ClO_4]$ is shown in Table V[3], along with the ν_{Pt-C} frequencies observed in this work.

TABLE V

Observed		Literature	
L	ν_{Pt-C} (cm^{-1})	L	ν_{Pt-C} (cm^{-1})
PPh_3	535	PPh_3	528
CO	545	CO	545
C_5H_5N	545	C_5H_5N	555
$P(OMe)_3$	555		
$P(OEt)_3$	568		
$P(OPh)_3$	570		

The trans-influence series observed from vibrational data is again similar to that expected from the literature. However, it must be stated that it is naive to consider the harmonic oscillator approach to be completely valid since each of the two parts of the molecule bound by the Pt-C bond are complex and probably do not act as hard spheres connected by a spring.

There has been some attempt made to correlate internal ligand vibrations of such species as C≡O or C≡N, bonded to platinum, with the trans-influence series[3]. It has not as yet proven possible to construct such series for carbonyl compounds due to complexities originating with the synergic bonding system. For platinum-nitrile systems the change in $\nu_{N\equiv C}$ has been interpreted in terms of the change in charge on the platinum[22]. The ν_{C-F} stretch was examined in complexes of the type trans-$[PtL(CF_3)(PMe_2Ph)_2]$ to determine if this frequency could be related to the trans-influence of L[23]. It was found that ν_{C-F} correlated not with the trans-influence of L, but with its mass. The ν_{C-F} absorption was noted at around 1100 cm^{-1}, with total variation over about 45 cm^{-1}.

The values of $\nu_{C=C}$ for the perfluorovinyl complexes show a spread of only 13 cm^{-1}. Values are given in Table VI.

These series obviously do not correlate either with the mass of the trans ligand or its trans-influence. Appleton et al[24] have studied complexes of the type trans-$[PtL(C(CF_3)=CHOCH_3)(PMe_2Ph)_2]$. They record the $\nu_{C=C}$ value but do not attempt to correlate it with

TABLE VI

OBSERVED AND LITERATURE VALUES OF $\nu_{C=C}$

X	$\nu_{C=C}(cm^{-1})$	L	$\nu_{C=C}(cm^{-1})$
Cl^-	1729	CO	1730
Br^-	1736	C_5H_5N	1732
I^-	1731	PEt_3	1731
NO_2^-	1735	PPh_3	1731
ONO_2^-	1736	$P(OMe)_3$	1741
CN^-	1728	$P(OEt)_3$	1733
N_3^-	1731	$P(OPh)_3$	1729

either the trans-influence or mass of L, nor are these correlations possible for the values obtained.

3.2.2. Nuclear Magnetic Resonance Spectra and the Trans-influence

In the complexes prepared there are four nuclei capable of giving rise to a nuclear magnetic resonance signal. These nuclei are tabulated in Table VII.

This Table indicates the most suitable nuclei for n.m.r. experiments are ^1H and ^{19}F. The ^1H spectra have been discussed.

Vinyl species 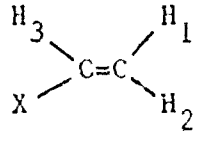 possess ABC spin systems

and their n.m.r. spectra are quite complex. The coupling constants are found to increase in the order $J_{12}(J_{gem}) < J_{13}(J_{cis}) < J_{23}(J_{trans})$

TABLE VII

MAGNETIC NUCLEI IN PERFLUOROVINYLPLATINUM(II) COMPLEXES

Isotope	Natural Abundance (%)	Relative Sensitivity for equal numbers of nuclei at constant field	Spin ($h/2\pi$)	Quadrupole moment (10^{-24} cm^2)
^{1}H	99.99	1.00	½	0
^{19}F	100.00	0.833	½	0
^{31}P	100.00	6.63×10^{-2}	½	0
^{195}Pt	33.8	9.94×10^{-3}	½	0

and both J_{cis} and J_{trans} decrease with increasing electronegativity of X[25]. When X is a magnetic nucleus J_{XH} increases with increasing electronegativity of X and the order J_{XH_3} (J_{gem}) $\approx J_{XH_2}$ (J_{cis}) $< J_{HX_1}$ (J_{trans}) is found. These overall orders of increasing coupling constants were found to hold for <u>trans</u>-$[PtBr(CH{=}CH_2)(PPh_3)_2]$[26].

The approximation is usually made that the coupling between hydrogen nuclei separated by one, two or three bonds is transmitted by the bonding electrons. Therefore, the coupling can be calculated by use of the Fermi contact term alone and through space coupling can be ignored[25]. The coupling constants in alkanes show some dependence on interatomic angles, but this angular dependence would be expected to be unchanged through a series of inyl compounds due to the double bond.

The magnetic resonance spectra of perfluorovinyl compounds are more amenable to interpretation than those of vinyl compounds since the chemical shifts are much larger and the spin systems are thus of the AMX type. The chemical shifts for

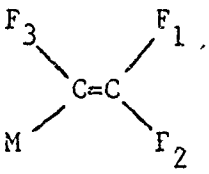

increase in the order $\sigma_{F_1} < \sigma_{F_2} < \sigma_{F_3}$ but there does not appear to be any correlation between the magnitude of the shift and the nature of M. As with vinyl systems the coupling constants are found to increase in the order $J_{12}(J_{gem}) < J_{13}(J_{cis}) < J_{23}(J_{trans})$[27]. However for M = Pt the coupling constants are in the order $J_{Pt-F_1}(J_{trans}) < J_{Pt-F_2}(J_{cis}) < J_{Pt-F_3}(J_{gem})$ which is opposite to the order usually found for vinyl systems. The large value of J_{Pt-F_3} has been explained on the basis of the spatial proximity of the platinum and fluorine nuclei, i.e., the coupling has a large through space component[21].

In the <u>trans</u>-influence literature the magnitude of $^1J_{Pt-A}$ for complexes trans-$[PtLAX_2]$ is related, by the equation given in 1.2.2.3.,

$$J_{Pt-A} \propto \left[\gamma_A \gamma_B S^2_{Pt6s}(0)\, S^2_A(0) \left| \psi_{Pt(6s)}(0) \right|^2 \left| \psi_{A(ns)}(0) \right|^2 {}^3\Delta_E^{-1} \right]$$

to the amount of platinum 6s orbital employed in the Pt-A bond. When couplings over more than one bond are examined another term f(Pt....A) is introduced which is postulated to include all electronic and stereo-

chemical factors influencing the coupling.

Appleton et al[28] have plotted $^2J_{Pt-F}$ for complexes of the type trans-$[PtL(CF_3)\{P(CH_3)_2C_6H_5\}_2]$ versus $^2J_{Pt-H}$ for complexes trans-$[PtL(CH_3)\{P(CH_3)_2C_6H_5\}_2]$. A straight line plot was obtained which passes, within experimental error, through the origin, Figure VI. This plot was interpreted by the authors as indicating that the above equation, based on only the Fermi contact coupling, adequately described the true coupling mechanism. Further work by the same authors[24] on complexes of the form

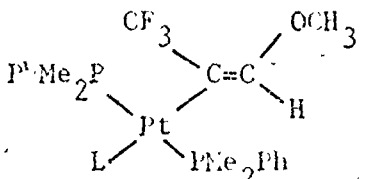

in which $^3J_{Pt-F}$ was plotted against $^3J_{Pt-H}$ again yielded a straight line, Figure VII, however, this plot did not pass through the origin, but intersected the $^3J_{Pt-F}$ axis at about 26 Hz ($^3J_{Pt-F}$ values ranged from 78 to 143 Hz). The authors felt one of the possible explanations for this was a constant through space contribution to both couplings. The existence of a through space coupling mechanism between fluorine atoms has long been accepted in organic chemistry[29].

It is necessary at this point to consider the various theories of the transmission of spin-spin couplings. The equation giving J_{Pt-A} above is a result of theoretical work carried out by Pople et al[30]. This mathematical approach applied time dependent perturbation theory

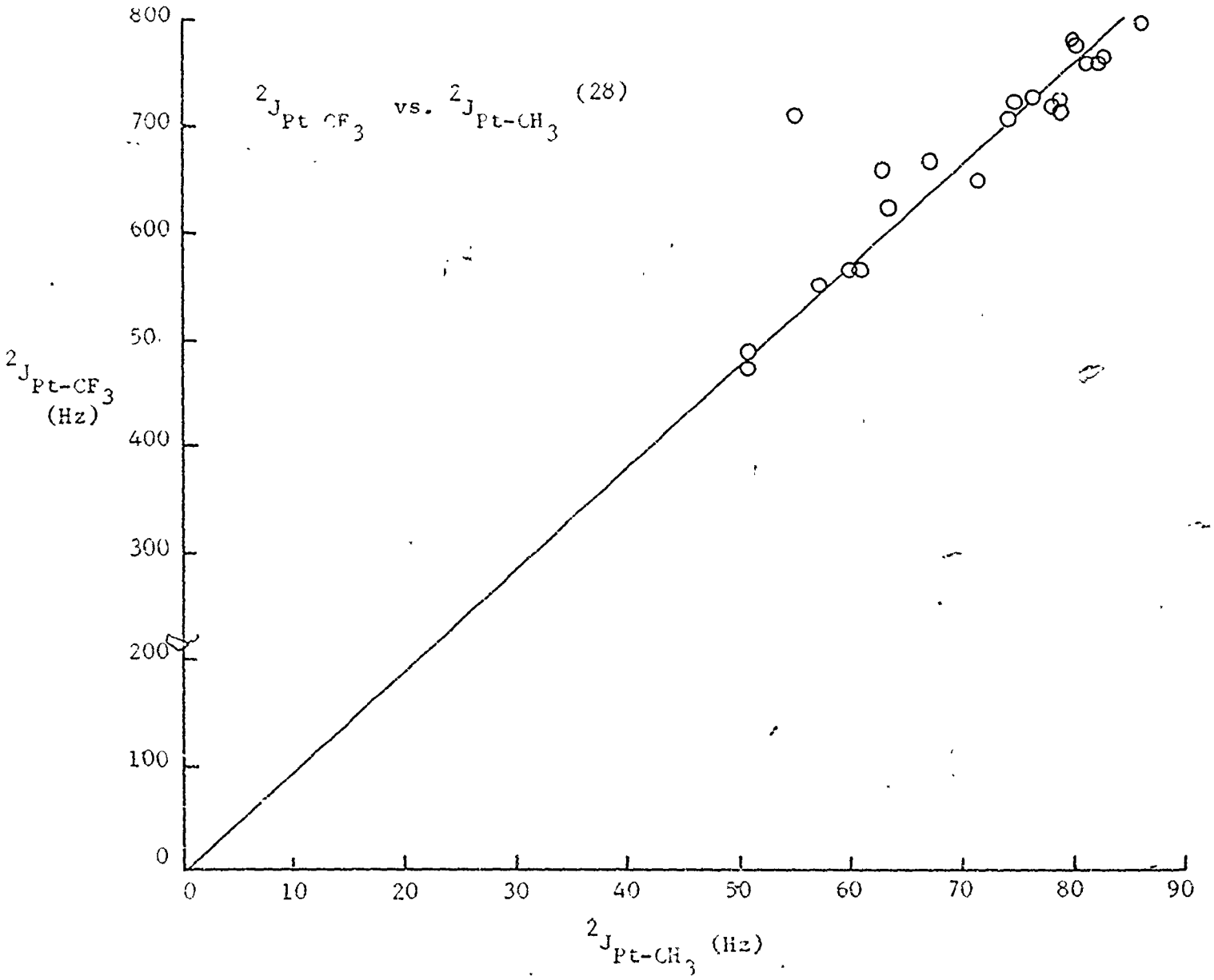
$^2J_{Pt\ CF_3}$ vs. $^2J_{Pt-CH_3}$ (28)
$^2J_{Pt-CF_3}$ (Hz)
800
700
600
50.
400
300
200
100
0
0
10
20
30
40
50
60
70
80
90
$^2J_{Pt-CH_3}$ (Hz)

Figure VI

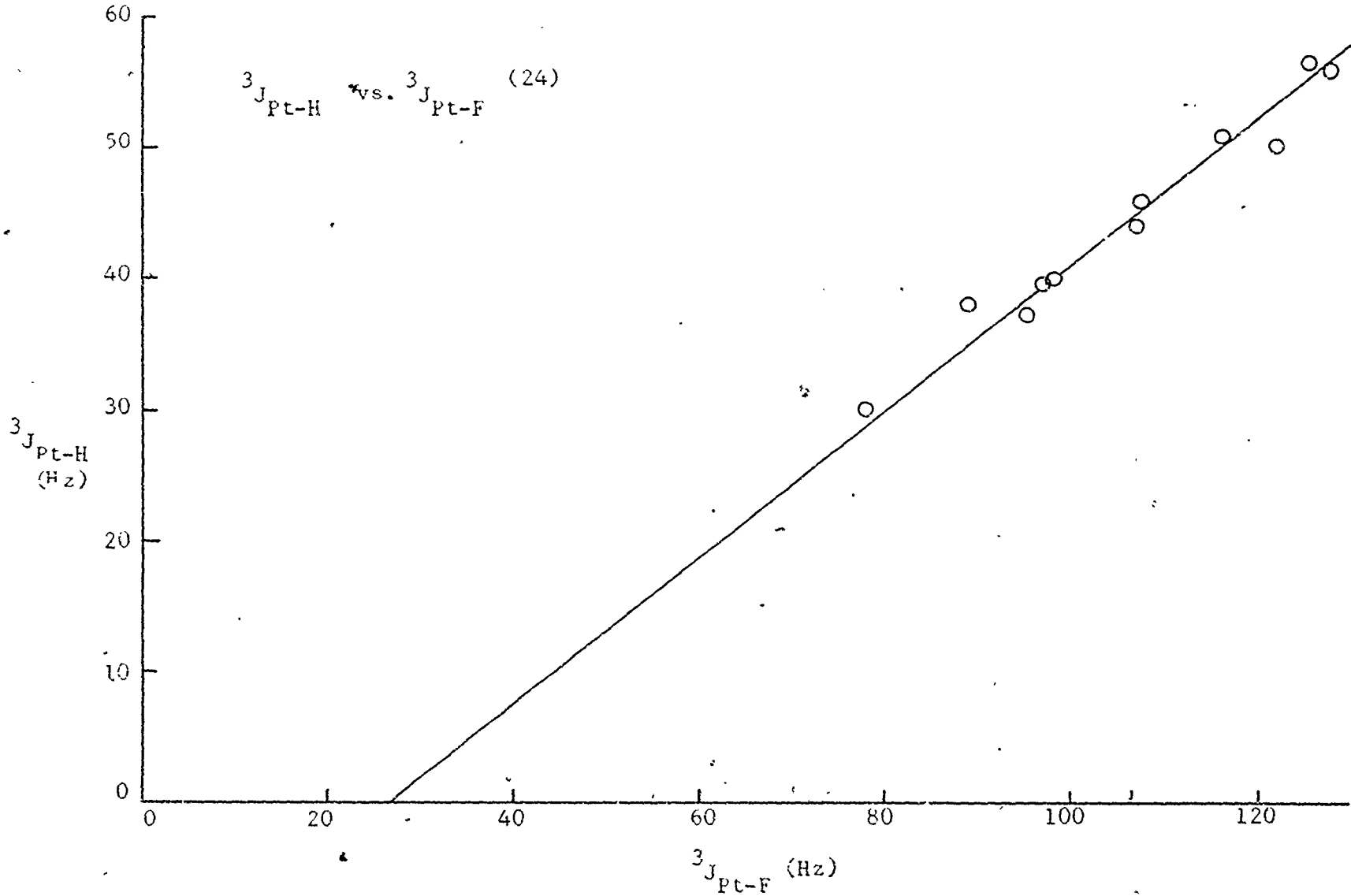
$^3J_{Pt-H}$ vs. $^3J_{Pt-F}$ (24)
$^3J_{Pt-H}$ (Hz)
$^3J_{Pt-F}$ (Hz)
0
10
20
30
40
50
60
0
20
40
60
80
100
120

Figure VII

to the problem and demanded a summation over all the excited states of the molecule. To avoid this difficulty the approximation was made that only triplet states were important and that, further, only a mean singlet-triplet excitation energy need be considered. However, Hinchliffe and Cook[31] have pointed out that the form of the triplet function employed has a marked effect on the computed value of the coupling constant, and they felt that the use of a minimal basis set of atomic orbitals in the calculation was not a reliable process.

Another objection to this theory deals with the fact that the theory assumes that the unperturbed wavefunction for a molecule is an eigenfunction of the molecular Hamiltonian, but the self-consistent wave functions employed in the calculations are actually eigenfunctions of the two electron Hartree-Fock Hamiltonians.

A later theory was developed by Pople et al.[32] to circumvent the difficulties inherent in the use of time dependent perturbation theory. Unfortunately the results of this second theory are not as easily visualized as are those of the first. The later theory examines changes brought about by the perturbing influence of a magnetic nucleus on the wave function for a molecule and is therefore a first order perturbation theory.

The contact contribution to the coupling can be written as

$$J_{AB} \propto \left[S_A^2(0) S_B^2(0) \left[\frac{\partial}{\partial hB} \rho^{spin}_{S_A S_A}(hB) \right]_{hB=0} \right] \qquad (1.13)$$

where $S_A(0)$ and $S_B(0)$ are the valence shell electron densities at

nuclei A and B. Changes in J_{AB} from compound to compound are thought to arise from changes in the valence shell electron spin density at nucleus A under the influence of a perturbing nucleus B. The effect of nucleus B is to modify, or perturb, the wave function for the molecule. This, in turn, modifies the spin density matrix, the diagonal of which is given by $\rho_{S_A S_A}$ [33].

The above two theories have been applied exclusively to Fermi contact contributions to the coupling constants. Blizzard and Santry[34] have developed a theory in which orbital and dipole-dipole, i.e., through space contributions are also considered. Their theory is based on Pople's first order perturbation theory and the overall coupling constant is given by

$$J_{AB} = a_{AB}J_c + b_{AB}(J_o + J_d) \qquad (1.14)$$

where J_c is the Fermi contact contribution and J_o and J_d the orbital and dipole-dipole contributions respectively. a_{AB} is given by $a_{AB} = S_A^2(0)S_B^2(0)$ and b_{AB} is given by $b_{AB} = \left\langle r^{-3} \right\rangle_A \left\langle r^{-3} \right\rangle_B$ where r is the position vector of a valence shell p electron centered on either A or B, and $S_A^2(0)$, $S_B^2(0)$ have the meanings given above.

In Blizzard and Santry's theory changes in the J_c term from molecule to molecule arise from changes in the bond order matrix corresponding to the valence s orbital on A under the perturbing influence of nucleus B on the molecular wave function. In a similar fashion changes occurring in the bond order matrix representing the orbital part of the three nonbonding valence shell p orbitals cause

changes in J_o while changes in the spin part of the bond order matrix for these same orbitals cause changes in J_d. J_c is isotropic while J_o and J_d are anisotropic. Unfortunately this theory is difficult to relate to easily visualized changes at a platinum nucleus when considering the n.m.r. trans-influence, eg., the dipole-dipole expression contains an imaginary bond order term.

In the theories considered the $S_A^2(0)$, $S_B^2(0)$ and $\langle r^{-3} \rangle$ terms are determined by the application of a least squares fit of theoretical values to experimental data.

The contact terms of the various theories can explain the coupling between a given nucleus and hydrogen with a reasonable degree of accuracy in most cases. The orbital and dipole-dipole terms are not required. This is not surprising since hydrogen has no p electrons through which these couplings can be transmitted, unless the coefficients of the 2p atomic orbitals for hydrogen in the overall wave function are large. When couplings between heavier nuclei, such as carbon-carbon, carbon-fluorine or fluorine-fluorine are considered the inclusion of terms involving orbital and dipole-dipole coupling give results which are closer to the experimental values than do calculations based on Fermi contact coupling alone.

Blizzard and Santry believe that in the case of fluorine-fluorine couplings the through space contributions can be larger than the contact contribution. Therefore in systems involving coupling between platinum and fluorine the coupling may have a significant

through space component, but it is unlikely that the through space component is of any magnitude for platinum-hydrogen couplings.

When $^{2}J_{Pt-H}$ for trans-$[PtL(CH_3)(PEt_3)_2]$ [35] is plotted against $^{1}J_{Pt-H}$ for trans-$[PtHL(PEt_3)_2]$ [36] a straight line plot which passes through the origin would be expected, since only Fermi contact coupling is possible. In fact when the values are plotted, Figure VIII, a straight line plot is obtained, but the plot intersects the $^{2}J_{Pt-H}$ axis at about 25 Hz. ($^{2}J_{Pt-H}$ ranges from 60.2 to 86.0 Hz). When this observation is coupled with that embodied in Figure VI with its interpretation the conclusion can be drawn that it is difficult, at this time, to closely relate n.m.r. trans-influence couplings to a theoretical base. Both contact and through space couplings seem to play some role.

The experimental observation is that when J_{Pt-A} for complexes trans-$[PtLAX_2]$ is plotted against J_{Pt-B} for complexes trans-$[PtLBX_2]$ a straight line plot is usually obtained. The X ligands are normally tertiary phosphines and their exact identity does not change the value of J_{Pt-A} significantly. The existence of the various plots for a) couplings over one and two bonds ($^{1}J_{Pt-H}$ versus $^{2}J_{Pt-CH_3}$); b) one and three bonds[24] ($^{1}J_{Pt-H}$ versus $^{3}J_{Pt-C=CH}$) and c) differing species[24, 26] ($^{1}J_{Pt-H}$ versus $^{2}J_{Pt-CF_3}$; $^{1}J_{Pt-H}$ versus $^{3}J_{Pt-C-CF_3}$; $^{3}J_{Pt-C-CF_3}$ versus $^{3}J_{Pt-C=CH}$) indicates that changing the trans ligand L exerts some influence at the platinum nucleus which changes the contact and through space components of the coupling in some proportional fashion,

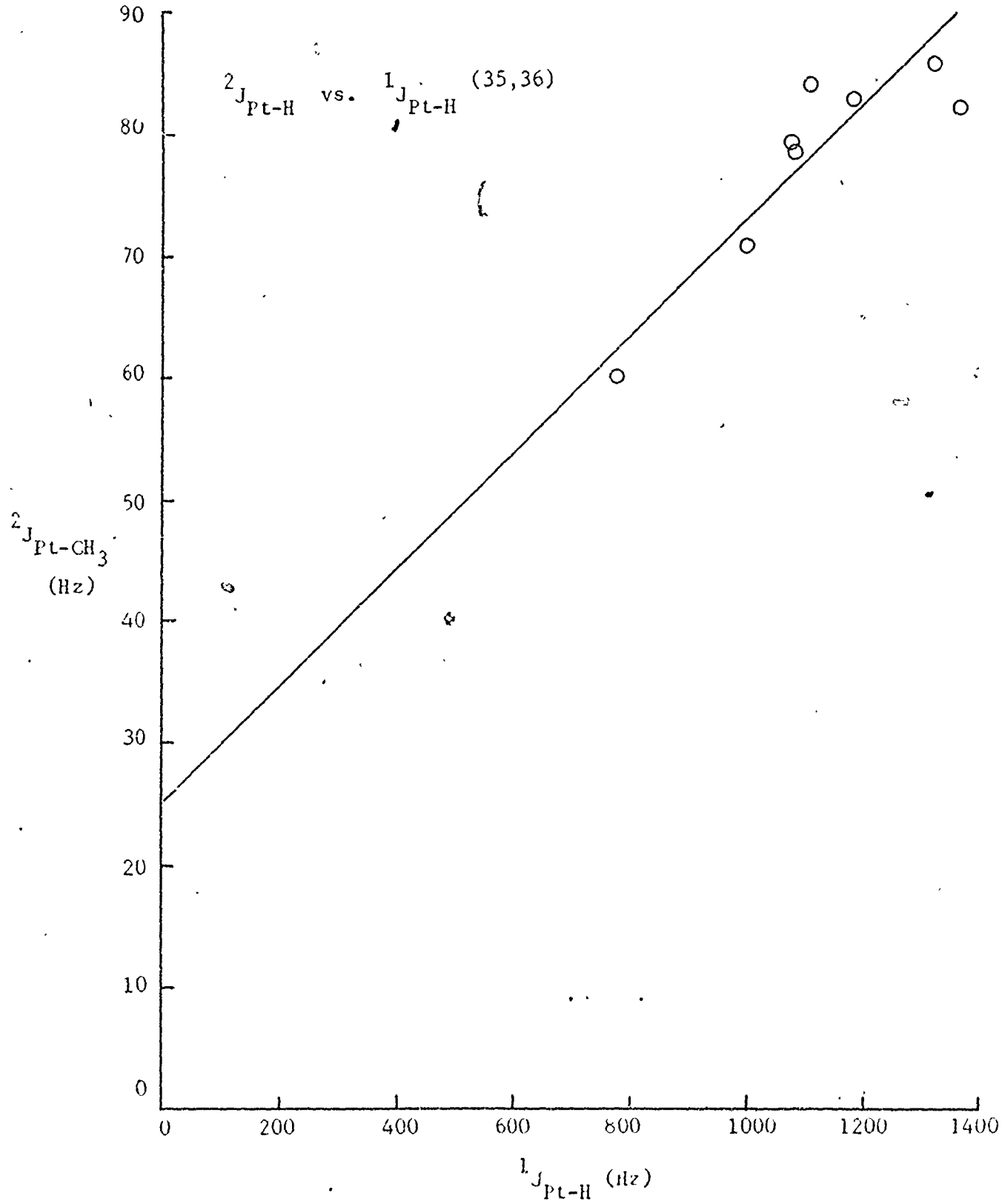
$^2J_{Pt-H}$ vs. $^1J_{Pt-H}$ (35,36)
$^2J_{Pt-CH_3}$ (Hz)
90
80
70
60
50
40
30
20
10
0
0
200
400
600
800
1000
1200
1400
$^1J_{Pt-H}$ (Hz)

Figure VIII

but theory and experiment do not yet allow an exact discussion of the phenomenon.

The work carried out by Appleton et al[24] is interesting in that it allows a comparison of $^3J_{Pt-F}$ and $^3J_{Pt-H}$ values in the same complex. Presumably a through space component would be expected for the former and none for the latter. The fact that a linear plot is obtained indicates either that the contact and through space terms are changing in some proportional fashion or that the through space term is very small.

With the present work there are three couplings which could give an indication of the trans-influence, $^2J_{Pt-F_3}$, $^3J_{Pt-F_1}$ and $^3J_{Pt-F_2}$. Examples of typical fluorine magnetic resonance spectra are given for trans-$[PtCl(CF{=}CF_2)(PEt_3)_2]$ and trans-$[Pt(CF{=}CF_2)(PEt_3)_2(PPh_3)][ClO_4]$ in Appendix 1. A plot of $^2J_{Pt-F_3}$ obtained in this work against $^2J_{Pt-F}$ for complexes trans-$[PtL(CF_3)\{P(CH_3)_2Ph\}_2]$ yields a linear plot, Figure IXa, as does a plot of $^2J_{Pt-F_3}$ against $^2J_{Pt-H}$ from trans-$[PtL(CH_3)(PEt_3)_2]$, Figure IXb. However the plots of $^3J_{Pt-F_1}$ and $^3J_{Pt-F_3}$ show a large amount of scatter, Figure X.

This is a different situation than that observed by Appleton et al, Figure VII. The question arises; why does $^2J_{Pt-F_3}$ show a linear plot against $^2J_{Pt-CH_3}$ while the plots of $^3J_{Pt-F_1}$ and $^3J_{Pt-F_2}$ are not linear with respect to $^2J_{Pt-F_3}$? The probable answer lies in the anisotropy of the through space coupling.

The Fermi contact term drops sharply with an increasing

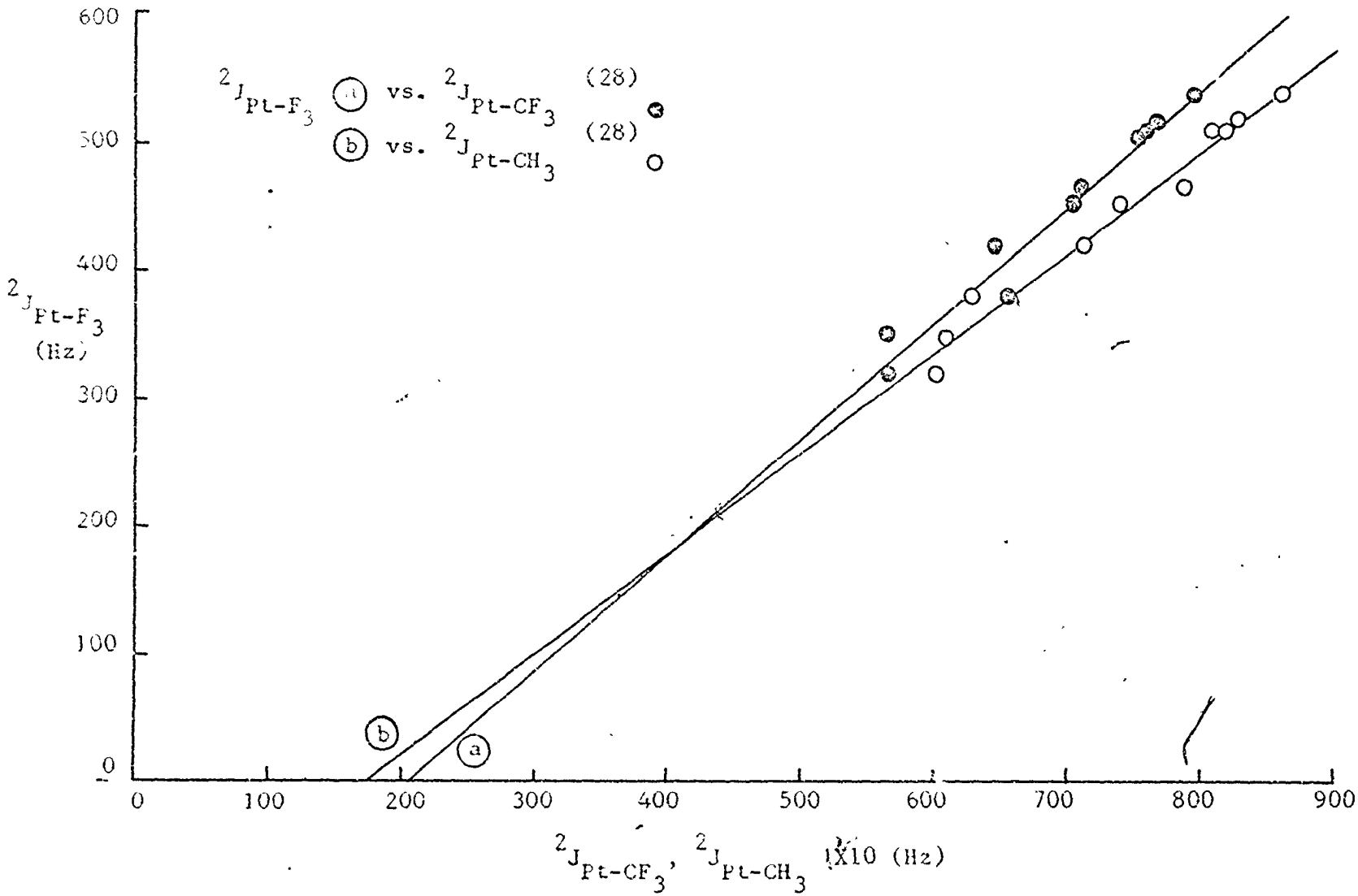
$^2J_{Pt-F_3}$ (a) vs. $^2J_{Pt-CF_3}$ (28)
(b) vs. $^2J_{Pt-CH_3}$ (28)
$^2J_{Pt-F_3}$ (Hz)
600
500
400
300
200
100
0
0
100
200
300
400
500
600
700
800
900
$^2J_{Pt-CF_3}$, $^2J_{Pt-CH_3}$ (X10 (Hz)
b
a

Figure IX

number of bonds between coupled nuclei, e.g., $^{1}J_{Pt-H}$ varies from 778 to 1369 Hz[36] while $^{2}J_{Pt-H}$ varies from 51 to 88 Hz[35]. With the perfluorovinyl compounds $^{2}J_{Pt-F_3}$ varies from 282 to 538 Hz while $^{3}J_{Pt-F_2}$ varies from 30.8 to 61.3 Hz. Assuming the plane of the perfluorovinyl group to be normal to the platinum square plane the distance from F_2 to platinum is 3.04 Å, while the distance from F_3 to platinum is about 2.92 Å. The through space couplings would be of roughly the same order of magnitude and $^{2}J_{Pt-F_3}$ would therefore appear to be dominated by the contact term.

The distance from platinum to F_1 is calculated at about 4.16 Å. Since the through space couplings decrease with distance[29], this contribution to $^{3}J_{Pt-F_1}$ should be smaller than that to $^{3}J_{Pt-F_2}$. From Tables II and III it can be seen that in all cases except those for CN^- and CO, where synergic bonding may be important, $^{3}J_{Pt-F_2}$ is larger than $^{3}J_{Pt-F_1}$. Since with vinyl systems $J_{MH(trans)}$ is usually greater than $J_{MH(cis)}$, and the opposite order is found here, the magnitude of the through space coupling can be estimated at roughly 5 to 25 Hz at a distance of about 3 Å.

Also, since through space coupling is anisotropic, its magnitude depends in part on the orientation of the perfluorovinyl plane with respect to the platinum square plane. The value of the coupling constant thus depends not only on the nature of the trans ligand but also on the angle between the two planes. Changes in this angle when the trans ligand was changed would cause variations in the coupling con-

stant which were unrelated to the trans-influence of the substituted ligand.

Changes in this angle would be of greatest importance in the case of $^{3}J_{Pt-F_2}$, since $^{2}J_{Pt-F_3}$ is dominated by the contact term, and the through space coupling to $^{3}J_{Pt-F_1}$ is probably small. Changes in angle would not influence $^{3}J_{Pt-F_3}$ by more than 5 or 10 Hz, i.e., a few percent and a straight line plot with respect to other n.m.r. trans-influence series would be expected and is found, Figure X. Changes of 5 to 10 Hz in $^{3}J_{Pt-F_2}$ could easily result in the observed scatter from a straight line plot of $^{3}J_{Pt-F_2}$ against $^{2}J_{Pt-F_3}$ as shown in Figure X. For $^{3}J_{Pt-F_1}$ against $^{2}J_{Pt-F_3}$, also Figure X, two linear plots are obtained, one for species trans-$[Pt(C_2F_3)L(PEt_3)_2][ClO_4]$ where L is a neutral ligand and another for trans-$[PtX(C_2F_3)(PEt_3)_2]$ where X is an anionic ligand. Pyridine and cyanide are the only ligands which lie off these plots. Appleton et al[28] have chosen to plot their data for trifluoromethylplatinum complexes in a similar fashion, but there has not as yet been any significant data gathered to indicate that anionic ligands should give rise to different plots of trans-influence series than those obtained for neutral ligands.

With the complexes trans-$[PtL\{C(CF_3)-CHOCH_3\}(PMe_2Ph)_2]$ prepared by Appleton et al[24] a straight line plot of $^{3}J_{Pt-F}$ against $^{3}J_{Pt-H}$ was obtained, Figure VII. This indicates that there is no orientation effect associated with the platinum-fluorine coupling. There are two possible reasons for this. First, the fluorine atoms

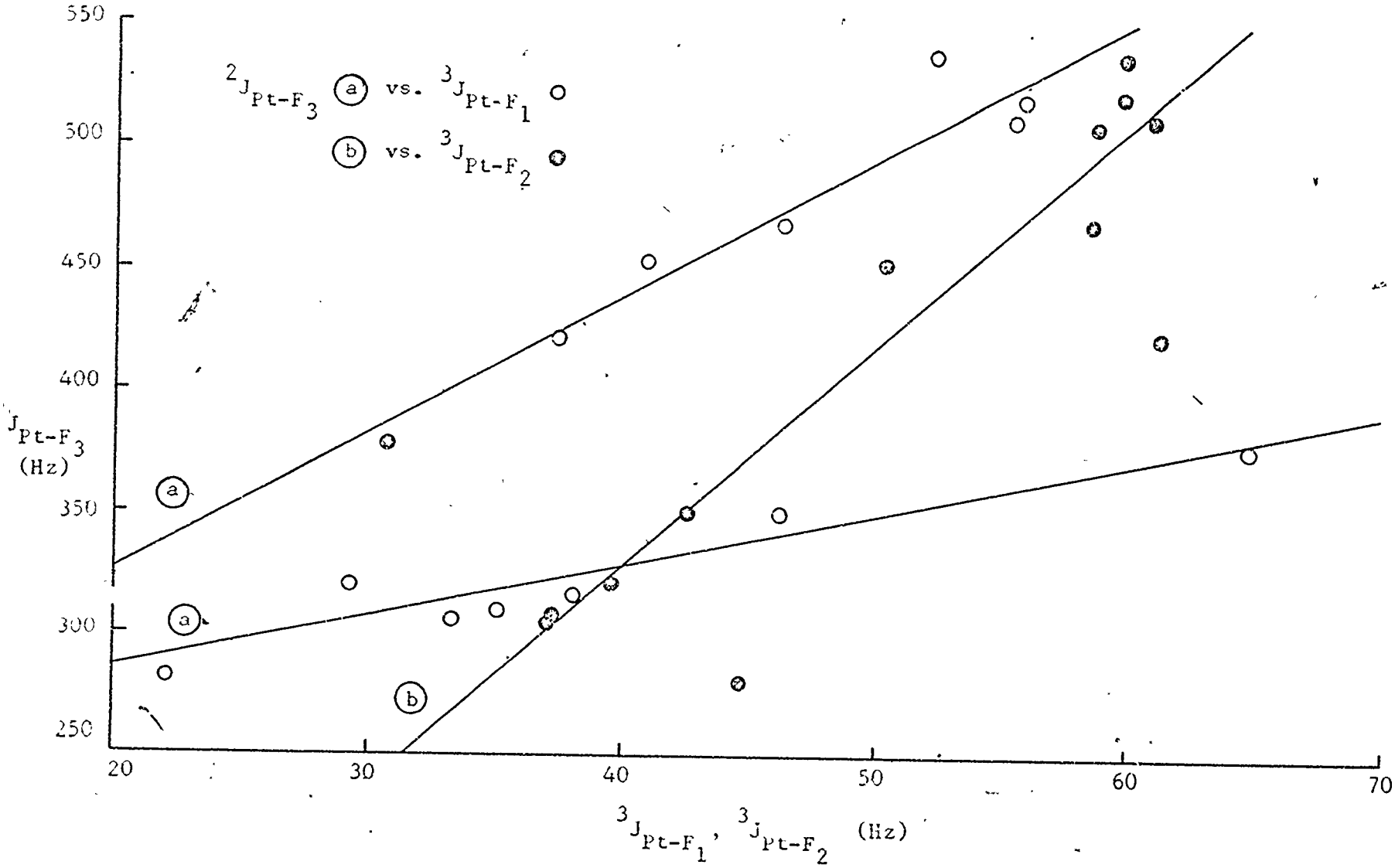
550
500
450
400
350
300
250
$^2J_{Pt-F_3}$ (a) vs. $^3J_{Pt-F_1}$
(b) vs. $^3J_{Pt-F_2}$
J_{Pt-F_3} (Hz)
20
30
40
50
60
70
$^3J_{Pt-F_1}$, $^3J_{Pt-F_2}$ (Hz)

Figure X

on the free rotating CF_3 group are an average of 3.45 Å from platinum, assuming the vinyl plane to be perpendicular to the platinum square plane. Therefore, the through space coupling would, in all probability, be small and slight variations to this component would not change the overall coupling significantly. Second, the bulkiness of the phosphine ligands and the $C(CF_3)=CHOCH_3$ indicator ligand tend to hold the indicator ligand in one orientation no matter what the identity of the trans ligand. Molecular models tend to support this contention.

The n.m.r. spectra of the chloro, carbonyl and triethylphosphite complexes were measured at different temperatures to ascertain if the coupling constants were temperature dependent, Table VIII. It was found that the coupling was temperature dependent, but not in a readily discernible pattern. For example the couplings $^3J_{Pt-F_2}$ decreased with decreasing temperature by from 0% for L=CO to 7.8% for L=$(EtO)_3P$. But $^2J_{Pt-F_1}$ increased by 2.7% for X=Cl^- and decreased 3.9% for L=$(EtO)_3P$. Also $^2J_{Pt-F_3}$ increased by 0.8% for X=Cl^- and decreased 3.9% for L=$(EtO)_3P$ as the temperature was decreased. Below about -20 °C viscosity broadening occurred and peak positions could not be obtained to accuracy better than about to 1 cps. It would be advisable to study somewhat less complex systems, e.g., methyl or trifluoroethyl platinum compounds at different temperatures before carrying out further work on this system.

In conclusion, $^2J_{Pt-F_3}$ correlates well with other types of the n.m.r. trans-influence; $^3J_{Pt-F_1}$ and $^3J_{Pt-F_2}$ do not. The reason

TABLE VIII

VARIATION OF COUPLING CONSTANTS WITH TEMPERATURE

Ligand	Temperature (°C)	$^3J_{Pt-F_1}$ (Hz)	$^3J_{Pt-F_2}$ (Hz)	$^2J_{Pt-F_3}$ (Hz)
Cl^-	-40	59.6	64.6	524
	0	-	66.0	-
	35	58.1	66.0	520
CO	25	64.9	31.6	379
	60	66.0	31.6	384
$(EtO)_3P$	-15	34.9	35.0	308
	25	33.6	37.3	309
	60	33.6	37.9	308

for the lack of correlation for this latter pair is thought to arise from a changing through space contribution to the coupling. This contribution probably varies with the trans-influence of the substituting ligand but also depends on the relative orientation of the perfluorovinyl group in the molecule and the distance from the platinum nucleus to each fluorine nucleus.

3.3. Suggestions for Further Work

Couplings of the type $^3J_{Pt-F}$ correlate in a linear fashion with other measures of the trans-influence for complexes trans-$[PtL\{C(CF_3) = CHOCH_3\}(PMe_2Ph)_2]$. For complexes trans-$[PtL(CF=CF_2)(PEt_3)_2]$ this linear correlation is not found. The difference is ascribed to a constant through space contribution to $^3J_{Pt-F}$ for the former and a changing through space contribution to $^3J_{Pt-I}$ for the latter. The constant contribution is felt due to the rigid orientation of the $C(CF_3) = CHOCH_3$ ligand, resulting from both its own bulk and the size of the phosphine ligands. A useful experiment would be to prepare complexes of the form trans-$[PtL\{C(CF_3) = CHOCH_3\}(PMe_3)_2]$, since the smaller trimethylphosphine groups should permit varying orientation of the $C(CF_3) = CHOCH_3$ group, hence a varying contribution to the through space contribution to $^3J_{Pt-F}$. Further, complexes of the form trans-$[PtL(CF=CF_2)(PMe_2Ph)_2]_2$ could also be prepared, and may well yield $^3J_{Pt-I}$ values which correlate in a linear fashion with other measures of the trans-influence, since the perfluorovinyl ligand would be restrained into one orientation, with respect to the platinum square plane by the bulky phosphine ligands.

CHAPTER IV

INTRODUCTION

Bridge Substitution in Pentaborane(9)

The Crystal Structure of Bis(diethylamino)dithiaboretane

4.1. General

Boron is typical of first row elements in that it displays some properties in common with the heavier elements of its group and differs in others. For example, the trihalides of boron and aluminum both function as Lewis acids and borate esters are physically similar to alkoxides. However the trivalent halides of aluminum, gallium and indium are associated whereas the boron halides are monomers. Boron trihalides hydrolyze more readily than do aluminum halides. Boric acid ($B(OH)_3$) is acidic while $Al(OH)_3$ is amphoteric. Boron has an extensive hydride chemistry while the hydride chemistries of other group IIIA elements are limited. The boranes are volatile and flammable whereas the lone binary hydride of aluminum is a polymeric solid.(37)

Boron, a metalloid, has a high melting point (2000 °C), behaves as a semiconductor and acts chemically as a nonmetal. The higher group IIIA elements are conductors, have relatively low melting points and act chemically as metals. Boron shows more similarities with silicon than with aluminum in the behaviour of its hydrides, acids, oxides and on the hydrolysis of its halides.(1)

4.2. Nomenclature

Knowledge in boron chemistry increased rapidly in the 1950's as a result of the search for high energy fuels. In response to the expansion of this field, the American Chemical Society, in 1968, pub-

lished a systematized nomenclature for boron compounds.[38] Those rules which are pertinent to this work are summarized below:

(1) The presence of boron and hydrogen in a compound is indicated by the term "borane".

(2) The number of hydrogen atoms in a molecule is designated by either a numeral in parentheses after the name or a numeral followed by H. The former convention is employed in this work.

Examples

(a) B_2H_6 is diborane(6)

(b) B_5H_9 is pentaborane(9)

(c) $B_{10}H_{14}$ is decaborane(14)

(3) Names are based solely on molecular topology, not on structure. It is therefore necessary to employ diagrams to impart structural information.

(4) Substituents are named in the normal way, i.e., $(CH_3)_2B_2H_4$ is 1,1- or 1,2- dimethyldiborane(6), $B(C_2H_5)_3$ is triethylborane.

(5) Boron atoms are numbered for purposes of identifying the position of substitution. The molecule is viewed as a plane projection from the direction of the open part of the molecular framework. Interior atoms are numbered before exterior and numbering is in a clockwise manner, beginning at the 12 o'clock position. In projection drawings of the

boranes, the bonding is indicated in conventional fashion, i.e., straight lines to represent binuclear sigma bonds. A BHB bridge bond is drawn as 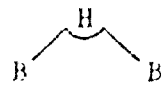 and a BBB three-center bond as either  or 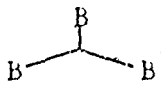 . For higher boranes the localized three-center BEB bond is not always adequate to describe the bonding, as will be shown below (Section 4.5.3.).

Examples:

(a) Pentaborane(9)

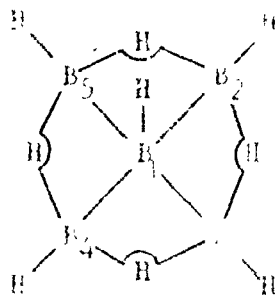

Figure XIa

(b) cis-1,2-dimethyldiborane(6)

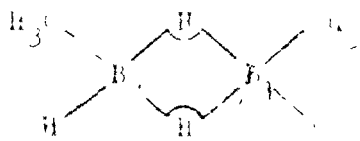

Figure XIb

(c) Bridged substituents are indicated by the symbol μ-. Example: μ-methylpentaborane(9)

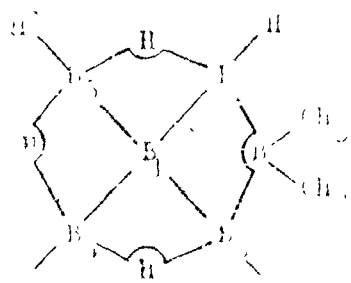

Example XII

(7) Some ring compounds containing boron and an atom from groups V or VI, in alternating fashion, are particularly stable. Trivial names have been widely used for these compounds and are accepted by the American Chemical Society. Examples:

(a) Borazine

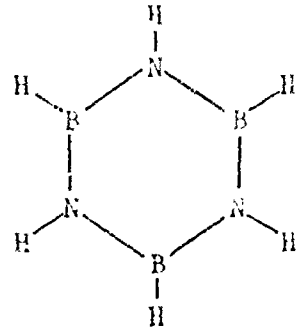

Figure XIIIa

(b) Borthi n

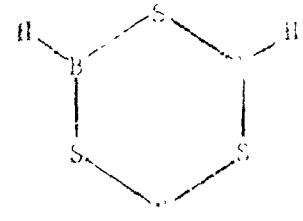

Figure XIIIb

(c) Dithiaboretane

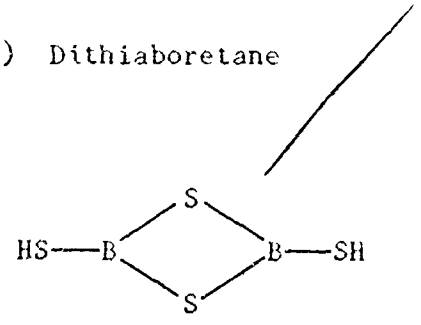

Figure XIIIc

4.3. The Boranes

4.3.1. Historical

The existence of the boranes was recognized by Sir Humphrey Davy (1778-1824). Almost one hundred years ago Jones prepared a volatile boron hydride by the action of hydrochloric acid on magnesium boride, Mg_3B_2[39]. No conclusive work was carried out until 1912 when Alfred Stock developed the techniques required to handle these volatile and pyrophoric materials.

Stock and his collaborators, in a brilliant series of investigations, synthesized and characterized B_2H_6, B_4H_{10}, B_5H_9, B_5H_{11}, B_6H_{10} and $B_{10}H_{14}$[40]. However, Stock did not have available to him the experimental and theoretical tools required to study the structures and bonding of the boranes. These tools were developed and employed after the Second World War.

A major part of the research into the structures and bonding of the boranes was conducted by W.N. Lipscomb and his collaborators[41].

The study of the syntheses, structures and bonding in the boranes remains one of the most interesting in chemistry.

4.3.2. The Structures of the Boranes

For those boron hydrides whose structures have been determined, the boron skeleton can usually be described as a fragment of an icosahedron with its edges 'sewn up' by bridging hydrogen atoms. An icosahedron (Figure XIV) is one of the most regular figures in nature. It has twenty equilateral triangles as faces, thirty edges and twelve vertices. The following boranes can be thought of as derived from one or more icosahedra: B_2H_6 (Figure XVa), B_4H_{10} (Figure XVb), B_6H_{10} (Figure XVc), B_8H_{12}, $B_{10}H_{14}$ (Figure XVd), $B_{18}H_{22}$ and $B_{20}H_{16}$.

There are some important boranes whose structures cannot be represented as icosahedral fragments. Pentaborane(9) has a square pyramidal boron skeleton (Figure XVi) and the borane anion $B_{10}H_{10}^{2-}$ has a bicapped square antiprismatic framework. The framework of decaborane(16) can be described as two pentaborane(9) molecules fused at the two apex positions.

The structures of many borane related species have also been determined and here again the icosahedrally related skeletal structures seem favored. The extensive group of carboranes (compounds with both boron and carbon atoms in skeletal positions) based on the $B_{12}H_{12}^{2-}$ anion all have icosahedrally related frameworks[37]. However, the lower molecular weight carboranes appear to favor the symmetries

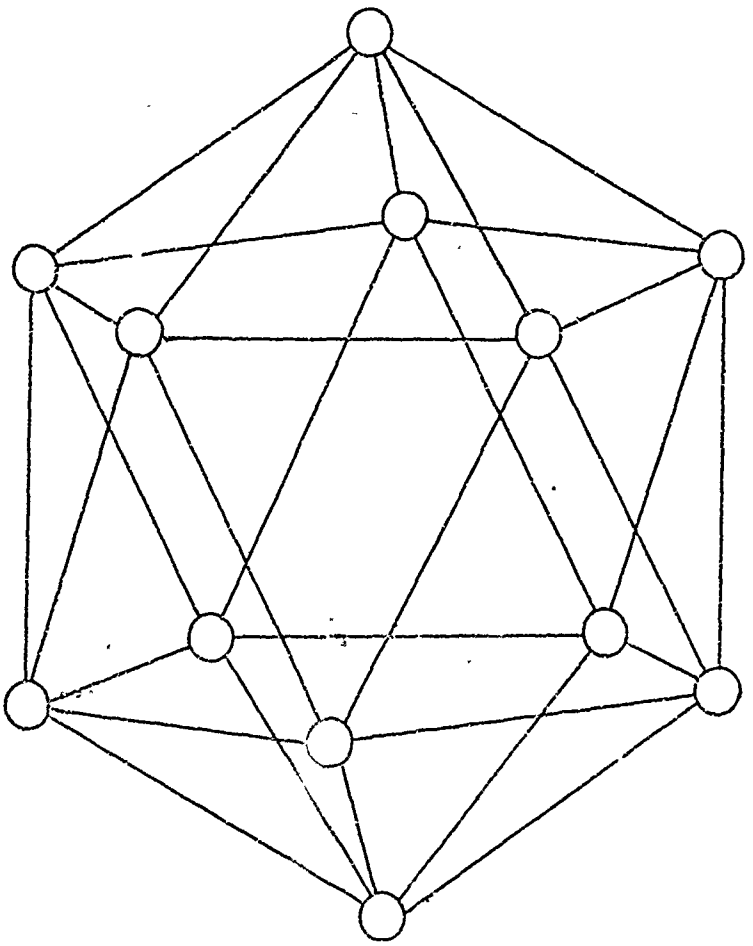

Figure XIV

An Icosahedron

commonly found in inorganic chemistry, i.e., the five atom skeleton of 1,6-$C_2B_3H_5$ is a trigonal bipyramid and the six membered framework of 1,6-$C_2B_4H_6$ is an octahedron.

4.3.3. Bonding in the Boranes

4.3.3.1. General

As soon as sufficient structural data [illegible] it became apparent that [illegible]

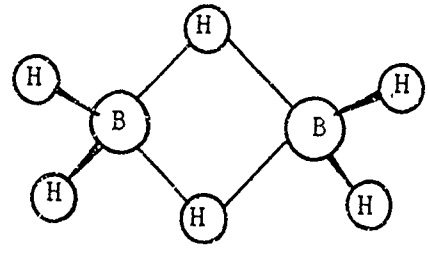

Figure XVa

Diborane(6)

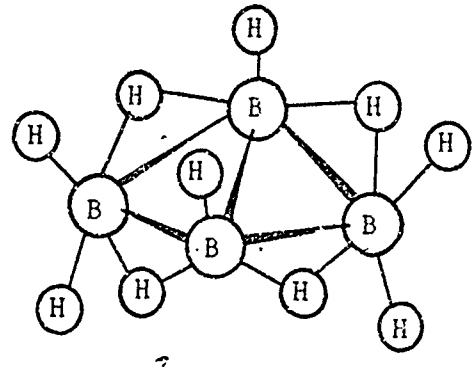

Figure XVb

Tetraborane(10)

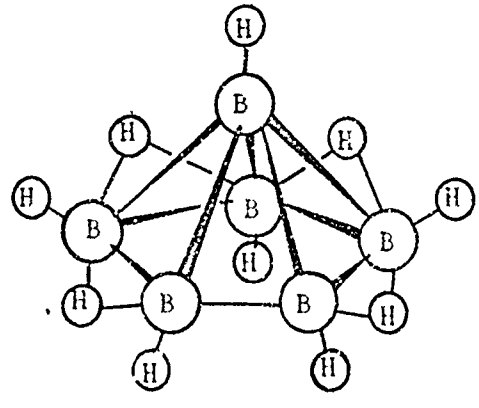

Figure XV

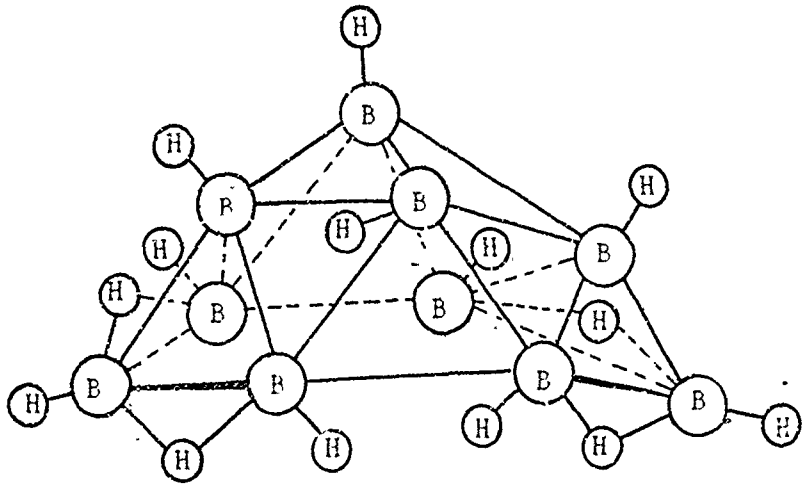

Figure XVd

Decaborane(14)

that were different than the 'normal' two-center, two-electron bond. The valence configuration of group IIIA is ns^2, np^1. Although this configuration indicates boron might be univalent, it is either tri- or tetravalent under normal laboratory conditions. As a trivalent element, boron has a vacant low energy orbital. The large number of

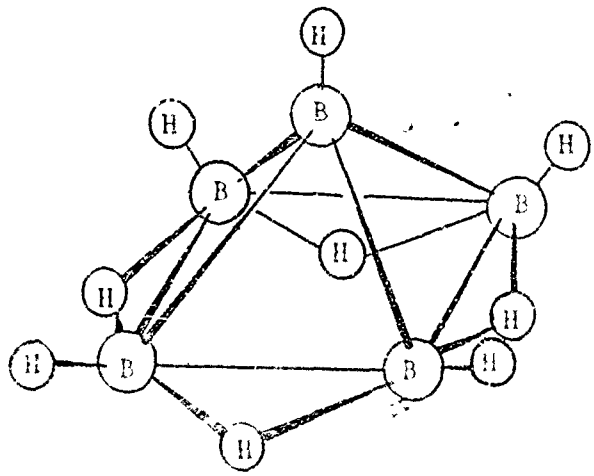

Figure XVI

Pentaborane(9)

compounds in which boron is tetravalent indicates this low energy orbital readily takes part in bonding. There are two possible ways in which boron and other group IIIA elements can form the fourth bond to another atom.

The first involves coordinate covalent bond formation. For example in the boron trifluoride etherate molecule, a lone pair of electrons on the oxygen atom of the ether is donated to the vacant boron orbital. Similarly aluminum trichloride dimerizes when an electron pair on a chlorine atom is donated to a vacant orbital on an aluminum atom. The strength of the coordinate bond is influenced

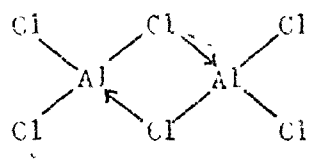

Figure XVII

Aluminum trichloride dimer

by the lewis acidity of the group IIIA atom and the Lewis basicity of the donor atom, (Section 4.4.1. below).

There are cases in which the formation of a coordinate bond can not be used to explain the bonding in electron deficient species, e.g., the dimerization of borane to form diborane or trimethylaluminum to form $[(CH_3)_3Al]_2$. Neither the hydrogen atoms of borane nor the carbon atoms of trimethylaluminum have a lone pair to donate to the vacant orbitals of the group IIIA atoms. In cases such as these the bonding is interpreted in terms of a three-center bond.

4.3.3.2. The Three-Center Bond

The description of the three-center bond involves the linear combination of an atomic orbital on each of three adjacent atoms. Of the three molecular orbitals formed one, symbolized E_+, is bonding, while the remaining two, Eo and E-, are usually antibonding but can become nonbonding in the limiting case of the two-center bond, Figure XVIII[41]. The hybridization of the orbitals used in forming the three-center bond is determined by the immediate environment of the atom providing the orbital.

If the three centers are labelled A, B, and C the following terms can be employed.

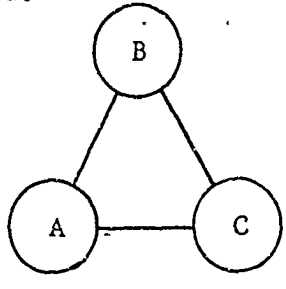

The exchange integrals, i.e., those quantities which measure the strength of interaction between atomic orbitals, are given as $H_{AB} = H_{BC} = \beta$ and $H_{AC} = \gamma$. The energies of the three molecular orbitals relative to a non bonded energy H_o are given by[42].

$$E_+ = Ho + \frac{\gamma}{2} + \left[\left(\frac{\gamma}{2}\right)^2 + 2\beta^2\right]^{\frac{1}{2}}$$

$$E_o = H_o - \gamma$$

$$E_- = Ho + \frac{\gamma}{2} - \left[\left(\frac{\gamma}{2}\right)^2 + 2\beta^2\right]^{\frac{1}{2}}$$

It should be noted that if β is zero and γ is nonzero a normal two-center, two-electron bond will be formed between atoms A and C. If γ is zero and β is nonzero an open three-center bond will be formed and if γ is approximately equal to β a closed three-center bond will be formed. Relative energy levels are shown in Figure XVIII from Lipscomb[41].

There are two types of open three-center bonds found in the boranes. In the first, a hydrogen atom functions as a bridge with the atomic orbitals being 1s from hydrogen and sp^2 or sp^3 from each boron

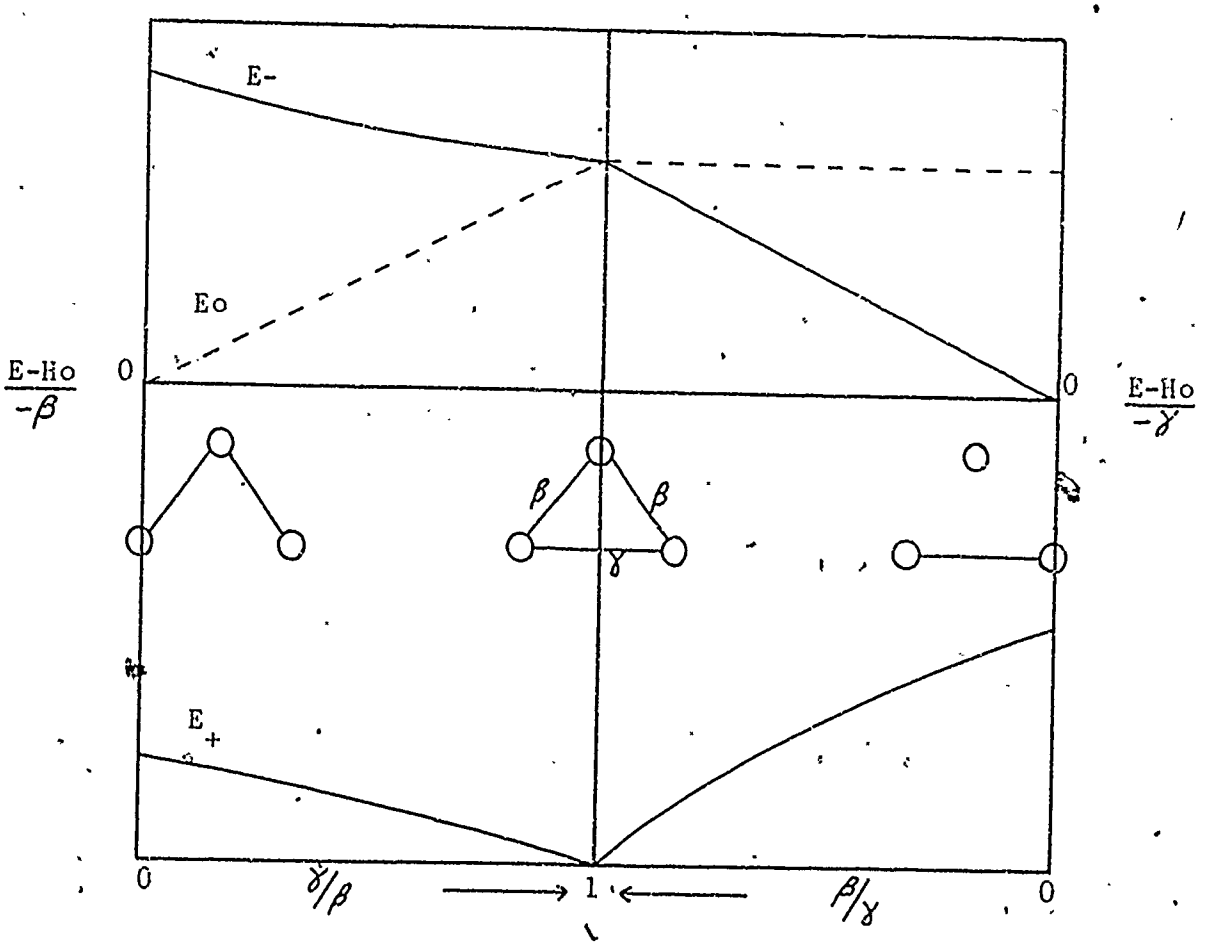

Figure XVIII

Relative Energy Levels in Three Center Bond

as shown in Figure XIXa. Boron atoms also bridge as shown in Figure XIXb. The bridging boron atom contributes a p orbital to the molecular orbital and the other boron atoms contribute as above. A closed three-center bond can be formed between three boron atoms as shown in Figure XIXc. Here the atoms may have sp, sp^2 or sp^3 hybridization. Figure

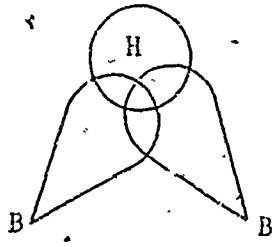

Figure XIXa

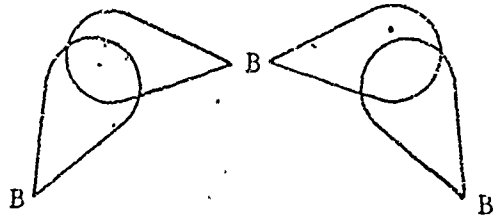

Figure XIXb

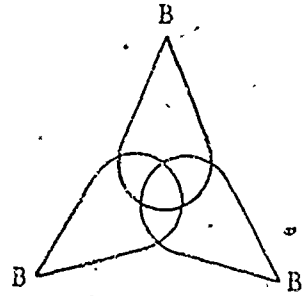

Figure XIXc

Types of Three Center Bond

XIXc corresponds to the center of Figure XVIII, i.e., where $\gamma/\beta = 1$. Figures XIXa and b correspond to $\gamma/\beta = 0$ while $\beta/\gamma = 0$ applies to a normal two center bond. The energy level diagram indicates that E_+ is always bonding, while E_o and E_- are antibonding except at $\gamma/\beta = 0$ and $\beta/\gamma = 0$ respectively, where they are nonbonding.

In diborane(6), Figure XVa, a total of twelve electrons and fourteen atomic orbitals are available for bonding. Eight of the electrons and eight of the atomic orbitals are employed in the formation of the four two-center terminal bonds between hydrogen and boron. The remaining six orbitals and four electrons are utilized in forming two hydrogen bridge bonds, each of which uses a hydrogen 1s orbital and one sp^3 orbital from each boron.

Pentaborane(9), Figure XVI, has 29 valence orbitals and twenty-four valence electrons. Ten of these orbitals and ten of the electrons are used to form the five terminal boron-hydrogen bonds. Further, each of the four basal boron atoms contributes two orbitals to the bridge bonds to the basal hydrogens and each of the four bridge bonded hydrogen atoms contributes one orbital. There are, therefore, twelve atomic orbitals involved in the hydrogen bridging system and eight electrons are accommodated, two in each of the four three-center bonding orbitals. A total of twenty-two orbitals and eighteen electrons have been used in bonding the hydrogen atoms to the molecular framework. Seven orbitals and six electrons remain to hold the framework together.

The valence s orbital and one of the valence p orbitals on the apex boron form an sp hybrid, with the axis of the hybrid pair along the C_4 axis of the molecule. The remaining p orbitals on the apex boron are oriented so that one orbital is in the plane of basal boron atoms 2 and 4 while the other orbital is in the plane of basal atoms 3 and 5. Each of the p orbitals overlaps with a pair of basal sp^3 orbitals to give an open three-center two-electron bond.

Of the two sp hybrid orbitals on the apex boron one is used to form a terminal boron-hydrogen bond as mentioned above. The other points into the molecular cage and overlaps with the four sp^3 orbitals originating on the basal atoms. This forms, in effect, a closed, five-center molecular orbital.

The final six electrons are therefore contained in three molecular orbitals, one a five-center bonding orbital, the other two orbitals being an open, three-center, degenerate pair of bonding orbitals.

Charge distribution calculations based on the molecular orbitals above give each basal boron a charge of +⅔ electronic charge while the apex boron carries -1 electronic charge. The dipole moment calculated from this model gives a value of 5.23 Debye. The actual dipole moment is 2.13 Debye[43]. Calculations including electronic repulsion terms give the apex boron atom a charge of about -0.36 charge units while the basal borons have charges of +0.09 charge units. This calculation yields a dipole moment of 1.88 Debye, in better agreement with the observed value.

4.3.4. Preparation of the Boranes

Neither this section nor the following on the reactions of the boron hydrides is meant to be comprehensive. The intention is to concisely present essential background information.

The most widely used method for the preparation of diborane(6) involves the addition of boron trifluoride etherate to a slurry of lithium aluminum hydride in diethyl ether[44]. Yields can be

$$4BF_3 + 3LiAlH_4 \longrightarrow 2B_2H_6 + 3LiF + 3AlF_3$$

stoichiometric.

Many of the higher boranes are obtained from diborane(6) by the input of energy. For example, tetraborane(10) can be synthesized in a hot-cold reactor operating at 120 °C and -78 °C. The same apparatus operating at 120 °C and -30 °C yields pentaborane(11)[45].

Pentaborane(9) is most efficien[t]ly prepared on an industrial scale. A recirculating flow system is used and a diborane(6)-hydrogen mixture in a 1:4 ratio is passed through the reactor at 200-240 °C. Residence time is two or three seconds, yields can reach 70% and conversion 30%[45]. Decaborane(14) can be prepared in 60% yield in a static system by the pyrolysis of diborane(6) for fifteen to thirty minutes at 150-160 °C[37]. The growth of interest in the boranes is shown by the fact that the above boranes, with the exception of pentaborane(11), are commercially available[46].

Over the past few years it has become apparent that a stepwise increase in the number of boron atoms in a borane is possible through the action of diborane(6) or substituted monoboranes on borate anions, as indicated by the following reactions:

$$MBH_4 + (CH_3)_2BCl \longrightarrow 1,1\text{-}(CH_3)_2B_2H_4 + MCl \quad (47)$$

$$MBH_4 + (BH_3)_2 \longrightarrow MB_3H_8 + H_2 \quad (48)$$

$$MB_3H_8 + (CH_3)_2BCl \longrightarrow 2,2\text{-}(CH_3)_2B_4H_8 + MCl \quad (47)$$

$$MB_4H_9 + \tfrac{1}{2}(BH_3)_2 \longrightarrow MB_5H_{12} \xrightarrow{HCl} B_5H_{11} + H_2 + MCl \quad (49)$$

$$MB_5H_8 + \tfrac{1}{2}(BH_3)_2 \longrightarrow MB_6H_{11} \xrightarrow{HCl} B_6H_{12} + MCl \quad (49)$$

$$MB_6H_{11} \xrightarrow[\text{to R.T.}]{\text{warm}} B_6H_{10}\ (20\%) \quad (50)$$

The borate anions can be prepared by the action of an alkali metal hydride on the parent hydride in diethyl ether (see Section 4.3.6. below). The synthetic possibilities inherent in the above reactions are only beginning to be explored.

4.3.5. Reactions of the Boranes

Wiberg[37] notes fifteen types of reaction possible with the boranes. Of these the most frequently employed are:

a) Cleavage reactions involving B-H double bridges. The cleavage process can be symmetric or asymmetric. For example, tetrahydrofuran cleaves diborane(6) symmetrically to yield the $THF:BH_3$ adduct[51]. Ammonia cleaves diborane(6) asymmetrically at low temperatures to yield $(NH_3)_2BH_2^+$ and BH_4^-[52]. Symmetrical cleavage of pentaborane(9) produces BH_3 and B_4H_6 while asymmetric cleavage with ammonia at low temperatures yields $(NH_3)_2BH_2^+$ and $B_4H_7^-$[53].

b) Electrophilic substitution reactions can be carried out under appropriate conditions. For example both pentaborane(9) and decaborane(14) are alkylated with alkylhalides and Friedel-Crafts catalysts[45]. The substitution positions are those expected from charge distributions calculated on the basis of molecular orbital theory, i.e., the apex boron is substituted in pentaborane(9) while the number 2 boron is the one initially substituted in decaborane(14).

c) Lewis bases such as hydride ions or carbanions remove protons from the boranes. This will be discussed in more detail in

Section 4.3.6. below.

d) Olefins or acetylenes react with diborane(6) or mono- or disubstituted alkyl boranes. The B-H bond adds across the multiple bond in an anti-Markownikoff fashion to yield a variety of organoboranes which can be further reacted to yield organic compounds. The total process, hydroboration, is of considerable value to the synthetic organic chemist[54].

4.3.6. Deprotonation of the Boranes

The two general types of hydrogen atoms in the boranes are bridging and terminal. Although early charge distribution calculations indicated that the bridging hydrogens were more negative than the terminal hydrogen atoms[41] recent calculations indicate the converse[55].

If a terminal proton is removed, a pair of valence electrons becomes available and thus marked changes in bonding in the rest of the molecule are likely. On the other hand if a bridging proton is removed, only small changes in bonding are expected as the B-H-B bridging unit becomes a B-B unit. Thus it is not surprising that the experimental evidence clearly shows that a bridging proton is removed when the boranes are deprotonated.

Decaborane(14) was the first borane to be deprotonated. Sodium hydride in diethyl ether was found to yield hydrogen and $NaB_{10}H_{13}$[56]. The parent hydride can be regenerated by the action of anhydrous acid on the sodium salt in aprotic solvents. Bases such

as OH^-, OR^-, and BH_4^- were also used to deprotonate decaborane(14). In all cases decaborane acts as a monoprotic acid. The position of substitution is uncertain. Neutralization of $NaB_{10}H_{13}$ with deuterium chloride in diethyl ether results in approximately 90% of the deuterium being found in a bridge position[57], but the obvious conclusion is complicated by the fact that there is considerable exchange between bridging and terminal positions of decaborane(14) in solutions of Lewis bases[58]. Evidence from nuclear magnetic resonance spectra is equivocal.

Lower molecular weight boranes are also deprotonated with suitable bases. Tetraborane(10) was deprotonated with methyllithium[59], ammonia or potassium hydride[60]. These deprotonations were carried out in diethyl ether at -78 °C. The compounds obtained, LiB_4H_9, $NH_4B_4H_9$ and KB_4H_9, appear to be stable at -78 °C but decompose on warming. The reaction of ammonia with tetraborane(10) is thought to be reversible. On standing at -65 °C a competing, irreversible, reaction between tetraborane(10) and ammonia also occurs resulting in the asymmetric cleavage product $[(NH_3)_2BH_2^+][B_3H_8^-]$[60].

On treatment of LiB_4H_9 with hydrogen chloride in diethyl ether, 75% of the parent hydride was recovered. On treatment of LiB_4H_9 with deuterium chloride μ-DB_4H_9 was recovered[61]. The conclusion that the D atom occupied a bridging position was based on the fact that a strong absorption occurred at 1583 cm^{-1} in the infrared spectrum. No absorption was noted at the frequency expected for the terminal B-D

stretch, i.e., 1946 cm^{-1}. On standing the band at 1583 cm^{-1} decreased in intensity and a new band appeared at 1946 cm^{-1}, due to intramolecular exchange of terminal hydrogen with bridging deuterium atoms[61].

Pentaborane(9) was reacted with sodium hydride in bis(2-methoxyethyl)ether (diglyme) at room temperature. An 82% yield of hydrogen on the basis of

$$B_5H_9 + NaH \longrightarrow NaB_5H_8 + H_2$$

was obtained but the parent hydride could not be regenerated by the action of hydrogen chloride[62]. Subsequently, pentaborane(9) was reacted in ether solvents at -78 °C with methyllithium or n-butyllithium to yield hydrocarbon and lithium octahydropentaborate(1-) (LiB_5H_8)[63]. Sodium and potassium octahydropentaborate(1-) species were prepared by the reaction of the alkali metal hydrides on pentaborane(9) in 1,2-dimethoxyethane (glyme) at -50 °C[64]. The parent hydride could be regenerated by the action of hydrogen chloride on LiB_5H_8[63].

During the reaction at -60 °C of pentaborane(9) with liquid ammonia, the boron n.m.r. spectrum initially indicated the presence of ammonium octahydropentaborate(1-), but on standing a short time the asymmetric cleavage product $[(NH_3)_2BH_2^+][B_4H_7^-]$ was formed. As with tetraborane(10), the deprotonation reaction was thought to be reversible and cleavage products formed by the slow, irreversible reaction of B_5H_9 with ammonia, rather than through a $B_5H_8^-$ intermediate[53].

Tetra-n-butylammonium octahydropentaborate(1-) was prepared

by a metathetical reaction of tetra-n-butylammonium iodide with potassium octahydropentaborate(1-) at -23 °C in methylene chloride-THF solutions[65]. Pentaborane(9) was regenerated by the action of hydrogen chloride.

Infrared, ^{11}B and ^{1}H n.m.r. spectra were used to assign the acidic proton in pentaborane(9) to a bridge position[63,64,66]. There is believed to be a rapid tautomerism of the bridge protons, but no interchange of bridge with terminal protons[66]. Thus only a single doublet resonance is noted for the chemically nonequivalent basal boron atoms in the ^{11}B n.m.r. spectrum of LiB_5H_8, even at low temperature. The proton n.m.r. spectrum indicates all basal terminal hydrogen to be equivalent, and all bridge hydrogens to be equivalent. However, Shore et al[67] deprotonated $2\text{-}CH_3B_5H_8$ with potassium hydride and found that the tautomerism could be slowed at low temperatures. Two resonances of relative area 2:1 were ascribed to the bridge protons. Since three chemically different bridge protons were expected, the results were interpreted as indicating tautomerism had slowed but not stopped.

Hexaborane(10) was deprotonated with methyllithium and sodium and potassium hydride[68]. As with tetraborane(10) and pentaborane(9), hexaborane(10) in liquid ammonia initially formed $NH_4B_6H_9$ but on warming the cleavage product $[(NH_3)_2BH_2^+][B_5H_8^-]$ was found[69]. Spectral evidence once again indicated that a bridge proton was removed when hexaborane(10) was deprotonated.

The Bronsted acidities of the above four boranes appears to decrease in the order $B_{10}H_{14} > B_6H_{10} \approx B_4H_{10} > B_5H_9$[61,68]. The relative order of acidity of the B_6H_{10}-B_4H_{10} pair has not been established. As expected, when electron withdrawing substitutents, such as chloride, were substituted for a terminal hydrogen atom the Brønsted acidity of the borane was enhanced. When a methyl group was substituted for a terminal hydrogen the Brønsted acidity decreased[67].

Of the borate (1-) salts only $B_{10}H_{13}^-$ is stable at room temperature. Thermal stability decreases in the order $B_{10}H_{13}^- > B_6H_9^- > B_5H_8^- > B_4H_9^-$[61]. The thermal stabilities of lithium, sodium and potassium borate(1-) species are similar. Some workers reported the lithium compounds to be slightly more stable than the sodium or potassium[66] whereas others reported the converse[60,61]. A considerable increase in stability occurred when the large tetramethylammonium cation was introduced[65].

Deprotonation rates appear to increase qualitatively in order of the Lewis base strength of the solvents employed. None of the deprotonation reagents employed to date was capable of deprotonating the boranes in either the absence of solvent or the presence of hydrocarbon solvent.

When a proton is removed from a borane, a B-H_μ-B unit becomes a B-B unit, and it is possible to protonate this B-B bond. As an extension to this, Shore et al[70] used HCl or DCl in BCl_3 at

-78 °C successfully to protonate the lone B-B bond in the base of hexaborane(10), Figure XVc to form the undecahydrohexaboronium(+1) ion[70].

Triborane(9) does not exist but the conjugate base, the thermally stable octahydrotriborate(1-) anion, was prepared by the reaction of diborane(6) with sodium borohydride at 60 °C in glyme[71]. This anion takes part in reactions of a type similar to the other borate(1-) species in some respects[47], but different in others[72], (see Section 4.3.7. below). The structure of the nonexistent parent is postulated as a trigonal plane of BH_2 groups joined by three bridge hydrogens. X-ray crystallographic work on $[(NH_3)_2BH_2^+][B_3H_8^-]$ indicated a bridging position was vacant[73]. The $B_3H_8^-$ ion was therefore considered structurally similar to the other borate(1-) species.

4.3.7. Bridge Substitution in the Boranes

When diborane(6) was passed over $[(NH_3)_2BH_2]BH_4$ at 85 °C μ-aminodiborane(6) ($\mu NH_2B_2H_5$) was obtained[74]. The amino group was shown by electron diffraction to be in a bridge position[75]. The bonds between the boron and nitrogen atoms are two center two electron bonds.

It is possible to prepare compounds in which an atom other than hydrogen is found in a bridging position and is bonded to the rest of the molecule with a three center two electron bond. The

precursors to these species are the borate(1-) anions.

Gaines and Iorns prepared the first of the compounds in which a heavier atom was substituted for a bridging proton[76]. They reacted lithium octahydropentaborate(1-) with trimethylchlorosilane in ether at -78 °C and obtained μ-trimethylsilylpentaborane(9) (μ-$(CH_3)_3SiB_5H_8$). This compound was brominated at the apex position to decrease its volatility and provide a heavy atom for a single crystal x-ray diffraction study[77]. This study unequivocally established that the silicon atom was in a basal bridge position.

Subsequently Gaines and Iorns prepared a series of compounds of the general formula μ-$R_3M_{IV}B_5H_8$ where M_{IV} = Si, Ge, Sn or Pb and R = H, CH_3 or C_2H_5[78]. The bridging position of the R_3M_{IV} group was confirmed by ^{11}B n.m.r. experiments. It was demonstrated that the silicon and germanium derivatives isomerized quantitatively, at room temperature in weak Lewis bases, to the 2-substituted derivatives. It was also determined in another study that μ-$H_3SiB_5H_8$ was chlorinated at the silicon atom by boron trichloride[79].

Burg and Heinen reacted dimethylchlorophosphine with lithium octahydropentaborate(1-) in diethyl ether at -78 °C[80] to form μ-dimethylphosphorylpentaborane(9), (μ-$(CH_3)_2PB_5H_8$). The bridging position of the phosphorus atom was confirmed by n.m.r. When bis(trifluoromethyl)chlorophosphine was employed as an insertion reagent, only 1-bis(trifluoromethyl)phosphorylpentaborane(9) was obtained.

Gaines and Iorns have prepared μ-dimethylborylpentaborane(9)

(μ-$(CH_3)_2BB_5H_8$) by the reaction of dimethylchloroborane(3) with lithium octahydropentaborate(1-) in diethyl ether at -78 °C. This compound isomerizes to 4,5-dimethylhexaborane(10) in diethyl ether at room temperature[81].

Gaines and Borlin prepared μ-dimethylaluminumtriborane(9) (μ-$(CH_3)_2AlB_3H_8$) and μ-dimethylgalliumtriborane(9) (μ-$(CH_3)_2GaB_3H_8$) by the action of the dimethylmetalchloride species on sodium octahydrotriborate(1-) at room temperature[72]. However these compounds are not triborane(9) molecules (Figure XXa) with a group IIIA metal replacing a bridging proton. The structure is thought to be as indicated in Figure XXb.

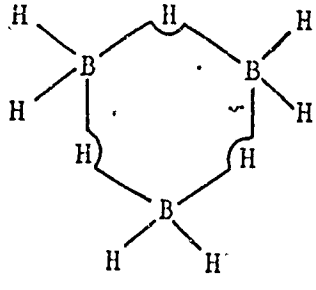

Figure XXa

Triborane(9)

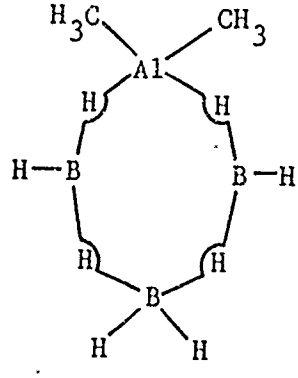

Figure XXb

Dimethylaluminumtriborane(9)

Nuclear magnetic resonance data indicated that the methyl groups, boron atoms and boron bound hydrogen atoms are involved in a rapid intramolecular exchange at room temperature[72].

In related studies, nido-2,3-dicarbahexaborane(8) (2,3-$C_2B_4H_8$) was deprotonated[82]. Chronologically this species was deprotonated prior to the boranes; with the exception of $B_{10}H_{14}$.

Nido-2,3 $C_2B_4H_8$ resembles a hexaborane(10) molecule with two of the basal boron atoms replaced by two carbon atoms. The base has only two hydrogen bridges, rather than the four of hexaborane(10). Compounds of the type μ-4,5 $R_3M_{IV}C_2B_4H_7$ have been prepared where M_{IV} = Si, Ge, Sn or Pb and R = H or CH_3[83,84]. The properties of the carboranes are significantly different from the properties of the boranes and they will not be discussed further.

As mentioned above (Section 4.3.4.) diborane will add to borate(1-) anions. In at least one of these cases, the addition of borane(3) to octahydropentaborate(1-), the borane enters the base of the molecule, probably in a bridging position. Hexaborane(10) is generated on warming to room temperature[50].

4.4. Boron Bonded to Group VA and Group VIA Elements

The species to be discussed in this section include those compounds in which boron is bonded to nitrogen or phosphorus, or oxygen or sulphur. In view of the vast literature in these areas no attempt will be made to be comprehensive. The intent is rather

to present a pertinent overview. Material for this section is to be found in Niedenzu[85], Nöth[86], Haiduc[87], Parshall[88], Coyle[89], Edwards[88], Torsell[89], Nesmeyanov[90], Nies[91], Mikhailov[86] and Meutterties[88]. Specific references to other sources are given.

4.4.1. Compound in which Boron is Tetracoordinate

Tricoordinate boron has a vacant low-energy orbital. Tricoordinate group VA atoms have a non-bonding pair of electrons and dicoordinate group VIA atoms have two non-bonding pairs of electrons. Therefore boron is capable of functioning as a Lewis acid and nitrogen, phosphorus, oxygen and sulfur as Lewis bases. When the Lewis acid-Lewis base neutralization reaction occurs the bond formed is a coordinate covalent bond. Electron density is transferred from the group VA or VIA element to boron. The classes of compounds formed are called amine-boranes ($R_3NBR'_3$) in the case of nitrogen, phosphine-boranes ($R_3PBR'_3$) in the case of phosphorus and simply coordination complexes for oxygen and sulfur ($R_2OBR'_3$, $R_2SBR'_3$). On complex formation, boron, nitrogen and phosphorus become four coordinate and oxygen and sulfur become three coordinate.

The complexes are usually prepared by the direct reaction of Lewis acids, eg., boron trihalides, diborane(6) or mono-, di- or trisubstituted boranes, with a wide variety of Lewis bases. These include primary, secondary or tertiary phosphines or amines,

ethers, and to a lesser extent aldehydes and ketones, as well as hydrogen sulfide, thioethers and mercaptans. A variety of other methods of formation exist. For example, $LiBH_4$ can be used as a source of borane, and stronger Lewis bases can be used to replace weaker, eg., transamination reactions.

The strength of the bond between boron and the donor atom depends on the relative strength of the Lewis acid and the Lewis base. Changes in the donor-acceptor bond strength with changing acid-base strengths frequently are monitored by means of the donor-acceptor stretching frequency in the infrared spectrum. Boron trihalides are stronger Lewis acids than either diborane(6) or substituted monoboranes due to the ability of the halogen atoms to remove electron density from the boron. Boron trifluoride might be thought the strongest Lewis acid of the boron trihalides but it is not. The reason it is not a strong acid is because molecular orbitals of pi symmetry are formed employing boron and fluorine p orbitals of appropriate symmetry. Energy is required to disrupt this double bonding and this reduces the stability of the coordinate complex.

The Lewis base strength of the donor atom is increased by the replacement of hydrogen atoms with alkyl or aryl groups. Thus while phosphine-borane (H_3PBH_3) is unstable, trimethylphosphine-borane ($(CH_3)_3PBH_3$) is relatively stable. As expected on the basis of electronegativities, the nitrogen-boron dative bond is normally

stronger than the phosphorus-boron dative bond, and the oxygen-boron bond is normally stronger than the sulfur-boron bond. The reference acids used to establish stabilities are usually the boron trihalides. When BH_3 is employed as the reference acid, the order of stabilities is reversed. The bond between boron and the heavier element is stronger than that between boron and the lighter. This phenomenon is rationalized by postulating that a d orbital on the second row atom is capable of participating in some form of bonding with a group orbital of the H_3 unit.

4.4.2. Compounds in which Boron is Tricoordinate

Compounds in which boron and groups VA and VIA atoms retain their 'normal' coordination number, i.e., three for boron, nitrogen and phosphorus and two for oxygen and sulfur, have been much more widely studied than those in which the above elements expand their coordination spheres.

With group VA the classes of compounds $R_2NBR'_2$ are called amino-boranes or, $R_2PBR'_2$, phosphinoboranes. These compounds can be obtained by pyrolysis of the amine or phosphine boranes if the boron atom has at least one hydrogen atom bonded to it. For example,

$$R_3NBR'_2H \xrightarrow{\Delta} R_2NBR'_2 + RH$$

The boron atom of the amino or phosphinoboranes can be mono-, di- or trisubstituted, eg., R_2NBX_2, $(R_2N)_2BX$ or $(R_2N)_3B$. As well as the above pyrolysis reaction, there are a wide variety of methods

available for preparing these compounds. Mixed derivatives ($RR'NBR''R'''$) can also be prepared.

The bond between boron and phosphorus in the phosphinoboranes can be described in terms identical to those used to describe the bond between boron and nitrogen in the aminoboranes. Therefore bonding will be discussed only for the aminoboranes. The bond between boron and nitrogen in the aminoboranes possesses double bond character. Each of the boron and nitrogen atoms can be considered as an sp^2 hybrid and a sigma bond is formed by the overlap of these hybrid orbitals. Boron has a vacant p_z orbital perpendicular to the plane of the sp^2 hybrid while nitrogen has a filled p_z orbital perpendicular to the same plane. These p_z orbitals overlap and a bond is formed by donation of electron density from nitrogen to boron. The strength of the B-N bond varies with the substituents on the two centers. The boron-nitrogen stretching frequency from the infrared spectrum increases, indicating a stronger bond, as the number of carbon atoms in alkyl substituents on each of boron and nitrogen decreases. Further, if the nitrogen atom has aryl substituents the frequency decreases, presumably because delocalization of the lone pair of electrons on nitrogen over the pi system on the aryl substituent decreases the availability of this lone pair for donation to boron.

Restricted rotation about the B-N bond is attributed to the double bond. The barrier to rotation, from n.m.r. data, is

about 10-15 kcal/mole. Molecular orbital calculations show that the nitrogen atom in monoaminoboranes carries a net negative charge of about 0.05 electronic units. This is thought due to the boron atom donating more charge to nitrogen through the sigma bond than it receives through the pi bond.

Bond lengths in amine boranes are about equal to the sum of the covalent radii of boron and nitrogen (1.57Å ±0.03). The bond length between boron and nitrogen in monoamino- and bisaminoboranes has not been established by x-ray methods. The trisaminoborane 1,8,10,9-triazaboradecalin (Figure XXI) has been examined by x-ray

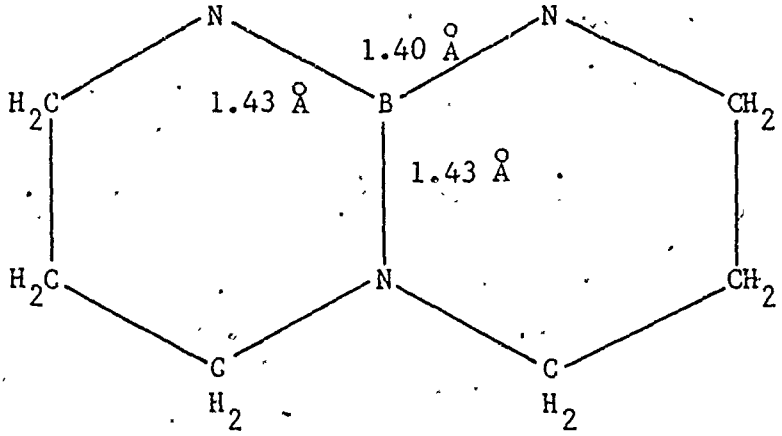

Figure XXI

1,8,10,9-triazaboradecalin

methods and the length of the boron-nitrogen bond established as 1.40-1.43Å (92).

The chemistry of the aminoboranes and phosphinoboranes is determined largely by the presence of both donor and acceptor atoms

in the molecule. Thus aminoboranes will dimerize or trimerize with both boron and nitrogen atoms becoming four coordinate. The possibility of oligimer formation depends on the strength of the acceptor and donor sites and on steric effects, but whether dimers, trimers or even tetramers are formed appears to depend on the conditions of the preparative reaction, i.e., solvents employed and temperatures used.

Even though the p_z orbital on boron is employed in bonding it is still possible for these compounds to function as Lewis acids. For example, trismethylaminoborane, $B(NHMe)_3$, will add $NHMe^-$ to form $B(NHMe)_4^-$. The nitrogen atoms can also function as donors, eg., tris(dimethylamino)borane will add aluminum trichloride.

Heterocyclic rings containing alternating boron and nitrogen or boron and phosphorus atoms are known. The former are very well known, and commonly contain tricoordinate boron and nitrogen. The latter are not well known and, when found, usually contain four coordinate boron and phosphorus. Phosphorus containing rings can be thought of as oligomers of phosphinoboranes. Phosphinoboranes form these rings so readily that it is frequently difficult to obtain the monomer.

The most studied boron-nitrogen ring compound is borazine, $(HBNH)_3$, Figure XIIIa. Borazine is of interest because of its electronic similarity to benzene. The bonding in borazine consists of a sigma system with bonding by overlap of sp^2 orbitals on adjacent

centers, and a pi system with bonding due to donation of electron density from a filled p_z orbital on nitrogen to a vacant p_z orbital on boron (z axis perpendicular to the plane of the B-N ring). Molecular orbital calculations indicate nitrogen to be slightly negative for the same reasons mentioned above for amino-boranes.

Under certain conditions, four membered boron-nitrogen heterocyclics are formed, although six membered rings are more common. The formation of four membered rings, which are favored by the presence of bulky substituents, is usually accomplished by pyrolysis of trisaminoboranes. The reaction is thought to proceed via an N-bridged intermediate, followed by amine elimination.

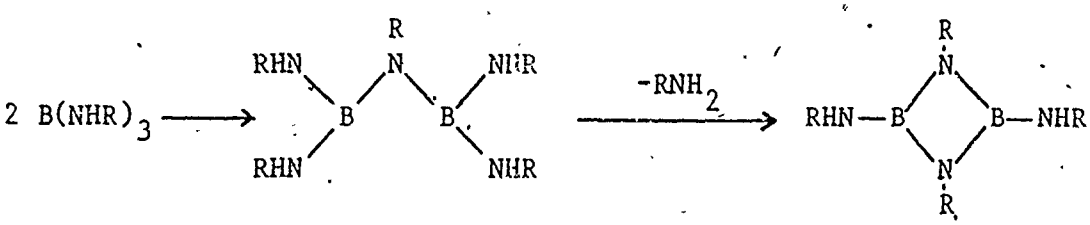

Mass spectrometric molecular weight determination and x-ray diffraction data for B-[bis(trimethylsilyl)amino]-N-trimethylsilylcyclodiborazane, Figure XXII[93], clearly establishes the existence of four membered rings.

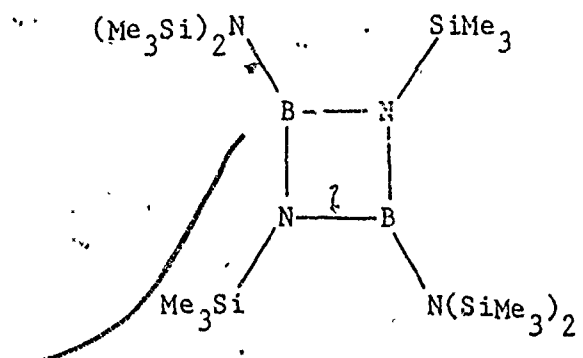

Figure XXII

Both oxygen and sulfur form compounds analogous to the aminoboranes. Borinates ($R_2B(OR)$), boronates ($RB(OR)_2$) and borates ($B(OR)_3$) are formed by the reaction of di, mono- or unsubstituted boron halides with alcohols. If the same boron halides are reacted with mercaptans, thioesters are obtained. Hydrolysis of both the esters and the thioesters yields oxyacids. Treatment of the thioesters with hydrogen sulfide yields the thioacids, with the exception of the sulfur analogue of boric acid, which has not been prepared.

The oxy acids of boron do not function as acids by donation of a proton but rather by accepting an hydroxyl ion. The vacant orbital on boron accepts an electron pair from the oxygen atom of the hydroxyl group, forming $B(OH)_4^-$, $RB(OH)_3^-$ and $R_2B(OH)_2^-$ species.

Thioesters of boron function as acceptors with donors such as amines. However the complexes decompose below room temperature to yield the mercaptan and aminoboranes.

The oxyacids of boron undergo facile intermolecular dehydration. On heating, orthoboric acid $B(OH)_3$, yields metaboric acid $(HOBO)_3$, while boronic and borinic acids dehydrate as shown below.

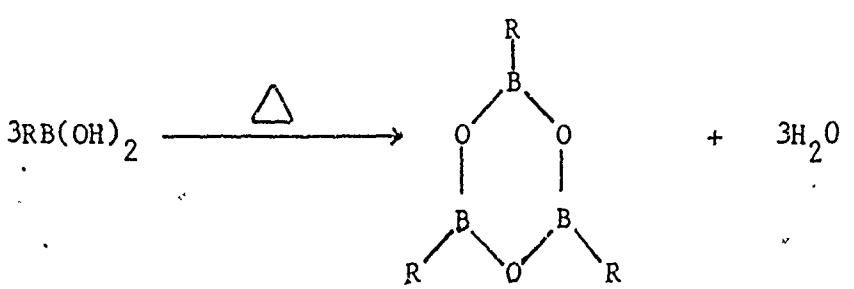

$$2R_2BOH \xrightarrow{\Delta} R_2B\text{-}O\text{-}BR_2 + H_2O$$

The thioacids undergo similar reaction somewhat more readily. Although the parent acid $B(SH)_3$ has not been isolated the dimer $(HSBS)_2$ and trimer $(HSBS)_3$ have.

The orthoboric acid molecule ($B(OH)_3$) has a trigonal planar structure, Figure XXIIIa, with each of the hydrogen atoms hydrogen bonded to an oxygen atom on another molecule, forming a pseudo-hexagonal network. The hydrogen atoms are not found at the midpoint of the oxygen-hydrogen-oxygen linkage. Metaboric acid $(HBO_2)_3$ has a

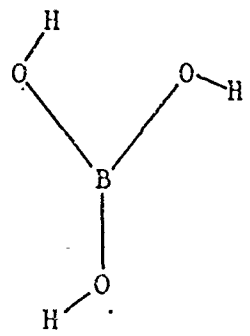

Figure XXIIIa

Orthoboric acid

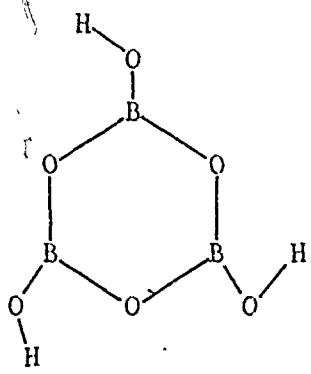

Figure XXIIIb

Metaboric acid

planar trimeric unit, Figure XXIIIb. Each hydrogen atom is bonded via a hydrogen bond to a non ring oxygen in another trimer. These hydrogen atoms are found at the midpoints of the oxygen-hydrogen-oxygen linkage.

There is a very strong tendency for oxygen-boron heterocyclic rings to be six membered. Only one four membered ring is known. This compound is formed by the dehydration of mesitylene

boronic acid. Steric effects may favor the formation of the four membered ring[94].

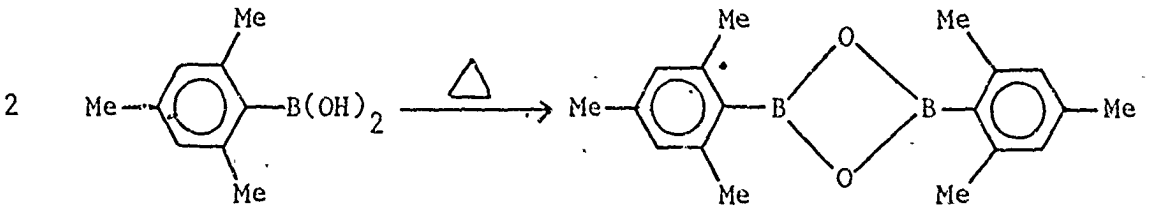

Sulfur-boron compounds, in contrast, form four membered rings readily. Hydrolysis of boron trihalides yields boric acid, which can then be dehydrated to form the six membered metaboric acid ring. When boron trihalides are treated with hydrogen sulfide the parent acid can not be isolated, but the products of a reaction similar to dehydration are formed, as shown below.

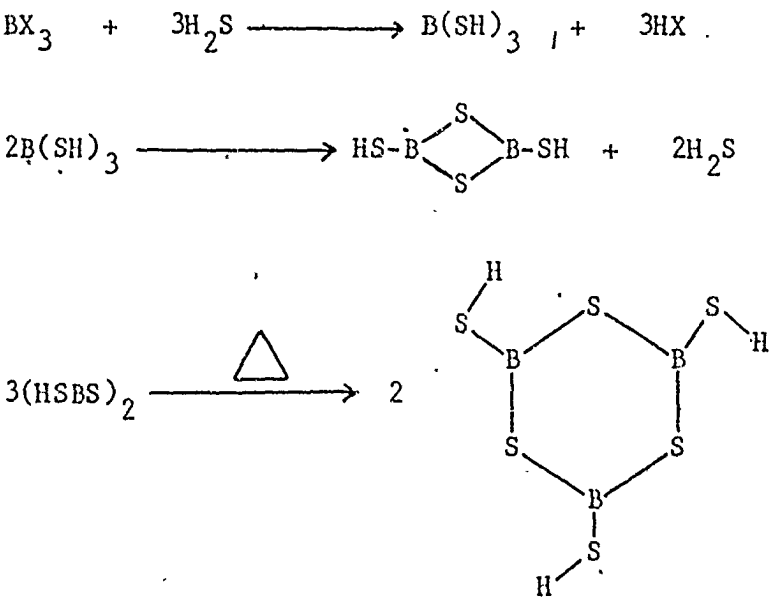

Initially a four membered ring (dithiaboretane or dithiol-

cyclodiborthiane) is formed. On heating, the six membered ring, (trithiaboretane or trithiolcyclotriborthiane), is irreversibly formed. Derivatives of the four membered ring can be formed, eg., heating triethylamine borane with hydrogen sulfide yields bis(diethylamino)dithiaboretane[95]. This compound is interesting in that it contains a monoamino linkage as well as the strained $(BS)_2$ four membered ring.

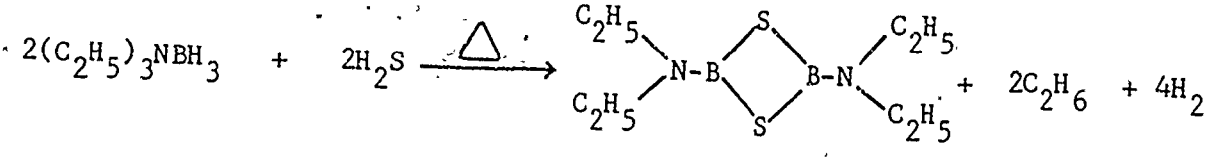

Due to the commercial importance of many oxygen-boron compounds detailed structural investigations have been carried out. The sum of the covalent radii for the boron-oxygen bond is 1.55 Å. However in both orthoboric and metaboric acids the boron-oxygen distance is 1.37 Å. Apparently there is donation of charge from the filled lone-pair orbitals on oxygen to the vacant boron orbital, resulting in π bond character. The puckered six membered $B_3O_6^{3-}$ ring found in potassium metaborate (KBO_2) has alternating boron and oxygen atoms 1.38 Å apart. The anion found in potassium metaborate tetrahydrate ($K_2O.5B_2O_3.8H_2O$) contains tricoordinate and tetracoordinate boron atoms, Figure XXIV. The bond distance from boron to the oxygen atoms in the hydroxyl group is 1.28 Å, whereas that between trigonal boron and ring oxygen is 1.53 Å. Tetrahedral boron has no capacity for double

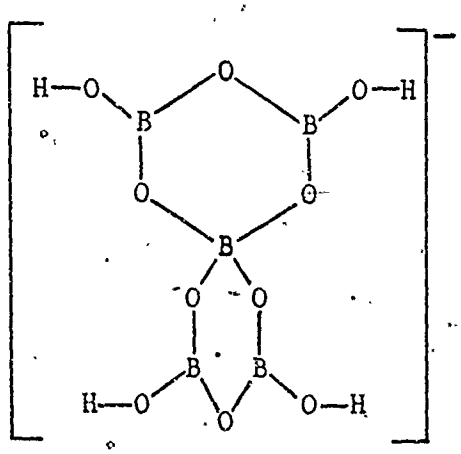

Figure XXIV

Potassium metaborate tetrahydrate anion

bond formation, and therefore the interatomic distances are about those expected on the basis of covalent radii.

Very little structural work has been carried out on boron-sulfur containing compounds. The crystal structure of $(BrBS)_3$ has been determined and the boron-sulfur distance was reported as 1.85 Å. As this is very close to the sum of the covalent radii (1.84 Å) it is unlikely that π electron density is being donated to the vacant boron orbital from the large, difuse, non-bonded electron pairs on sulfur.

4.5. Spectral Techniques in the Study of Boron Chemistry

4.5.1. Infrared Spectroscopy

Historically, infrared spectra have been important in the study of boron containing compounds. For example, the structure of

diborane(6) was elucidated on the basis of infrared spectra[96]. Isotope exchange has frequently been employed in the interpretation of spectra[97] and stretching frequencies are used to determine the degree of multiple bonding present in compounds such as amino- and phosphinoboranes[85]. However today infrared spectroscopy is used mainly as an identification tool, since structural information is more readily obtained by study of n.m.r. spectra.

4.5.2. Mass Spectroscopy

Boron has two naturally occurring isotopes, ^{10}B and ^{11}B, which are found in relative abundances of approximately 1:4 respectively. Thus the parent ion peaks of pentaborane(9) are spread over six mass units due to $^{11}B_5$, $^{11}B_4\,^{10}B_1$, $^{11}B_3\,^{10}B_2$, $^{11}B_2\,^{10}B_3$, $^{11}B_1\,^{10}B_4$ and $^{10}B_5$ species. Further spreading is caused by the successive elimination of hydrogen. The fragment resulting after elimination of a boron atom from B_5H_9 shows a spread of five mass units for the boron cage and further spreading by hydrogen atom elimination. Thus an identifiable pattern exists for each of the boron hydrides. Mass spectroscopy, as is the case with infrared spectroscopy, is used mainly as an identification tool rather than as a means of obtaining information about structure or bonding.

4.5.3. Nuclear Magnetic Resonance Spectroscopy

Proton n.m.r. spectra have been used in the study of boron

containing compounds with considerably less success than has been the case in carbon chemistry. The ^{11}B isotope has a nuclear spin of 3/2 while the ^{10}B isotope has a nuclear spin of 3. Thus a hydrogen atom bonded to ^{11}B shows a spin multiplet of multiplicity four, and a hydrogen atom bonded to ^{10}B a multiplicity of seven. Therefore the relative intensities of each member of a multiplet are lower, by a factor of either four or seven, than the intensities of a single hydrogen bonded to carbon. Furthermore, since the two boron isotopes have quadrupole moments, there is an indirect mechanism for rapid transition of the hydrogen nucleus from a higher to a lower energy spin state. This considerably broadens the resonance line. Hydrogen atoms bound to carbon normally have half height widths of a few Hz, but hydrogen atoms bonded to boron have half height widths of 30-60 Hz. This broadening results in poor resolution of proton n.m.r. spectra of compounds containing hydrogen atoms bonded to boron. In practice the septet for ^{10}B bonded hydrogen is usually obscured by background noise.

As mentioned above, ^{10}B has a lower abundance than ^{11}B. It also has a larger quadrupole moment and a lower sensitivity in n.m.r. experiments. In compounds containing boron of natural abundance the n.m.r. signal for ^{10}B nuclei is only about 0.03 times as intense as that of ^{11}B, and it is broader. For this reason ^{10}B n.m.r. spectra are used only to study isotope effects.

^{11}B n.m.r. spectra can provide useful structural information. These spectra are somewhat more difficult to obtain than hydrogen spectra

as the relative sensitivity of the ^{11}B nucleus is only 0.165 that of an equal number of hydrogen nuclei at constant field. Further, the quadrupole moment of the ^{11}B nucleus provides a direct means by which spin-lattice relaxation can occur. Consequently, signals are considerably broadened. In spite of these difficulties satisfactory spectra can be obtained. The interpretation of these spectra is based on the following general rules:

1) Boron bonded only to boron, carbon, nitrogen or halogen atoms (or combinations of these) gives rise to a single resonance.

2) To a first approximation, spin-spin splitting of a ^{11}B resonance arise only from interaction with hydrogen atoms bonded directly to the boron atom in question. However, bridging protons do not cause splittings. If ^{11}B is coupled to a single proton a 1:1 doublet results, with two protons a 1:2:1 triplet; with three protons (as in trimethylaminoborane) a 1:3:3:1 quartet and with four protons (as in sodium borohydride) a 1:4:6:4:1 quintet.

3) In general the value of the coupling constant decreases with an increasing number of hydrogen atoms bonded to boron, due to the decreasing s character of the boron-hydrogen bond.

4.6. Structure Determination by X-ray Methods

4.6.1. General

The following sections are based on material from Glusker and Trueblood[98] and Stout and Jensen[99].

An increase in the apparent visual size of a small object can be achieved with a microscope. The microscope has a lens system for gathering polychromatic light scattered by the object. But the wavelength of light used is long compared to atomic or molecular sizes, therefore light microscopy can not be used to examine objects with dimensions on the atomic or molecular scale. Radiation of wavelength suitable for scattering by particles of atomic size can be employed. This radiation can be in the form of x-rays, thermal neutrons from reactors, or electrons with energies in the 10-50 keV range. X-rays are scattered by electrons in atoms, neutrons by nuclei in atoms, and electrons by atomic electric fields. But in practice no lens systems capable of focusing x-rays or neutrons are known, and electrons in the energy range required can not be focused well enough to provide resolution of individual atoms. Scattering of radiation as employed in optical microscopes, can not, therefore, be used to provide accurate information about structure on the atomic level. However, it is possible to study structure at the atomic and molecular level by employing the diffractive properties of waves.

When monochromatic light is passed through a grating composed of many parallel slits, spaced about the same distance apart as the

wavelength of the light, a diffraction pattern can be observed on a screen behind the grating. This pattern consists of bright and dark lines and can be explained by considering that each slit acts as a light source. The bright lines occur where the light from the series of slits reaches the screen in phase and the dark lines occur where the light waves reaching the screen are out of phase. Further, if the slits are replaced by tiny holes with the same spacing as the slits a similar diffraction pattern is obtained. The diffraction lines are perpendicular to the rows of tiny holes. The sine of the angle at which diffraction maxima are found is inversely proportional to the spacing of the tiny holes, i.e., there is a type of reciprocal relationship between the arrangement of the point light sources (pinholes) and the diffraction pattern obtained.

Now if the original grating consisting of a row of tiny holes is replaced by a grating with many rows of tiny holes a diffraction pattern consisting of dots, not lines, is obtained, Figure XXV. The dots occur at places where the light from the point sources reaches the screen in phase, and the dark areas between the dots occur at places where the light reaching the screen is out of phase. Again, the sine of the angle at which the diffraction maxima occur is inversely proportional to the spacing of the point sources. Stated another way, the diffraction pattern obtained from a particular lattice of point sources can be shown to be the reciprocal of that lattice. This reciprocal arrangement holds for a three dimensional array of

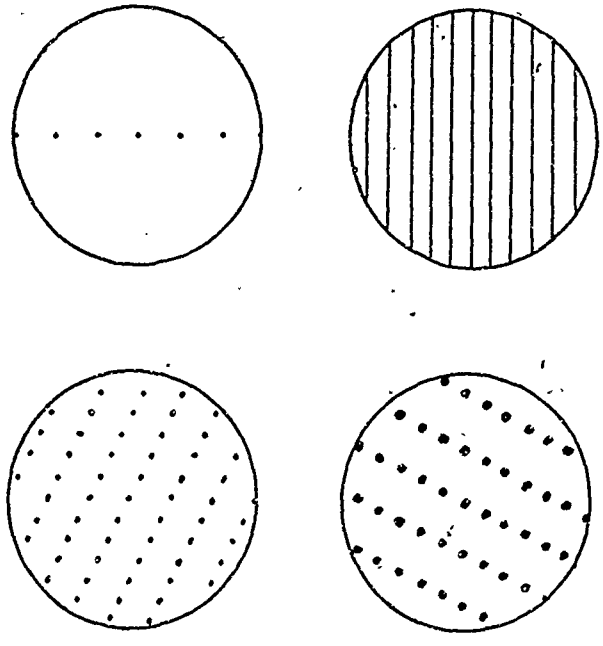

Figure XXV

Diffraction Patterns Resulting from One and Two Dimensional Arrays of Point Sources

point sources as well as the two dimensional array described above.

A crystal is composed of atoms arranged in a regular repetitive array. The crystal can be considered as a three dimensional diffraction grating. A lattice which is the reciprocal of the original crystal lattice can once again be used to describe the diffraction pattern resulting on irradiation of the crystal with monochromatic x-ray radiation.

There are certain specific conditions which must be met before a beam of x-rays is diffracted by a crystal. These conditions are commonly stated in terms of the Miller indices of planes within the

unit cell. The shape of the crystal unit cell is expressed in terms of the axial lengths, a, b and c and the interaxial angles. α is the angle between b and c, β is the angle between a and c, and γ is the angle between a and b. Bragg's condition for diffraction to occur is expressed by

$$2d_{hkl}\sin\theta_{hkl} = \lambda \qquad (4.1)$$

Here λ is the wavelength of radiation employed, θ_{hkl} is one-half the angle between the incident and diffracted x-ray beams and d_{hkl} is the distance between the parallel sets of planes defined by the Miller indices h,k and l. The set of planes designated by h, k and l intersect the a axis at a/h, the b axis at b/k and the c axis at c/l. The Miller indices may have only integral values.

The diffraction pattern obtained by using the crystal as a diffraction grating has axial dimensions of a*, b* and c* and interaxial angles as above of α^*, β^* and γ^*. The relationships between the crystal unit cell and the lattice of the diffraction pattern can be stated in vector algebra notation as

$$\vec{a}^*\cdot\vec{a} = \vec{b}^*\cdot\vec{b} = \vec{c}^*\cdot\vec{c} = 1 \qquad (4.2)$$

$$\vec{a}\cdot\vec{b}^* = \vec{a}\cdot\vec{c}^* = \vec{b}\cdot\vec{a}^* = \vec{b}\cdot\vec{c}^* = \vec{c}\cdot\vec{a}^* = \vec{c}\cdot\vec{b}^* = 0 \qquad (4.3)$$

From the above it can be seen that $\vec{a}^*$ is perpendicular to the $\vec{b}\cdot\vec{c}$ plane. $\vec{a}^*$ can also be given by

$$\vec{a}^* = \frac{\vec{b}\times\vec{c}}{\vec{a}\cdot(\vec{b}\times\vec{c})} \qquad (4.4)$$

A number of points may now be stressed.

1) The diffraction pattern obtained from a single crystal composed of a large number of unit cells can be considered to be a scaled up sampling of the diffraction pattern of the unit cell.

2) The angles at which diffraction maxima occur depend only on the lattice of the diffracting crystal, not the contents of the unit cell.

3) The axial lengths and interaxial angles of the unit cell can be obtained by measurement of the diffraction pattern.

4) The reciprocal lattice has the same symmetry as the direct lattice.

5) The positions of the diffraction maxima give only information about the dimensions and symmetry of the unit cell. The intensities of the maxima contain information about the contents of the unit cell.

4.6.2. Recording the Diffraction Pattern

The x-rays diffracted by a crystal are usually collected by a photographic plate or by a scintillation counter mounted on a diffractometer. Each method has its advantages. The film method can be used to gather many diffraction points at one time whereas the

counter method observes only one point at a time. However the counter method allows accurate measurement of intensities, which the film method does not. The film method allows the researcher to establish rapidly the geometry of the unit cell.

Photographic cameras are normally of three types.

1) Oscillation Camera. This device oscillates a crystal about an axis perpendicular to the x-ray beam. The resulting diffraction pattern is recorded on a film held in a cylindrical cassete with the axis of the cylinder colinear with the oscillation axis of the crystal. The pattern obtained consists of dots in rows called layer lines. Each layer line is one layer of reciprocal space, projected edgewise.

2) Weissenberg Camera. This device is based on the oscillation camera. One row of dots, i.e., one layer of reciprocal space is collected by placing a slotted screen between crystal and film. The film holder is given a translational motion along the axis of the crystal oscillation. By this method one of the layer lines obtained from an oscillation photograph is spread over the two dimensional film. By positioning the screen to allow only the desired layer line to reach the film, zero, first, second, etc., layer Weissenberg photographs are obtained. Each of these photographs gives a distorted view of a reciprocal lattice plane.

3) Precession Camera. This camera provides a powerful photographic technique in that it allows the undistorted recording of one layer of reciprocal space. The film result may be interpreted in

a very simple manner. The crystal is mounted in such a fashion that one of its axes is allowed to precess about the axis of a beam of x-rays. The film holder is also allowed to precess in such a manner that one layer of reciprocal space is always parallel to the film, i.e., the precessing crystal axis is perpendicular to the film. An annular screen is used to exclude all reciprocal lattice layers but one.

The oscillation photograph can be used to obtain the length of one real axis; the Weissenberg photograph yields two reciprocal axial lengths and a reciprocal interaxial angle, as does the precession photograph. Both Weissenberg and precession photographs yield symmetry information, but the precession photograph is much easier to interpret.

A scintillation counter is employed as an integral part of a diffractometer. The diffractometer has four axes which allow the crystal to be aligned so that the diffracted beam from any set of crystal planes can be collected by the counter. Thus it is possible to measure the intensity of a reflection as well as its position.

The crystallographer is concerned with the symmetry of crystals. By an examination of the diffraction pattern of a crystal it is possible to determine which of the seven crystal systems (cubic, hexagonal, rhombohedral, tetragonal, orthorhombic, monoclinic or triclinic, can be used to describe the crystal. It is also possible to determine whether the crystal unit cell is primitive, i.e., contains one lattice point per unit cell, or non-primitive. Finally it

is possible to determine which of the 230 space groups will describe the symmetry of the crystal structure. Once the space group is determined the equivalent positions within the unit cell are known. These are the symmetry related positions. For example with eight equivalent positions in a unit cell one atom can be placed and the other seven generated by symmetry. Thus the structure factor calculation, refinement and the Fourier synthesis need only be carried out for the asymmetric unit within the unit cell. Knowledge of the point group is also a necessary prerequisite to the use of the Patterson function as a tool in placing heavy atoms within the unit cell.

4.6.3. Structure Determination

The accurate measurement of intensity data is of paramount importance in determining the positions of atoms within the unit cell. A general expression for the intensity of a specific reflection is given by

$$\text{Intensity} = (K)|F|^2(Lp)(Tv)(Abs) \qquad (4.5)$$

The term (Lp) represents two factors. The first is called the Lorentz factor. During data collection the crystal is rotated or precessed at a constant rate, but the rate at which two different sets of crystal planes pass through the diffraction condition may be quite different. This has an effect on the intensity. The second factor is the polarization factor. This accounts for the decrease in intensity caused by the partial polarization of the diffracted beam by the crystal. The

Lorentz and polarization factors depend only on some function of the angle θ and can be calculated without knowledge of the atomic arrangement within the unit cell.

The term (Abs) is an absorption correction and it arises because two different diffracted beams may travel quite different lengths of path within the crystal.

This correction requires a calculation of the length of path followed by the x-ray beam through the crystal, and thus a knowledge of the dimensions and orientation of the crystal. Calculation of the absorption correction is quite time consuming, therefore the (Abs) term is not always employed.

The effect of the term (Tv) is to reduce the scattering power of a given atom in the direction of diffraction. This reduction arises due to the spreading out of the electron density of an atom by thermal motion.

(K) is a scale factor. The intensities of the various reflections are measured relative to some standard reflection and the scale factor converts the relative intensities to absolute intensities. The first order estimation of this quantity does not require a knowledge of the positions of atoms within the unit cell. It is determined by comparing average observed intensities with the theoretically expected intensities for a cell of the same contents.

The term $|F|^2$ is the quantity which relates the intensity of the diffraction maxima to the arrangement of the atoms within the unit cell.

The vector $\vec{F}_{hkl}$ is called the structure factor and is used to represent the resultant of the many individual waves scattered in a specific direction by the crystal. $\vec{F}$ can be represented exponentially $\vec{F}_{hkl} = |F_{hkl}| e^{i\alpha(hkl)}$, where $|F_{hkl}|$ is the amplitude of the resultant wave and α is its phase, or as a complex number, $\vec{F}_{hkl} = A_{hkl} + i B_{hkl}$. Both representations are employed in the solution of the crystallographic problem. For a particular reflection the structure factor amplitude is given by

$$|F_{hkl}| = \sqrt{A_{hkl}^2 + B_{hkl}^2} \tag{4.6}$$

where $$A_{hkl} = \sum_j f_j \cos 2\pi (hx_j + ky_j + lz_j) \tag{4.7}$$

and $$B_{hkl} = \sum_j f_j \sin 2\pi (hx_j + ky_j + lz_j) \tag{4.8}$$

Each summation is carried out over all the j atoms in the unit cell. The coordinates of each atom in the unit cell are given by x_j, y_j and z_j, while h, k and l are the Miller indices corresponding to the particular reflection. f_j is the amplitude of the scattering factor for the jth atom. The scattering power of an atom is highest in the direction of the incident beam and falls off as the angle of diffraction increases. This decrease is due to the discrete size of the electronic cloud of the atom, i.e., only in the direction of the incident beam does the whole atom scatter in phase. The scattering factor of an atom is usually related to the scattering power of a single electron. It has a value equal to the atomic number in the

direction of the incident beam and falls off as a function of 0. The temperature correction mentioned above (Tv) is applied to the f_j term and has the effect of reducing f_j. The proper scattering factor for the jth atom can be given as

$$f_j = f_o e^{\frac{-B(\sin^2\theta)}{\lambda^2}} \qquad (4.9)$$

where 0 and have the usual meanings and

$$B = 8\pi^2\mu^2 \qquad (4.10)$$

where μ^2 is the mean square amplitude of atomic vibration. fo is the atomic scattering factor without correction for thermal vibration.

If the positions of atoms in the unit cell were known it would be possible to calculate the intensities of all reflections. However, the crystallographer begins with the intensities and calculates the structure factor amplitude, $|F|$, from these. This amplitude is termed $|F|_{obs}$. A Fourier synthesis using these $|F|_{obs}$ values could then be carried out to obtain a map of the electron density of the unit cell if one more factor were known.

The electron density at a point x, y, z in the unit cell is given by the Fourier summation

$$\rho(xyz) = \frac{1}{V_c} \sum_{\text{all}} \sum_{h,k,l} \sum |F| \cos\left[2\pi(hx + ky + lz) - \alpha\right] \qquad (4.11)$$

V_c is the volume of the unit cell and the triple summation is carried out over all values of h, k and l. $|F|$ is the value of the

structure factor amplitude for a particular set of h, k and l, and is simply the $|F|_{obs}$ value. Thus if α were known it would be possible to calculate the electron density ρ, at all points x, y and z, or rather, to prepare three dimensional electron density maps.

α, the phase angle, should not be confused with the α used to describe a real unit cell interaxial angle. α can be represented graphically by Figure XXVI, which also shows the relationship of the structure factor to the A and B terms of equation (4.6).

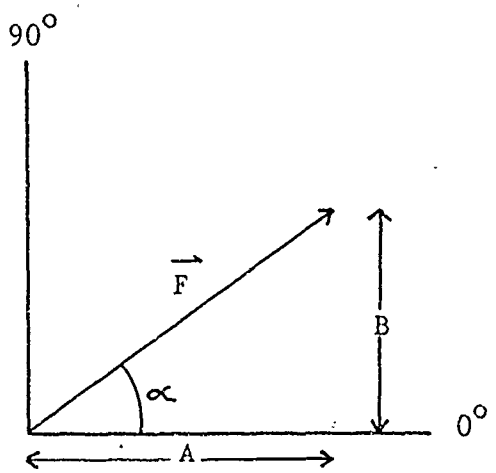

Figure XXVI

The Structure Factor F and the Phase Angle

The necessity to consider the phase angle α arises from the fact that not all, or perhaps none, of the atoms which scatter to give rise to a particular hkl reflection lie on that set of Miller planes. Atoms which lie off the plane will scatter x-radiation with a phase difference from those atoms which lie on the plane. The phase difference is proportional to the perpendicular distance from the plane to the atom in question.

The structure or $\overrightarrow{F}_{hkl}$ for a particular set of planes

is actually the vector sum of the structure factors of the individual atoms giving rise to the hkl reflection. This is shown for three atoms in Figure XXVII, where the individual atomic structure factors are f_1, f_2 and f_3.

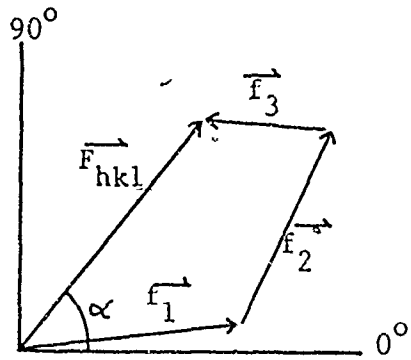

Figure XXVII

The Individual Atomic Structure Factors and the Overall Structure Factor

From Figure XXVI it can be seen that

$$\tan \alpha = \frac{B}{A} \qquad (4.12)$$

Thus both A and B must be evaluated before α can be determined. A and B can be evaluated from equations (4.7) and (4.8) if the atomic positions are known. In practice the crystallographer makes educated guesses about the positions of one or more atoms in the unit cell and calculates a set of structure factor amplitudes. If the guess is a good one the $|F|_{calc}$ values approximate the $|F|_{obs}$ values. The α values obtained, used in conjunction with the $|F|_{obs}$ values, allow computation of a Fourier map which is biased toward the correct solution by use of the $|F|_{obs}$ values.

To choose the initial atom positions a Patterson function is frequently employed. The Patterson function is given by

$$P_{(uvw)} = \frac{1}{V_c} \sum_{all} \sum_{h,k,l} |F|^2 \cos 2\pi(hu + kv + lw) \qquad (4.13)$$

and is evaluated at all points in space to yield a Patterson map. The Patterson function is actually a Fourier series for which only h, k and l, plus the $|F|_{obs}$ values are needed. The resulting map is the sum of the appearances of the structure when viewed from each atom in turn. The peaks in the map correspond to vectors originating at one atom and terminating at another. The size of the peak is proportional to the products of the atomic numbers of the atoms at which the vector begins and terminates. Thus peaks corresponding to vectors between two heavy atoms are large and can usually be readily picked out. A careful study of these large peaks often allows the heavy atoms to be placed approximately in the unit cell. The $|F|^2$ values do not contain any phase information, therefore, the Patterson function resulting from their use contains less information about the unit cell than does the Fourier function. As a result the Patterson function belongs to only one of 24 space groups while the real crystal can be one of 230 space groups. The space group of the Patterson function can be derived by replacing screw axes with rotation axes, glide planes with mirror planes and adding a center of symmetry. The Patterson map contains N^2 peaks for the N atoms in the unit cell. As

the Patterson cell is the same size as the unit cell a considerable number of peaks may overlap. Thus, a variety of trial structures may correspond well with the gross features of the Patterson function but be incorrect solutions to the crystallographic problem.

If a heavy atom is present in a cell the phase angle α determined on the basis of the heavy atom alone will be close to the proper phase angle for the particular reflection. A graphical representation of this is shown in Figure XXVIII.

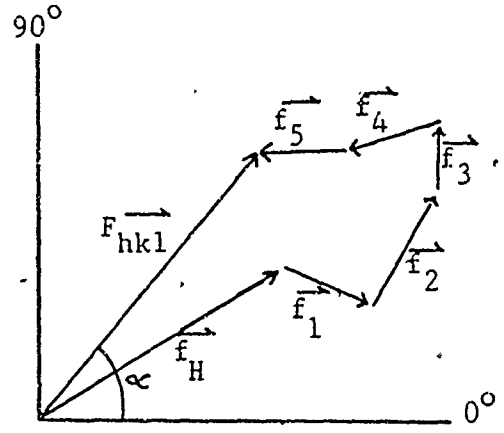

Figure XXVIII

The Heavy Atom Scattering Factor

The individual atomic scattering factors sum to give the overall scattering factor for the reflection. The scattering factor for the heavy atom, $\vec{f}_H$, is usually fairly close to the total scattering factor as regards the phase angle α. Therefore if a heavy atom is placed correctly the structure factor amplitudes calculated on the basis of the heavy atom, $|F|_{calc}$, will approximate the observed structure factor amplitudes $|F|_{obs}$.

A measure of the validity of a structure is the discrepancy

index, R, given by

$$R = \frac{\sum(|F|_{obs} - |F|_{calc})}{\sum(|F|_{obs})} \qquad (4.14)$$

At present R values in the range 0.08 to 0.03 or lower are considered to indicate reliable structure determination.

Structure refinement is carried out via two methods, both of which are commonly used. The first employs a Difference Fourier synthesis. This is a Fourier synthesis employing $(|F|_{obs} - |F|_{calc})$ rather than $|F|_{obs}$. If the structure is correct the difference map is virtually featureless, with only minor, random undulations.

The method of least squares is also widely applied in the refinement of crystal structures. With this method the parameters which are employed in the computation of the calculated structure factor $|F|_{calc}$, are varied in such a way as to minimize the quantity Q, defined by

$$Q = \sum\left[W_{hkl}(\triangle|F_{hkl}|)^2\right] \qquad (4.15)$$

Here $\triangle|F_{hkl}| = |F|_{obs} - |F|_{calc}$ and $(W_{hkl})^{-\frac{1}{2}}$ is the standard deviation of the experimental value of $|F|_{obs}$.

As many as nine parameters can be used for each atom (three positional and six to define a thermal ellipsoid), therefore, including the general scale factor, equation (4.15) must be minimized for (9N+1)

parameters for N atoms. This process results in (9N+1) simultaneous equations, demanding at least this number of observations. A more suitable number of observations is usually 5(9N+1) to 10(9N+1), since the intensities of the observation maxima usually have significant experimental uncertainty.

The equations derived from (4:15) are not linear; they contain both trigonometric and exponential functions. The method of least squares requires linear equations. If the total structure is a reasonable approximation of the true structure a set of linear equations can be derived in which the variables are the shifts of trial parameters rather than the parameters themselves. The shifts are then calculated by the method of least squares.

4.7. Objects of the Research

The objects of the research in boron chemistry were twofold. First, to attempt to synthesize compounds of the type $R_2M_{III}B_5H_8$, where R is an alkyl group and M_{III} a group IIIA element, and second, to determine the crystal structure of bis(diethylamino)dithiaboretane by x-ray methods.

CHAPTER V

EXPERIMENTAL

Bridge Substitution in Pentaborane(9)

The Crystal Structure of Bis(diethylamino)dithiaboretane

5. Experimental

5.1. Bridge Substitution in Pentaborane(9)

5.1.1. Chemicals, Instrumentation and Techniques

The identification and purity of chemicals employed was determined by spectroscopic techniques. Mass spectra were obtained on a Hitachi Perkin-Elmer RMU-6E double focusing spectrometer at an ionization chamber potential of 70 eV. Infrared spectra were recorded between 4000 cm^{-1} and 600 cm^{-1} on a Perkin-Elmer 337 spectrometer as either nujol mulls between sodium chloride plates or as gas samples in a 10 cm path length cell fitted with sodium chloride windows. Proton magnetic resonance spectra were obtained using either the Perkin-Elmer model R12A spectrometer noted in 2.1.2. above or with the Varian HA. 60 I.L. instrument mentioned in the same section. The Varian machine was also used for ^{11}B spectra, at a frequency of 19.250 MHz.

Due to the pyrophoric and hydrolytic nature of some of the chemicals, high vacuum and inert atmosphere techniques were employed throughout the research. Except where indicated, vacuum manipulations were carried out in the manner described by Sanderson[100], and Shriver[101]. Low temperature baths employed were liquid nitrogen (-196 °C), petroleum ether slush (-140 °C), toluene slush (-95 °C), dry ice-acetone (-78 °C), chloroform slush (-63 °C), chlorobenzene slush (-45 °C), bromobenzene slush (-31 °C) and carbon tetrachloride

slush (-23 °C).

A Labconço fiberglass glove box with an evacuable port was employed in the transfer of nonvolatile materials. A nitrogen atmosphere, slightly above ambient pressure, was maintained in the box by the evaporation of liquid nitrogen into it through a molecular sieve drying train. The glove box atmosphere was recirculated continuously through a molecular sieve drying train.

5.1.2. Preparations

5.1.2.1. The Preparation of Diborane(6)

The apparatus employed in the preparation of diborane(6) is shown in Figure XXIX. The method employed was that of Shapiro et al[102] which involved the reaction of lithium aluminum hydride with boron trifluoride, as the etherate. The reaction proceeds in two steps:

$$BF_3 + LiAlH_4 \longrightarrow LiBH_4 + AlF_3$$

$$BF_3 + 3LiBH_4 \longrightarrow 2B_2H_6 + 3LiF$$

The overall reaction is given by:

$$4BF_3 + 3LiAlH_4 \longrightarrow 2B_2H_6 + 3LiF + 3AlF_3$$

Yields are virtually quantitative.

As an example of an actual preparation, the apparatus in Figure XXIX was flushed with hydrogen and then lithium aluminum hydride

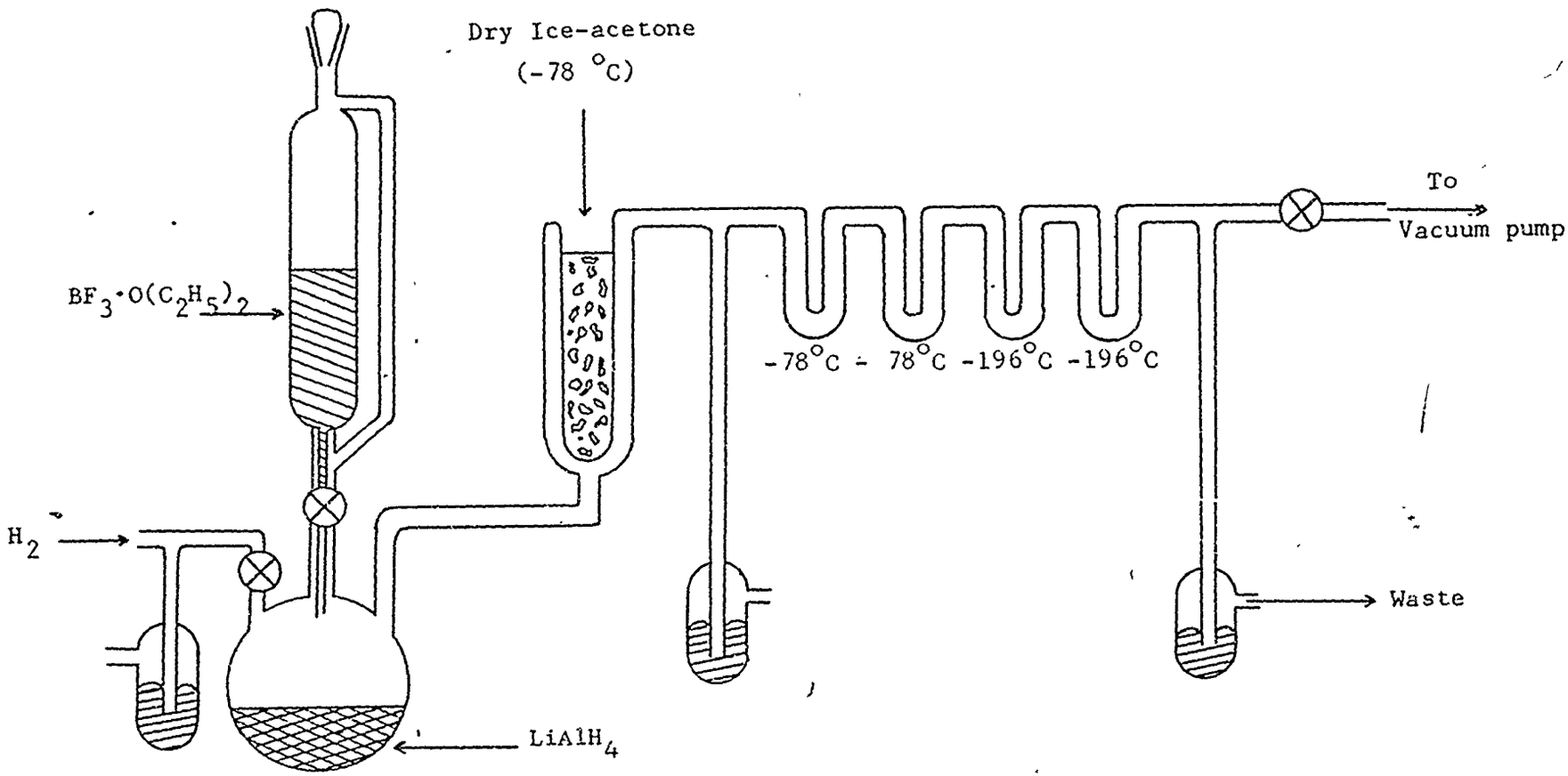

Figure XXIX

Apparatus Employed in the Preparation of Diborane(6)

(12.5 g, 0.33 moles) was placed in the flask followed by 200 ml anhydrous diethyl ether. The system was flushed slowly with hydrogen to remove all traces of air. Boron trifluoride-diethyl etherate (70ml, density 1.125 g/ml, 79 g, 0.56 moles) was placed in the dropping funnel. The etherate was added dropwise during a period of about three hours to the stirred lithium aluminum hydride ether mixture. The hydrogen flow was turned off during the addition of the etherate as it was found that when the flow was on ether was forced through the dry ice-acetone cold trap. On completion of the reaction, the system was gently flushed with hydrogen for about thirty minutes. The diborane(6) reaction product was purified by passing it through two traps cooled to -140 °C. Diborane (6) will pass through traps at this temperature whereas diethyl ether will not. The diborane(6) was shown to be free of impurities by mass and infrared spectra.

5.1.2.2. The Preparation of Pentaborane(9)

The majority of methods for the preparation of pentaborane(9) are of industrial importance only[37,45], and can not be readily adapted to laboratory scale preparations. A laboratory method of decomposing diborane(6) in a single pass silent electric discharge was reported by Kotlensky and Schaeffer[103]. One of the products obtained, in about 20% yield, was pentaborane(9).

A schematic diagram of the all glass, circulating type, silent electric discharge apparatus employed in this research is shown in

Figure XXX. The apparatus consisted of a discharge tube, a pump, a product condensation trap, a ballast section which increased volume and promoted mixing and a Torricelli manometer. The pump was an all glass double stroke type. The piston, a cylinder of iron enclosed in glass, was moved by an external permanent magnet attached to a motor. The valves were microscope cover glasses. The discharge section consisted of two concentric tubes, 15 and 20 mm in diameter, one meter in length. The outer tube was wrapped with brass shim stock and the inner was filled with 1 M cupric sulphate solution. An a.c. potential was applied between the inner and outer tubes by means of a 30 kV, 15 mA, fluorescent tube transformer (Allanson Manufacturing Corp., Toronto, Canada). A number of small indentations in the outer tube were required to steady the inner tube, as there was considerable vibration during operation.

Diborane(6) was subjected to the silent discharge. After three and one-quarter hours, the pressure had decreased from 575 Torr to 517 Torr. The pressure then began to rise until, after one hundred and sixteen hours, it reached 864 Torr. An increase in pressure was expected, due to hydrogen production, for the formation of all the boranes except tetraborane(10) and pentaborane(11). An infrared spectrum of the material formed after three and one-quarter hours running time showed this material to be rich in tetraborane(10). This finding is discussed in more detail in reference (104).

After cooling the product condensation trap to -196 ^{o}C the

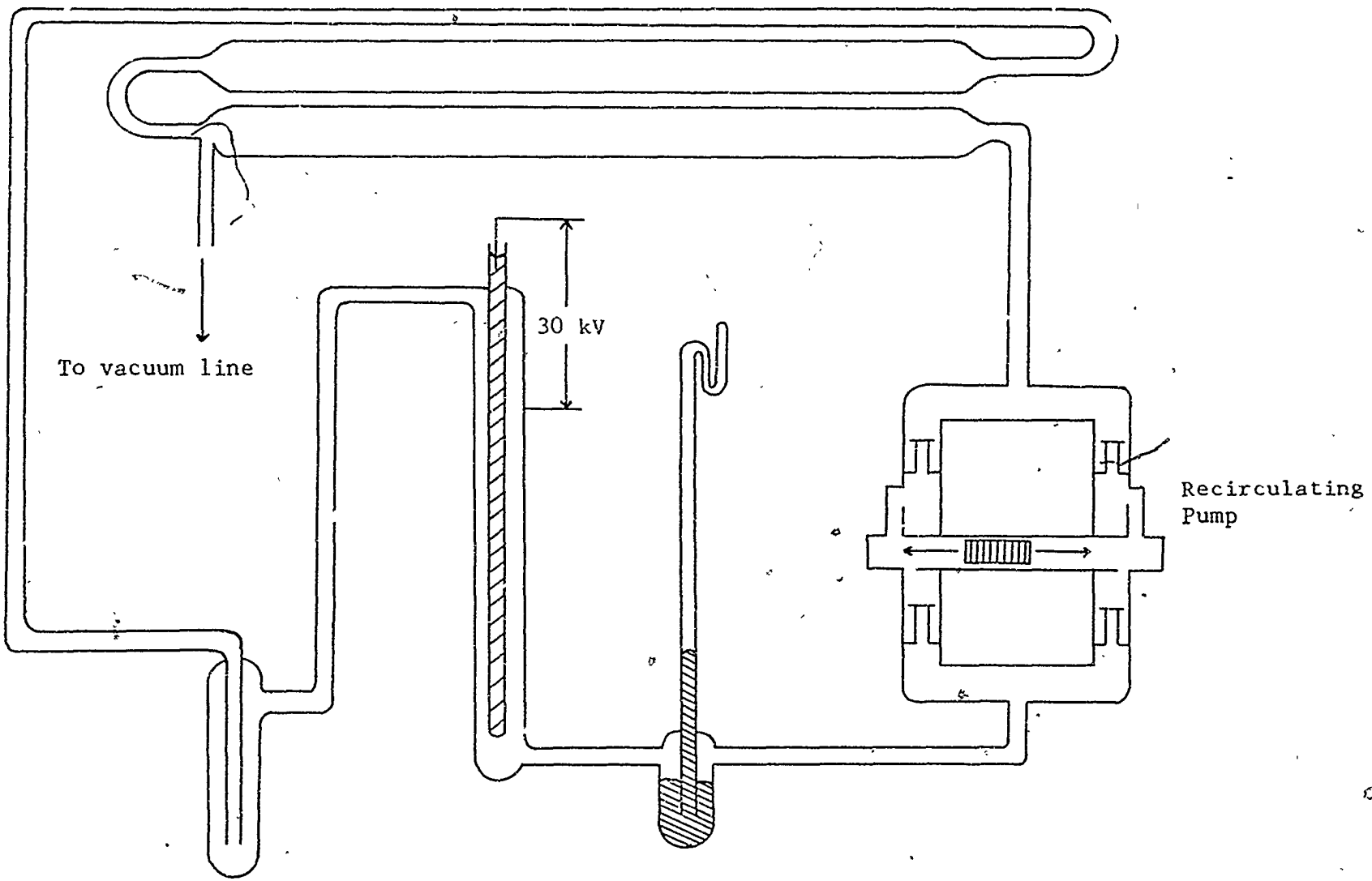

Figure XXX

Silent Electric Discharge Apparatus

hydrogen produced in the discharge apparatus was removed. The product condensation trap was slowly warmed to room temperature while the volatile products were passed through traps cooled to -63 °C and -140 °C and condensed into traps cooled to -196 °C. Less than 1 liquid ml condensed in the trap cooled to -63 °C. This material was removed from the vacuum line and stored. The traps cooled to -196 °C were empty, and only a trace of diborane(6) was found in the products condensed in the traps cooled to -140 °C. Therefore it was felt the conversion of diborane(6) to higher boranes was virtually complete. The contents of the traps cooled to -140 °C, about 5 liquid ml, were slowly passed through traps maintained at -95 °C. This distillation served to remove the more volatile tetraborane(10), which amounted to about 4 ml. The material retained in the -95 °C trap was then passed repeatedly through traps at -78 °C in an attempt to separate pentaborane(9) from pentaborane(11). Eventually 1.6 mmol pentaborane(9) was obtained. This represented about a 2% yield on the basis of

$$5B_2H_6 \longrightarrow 2B_5H_9 + 6H_2$$

The three boranes (B_4H_{10}, B_5H_9 and B_5H_{11}) were identified by their infrared spectra[105]. These spectra indicated that the reaction products were contaminated with diborane(6).

In view of the low yield of pentaborane(9) it was decided to obtain pentaborane(9) from a commercial source. The Callery Chemical Co. of Callery, Pennsylvania, was able to supply this borane in large

quantities. As mass, infrared and nuclear magnetic resonance spectra established that the commercial product was free of impurities, it was employed as supplied in subsequent experiments. The infrared and nuclear magnetic resonance spectra are reproduced in Appendix II as IR I, NMR I and NMR VIII.

5.1.2.3. Lithium Octahydropentaborate(1-) Preparation and Properties

This preparation was based on the method of Gaines and Iorns[63], namely

$$LiCH_3 + B_5H_9 \longrightarrow LiB_5H_8 + CH_4$$

They carried out this reaction in diethyl ether at temperatures varying from -78 °C to -30 °C. As it is difficult to separate pentaborane(9) from diethyl ether by fractional condensation dimethyl ether (B.P. -25 °C) was used in the present work as reaction solvent.

The concentration of the methyllithium (Alfa Inorganics) employed in this and other preparations was determined by hydrolyzing a known volume of methyllithium solution

$$LiCH_3 + H_2O \longrightarrow LiOH + CH_4$$

and determining the quantity of methane produced after transferring the methane to a standard volume with a Toeppler pump.

The apparatus used in the preparation of LiB_5H_8 is shown in Figure XXXI. In a typical preparation the reaction flask was evacuated, then filled to atmospheric pressure with dry nitrogen. Methyllithium (5.0 ml, 2.3 M in diethyl ether, 11 mmol) was syringed into the flask.

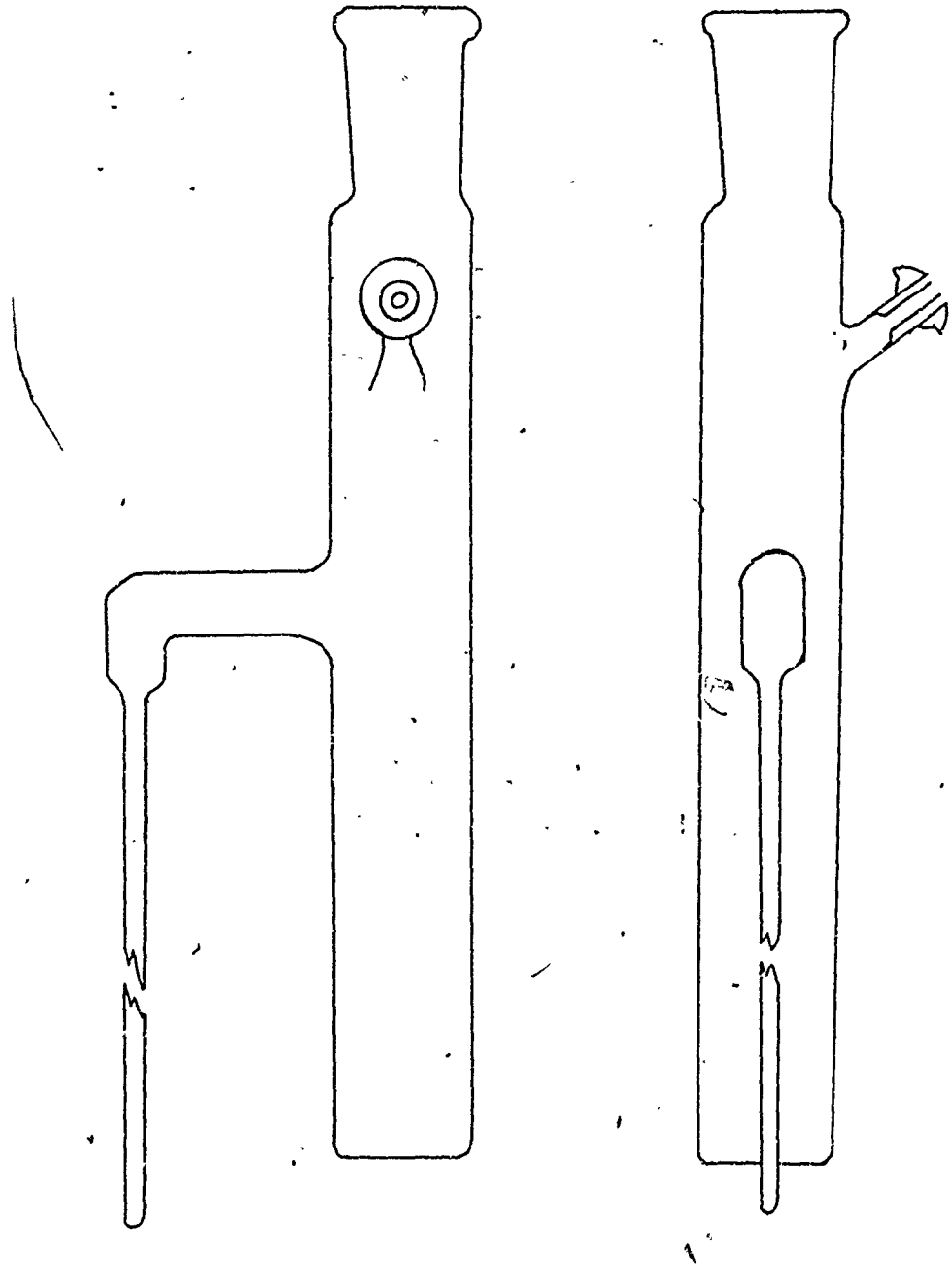

Figure XXXI

The flask was cooled carefully to -196 °C, evacuated and slowly warmed to room temperature. During the warming step the diethyl ether was removed by distillation. The reaction flask was cooled again to -196 °C and dimethyl ether (0.1 moles) followed by pentaborane(9) (10.0 mmol) condensed onto the methyllithium. The flask was warmed to -78 °C for fifteen minutes, then to -45 °C for an additional forty-five minutes. The methane produced (9.8 mmol) corresponded to a 98% yield of lithium octahydropentaborate(1-). The methane was identified by mass and infrared spectra. The reaction flask was allowed to stand at -45 °C until the lithium hydroxide had settled. The entire flask, including the n.m.r. tube, was cooled to -78 °C and the liquid decanted into the n.m.r. tube. Both the n.m.r. tube and the reaction flask were then cooled to -196 °C and the n.m.r. tube sealed off and removed. The ^{1}H and ^{11}B magnetic resonance spectra of lithium octahydropentaborate are shown in Appendix II as NMR II and NMR IX.

Many other preparations similar to the above were conducted in an attempt to become familiar with some of the properties of LiB_5H_8. In one of these experiments, employing 10 mmol of pentaborane(9) and 11 mmol of methyllithium, the solvent was removed by pumping for eighteen hours on a sample maintained at -30 °C. It was found that all but 7 mmol of solvent were removed after two and one-half hours and all but 5 mmol after eighteen hours. Thus after prolonged pumping the molar ratio of octahydropentaborate(1-) to solvent

was 2:1, indicating strong solvation. The material in the flask became viscous and after a time resembled modelling clay in consistency. The flask was cooled to -196 °C, removed to the dry box where a sample of the clay-like material was taken and an infrared spectrum obtained as quickly as possible (about fifteen minutes). The spectrum was redetermined after twenty-four hours. These spectra are shown in Appendix II as IR IIa and IR IIb.

Apparently removal of solvent led to decomposition of the lithium octahydropentaborate(1-). To test this hypothesis the experiment was repeated. After solvent removal the reaction flask was cooled to -196 °C, and the solvent was replaced, followed by anhydrous hydrogen chloride (20.0 mmol). Gaines and Iorns regenerated pentaborane(9) in this way[63].

$$LiB_5H_8 + HCl \longrightarrow LiCl + B_5H_9$$

However in the present work pentaborane(9) could not be regenerated after solvent had been removed. Hydrogen gas was evolved instead, indicating decomposition.

5.1.2.4. The Preparation of μ-dimethylborylpentaborane(9)

To gain familiarity with the general type of preparation which would be employed in the attempts to prepare higher members of the bridged group IIIA -pentaborane(9) species μ-dimethylborylpentaborane (9) was prepared. The original preparation was reported by Gaines and Iorns[81] who reacted lithium octahydropentaborate(1-) with di-

methylboron chloride at temperatures between -78 °C and -40 °C in diethyl ether. They characterized the product by mass, infrared, ^{1}H and ^{11}B n.m.r. spectra.

The reaction flask used in this preparation was similar to that shown in Figure XXXI without the n.m.r. tube. Lithium octahydropentaborate(1-) was prepared by reacting methyllithium (11 mmol) with pentaborane(9) (10.0 mmol) in 0.12 moles of dimethyl ether. Methane production corresponded to a 94% yield of lithium octahydropentaborate(1-).

Dimethylboron bromide (Alfa Inorganics) was tested for purity by mass spectrometry. Ten mmol of this material was condensed into a reaction flask cooled to -196 °C. On warming the reaction flask to -78 °C the solution of octahydropentaborate in dimethyl ether remained solid but the dimethylboron bromide melted. The flask was warmed to -45 °C and maintained at this temperature, with stirring, for one hour. The solution turned yellow-orange and the vapor pressure above the solution varied from 225 to 260 Torr. (Expected for dimethyl ether at -45 °C is 283 Torr.)

A distillation was carried out while allowing the flask to warm from -45 °C to room temperature over a two hour period. The volatile materials were pumped through a distillation train made up of two traps cooled to -63 °C, one cooled to -78 °C and two cooled to -196 °C. The material found in the coldest traps was shown, by vapor pressure measurements, to be pure dimethyl ether. The material in the three higher

temperature traps was condensed into an n.m.r. tube which was sealed by flame and removed from the vacuum line. Proton n.m.r. and ^{11}B n.m.r. spectra were obtained at -20 °C. These spectra, reproduced in Appendix II as NMR III and NMR X, establish by comparison with published spectra[81], that the compound prepared was μ-dimethylborylpentaborane(9).

5.1.2.5. The Attempted Preparation of μ-dimethylaluminumpentaborane(9)

The apparatus used in the attempt to prepare μ-diethylaluminumpentaborane(9) was identical to that used to prepare μ-dimethylborylpentaborane(9). The octahydropentaborate(1-) was prepared as previously described, by reacting methyllithium (11 mmol) with pentaborane(9) (10 mmol) in dimethyl ether. The methane produced corresponded to a 97% yield of lithium octahydropentaborate(1-).

The reaction flask was cooled to -196 °C and dry nitrogen introduced. Diethylaluminum chloride (Texas Alkyls) (1.5 ml, density 0.961 g/ml, 1.44 g, 12 mmol) was syringed into the flask which was then evacuated. The flask was warmed to -45 °C, and the viscous solution was stirred for one hour. The only volatile material obtained by distillation from the reaction flask at -45 °C was dimethyl ether, which was identified by its mass spectrum. As in the case of μ-dimethylborylpentaborane(9), the reaction flask was warmed slowly to room temperature while its contents were transferred to traps cooled to -196 °C. After two hours some material was found in the first cold

trap. A distillation was carried out by warming this trap to -31 °C and passing the gas through two traps cooled to -95 °C into two traps cooled to -196 °C. The first -196 °C trap contained dimethyl ether, while the first -95 °C trap contained 0.8 mmol triethylborane. Both materials were identified by infrared spectroscopy.

The reaction flask containing the paste-like residue was removed to the dry box, opened and a sample drawn. An infrared spectrum of this residue, IR III in Appendix II, had some absorptions in common with those of IR II, i.e., the decomposition products of lithium-octahydropentaborate(1-). As some of the other absorptions might have been due to diethylaluminum chloride, an infrared spectrum of this material was obtained. This spectrum, IR IV in Appendix II, did not correlate with the reaction product spectrum. A sample of diethyl-aluminum chloride-dimethyl etherate was prepared by reacting diethyl-aluminum chloride with excess dimethyl ether at -45 °C. The infrared spectrum of the etherate, IR V in Appendix II, did show absorptions in common with those of the reaction product. The above spectra, IR II, III, IV and V will be discussed below.

5.1.2.6. The Attempted Preparation of μ-dimethylthalliumpentaborane(9)

The reaction flask shown in Figure XXXII was employed in this attempted preparation. The flask was designed to allow generation of lithium octahydropentaborate(1-) as in 5.1.2.3., followed by the addition of dimethylthallium bromide as a powder by rotating the

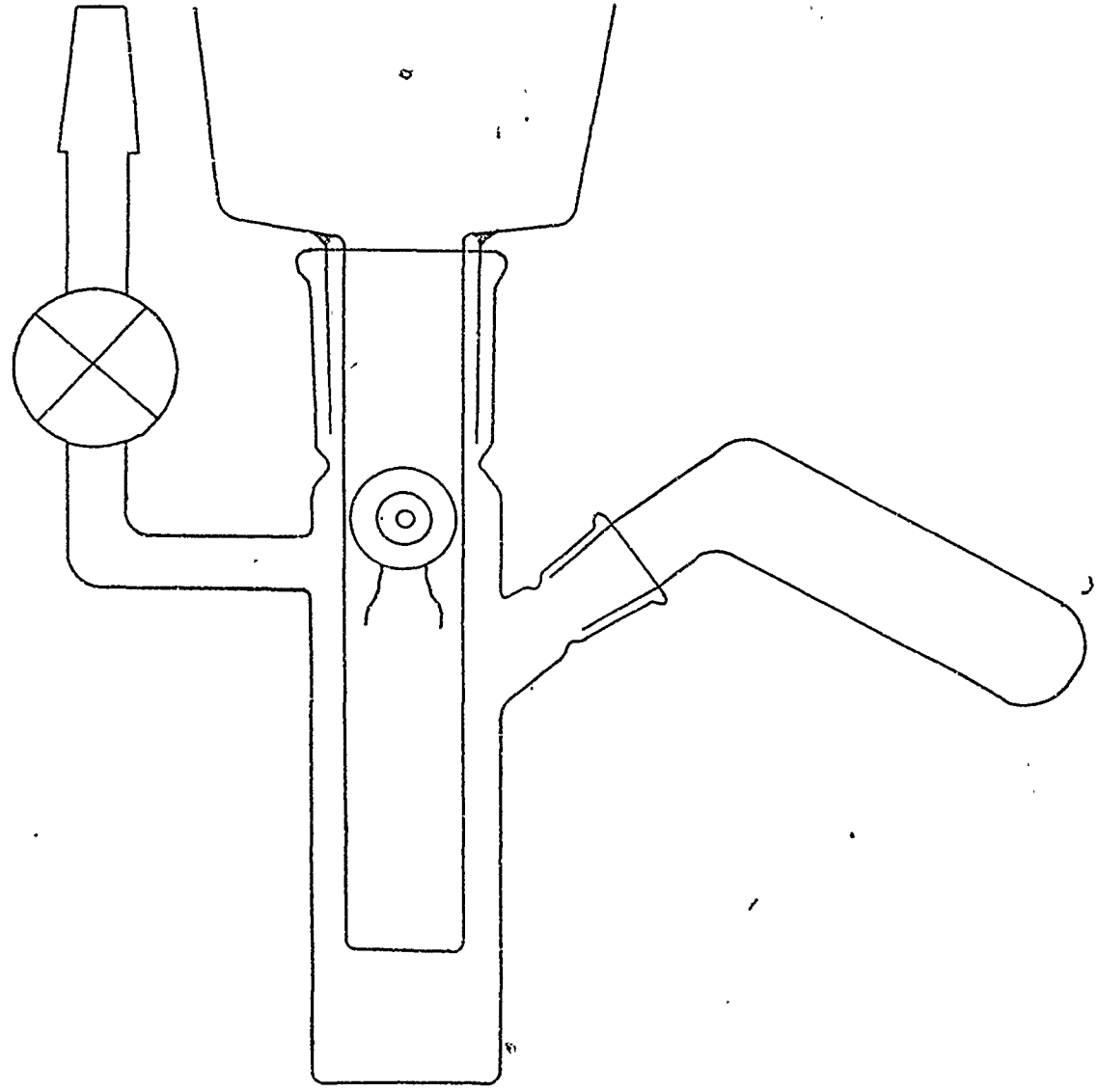

Figure XXXII

Reaction Flask Employed in the Attempted Preparation of

μ-dimethylthalliumpentaborane(9)

side arm. Since the desired product would have a molecular weight of 296 g/mole, its volatility would probably be low at the temperatures required to prevent decomposition. Therefore provision was made in the design of the reaction flask to allow a low temperature sublimation. Dimethylthallium bromide (3.14 g, 10.0 mmol) was weighed into the side arm of the reaction flask. The flask was attached to the vacuum line, evacuated and then filled with dry nitrogen gas. Methyllithium (11 mmol) was injected into the reaction flask. The flask was slowly cooled to -196 °C, evacuated, then warmed slowly while the diethyl ether which had acted as solvent for the methyllithium was removed by distillation. The reaction flask was again cooled to -196 °C and dimethyl ether (0.12 mole) and pentaborane(9) (10 mmol) added. The flask was warmed slowly to -45 °C and the solution was then stirred continuously for fifty minutes. Methane production corresponded to a 100% yield of lithium octahydropentaborate(1-).

The dimethylthallium bromide was then poured into the reaction flask by turning the side arm. The solution was warmed to -45 °C while the cold finger was maintained at -78 °C. The dimethyl ether solvent, which condensed on the cold finger and dripped back into the solution, froze the reaction mixture. The dry ice in the cold finger was allowed to sublime and the reaction flask was warmed to -23 °C. At this temperature the pressure in the flask was approximately 760 Torr. After stirring the mixture for two hours, the flask was cooled to -45 °C and the cold finger to -78 °C. A fractional con-

densation through two traps cooled to -78 °C into two traps cooled to -196 °C was carried out. The only volatile material recovered from this condensation was dimethyl ether. The flask and cold finger were warmed to -23 °C and pumping carried out for seven hours. As before the only material recovered was dimethyl ether. Some material spattered onto the cold finger due to bumping of the solution.

The reaction flask was filled with dry nitrogen, removed to the dry box, opened and a sample drawn from the cold finger for infrared analysis. Although this spectrum, IR VI in Appendix II, was similar to IR II, there were additional peaks.

If μ-dimethylthallium pentaborane(9) were formed lithium bromide would be a likely product, i.e.,

$$\mu\text{-}LiB_5H_8 + (CH_3)_2TlBr \longrightarrow \mu\text{-}(CH_3)_2TlB_5H_8 + LiBr$$

Powder photography was used to test for the presence of lithium bromide. A sample of the reaction residue was placed in a 0.5 mm Lindeman tube and a powder photograph, employing Cu Kα radiation, taken. A twenty-four hour exposure showed the presence of dimethylthallium bromide but failed to show any lithium bromide.

At this time it was learned that Gaines had attempted substantially the same experimental work and obtained the same results[106]. He felt the problems were solvent related. This point of view was held in the present work. Two experiments to prepare bridge substituted compounds in the absence of solvent had been attempted and these are detailed below.

5.1.2.7. The Reaction of Pentaborane(9) with Trimethylaluminum

There is evidence to suggest that trimethyl group IIIa species can react with compounds containing active hydrogen and eliminate methane[107,108]. Thus it appeared there might be a possibility of the following reaction

$$\tfrac{1}{2}[(CH_3)_3Al]_2 + B_5H_9 \longrightarrow \mu\text{-}(CH_3)_2AlB_5H_8 + CH_4$$

It was decided to attempt this reaction, both in the presence and absence of solvent.

Trimethylaluminum (Texas Alkyls,, 0.5 ml, density 0.752 g/ml, 0.4 g, 5 mmol) was syringed into a reaction flask (Figure XXXI). The flask was cooled to -196 °C, evacuated, and dimethyl ether (0.1 moles) and pentaborane(9) (5.0 mmol) added. The solution was warmed to -45 °C and stirred for one hour. No methane was produced. The reaction flask was warmed to -23 °C and then to room temperature. Again no methane was found. A sample of the liquid in the bottom of the flask was drawn for ^{11}B n.m.r. This spectrum revealed only pentaborane(9).

The experiment was repeated in the absence of solvent, since trimethylaluminum-dimethyl etherate forms readily at the temperatures employed. Trimethylaluminum (0.24 ml, 2.5 mmol) was syringed into an n.m.r. tube which was then affixed to the vacuum line, cooled and evacuated. Pentaborane(9) (2.5 mmol) was added. As above, the sample was warmed first to -45 °C, then -23 °C and finally to room temperature. No methane was found. The sample was heated to 60 °C for one hour but again no methane was found. The n.m.r. tube was flame sealed and a

^{1}H n.m.r. spectrum run. The largest peak corresponded to the methyl proton resonance of trimethylaluminum, 0.5 p.p.m. upfield from T.M.S., by tube interchange. Pentaborane(9) resonances were also readily identified and several other small, unidentified, peaks were noted as well. The n.m.r. tube was heated to 60 °C for an additional eleven hours and the spectrum redetermined. The peak due to the methyl protons had decreased in intensity and a new peak 0.9 p.p.m. downfield from T.M.S. (by tube interchange) was noted. The n.m.r. tube was heated to 95 °C for two and one-half, then four hours. The new peak was seen to increase in intensity after heating, while the trimethylaluminum proton resonance decreased in intensity. These spectra are designated NMR IVa and b in Appendix II. The ^{11}B spectrum taken after the final heating is NMR XI.

The vessel shown in Figure XXXIII was designed to allow the opening of the n.m.r. tube, separation of volatile from nonvolatile material, and the preparation of a solution of the nonvolatile products for n.m.r. purposes. When the tube was opened only 0.01 mmol of non-condensable gas was found indicating negligible production of hydrogen or methane. The tube contained 2.41 mmol of volatile products. From this mixture, a fraction (0.81 mmol) was obtained which condensed in a trap cooled to -78 °C. This material was identified as pentaborane(9) by its infrared spectrum. A second fraction (1.45 mmol) which passed a trap cooled to -140 °C, was shown, by its infrared spectrum, to be trimethylborane. A third fraction (0.14 mmol) passed a trap cooled to -78 °C but would not pass one cooled to -140 °C and was identified

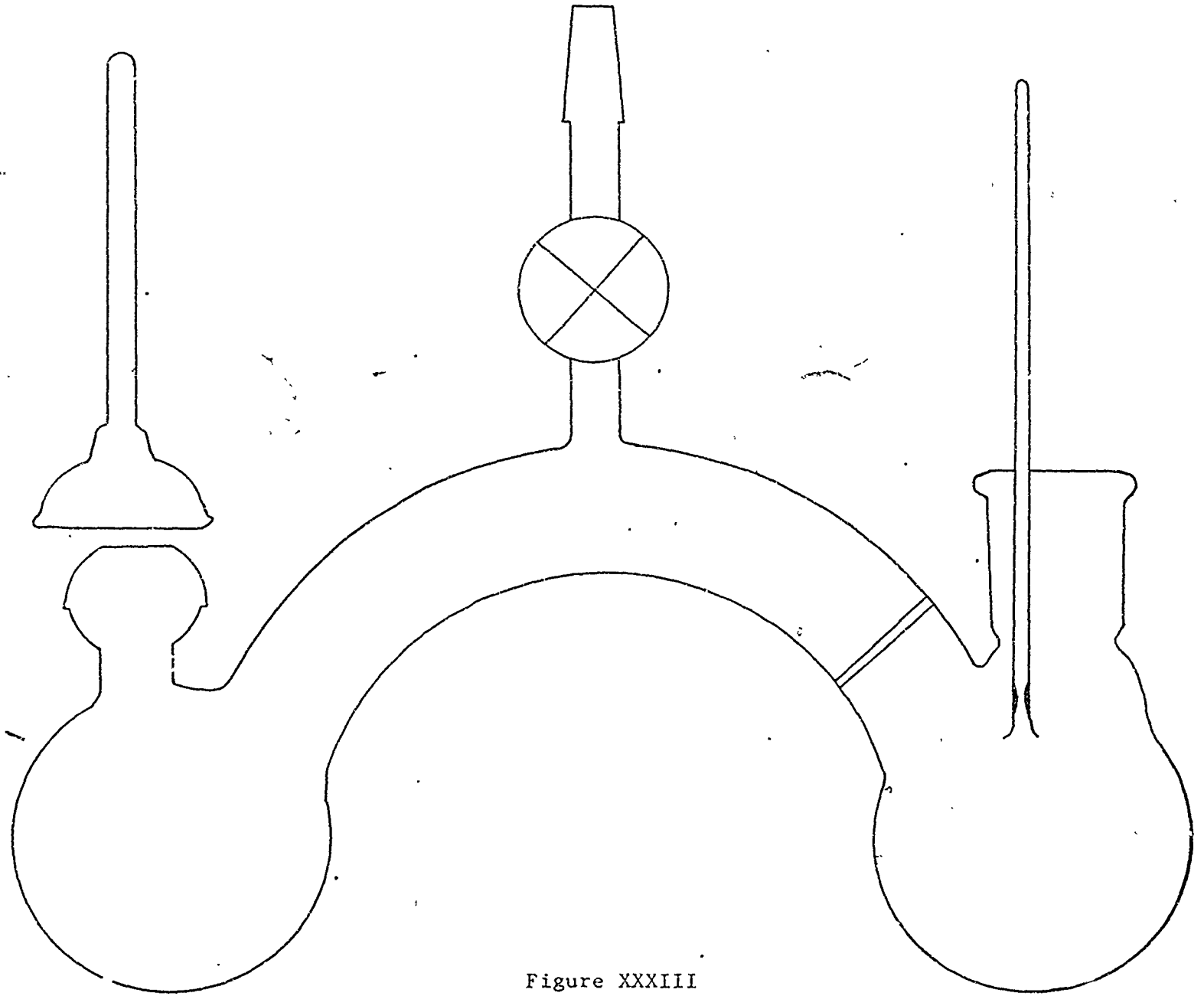

Figure XXXIII

Vessel Designed to open n.m.r. Tube

as a mixture of 1,1-dimethyldiborane(6) and 1,2-dimethyldiborane(6) by infrared and mass spectrometry.

A sample of the yellow nonvolatile reaction product remaining in the flask was taken for an infrared spectrum, IR VII in Appendix II. The yellow solid was treated with dry benzene. A small amount dissolved in benzene and a proton n.m.r. spectrum was obtained. This spectrum, NMR V in Appendix II, shows a single, sharp absorption 0.3 p.p.m. upfield from T.M.S., by tube interchange. The yellow powder in the flask turned white under the benzene overnight. No further work was conducted on this reaction.

5.1.2.8. The Reaction of Pentaborane(9) with Trimethylborane

As the dimeric character of trimethylaluminum might have inhibited the desired reaction, a reaction employing the monomeric trimethylborane was attempted. Trimethylborane (B.P.-20 °C) was prepared by the method of Brown[109], eg.,

$$BF_3 + 3CH_3MgCl \longrightarrow (CH_3)_3B + 3MgClF$$

Methyl magnesium chloride solution (Alfa Inorganics, 85 ml, 3M, 0.25 mole) was placed in a dried, nitrogen filled 500 ml three neck round bottom flask. The flask, fitted with a pressure equalized dropping funnel and a nitrogen inlet, was connected to the vacuum line through a water cooled condenser. The solution was stirred with a magnetic stirrer. Boron trifluoride-diethyletherate (34 ml, density 1.125 g/ml, 38 g, 0.27 mole) was added dropwise over a period of one and one-half

hours. The heat generated caused the solvent to reflux gently. When reaction was complete, the flask was cooled to -78 °C. Pumping was initiated and the trimethylboron collected in a trap at -196 °C. The product was purified by two distillations through traps cooled to -95 °C. The yield was quantitative on the basis of the Grignard reagent, and the product was identified as trimethylboron by its mass and infrared spectra.

Several attempts to react trimethylborane with pentaborane(9) were carried out. The reaction vessel used in all attempts was a 250 ml round bottom flask fitted with a Springham greaseless stopcock (C. Springham & Co. Ltd., England). No reaction occurred at temperatures from -78 °C to 175 °C with reaction periods up to three hours in either the presence or absence of solvent. Both reactants were quantitatively recovered. When pentaborane(9) (2.0 mmol) was heated with trimethylborane (2.1 mmol) to 175 °C for twenty-two hours 0.29 mmol trimethylborane and 0.35 mmol pentaborane(9) were consumed. A small amount (0.16 mmol) of a mixture of hydrogen and methane was produced. When a reaction was conducted at 175 °C for sixty-eight hours employing 2.21 mmol pentaborane(9) and 2.11 mmol trimethylborane, 0.52 mmol pentaborane(9) and 0.46 mmol trimethylborane were consumed. A mixture of hydrogen and methane (0.89 mmol) was again produced, as well as 0.07 mmol 2,3-dimethylpentaborane(9), which was identified by mass and infrared spectra.

At this point work on this reaction was discontinued.

5.2. The Structure of Bis(diethylamino)dithiaboretane

5.2.1. Chemicals, Instrumentation and Techniques

Very few chemicals were employed in this research. The purity of hydrogen sulfide (Fisher) was established by mass spectroscopy. Diethyl ether (Fisher, anhydrous) was dried over sodium wire immediately prior to use. Pentane was distilled from phosphorus pentoxide and stored over sodium wire, then molecular sieve. Triethylamine hydrochloride (Baker) was dried under vacuum at 100 ^{o}C and lithium borohydride (Alfa Inorganics) was used as supplied.

Throughout this work inert atmosphere techniques were employed. Extensive use was made of the dry box noted in 5.1.1. Specific techniques, such as crystal mounting, will be mentioned where appropriate. Infrared, mass and n.m.r. spectrometers were described in Sections 2.1.2. and 5.1.1.

Two x-ray generators were employed. For photographic work Cu Kα radiation, λ= 1.542 Å, was supplied by a Phillips PW 1009/30 generator operated at a voltage of 30 kV and a current of 20 mA. The four circle diffractometer was mounted on a Picker model 6238 x-ray generator fitted with a molybdenum tube, λ= 0.71069 Å, and run at 40 kV, 16 mA. In the case of copper radiation, a nickel filter was used to remove Kβ radiation, and with the molybdenum tube a zirconium filter served the same purpose.

Two cameras were employed in the photographic work. A Charles Supper camera was used for oscillation and Weissenberg pictures, while

an STOE camera was used for precession photographs. A scintillation counter was employed on the diffractometer to measure intensities.

5.2.2. Preparations

5.2.2.1. The Preparation of Triethylamineborane

Triethylamineborane $[(C_2H_5)_3NBH_3]$ was prepared by the method of Greenwood and Morris[110], i.e.,

$$(C_2H_5)_3NHCl + LiBH_4 \longrightarrow LiCl + (C_2H_5)_3NBH_3 + H_2$$

Triethylamine hydrochloride (30 g, 0.22 mole) was dissolved in 200 ml diethyl ether in a 500 ml 3 neck round bottom flask. Lithium borohydride (4.0 g, 0.18 mole) was added, as a slurry in 40 ml diethyl ether, over a period of one hour. The reaction was carried out under nitrogen, at room temperature, with continuous stirring. After reaction the diethyl ether was removed by pumping and the triethylamineborane vacuum distilled. The yield of amine-borane was 15.5 g, 0.13 mole, 72% on the basis of lithium borohydride. The purity of the product was established by n.m.r., infrared and mass spectroscopic analyses. The amine-borane was stored over molecular sieve in the dry box.

5.2.2.2. The Preparation of Bis(diethylamino)dithiaboretane

This preparation was based on a procedure by Forstner and Muetterties[95], i.e., the reaction of hydrogen sulfide with triethylamineborane at 200 °C in a stainless steel bomb. In the current

work a 25 cc capacity stainless steel bomb, manufactured by Baskerville and Lindsay Ltd. was used. The bomb was dried at 100 °C and placed in the dry box. A syringe was used to transfer a sample of triethylamineborane into the bomb. Sample weight was determined by difference.

For the initial preparation, triethylamineborane (3.13 g, 27.2 mmol), was placed in the bomb which was then connected to the vacuum line and evacuated. The bomb was cooled to -196 °C and hydrogen sulfide (49.4 mmol) added. The bomb was sealed, warmed to room temperature and then heated to 200 °C for three hours. After cooling to room temperature the bomb was vented and the gaseous reaction products were burned in a gas oxygen flame. The bomb was opened in the dry box. A white solid, covered with a clear liquid, was found in the bottom of the bomb. This material was stirred and transferred to a sublimation apparatus. A sublimation was carried out from a temperature of 200 °C to a cold finger at -78 °C. White powder, wetted with liquid, was found on the cold finger.

The liquid, presumably unreacted triethylamineborane, was removed from the cold finger by washing with pentane. The infrared spectrum of the white solid remaining (IR VIII of Appendix II) correlated reasonably well with the published spectra of bis(diethylamino)dithiaboretane[95], however the solubility of the white material was not as expected. For example the material was reported to be soluble in pentane, chloroform, carbon tetrachloride and benzene. Of these solvents only carbon tetrachloride dissolved sufficient sample to allow an n.m.r. spectrum to be obtained. This spectrum, NMR VI of Appendix II,

possessed broad, unresolved, absorptions at 1.1 and 3.1 p.p.m. downfield from T.M.S. The absorptions reported for bis(diethylamino)-dithiaboretane were a well resolved methyl triplet and methylene quartet at 1.2 and 3.3 p.p.m. downfield respectively[95]. A mass spectrum of the white solid possessed a cut-off at m/e 347. This indicated the white solid was not $[(C_2H_5)_2NBS]_2$ but rather $[(C_2H_5)_2NBS]_3$, i.e., the six membered ring had been prepared. This mass spectrum is recorded in Appendix II as MS I.

Several other attempts were made to prepare the four membered ring. The following is an example of a successful preparation. Triethylamineborane (1.4 g, 12 mmol) was syringed into the 25 cc capacity bomb in the dry box. The bomb was assembled, connected to the vacuum line, evacuated and cooled to -196 °C. Hydrogen sulfide (52 mmol) was condensed into the bomb, which was then placed in an oven and heated to 175 °C for twenty-four hours. The bomb was vented and the gaseous products were burned. The bomb was disassembled in the dry box and benzene added. The reaction mix was dissolved in benzene and then transferred to a sublimation apparatus. The benzene solution was boiled to remove all traces of hydrogen sulfide, the sublimation apparatus was connected to the vacuum line, cooled to -196 °C and evacuated. The benzene was removed while slowly warming the sublimation apparatus. A sublimation was carried out from a hot temperature of 75 °C to a cold of -78 °C. The sublimation apparatus was opened in the dry box and the white material on the cold finger recrystallized from pentane. The yield was 1.0 g, 4.3 mmol, 56%. This yield may be high,

as it was calculated on the basis of amount of material removed from the cold finger, rather than the amount recrystallized.

The bis(diethylamino)dithiaboretane reaction product was identified by means of mass, infrared and proton magnetic resonance spectra, which are given in Appendix II as MS II, IR IX and NMR VII.

5.2.3. Analysis of the Crystal Structure of Bis(diethylamino) dithiaboretane

5.2.3.1. Crystal Mounting and Photographic Work

As bis(diethylamino)dithiaboretane is rapidly hydrolyzed by atmospheric moisture, all handling was done in a dry box. The compound was dissolved in a small amount of n-pentane at room temperature. The pentane solution was cooled on a Model TCP-2 Thermoelectric Cold Plate (Thermoelectrics Unlimited, Inc., New Jersey, U.S.A.) until crystals of an acceptable size (approximately 0.4 X 0.4 X 0.1 mm) were obtained. A crystal was then removed from the solution and placed in the mouth of a Lindemann tube. A glass fibre was used to push the crystal down the tube until it wedged. The Lindemann tube was placed on a glass slide and broken off about 6 mm from the crystal with a scalpel. The broken end was sealed by quickly dipping the end of the tube in molten black wax. This cutting and sealing operation was repeated 6 mm below the crystal.

The Lindemann tube was removed from the dry box to a polarizing microscope and examined to determine if the crystal it contained was a single crystal. If the crystal was acceptable the Lindemann tube was mounted on a goniometer head using black wax.

Practical difficulties included cleaving the crystals while wedging them in the tubes, and melting the crystals while sealing the tubes.

In all, over forty crystals were mounted. Of these only four

were of sufficient quality for further work. Three of these four were not single crystals but were acceptable for photographic work. Only one of the crystals mounted was of sufficient quality for use on the diffractometer.

A further difficulty arose in that the crystals began to "melt", or lose crystallinity, at the contact points between the crystal and the Lindemann tube. Once this process started the crystal lost crystallinity rapidly, thus crystals were suitable for data collection only for two to five days after mounting.

The dimensions and angles of the unit cell were determined from Weissenberg and precession photographs. The unit cell was found to be tetragonal, i.e., $a = b \neq c$ and $\alpha = \beta = \gamma = 90^{\circ}$. Accurate cell dimensions were determined by mounting a crystal on the diffractometer and measuring the angles at which diffraction maxima occurred for 28 reflections. The cell dimensions were then refined by the method of least squares. Crystal data are given in Table IX.

Two possible space groups were indicated by the Weissenberg and precession photographs. These were either $P_{4_1}22$ (No. 91) or $P_{4_1}2_12$ (No. 92). The general conditions limiting reflections for these groups differ only in that no conditions are imposed on h00 reflections for $P_{4_1}22$ while $P_{4_1}2_12$ imposes conditions h00 = 2n. The reflections 100, 300, 500, etc., were not observed. This suggested the space group was $P_{4_1}2_12$, as was later confirmed by structure refinement.

The crystal density was determined by growing a large crystal,

which was weighed and then measured on a travelling microscope (E.E. Becker and Co., London, England). The density was found to be 1.08 $\pm$ 0.08 gm cm^{-3}. The density calculated on the basis of eight molecules per unit cell was 1.10 gm cm^{-3}.

TABLE IX

CRYSTAL DATA FOR BIS(DIETHYLAMINO)DITHIABORETANE

System	Tetragonal
Space Group	$P4_12_12$
Molecular Weight	230.01 gm $mole^{-1}$
Cell Dimensions	a = 10.396 $\pm$ 0.003Å
	b = 10.396 $\pm$ 0.003Å
	c = 25.589 $\pm$ 0.007Å
	$\alpha = \beta = \gamma =$ 90.00°
Cell Volume	2765 X 10^{-24} cm^3
Density (measured)	1.08 $\pm$ 0.08 gm cm^{-3}
Density (calculated)	1.10 gm cm^{-3}
Molecules per cell	8

5.2.3.2. Diffractometry

The crystal habit of $[(C_2H_5)_2NBS]_2$ is a tetragonal tablet showing the 110, $1\bar{1}0$ and 001 faces. It was necessary to mount the crystals in the Lindemann tubes with the 110 (or $1\bar{1}0$) planes approx-

imately parallel to the tube axis. The tube was mounted on the diffractometer with its axis approximately colinear with the ϕ axis, i.e., with the 110 set of planes parallel to the ϕ axis.

For purposes of intensity data collection it was decided to treat the unit cell as face-centered rather than primitive. The new axes were chosen along the diagonals of the primitive cell. The transformations involved were:

$$h_F = k_p + h_p$$
$$k_F = k_p - h_p$$
$$l_F = l_p$$

or

$$h_p = \tfrac{1}{2}(h_F - k_F)$$
$$k_p = \tfrac{1}{2}(h_F + k_F)$$
$$l_p = l_F$$

where h_F, k_F, l_F and h_p, k_p, l_p are the Miller indices for the face-centered cell and primitive cells respectively.

A total of 654 reflections, up to $2\theta = 30^\circ$, were measured. The scan was in 2θ, for one minute, at a rate of 2° per minute and background measurements were taken for thirty seconds at the beginning and end of each scan. A standard reflection was measured every hour, i.e., about every 20 reflections. It was found necessary to check the orientation of the crystal every hour, particularly in the latter stages of data collection, due to the crystal "melting" at the contact points with the Lindemann tube. This "melting" phenomenon also accounted for the fact that the intensity of the reflection from the standard set

of planes dropped from 45200 counts/minute at the beginning of the data collection to 9617 counts/minute at the end, fifty-nine hours later. Seventy-six hours after data collection was initiated the count rate from the standard reflection had dropped to 2576 counts/minute.

Lorentz and polarization corrections were applied to the data but an absorption correction was not. The Miller indices were transformed from the face-centered unit cell to the primitive unit cell before the calculation of these corrections.

As the Laue symmetry was 4/mmm the intensity of the reflection due to the hkl set of planes was equal to that of the khl set, i.e., $|F_{(hkl)}| = |F_{(khl)}|$. As a complete octant had been gathered (to $2\theta = 30^{\circ}$) it was possible to compare $|F_{(hkl)}|$ values with $|F_{(khl)}|$ values. Where these were less than 5% apart they were averaged, and where greater than 5% apart they were rejected. Only four sets of reflections were rejected. The averaging and rejection process reduced the size of the data set to 373 points.

5.2.3.3. Structure Determination

The atomic scattering factor curves for boron, carbon, nitrogen and sulfur were obtained from the International Tables for X-ray Crystallography[111]. The atoms were assumed to be uncharged.

The three-dimensional Patterson map showed several peaks which appeared to correspond with sulfur-sulfur vectors. On the basis

of these peaks sulfur positions were assigned and a structure factor calculation and least square refinement carried out. The R value at this stage was 0.515, weighted R was 0.544. Fourier and difference Fourier maps were obtained employing the phasing derived from the structure factor calculation. These maps allowed the assignment of two carbon atoms (C_1 and C_2) and another refinement cycle was carried out. The R value dropped to 0.496, weighted R to 0.483. The positions of the boron and nitrogen atoms, plus two more carbon atoms (C_3 and C_4) were predicted on the basis of Fourier and Difference Fourier maps. At this stage the R value dropped to 0.306, weighted R to 0.289. The positioning of the final four carbon atoms was suggested by a difference Fourier map. With these atoms positioned, two refinement cycles reduced the R value to 0.127, weighted R to 0.093. Slight changes in atomic positions reduced the R value to 0.120 (0.109 omitting zeroes) with a final weighted R of 0.091 (0.088 omitting zeroes). At this point no shift was greater than 0.08 of a standard deviation, and the highest peak in the difference Fourier was 0.381 electrons Å^3.

An absorption correction was considered since one dimension of the crystal was shorter than the other two (0.4 X 0.4 X 0.1 mm). A calculation showed the intensities would vary by $\pm$10% about a mean value, with the maximum and minimum absorption occurring with the beam along the long and short crystal dimensions respectively, i.e., at $\theta = 0^\circ$ and $\theta = 90^\circ$. An absorption correction was not made since much of the data was collected away from $\theta = 0^\circ$ or 90° and therefore the average in-

tensity variation would be less than $\pm$10%.

The use of anisotropic thermal parameters was prevented by the small size of the data set. A complete set of anisotropic thermal parameters would require 137 variable parameters, giving only three reflections per parameter. This is not a sufficient overdetermination.

An analysis of the various residuals, R, was carried out to see if there were systematic variations in the value of R. It was found that R increased as $|F_{obs}|$ decreased, i.e., for $|F_{obs}|$ above 24.1 R was less than 0.101 while for $|F_{obs}|$ below 10.6 the R values were greater than 0.280. This variation can be related to the greater degree of uncertainty in the experimental collection of weaker intensity reflections. It was also found that planes with Miller indices h + k = 2n the average $|F_{obs}|$ was 34.0, while for planes h + k = 2n + 1, the average $|F_{obs}|$ was 13.4. As a result of the relatively low intensities for the latter planes the R value associated with h + k = 2n + 1 was 0.215, while that of the planes h + k = 2n was 0.058.

The values of the residual indicated that the refinement process had been dominated by the more intense reflections. Since it was believed that a significant amount of information about the structure was contained in the reflections of low intensity a weighting scheme was employed which reduced the weights of the more intense reflections. Specifically, reflections with $|F_{obs}|$ greater than 25.0 (113 reflections in all) were assigned weights by the formula

$$\text{weight} = \left[\frac{25.0}{\text{Sc} \times |F_{obs}|}\right]^2$$

Here Sc is the scale factor used to scale $|F_{obs}|$ to $|F_{calc}|$. For reflections with $|F_{obs}|$ less than 25.0 weights were assigned by

$$\text{Weight} = \left[\frac{1}{Sc}\right]^2$$

No shifts in atomic or thermal parameters were observed on application of this weighting scheme. The use of a weighting other than unity for reflections with $|F_{obs}|$ below 25.0 was not warranted due to the experimental uncertainty in the measurement of the intensity of the weak reflections. The accuracy of the data associated with the low intensity reflections would have been improved by counting each reflection over a longer time period than the one minute scan employed, but the rapid degradation of the crystal precluded this approach.

The positional and thermal parameters derived from the last cycle of least squares refinement, with their standard deviations, are presented in Table X. The final values of observed and calculated structure factors are recorded in Appendix III.

TABLE X

FRACTIONAL ATOMIC COORDINATES AND ISOTROPIC THERMAL PARAMETERS FOR BIS(DIETHYLAMINO)DITHIABORETANE

Atom	X	Y	Z	B
S1	0.3793(8)	-0.3845(9)	0.3072(4)	5.34(28)
S2	-0.1112(8)	0.1214(8)	0.3059(3)	4.71(26)
C1	0.1398(28)	-0.1735(30)	0.3007(10)	4.83(83)
C2	0.0134(34)	-0.2369(36)	0.3099(12)	8.14(98)
C3	-0.3799(31)	0.4036(32)	0.3002(11)	6.29(90)
C4	-0.2559(34)	0.4733(32)	0.3134(11)	7.22(93)
C5	0.1058(28)	0.3509(27)	0.2947(10)	4.73(78)
C6	0.2332(34)	0.2712(35)	0.3061(11)	8.61(91)
C7	0.0855(33)	0.3427(34)	0.1927(12)	7.40(103)
C8	0.0223(32)	0.4743(34)	0.1796(10)	6.72(83)
B1	0.3071(91)	-0.3071	0.2500	9.48(184)
B2	0.4543(81)	-0.4543	0.2500	8.62(151)
B3	0.0394(32)	0.2006(34)	0.2473(13)	4.77(86)
N1	0.2124(45)	-0.2124	0.2500	4.88(84)
N2	-0.4480(91)	0.4479	0.2500	6.49(95)
N3	0.0493(23)	0.2912(22)	0.2446(9)	5.71(62)

Standard Deviations in Parentheses

CHAPTER VI

DISCUSSION

Bridge Substitution in Pentaborane(9)

The Crystal Structure of Bis(diethylamino)dithiaboretane

6. Discussion

6.1. Bridge Substitution in Pentaborane(9)

6.1.1. Properties of lithium octahydropentaborate(1-)

The reaction between methyllithium and pentaborane(9) to form lithium octahydropentaborate(1-) proceeds readily at -78 °C in dimethyl ether. The ^{11}B n.m.r. and ^{1}H n.m.r. spectra of this borate(1-) compound are labelled NMR IX and NMR II respectively in Appendix II. Their overall resemblance to the spectra of pentaborane(9) is apparent. However, the presumption of LiB_5H_8 formation was based primarily on its ability to react further with dimethylboron bromide to yield the readily identified dimethylborylpentaborane(9).

As the octahydropentaborate(1-) ion cannot be formed in hydrocarbon solvent, or in the absence of solvent[66], it must be concluded that the solvent plays a significant role. It was found in the current work that not all the solvent could be removed from a sample maintained at -30 °C. The amount of solvent remaining corresponded to an empirical formula of $LiB_5H_8 \cdot \frac{1}{2} (CH_3)_2O$. It was also apparent that solvent removal caused decomposition, as pentaborane(9) could not be generated on addition of solvent and hydrogen chloride to the solid borate(1-) salt. The infrared spectra of a sample of $LiB_5H_8 \cdot \frac{1}{2} (CH_3)_2O$ (IR 11a and b) provided the following additional evidence of decomposition:

1) Gaines and Iorns[78] reported the infrared spectra of

a variety of Group IVA bridged pentaborane(9) compounds. All show an absorption in the region 1810-1830 cm^{-1}. This is the frequency assigned to bridging B-H-B stretch in pentaborane(9)[112]. This band is not present in IR IIa or b.

2) Although lithium octahydropentaborate(1-) is known to decompose rapidly at room temperature[63], the infrared spectrum of the sample from which solvent had been removed showed only minor changes after twenty-four hours.

3) When lithium octahydropentaborate(1-) decomposes the products are the borohydride (BH_4^-) anion (n.m.r. evidence) and other unidentified species[63]. Infrared spectra IIa and b show absorptions at 2315 and 1080 cm^{-1}, which are comparable to those expected for lithium borohydride at 2320 and 1096 cm^{-1}[113].

Therefore, in addition to the previously known thermal instability of LiB_5H_8[63], the current study has established that LiB_5H_8 decomposes when solvent is removed from a sample maintained at a temperature at which the octahydropentaborate(1-) salt is thermally stable.

6.1.2. μ-Dimethylborylpentaborane(9)

Dimethylboron bromide was reacted with lithium octahydropentaborate(1-) to form μ-dimethylborylpentaborane(9). The formation of this product was confirmed by its ^{11}B n.m.r. spectrum. Assignment of this spectrum (XIII X) was based on that of Gaines and Iorns[81].

The high field doublet of relative area one was assigned to the apical boron. The triplet of relative area four consists of two overlapping doublets, one for chemically equivalent B_2 and B_3 (see Figure XII) and the other for chemically equivalent B_4 and B_5. These doublets are assigned to boron bonded to hydrogen. The low field singlet of relative area one is partially obscured by the high field doublet of the side band. This singlet was assigned to the bridged boron atom which is not bonded to a hydrogen atom. The ^1H n.m.r. spectrum of μ-dimethylborylpentaborane(9) (NMR III) is similar to that of pentaborane(9) (NMR I) as would be expected. Some impurity peaks were present as elaborate steps were not taken to purify the sample. The line widths of the impurity peaks indicate that these peaks are due to carbon bound protons. The high intensity absorption due to the six methyl protons precluded effective integration to determine the relative numbers of bridging and terminal protons. The overall appearance of the spectrum is very similar to that published by Gaines and Iorns[81], making allowances for the differing chemical shifts obtained on their 100 MHz instrument compared with the 60 MHz machine used to obtain NMR III.

6.1.3. Attempts to Prepare Bridged Group IIIA Pentaborane(9) Derivatives

6.1.3.1. The Attempted Reaction of Diethylaluminum Chloride with Lithium Octahydropentaborate

An attempt was made to prepare μ-diethylaluminumpentaborane(9)

by the addition of diethylaluminum chloride to a solution of lithium octahydropentaborate(1-) in dimethyl ether at -45 °C. The desired product was expected to have sufficient volatility to permit distillation directly from the reaction flask, since its molecular weight would be between that of μ-dimethylborylpentaborane(9) (103 g mole^{-1}) and μ-triethylsilylpentaborane(9) (177 g mole^{-1}). Both these latter compounds have been distilled directly from reaction flasks at temperatures below -20 °C[81,78]. Also dimethylaluminumtriborane(9), while not a bridged species, is similar to the bridged species and has a vapor pressure of 13 torr at 0 °C[72].

Thus it was felt that a successful reaction would yield a product which could be distilled directly from the reaction flask. The appearance of lithium chloride would have indicated a successful reaction, but detection of this salt was prohibited by the murky appearance of LiB_5H_8 solutions. Powder photography was not employed as a test for lithium chloride.

When the reaction was carried out no volatile material, other than solvent, was recovered from the reaction flask at -45 °C. On the basis of this, and subsequently discussed spectral observations, it was concluded that the bridged aluminum compound was not present.

On warming the flask slowly to room temperature triethylborane was obtained. This raised a question as to whether μ-dimethylaluminopentaborane(9) had decomposed to yield triethylborane, or was the triethylborane a product of the reaction between diethylaluminum chloride and

the decomposition products of lithium octahydropentaborate(1-)? A third mode of formation of triethylborane, the reaction between diethylaluminum chloride and lithium octahydropentaborate(1-) at room temperature was rejected due to 1), the instability of lithium octahydropentaborate at room temperature and 2), the fact that lithium octahydropentaborate decomposes when the solvent is removed.

While there is no direct evidence to support either of the two postulated schemes for the formation of triethylborane, the following indirect evidence does exist:

1) μ-dimethylborylpentaborane(9) and the Group IVA pentaborane(9) species all have sufficient thermal stability to allow their spectra to be obtained at room temperature[81,78]. Therefore, it seemed likely that, had the bridged aluminum compound been present it would have been possible to obtain its spectrum at room temperature. The presence of a bridged compound would have been indicated by a band in the region 1810-1830 cm^{-1} in the spectrum[78,112].

This band is missing in the infrared spectrum (IR III) of the reaction products. Had no reaction occurred between the two reactants the infrared spectrum should show the presence of both diethylaluminum chloride-dimethyl etherate and the decomposition products of lithium octahydropentaborate(1-). A comparison of IR III with IR II and IR V shows the presence of both reactants. In fact the only absorptions not assignable to these species occur at 800, 820 and

1100 cm^{-1} and are indicated on IR III with arrows. The bands at 800 and 1100 cm^{-1} correspond with bands present in the infrared spectrum (IR X) of the silicone grease used on the apparatus. All the other bands in the spectrum of the grease also correspond with one or another of the bands present in IR II or IR V.

Therefore the infrared spectrum of the reaction residue fails to give any indication of the presence of μ-dimethylaluminumpentaborane(9). Furthermore, only one band, that at 820 cm^{-1}, indicated that any reaction, other than the formation of diethylaluminum chloride-dimethyl etherate and the decomposition of lithium octahydropentaborate had occurred.

2) Alkylaluminum compounds are known to be effective alkylating agents in either the presence or absence of solvent. Trimethylaluminum reacts with both diborane(6)[114] and pentaborane(9) (see 5.1.2.7) to yield trimethylborane.

3) As pyrolysis of μ-dimethylborylpentaborane(9) failed to yield any trimethylborane it seems reasonable to assume that pyrolysis of μ-diethylaluminumpentaborane(9) should not yield triethylborane.

These points, considered together, support the suggestion that the triethylborane found on warming the reaction flask to room temperature was a product of some reaction other than the decomposition of μ-diethylaluminumpentaborane(9).

The thermodynamic driving force for the reaction between lithium borate(1-) salts and halide containing compounds is presumably

the formation of the ether insoluble lithium halides, eg.,

$$(CH_3)_2BBr + LiB_5H_8 \longrightarrow \mu\text{-}(CH_3)_2BB_5H_8 + LiBr$$

Failure to prepare μ-$(C_2H_5)_2AlB_5H_8$ can be attributed to the rapid formation of the dimethyl etherate of diethylaluminum chloride. Rapid formation of this etherate was indicated since the vapor pressure above an equimolar mixture of dimethyl ether and diethylaluminum chloride remained at zero when the mixture was warmed from -196 °C to -45 °C. Ether complexes of the dialkylaluminum halides are known to be very stable and may be distilled without dissociation[90].

In contrast dialkyl boron halides, unlike boron trihalides, do not readily form isolable etherates, and may, in fact, be distilled in uncomplexed form from etheral solvents[90]. The ether group on diethylaluminum chloride-dimethyl etherate increases the bulk of the aluminum compound, thus hindering the attack of this species on the octahydropentaborate(1-) ion. As well, the ether group occupies the site at which the aluminum atom might itself be attacked, i.e., the vacant 3p orbital.

6.1.3.2. The Attempted Reaction of Dimethylthallium Bromide with Lithium Octahydropentaborate

An attempt was made to prepare μ-dimethylthalliumpentaborane(9) by the reaction of dimethylthallium bromide with lithium-octahydropentaborate(1-) in dimethyl ether at -45 °C. As the desired product would have had low volatility due to its' high molecular weight

(296 g mole^{-1}), the reaction flask was designed to allow a sublimation to be carried out directly from the reaction mixture.

The only volatile material obtained was solvent. Some material collected on the cold finger due to the solution bumping as the solvent was removed. An infrared spectrum of this material (IR VI) showed three peaks not present in IR II, the decomposition product of lithium octahydropentaborate(1-). One of these, at 800 cm^{-1}, was due to dimethylthallium bromide, but the origin of the other two peaks at 730 and 965 cm^{-1}, and indicated by arrows on IR VI, is unknown. The absence of a band in the region 1810 - 1830 cm^{-1} was evidence that the bridged species was not present.

It was suggested by the stoichiometry of the desired reaction

$$(CH_3)_2TlBr + LiB_5H_8 \longrightarrow \mu\text{-}(CH_3)_2TlB_5H_8 + LiBr$$

that a powder photograph of the reaction residue would reveal the presence of lithium bromide if the reaction were successful. The powder photograph showed only dimethylthallium bromide.

Powder photography will detect a constituent in a mixture only if, as a rule of thumb, it is present in a quantity greater than about 5% by weight[115]. Making allowances for the facts that the major scattering atoms are thallium and bromine, and that lithium bromide has a cubic unit cell while dimethylthallium bromide has a tetragonal unit cell, the conclusion was reached that if the reaction were less than about 15% complete lithium bromide might not be detected in the reaction residue.

It is concluded on the basis of infrared spectroscopy and

powder photography that the bridged compound μ-$(CH_3)_2TlB_5H_8$ was not present. The reason for the failure to form the bridged compound could be thermodynamic in nature. Dimethylthallium bromide is an ionic solid and the energy required to disrupt the ionic lattice could be sufficient to prevent reaction. Also, the two phase reaction system resulting from the ether insolubility of the thallium compound could have inhibited reaction.

6.1.3.3. The Reactions Between Pentaborane(9) and 1) Trimethylaluminum and 2) Trimethylborane

It has been well established that trialkyl Group IIIA species can react with compounds containing active hydrogen and eliminate hydrocarbon. This elimination is frequently preceeded by the formation of an isolable complex, eg.,

$$\tfrac{1}{2}[(CH_3)_3Al]_2 + NH(CH_3)_2 \longrightarrow (CH_3)_3Al{:}NH(CH_3)_2 \longrightarrow (CH_3)_2Al{:}N(CH_3)_2 + CH_4 \quad (116)$$

$$\text{or } (CH_3)_3B + NH_3 \longrightarrow (CH_3)B{:}NH_3 \longrightarrow (CH_3)_2BNH_2 + CH_4 \quad (117)$$

but formation of an isolable complex is not absolutely necessary, eg.,

$$\tfrac{1}{2}[(C_2H_5)_3Al]_2 + C_4H_9C{\equiv}CH \longrightarrow C_4H_9C{\equiv}CAl(C_2H_5)_2 + C_2H_6 \quad (118)$$

$$\text{or } (C_2H_5)_3B + CH_3COOH \longrightarrow (C_2H_5)_2BOCOCH_3 + C_2H_6 \quad (119)$$

In general these reactions proceed more readily for the aluminum trialkyls than for those of boron. For example, trimethylborane does not hydrolyze at room temperature, whereas trimethylaluminum undergoes hydrolysis almost explosively.

If reactions of the type

$$\tfrac{1}{2}\left[(CH_3)_2Al\right]_2 + B_5H_9 \longrightarrow \mu\text{-}(CH_3)_2AlB_5H_8 + CH_4$$

$$(CH_3)_3B + B_5H_9 \longrightarrow \mu\text{-}(CH_3)_2BB_5H_8 + CH_4$$

were successful methane, which is easily identified, would be produced.

When trimethylaluminum was mixed with pentaborane(9) in dimethyl ether at temperatures varying from -45 °C to room temperature no methane was produced. As trimethylaluminum-dimethyl etherate, which might have retarded reaction, formed readily at the temperatures employed, the reaction was repeated in the absence of solvent. Again no methane was produced, indicating the desired reaction had not occurred. It was then decided to heat the solvent free mixture to determine if methane would form at higher temperatures. If methane were produced, a hot-cold type of reactor could be employed in an attempt to produce the bridged species. At temperatures up to 95 °C no methane was produced, but another reaction, whose nature was not established, did occur. The following points can be made about this reaction:

1) As shown in NMR IVa and b the peak due to the proton resonance of trimethylaluminum decreased in intensity while another peak, subsequently identified as originating with trimethyiborane, of which a substantial amount was produced, increased in intensity. Therefore the reaction appeared to be of the type

$$4B_2H_6 + \left[(CH_3)_3Al\right]_2 \longrightarrow 2Al(BH_4)_3 + 2(CH_3)_3B \quad (120)$$

2) A small amount of a volatile substance was formed.

Infrared and mass spectroscopy established this material was predominantly 1,2-dimethyldiborane(6) along with some 1,1-dimethyldiborane(6).

3) As no hydrogen was produced by the reaction, the residue must be rich in hydrogen.. This indicated the presence of borohydride $(BH_4)^-$, tetrahydroaluminate $(AlH_4)^-$, or an alane, i.e., a hydrogen bridged aluminum polymer. But the infrared spectrum of the residue (IR VII) fails to show the intense absorption expected at about 1100 cm^{-1} for a borohydride[113], or the broad, moderate intensity band expected at about 1700 cm^{-1} for tetrahydroaluminate[121]. Nor does this spectrum show the absorption expected for an alane at about 1750 - 1800 cm^{-1}[37]. Therefore the composition of this hydrogen rich residue remains undetermined. It should be mentioned that the only bands identifiable in IR VII are those originating with the mulling agent, nujol, at 1370, 1460 and 2900 cm^{-1}.

In spite of the existing, facile method of preparation of μ-dimethylborylpentaborane(9) it was decided to attempt to prepare this material by the direct reaction of trimethylborane and pentaborane(9). A successful reaction with the monomeric trimethylborane would have indicated that the failure of trimethylaluminum to react under similar circumstances could be related to the dimeric character of trimethylaluminum.

At temperatures up to 100 °C no reaction whatever occurred and the reactants were quantitatively recovered. Had a successful reaction occurred the products would have been methane and methyl-

diboranes, since pyrolysis of μ-dimethylborylpentaborane(9) at 100 °C is known to produce methyldiboranes[81].

It was only on prolonged heating at 175 °C that any reaction occurred. Less than 25% of the reactants were consumed, but methane was produced, along with traces of 2,3-dimethylpentaborane(9). However even this bit of evidence for the production of a bridged species is of dubious value, since it is known that the pyrolysis of trimethylborane alone, albeit at 400 °C, produces a mixture of hydrogen and methane[122]. Further, none of the methyldiboranes expected from the pyrolysis of the bridged species were detected. The methyldiboranes have sufficient thermal stability to allow their preparation, in small amounts, from the reaction of diborane(6) with trimethylborane at 300 °C[45]. Therefore it was believed that the methyldiboranes would not have decomposed at 175 °C, and their detection, if formed, would have been possible.

In conclusion it appears that the reactions of trimethylborane and trimethylaluminum with pentaborane(9) at elevated temperatures can best be considered as pyrolysis reactions whose nature has not been determined in this work.

6.2. The Crystal Structure of Bis(diethylamino)dithiaboretane

6.2.1. The Preparation of Bis(diethylamino)dithiaboretane

Bis(diethylamino)dithiaboretane, $[(C_2H_5)_2NBS]_2$ was origin-

ally prepared by Forstner and Muetterties[95] by the reaction of hydrogen sulfide with triethylaminoborane for three hours at 200 °C. When their work was repeated in the current study, spectral evidence (MS I, IR VIII and NMR VI) indicated the six membered ring, i.e., tris(diethylamino)trithiaboretane $[(C_2H_5)_2NBS]_3$, had been formed. This conclusion was based on the mass spectrum which showed a cut-off at m/e = 347 and a parent molecule ion at m/e = 345. The infrared spectrum of the dimeric compound (IR IX) is similar to that of the trimer (IR VIII), and the n.m.r. spectrum of the dimer (NMR VII) shows absorptions in the same region as those of the trimer (NMR VI). The solubility of the dimeric compound in organic solvents is much higher than that of the trimer. The low solubility of the trimer resulted in very poor resolution of the n.m.r. spectrum whereas the splitting pattern due to the coupling of methyl and methylene protons is clearly resolved in the case of the dimer.

The B-N stretching band in the infrared spectrum of aminoboranes occurs in the region 1350 - 1530 cm^{-1}. Both IR VIII and IX show bands in this region. Both spectra were obtained as mulls in nujol which itself absorbs at 1466 and 1381 cm^{-1}. Therefore assignment of the B-N stretch for the trimeric $[(C_2H_5)_2NBS]_3$ is difficult. For the dimeric $[(C_2H_5)_2NBS]_2$, the B-N stretching frequency could be assigned to the band at 1485 cm^{-1}. This compares with the B-N stretch in diethylaminodiethylborane $(C_2H_5)_2NB(C_2H_5)_2$ at 1490 cm^{-1}[85] and suggests the B-N bond in the dimer is fairly strong (see Section 4.4.2.).

The B-S stretching frequency is known to occur at about 915 cm^{-1} for thioboranes $(RS)_{3-n}BX_n$ [123]. However the B-S stretch for ring compounds has not been assigned. There are two bands in this region in IR IX, one at 890 cm^{-1} and one at 945 cm^{-1}, but it is not known if these bands are due to B-S stretch.

It is possible to suggest a reaction mechanism based on the material presented in Section 4.4. The initial step involves the conversion of the triethylamine borane to diethylaminoborane by heating[124]. As the boron atom in the diethylaminoborane is capable of functioning as a Lewis acid, it is proposed that hydrogen sulfide attacks in a manner analogous to the reaction of trichloroborane with mercaptan, i.e.,

$$BCl_3 + RSH \longrightarrow Cl_3B.S\begin{matrix}R\\H\end{matrix} \qquad (125)$$

is possible.

The resulting isolable complex eliminates hydrogen chloride on heating. It is also known that heating dialkylthioboranes with mercaptans yields alkylthioborates and hydrogen,

$$(RS)_2BH + RSH \xrightarrow{150\ ^{\circ}C} B(SR)_3 + H_2 \qquad (126)$$

The hydrogen sulfide attack would be followed by an intermolecular elimination of one molecule of hydrogen sulfide, forming a sulfur bridged intermediate. Examples of this type of elimination are known for both boron-nitrogen and boron-oxygen compounds, eg., amine elimination for trisaminoboranes, and boronic and borinic acid dehydrations. The final step in the reaction mechanism would involve the intramolecular elimination of hydrogen sulfide. The overall mechanism could

then be:

1) $(C_2H_5)_3NBH_3 \longrightarrow (C_2H_5)_2NBH_2 + C_2H_6$

2) $(C_2H_5)_2NBH_2 + 2H_2S \longrightarrow (C_2H_5)_2NB(SH)_2 + 2H_2$

3) $2(C_2H_5)_2NB(SH)_2 \longrightarrow (C_2H_5)_2NB\begin{smallmatrix}S\\SH\end{smallmatrix}\begin{smallmatrix}S\\HS\end{smallmatrix}BN(C_2H_5)_2 + H_2S$

4) $(C_2H_5)_2NB\begin{smallmatrix}S\\SH\end{smallmatrix}\begin{smallmatrix}S\\HS\end{smallmatrix}BN(C_2H_5)_2 \longrightarrow (C_2H_5)_2NB\begin{smallmatrix}S\\S\end{smallmatrix}\begin{smallmatrix}S\\S\end{smallmatrix}BN(C_2H_5)_2 + H_2S$

If the reaction mixture is heated to 200 °C the dimer is converted into the trimer.

A number of methods exist by which this mechanism could be tested. For example the preparation could be undertaken employing the aminoborane rather than the amine borane. Isotopic labelling of the boron bound hydrogen should result in all the deuterium being found in the hydrogen formed in the second step, while isotopic labelling of the hydrogen sulfide should show half the deuterium in the hydrogen while half would be found in the hydrogen sulfide.

6.3. The Crystal and Molecular Structure of Bis(diethylamino) dithiaboretane

Bis(diethylamino)dithiaboretane was found to crystallize in a tetragonal unit cell with a = b = 10.396 ± 0.003Å, c = 25.589 ± 0.007Å and $\alpha = \beta = \gamma = 90^{\circ}$. For purposes of description, the important symmetry elements in the space group, $P_{4_1 2_1 2}$, are the two-fold rotation axes along the cell diagonals at Z values of 0, 1/4, 1/2, 3/4 and 1.

A diagram of a single molecule of $\left[(C_2H_5)_2NBS\right]_2$ is given in Figure XXXIV. In the crystal these molecules can be visualized as occurring in pairs. In each molecule the sulfur atoms lie almost vertically above each other. In one molecule the two-fold rotation axis is along the two boron-nitrogen bond axes and in the other molecule this same axis is perpendicular to the 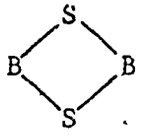 plane and passes through its center. The orientation of a pair of molecules is shown in Figure XXXV. Here the two-fold rotation axis is through the center of the boron-sulfur plane of the molecule in the foreground and along the boron-nitrogen axis of the molecule in the background.

The space group also has two and four-fold screw axes parallel to the c axis. These can be considered to generate the remaining pairs of molecules throughout the unit cell. The contents of a unit cell, in outline form, are shown in Figure XXXVI. The molecular pair shown in Figure XXXV correspond to the second pair of molecules in the c direction.

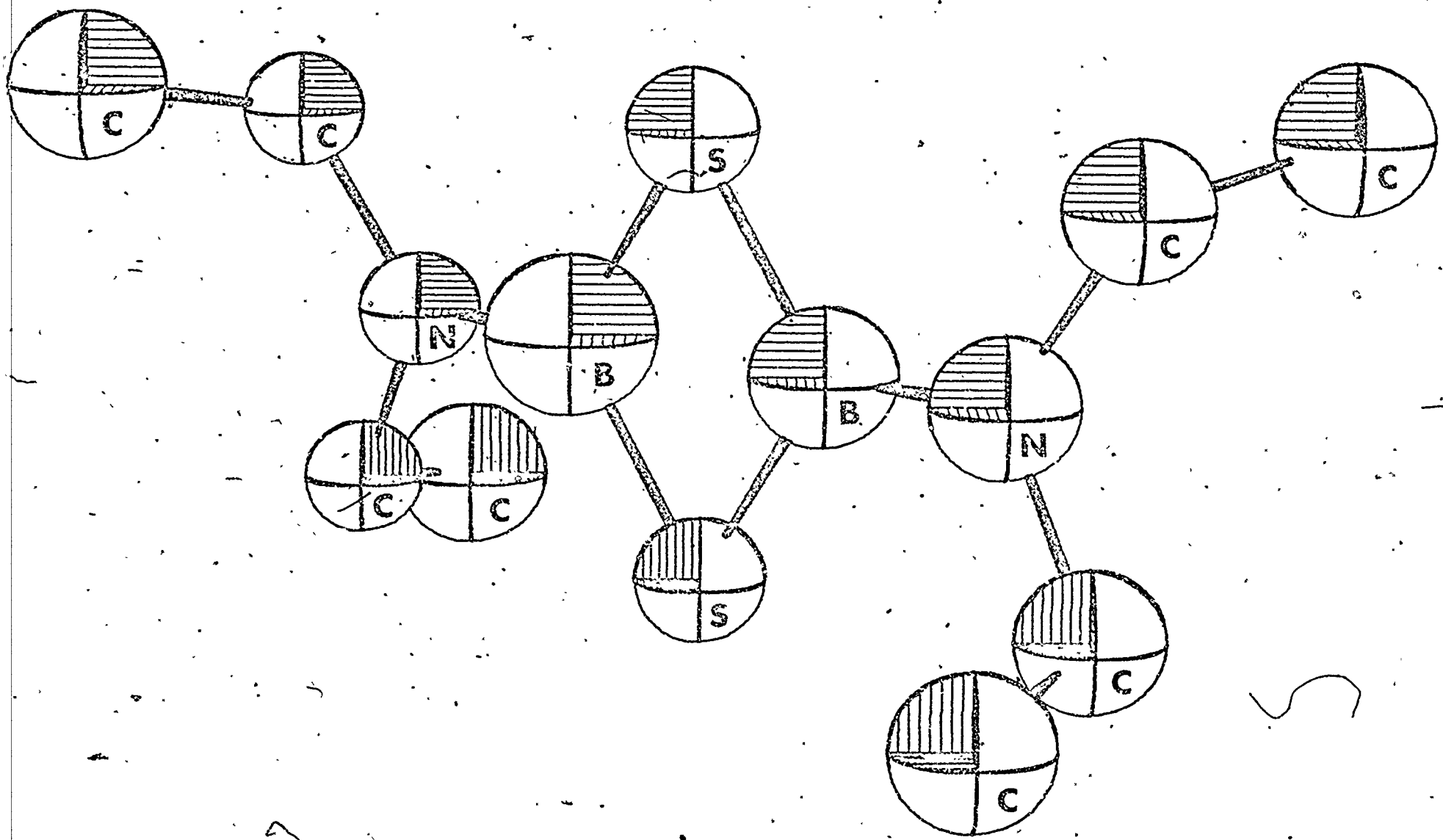

Figure XXXIV

Bis(diethylamino)dithiaboretane: Single Molecule

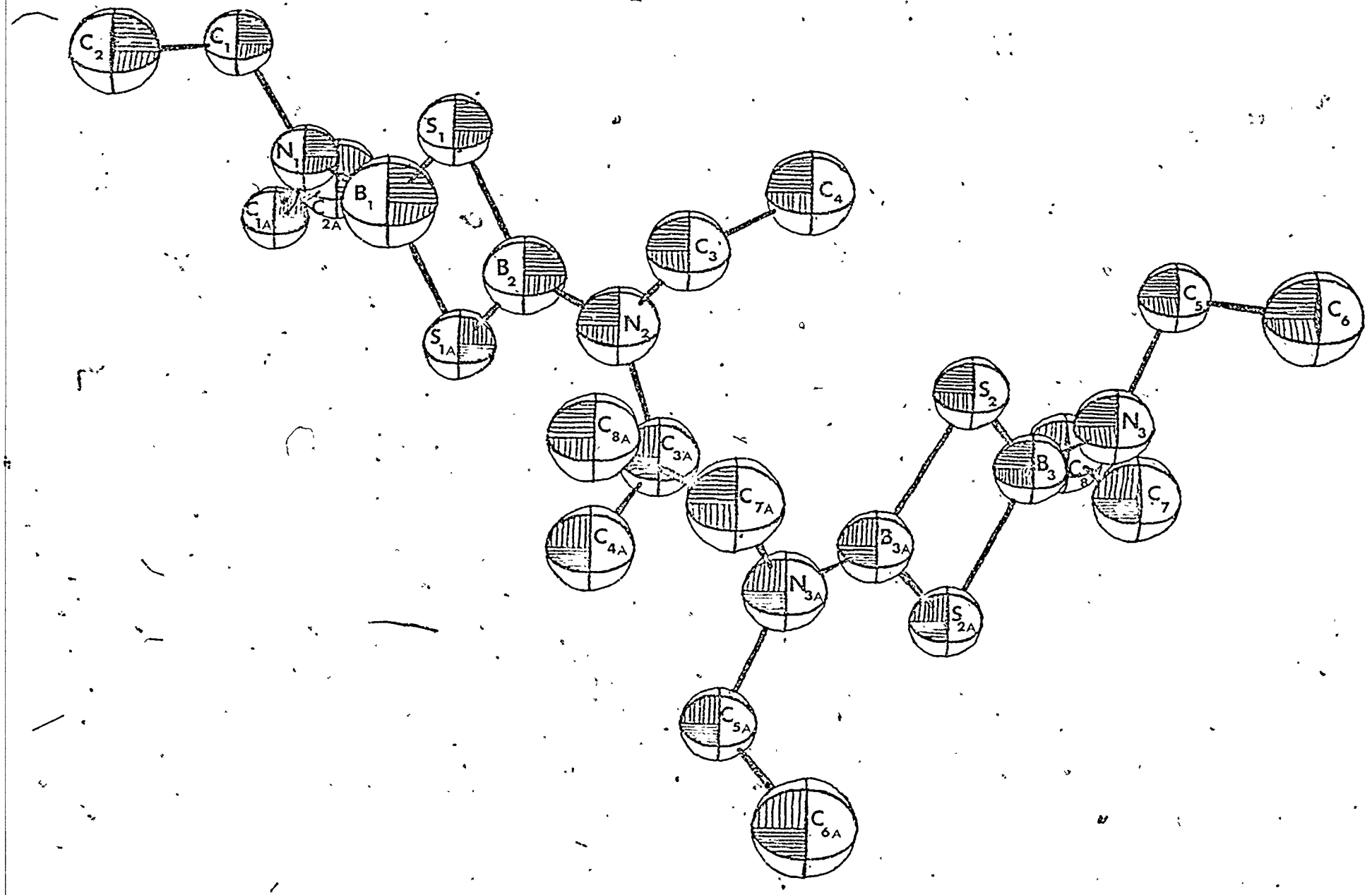

Figure XXXV -

Bis(diethylamino)dithiaboretane: Molecular Pair.

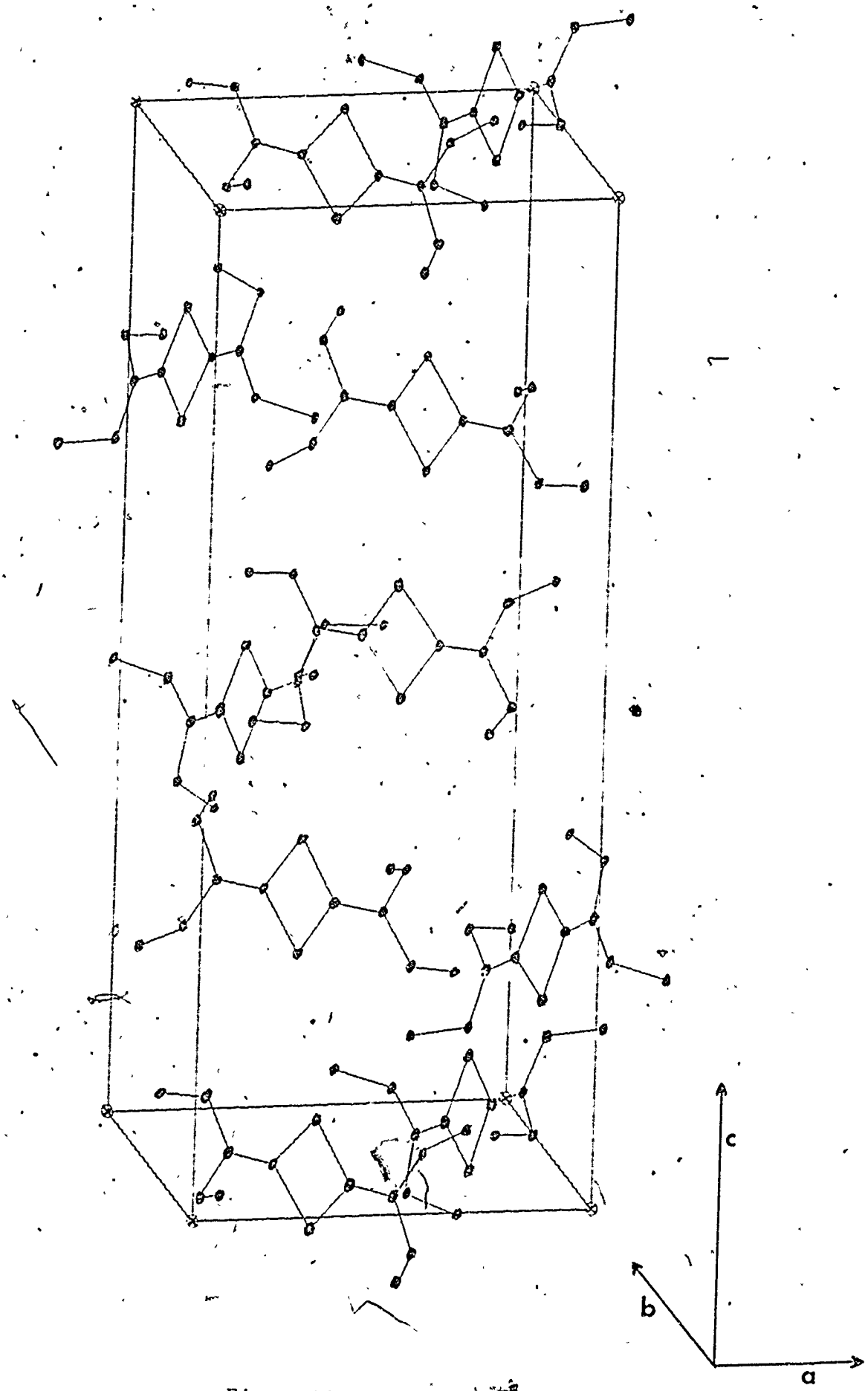

Figure XXXVI

Bis(diethylamino)dithiaboretane: Unit Cell Contents

The bond distances, with standard deviations, found in $[(C_2H_5)_2NBS]_2$ are given in Table XI. Bond angles, again with standard deviations, are given in Table XII. The atom designations are as in Figure XXXV.

TABLE XI

BOND LENGTHS WITH STANDARD DEVIATIONS

Bond	Length (Å)	Bond	Length (Å)
S_1-B_1	1.83 ± 0.04	N_1-C_1	1.55 ± 0.03
S_1-B_2	1.81 ± 0.04	N_2-C_3	1.54 ± 0.03
S_2-B_3	1.85 ± 0.04	N_3-C_5	1.48 ± 0.03
S_2-B_{3_A}	1.87 ± 0.04	N_3-C_7	1.54 ± 0.03
B_1-N_1	1.39 ± 0.06	C_1-C_2	1.52 ± 0.04
B_2-N_2	1.44 ± 0.05	C_3-C_4	1.49 ± 0.04
B_3-N_3	1.32 ± 0.03	C_5-C_6	1.59 ± 0.04
		C_7-C_8	1.55 ± 0.04

A great deal of information can be derived from these results as explained under the following headings:

1) The $[(C_2H_5)_2NBS]_2$ molecule shows approximately 222 (D_2) symmetry, with three orthogonal two-fold axes. From Figure XXXV, one of these axes passes along the B-N bonds, the second through the sulfur

TABLE XII

BOND ANGLES WITH STANDARD DEVIATIONS

Bonds	Angle (degrees)	Bonds	Angle (degrees)
S_1-B_1-S_{1_A}	106 ± 4	B_1-N_1-C_1	122 ± 2
S_1-B_2-S_{1_A}	108 ± 3	B_2-N_2-C_3	122 ± 2
S_2-B_3-S_{2_A}	101 ± 2	B_3-N_3-C_5	119 ± 3
		B_3-N_3-C_7	119 ± 3
B_1-S_1-B_2	73 ± 2		
B_3-S_2-B_{3_A}	79 ± 2	N_1-C_1-C_2	116 ± 3
		N_2-C_3-C_4	116 ± 3
S_1-B_1-N_1	127 ± 2	N_3-C_5-C_6	105 ± 2
S_1-B_2-N_2	126 ± 2	N_3-C_7-C_8	114 ± 3
S_2-B_3-N_3	130 ± 3		

atoms and the third is perpendicular to, and passes through, the center of the 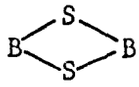 plane. In the crystal one of these axes lies along a diagonal of the unit cell and the second is at a small (less than 10^{o}) angle to another diagonal. The third C_2 axis, that through the sulfur atoms, is at a small angle (less than 10^{o}) to the c axis of the unit cell.

2) The existence of an alternating boron-sulfur four membered ring has been clearly established. Thus crystallographic data is now available substantiating the existence of the $(BS)_2$ ring as well as the $(BN)_2$ ring[93]. The existence of $(BP)_2$[87] and $(BO)_2$[94] rings remains

to be established by x-ray methods. The length of the boron-sulfur bond is within a standard deviation of the sum of the covalent radii of boron and sulfur (1.84Å), and is similar to that obtained (1.85Å) in a crystallographic study of $(BrBS)_3$[88]. On the basis of this distance it can be stated that the bond between boron and sulfur is a single bond, i.e., there is no donation of electron density from the filled, non bonding sulfur p orbitals to the vacant boron p orbital.

The ring is obviously strained. Expected angles for tri-coordinate boron and dicoordinate sulfur are 120° and 109° respectively. The angles found are approximately 105° for S-B-S and 75° for B-S-B. Nevertheless $[(C_2H_5)_2NBS]_2$ is stable at the preparation temperature (175 °C) and sublimes readily without decomposition at 75 °C.

The angles about the boron atom can not be compared with those found in the four membered B-N ring shown in Figure XXII, as these latter angles were not given[93].

3) To date the only aminoborane bond lengths reported have been for the compounds shown in Figures XXI and XXII. The B-N bond lengths in these compounds vary from 1.40 to 1.43Å, with the exception of the exocyclic B-N bond in the compound in Figure XXII, which is 1.47Å. These bond lengths may be compared with borazine, at 1.44Å.

The current study is the only structure analysis undertaken to date on a monoaminoborane, although space group determinations have previously been carried out[127].

Two of the three B-N bond lengths are within a standard

deviation of the previous results while the third is somewhat shorter. However, a statistical calculation[128] indicated a 36% probability, i.e., approximately 1 chance in 3, of finding another bond at 1.32Å, even if the B-N bond length was accepted as the average of the two longer lengths. This is a result of the sizable standard deviations.

The experimental results provide three indications of multiple bond character in the bond between boron and nitrogen. These are the short bond length, the bond angles about both boron and nitrogen and the coplanarity of the C-N-C and S-B-S-B planes.

The bond lengths obtained are all less than the sum of the covalent radii of boron and nitrogen (1.49Å). This is the strongest indicator of multiple bond formation. The bond angles about nitrogen are within a standard deviation of 120°, and therefore the nitrogen atom can be considered to be an sp^2 hybrid. Although the angles about the boron atoms are constrained by the boron-sulfur ring, the S-B-N angles suggest that the boron atom can also be considered as an sp^2 hybrid. The sp^2 hybrids on boron and nitrogen are at an angle of less than 10° to each other, and are therefore of appropriate symmetry for π bond formation.

If the boron-nitrogen bond is a double bond it would be expected that the C-N-C and S-B-S-B groups would be coplanar. Of the six planes of interest in the molecule five are planar due to having only 3 members or by symmetry. The sixth, B_3-S_2-B_{3_A}-S_{2_A} is not required by symmetry to be planar, but a least squares calculation

shows the sulfur atoms to be only 0.004Å off a mean plane through the group while the boron atoms lie 0.05Å off the same plane. The normals to the planes in question can be used to establish coplanarity, and are shown in Table XIII.

TABLE XIII

PLANES IN BIS(DIETHYLAMINO)DITHIABORETANE

Plane I	Plane II	Angle between normals(degrees)
B_1-S_1-B_2-$S_1{}_A$	C_1-N_1-$C_1{}_A$	9.32
B_1-S_1-B_2-$S_1{}_A$	C_3-N_2-$C_3{}_A$	170.73
B_3-S_2-$B_3{}_A$-S_2	C_5-N_3-C_7	5.70
B_3-S_2-$B_3{}_A$-$S_2{}_A$	$C_5{}_A$-$N_3{}_A$-$C_7{}_A$	174.40

This Table shows that in each molecule the planes in question are approximately, but not exactly, coplanar. In one molecule the C-N-C planes are rotated 9.32° and 9.27°, in opposite senses, to the S-B-S-B plane. In the other molecule the rotations are 5.60° and 5.70°, again in opposite senses. The observation that the rotations are almost identical, and in opposite senses, supports the 222 symmetry assignment for the molecule. The approximate coplanarity of the C-N-C and S-B-S-B planes also provides evidence for formation of a B-N multiple bond, but the evidence is not in itself sufficient since co-

planarity may also be a result of crystal packing.

Of interest is the fact that the long (1.47Å) exocyclic B-N bond found in B-[bis(trimethylsilyl)amino] -N-trimethylsilylcyclodiborazane, Figure XXII, has been ascribed to the fact that the Si-N-Si plane is at right angles to the $(B\text{-}N)_2$ ring, preventing overlap of the non-bonding p orbitals on nitrogen with the vacant p orbital on boron, and thereby inhibiting multiple bond formation.

4) The accepted carbon-carbon single bond length is 1.541Å (127). Again, there is some scatter in the values obtained for these bond lengths in $[(C_2H_5)_2NBS]_2$, with three being within a standard deviation of the accepted value and one shorter.

Three of the N-C-C bond angles are grouped about 115°, while the fourth is considerably smaller at 105°. The "Tables of Interatomic Distances"(127) contain many examples of angles about tetrahedral carbon in the range from 105° to 118°. The N-C-C angle found in triethylamine is 113° ± 3° and three of the four angles measured in this study are within a standard deviation of this value.

5) The average nitrogen-carbon bond distance obtained in this work was 1.53Å , which is two estimated standard deviations removed from the accepted value of 1.47Å (129).

6) Some of the physical properties of $[(C_2H_5)_2NBS]_2$ are consistent with the intermolecular distances in the crystal. For purposes of description the packing of the molecules can be artificially considered as occurring in two steps; first the packing of molecules in a manner suggested by Figure XXXV to form a two-dimensional sheet,

and second, the packing of these sheets to form a three-dimensional network.

Within a sheet the important distances, i.e., those of closest approach, are those from a sulfur atom in one molecule to the methyl and methylene groups of adjacent molecules. Table XIV shows the distances from sulfur to the methyl and methylene carbon atoms.

TABLE XIV

INTERMOLECULAR DISTANCES (SAME LAYER)

Sulfur - Methyl Carbon		Sulfur - Methylene Carbon	
Atoms	Distance(Å)	Atoms	Distance(Å)
S_2-C_1	4.03	S_1-C_6	3.89
S_2-C_2	4.05	S_1-C_{8_A}	4.08
S_1-C_5	3.97	S_2-C_2	3.95
S_1-C_{7_A}	4.25	S_2-C_4	3.96

These distances show that the ethyl group is oriented in such a way as to minimize repulsions between the sulfur atom and methyl and methylene groups.

The sulfur atoms in a higher layer are roughly equidistant from the sulfur and carbon atoms in a lower layer. For example, S_2 in a higher layer fits into the triangle formed by S_1, C_2 and C_6 in

a lower layer, and is roughly equidistant from these three atoms. Similarly the carbon atoms in an upper layer fit into triangles formed by sulfur and carbon in a lower layer and are again roughly equidistant from the three atoms forming the triangle. These intermolecular distances are given in Table XV.

TABLE XV

INTERMOLECULAR DISTANCES (BETWEEN LAYERS)

Atoms	Distance (Å)	Atoms	Distance (Å)
S_1-S_2	4.28	S_2-S_1	4.28
S_1-C_2	4.10	S_2-C_2	4.41
S_1-C_{7_A}	4.25	S_2-C_6	4.04
C_1-S_1	4.57	C_2-S_2	4.41
C_1-C_4	4.20	C_2-C_1	4.74
C_1-C_{7_A}	4.41	C_2-C_6	4.26
C_5-S_2	4.83	C_{7_A}-S_1	4.18
C_5-C_2	4.77	C_{7_A}-C_4	4.54
C_5-C_{8_A}	3.97	C_{7_A}-C_5	4.15

Tables XIV and XV show that the intermolecular distances between molecules in the same layer tend to be slightly shorter than those between molecules in different layers.

The Van der Waal's radius for sulfur is given at 1.85Å and the same radius for methyl and methylene groups is 2.0Å (130) The intermolecular distances are rather longer than the sum of the Van der Waal's radii. This fact correlates with the observed properties of $[(C_2H_5)_2NBS]_2$, i.e., low melting point (70 °C), facile sublimation, low density and the property of the crystal "melting" at the contact points with the Lindemann tubes.

In conclusion, the crystal and molecular structure of bis(diethylamino)dithiaboretane, have been determined. This determination establishes, for the first time, the existence of a four membered boron-sulfur ring and shows the S-B bond is a single bond. The results are also the first report of the B-N bond in a monoaminoborane and show this bond to have multiple bond character. The molecular symmetry has been shown to be approximately 222 (D_2), and the properties of the solid material are consistent with the crystal structure.

6.4. Suggestions for Further Work

The residue from the reaction of trimethylaluminum and pentaborane(9) was found to have an empirical formula of $Al(CH_3)_{1.1}B_{2.7}H_{6.0}$. The exact identity of this non-volatile hydrogen rich solid would be of great interest.

Further work should be carried out in the area of Group IIIA bridge substituted pentaborane(9) species. For example, the solubilities of other octahydropentaborate(1-) salts, such as μ-$(CH_3)_4NB_5H_8$ should be investigated with a view to finding borate(1-) salts which would be soluble in non etheral solvents.

The preparation of bis(diethylamino)dithiaboretane is relatively simple. It would be interesting to examine the chemistry of this ring compound. The reaction mechanism postulated in 6.2.1. should also be tested.

BIBLIOGRAPHY

1. F.A. Cotton and G. Wilkinson, "Advanced Inorganic Chemistry", Interscience Publishers, New York, 1966.

2. M.L. Tobe, "Inorganic Reaction Mechanisms", Thomas Nelson and Sons, Ltd., London, 1972.

3. T.G. Appleton, H.C. Clark and L.E. Manzer, Coord. Chem. Rev., 10, 335(1973).

4. F.R. Hartley, Chem. Soc. Revs., 2, 163(1973).

5. A. Pidcock, R.E. Richards and L.M. Venanzi, J. Chem. Soc. A., 1707(1966).

6. A.A. Grinberg, Acta. Physicochim URSS, 3, 573(1935).

7. Y.K. Syrkin, Izvest. Acad, Nauk SSSR, Otdel. Khim. Nauk, 69(1948).

8. S.S. Zumdahl and R.S. Drago, J. Amer. Chem. Soc., 90, 6669(1968).

9. C.H. Langford and H.B. Gray, "Ligand Substitution Processes", W.A. Benjamin, Inc., New York, 1965.

10. P.W. Atkins, J.C. Green and M.L.H. Green, J. Chem. Soc. A., 2275(1968).

11. G.G. Mather, A. Pidcock and G.J.N. Rapsey, J. Chem. Soc., Dalton, 2095(1973).

12. J. Chatt and B.L. Shaw, J. Chem. Soc., 5075(1962).

13. G. Socrates, J. Inorg. Nucl Chem., 31, 1667(1969).

14. H.C. Clark and W.S. Tsang, J. Amer. Chem. Soc., 89, 529(1967).

15. A.J. Rest, D.T. Rosevear and F.G.A. Stone, J. Chem. Soc. A., 66(1967).

16. H.C. Clark, K.R. Dixon and W.J. Jacobs, J. Amer. Chem. Soc., 90, 2259(1968).

17. K.R. Dixon, K.C. Moss and M.A.R. Smith, In Press.

18. H.C. Clark and J.D. Ruddick, Inorg. Chem., 9, 1226(1970).

19. M.J. Church and M.J. Mays, J. Chem. Soc. A., 3074(1968).

20. J.M. Jenkins and B.L. Shaw, Proc. Roy. Soc., 279(1963).

21. H.C. Clark and W.S. Tsang, J. Amer. Chem. Soc., 89, 533(1967).

22. H.C. Clark and L.E. Manzer, Inorg. Chem., 10, 2699(1971).

23. D.M. Adams, J. Chatt and B.L. Shaw, J. Chem. Soc., 2047(1960).

24. T.G. Appleton, M.H. Chisholm, H.C. Clark and L.E. Manzer, Can. J. Chem., 51, 2243(1973).

25. J.W. Emsley, J. Feeney and L.H. Sutcliffe, "High Resolution Nuclear Magnetic Resonance Spectroscopy", Vols. I and II, Pergamon Press, Oxford, 1965.

26. B.E. Mann, B.L. Shaw and N.I. Tucker, J. Chem. Soc. A, 2667(1971).

27. T.D. Coyle, S.L. Stafford and F.G.A. Stone, Spectrochimica Acta, 17, 968(1961).

28. T.G. Appleton, M.H. Chisholm, H.C. Clark and L.E. Manzer, Inorg. Chem., 11, 1786(1972).

29. F.B. Mallory, J. Amer. Chem. Soc., 95, 7747(1973), and references therein.

30. J.A. Pople and D.P. Santry, Mol Phys., 8, 1(1964).

31. A. Hinchliffe and D.B. Cook, Theoret. Chim. Acta. (Berl.), 17, 91(1970).

32. J.A. Pople, J.W. McIver, Jr. and N.S. Ostlund, J. Chem. Phys., 49, 2960(1968).

33. J.A. Pople, J.W. McIver, Jr. and N.S. Ostlund, J. Che. Phys., 49, 2965(1968).

34. A.C. Blizzard and D.P. Santry, J. Chem. Phys., 55, 950(1971).

35. F.H. Allen and A.Pidcock, J. Chem. Soc. A, 2700(1968).

36. J. Powell and B.L. Shaw, J. Chem. Soc., 3879(1965).

37. E. Wiberg and E. Amberger, "Hydrides of the Elements of Main Groups I-IV", Elsevier Publishing Co., Amsterdam, 1971.

38. Inorg. Chem., 7, 1945(1968).

39. F. Jones, J. Chem. Soc., 35, 41(1879).

40. A. Stock, "Hydrides of Boron and Silicon", Cornell University Press, Ithaca, New York, 1957.

41. W.N. Lipscomb, "Boron Hydrides", W.A. Benjamin, Inc., New York, 1963.

42. W.H. Eberhardt, B. Crawford and W.N. Lipscomb, J. Chem. Phys., 22, 989(1954).

43. H.J. Hrostowski and G.C. Pimentel, J. Chem. Phys., 20, 518(1952).

44. I. Shapiro, H.G. Weiss, M. Schmich, S. Skolnik and G.B.L. Smith, J. Am. Chem. Soc., 74, 901(1952).

45. R.T. Holzmann, "Production of the Boranes and Related Research", Academic Press, New York, 1967.

46. Callery Chemical Co., Callery, Pennsylvania.

47. D.F. Gaines, J. Am. Chem. Soc., 91, 6503(1969).

48. H.C. Miller, N.E. Miller and E.L. Meutterties, Inorg. Chem., 3, 1456(1964).

49. H.D. Johnson and S.G. Shore, J. Am. Chem. Soc., 93, 3798(1971).

50. R.A. Geanangel, H.D. Johnson and S.G. Shore, Inorg. Chem., 10, 2363(1971).

51. B. Rice and H.S. Uchida, J. Phys. Chem., 59, 650(1955).

52. D.R. Schultz and R.W. Parry, J. Am. Chem. Soc., 80, 4(1958).

53. G. Kodama, U. Engelhardt, C. Lafrenz and R.W. Parry, J. Am. Chem. Soc., 94, 407(1972).

54. H.C. Brown, "Hydroboration", W.A. Benjamin, Inc., New York, 1962.

55. W.E. Palke and W.N. Lipscomb, J. Am. Chem. Soc., 88, 2384(1966).

56. W.V. Hough and J.L. Edwards, "Advances in Chemistry", Volume 32, 1961.

57. J.J. Miller and M.F. Hawthorne, J. Am. Chem. Soc., 81, 4501(1959).

58. J.A. Dupont and M.F. Hawthorne, J. Am. Chem. Soc., 84, 1804(1962).

59. A.C. Bond and M.L. Pinsky, J. Am. Chem. Soc., 92, 7585(1970).

60. H.D. Johnson and S.G. Shore, J. Am. Chem. Soc., 92, 7586(1970).

61. M.L. Pinsky and A.C. Bond, Inorg. Chem., 12, 605(1973).

62. T. Onak, G.B. Dunks, I.W. Searcy and J. Spielman, Inorg. Chem., 6, 1465(1967).

63. D.F. Gaines and T.V. Iorns, J Am. Chem. Soc., 89, 3375(1967).

64. R.A. Geanangel and S.G. Shore, J. Am. Chem. Soc., 89, 6771(1967).

65. V.T. Brice, H.D. Johnson, D.L. Denton and S.G. Shore, Inorg. Chem., 11, 1135(1972).

66. H.D. Johnson, R.A. Geanangel and S.G. Shore, Inorg. Chem., 9, 908(1970).

67. V.T. Brice and S.G. Shore, Inorg. Chem., 12, 309(1973).

68. H.D. Johnson, S.G. Shore, N.L. Mock and J.C. Carter, J. Am. Chem. Soc., 91, 2131(1969).

69. G.L. Brubaker, M.L. Denniston, S.G. Shore, J.C. Carter and F. Swicher, J. Am. Chem. Soc., 92, 7216(1970).

70. H.D. Johnson, V.T. Brice, G.L. Brubaker and S.G. Shore, J. Am. Chem. Soc., 94, 6711(1972).

71. W.V. Hough, L.J. Edwards and A.D. McElroy, J. Am. Chem. Soc., 78, 689(1956).

72. J. Borlin and D.F. Gaines, J. Am. Chem. Soc., 94, 1367(1972).

73. C.R. Peters and C.E. Nordman, J. Am. Chem. Soc., 82, 5758(1960).

74. H.I. Schlesinger, D.M. Ritter and A.B. Burg, J. Am. Chem. Soc., 60, 2297(1938).

75. K. Hedberg and A. Stosik, J. Am. Chem. Soc., 74, 954(1952).

76. D.F. Gaines and T.V. Iorns, J. Am. Chem. Soc., 89, 4249(1967).

77. J.C. Calabrese and L.F. Dahl, J. Am. Chem. Soc., 93, 6042(1971).

78. D.F. Gaines and T.V. Iorns, J. Am. Chem. Soc., 90, 6617(1968).

79. T.C. Geisler and A.D. Norman, Inorg. Chem., 9, 2167(1970).

80. A.B. Burg and H. Heinen, Inorg. Chem., 7, 1021(1968).

81. D.F. Gaines and T.V. Iorns, J. Am. Chem. Soc., 92, 4571(1970).

82. T.P. Onak and G.B. Dunks, Inorg. Chem., 5, 439(1966).

83. M.L. Thompson and R.N. Grimes, Inorg. Chem., 11, 1925(1972).

84. A. Tabereaux and R.N. Grimes, Inorg. Chem., 12, 792(1973).

85. K. Niedenzu and J.W. Dawson, "Boron-Nitrogen Compounds", Academic Press Inc., New York, 1965.

86. R.J. Brotherton and H. Steinberg, "Progress in Boron Chemistry", Volume 3, p. 211, Pergamon Press Inc., Oxford, 1970.

87. I. Haiduc, "The Chemistry of Inorganic Ring Systems", Part I, Wiley-Interscience, London, 1970.

88. E.L. Meutterties, Editor, "The Chemistry of Boron and its Compounds", John Wiley & Sons, Inc., New York, 1967.

89. H. Steinberg and A.L. McCloskey, Editors, "Progress in Boron Chemistry", Volume I, Pergamon Press, Oxford, 1964.

90. A.N. Nesmeyanov and R.A. Sokolik, "Methods of Elements-Organic Chemistry", Volume I, The World Publishing Co. Cleveland, 1967.

91. R.M. Adams, Editor, "Boron, Metallo-Boron Compounds and Boranes", Interscience Publishers, New York, 1964.

92. G.J. Bullen and N.H. Clark, Chem. Comm., 670(1967).

93. H. Hess, Angew. Chem. Intern. Ed. Engl., 6, 975(1967).

94. R.T. Hawkins, W.J. Lennerz and H.R. Snyder, J. Am. Chem. Soc., 82, 3053(1960).

95. J.A. Forstner and E.L. Meutterties, Inorg. Chem., 5, 164(1966).

96. W.C. Price, J. Chem. Phys., 15, 614(1947).

97. W.J. Lehman, C.O. Wilson, J.F. Ditter and I. Shapiro, Adv. in Chem. Series, 32,127(1961).

98. J.P. Glusker and K.N. Trueblood, "Crystal Structure Analysis: A Primer", Oxford University Press, London, 1972.

99. G.H. Stout and L.H. Jensen, "X-ray Structure Determination", The MacMillan Co., New York, 1968.

100. R.T. Sanderson, "Vacuum Manipulation of Volatile Compounds", John Wiley, New York, (1948).

101. D.F. Shriver, "The Manipulation of Air-Sensitive Compounds", McGraw-Hill Book Co., New York, 1969.

102. I. Shapiro, H.G. Weiss, M. Schmick, S. Skolnik and G. B. L. Smith, J. Am. Chem. Soc., 74, 901(1952).

103. W.V. Kotlensky and R. Schaeffer, J. Am. Chem. Soc., 80, 4577(1958).

104. J.W. Owen, Master of Science Dissertation, University of Victoria, 1972.

105. L.V. McCarty, G.C. Smith and R.S. McDonald, Anal. Chem., 26, 1027(1954).

106. D.F. Gaines, private communication.

107. G.E. Coates,M.L.H. Green and K. Wade, "Organometallic Compounds", Third Edition, Volume I, Methuen and Co. Ltd., (London) 1967.

108. K. Yasuda and R. Okawara, Organomet. Chem. Rev., 2, 255(1967).

109. H.C. Brown, J. Am. Chem. Soc., 67, 1765(1945).

110. N.N. Greenwood and J.H. Morris, J. Chem. Soc., 2922(1960).

111. J.A. Ibers, "International Tables for X-ray Crystallography", Vols III, Kynoch Press, Birmingham, England, 1952.

112. H.J. Hrostowski and G.C. Pimentel, J. Am. Chem. Soc., 76, 998(1954).

113. W.C. Price, J. Chem. Phys. 17, 1044(1949).

114. H.I. Schlesinger, H.C. Brown, H.R. Holkstra and L.R. Rapp, J. Am. Chem. Soc., 75, 199(1953).

115. R.M. D'Eye and E. Wait, "X-ray Powder Photography in Inorganic Chemistry", Academic Press, New York, 1960.

116. F.G.A. Stone, Chem. Rev. 58, 116(1958).

117. E. Wiberg, K. Hertwig and A. Bolz, Z. Anorg. allgem. Chem., 256, 177(1948). Chem. Abstr. 43, 5690a(1949).

118. R. Rienacker and D. Schwengers, Justus Liebigs Ann. Chem. 737, 182(1970). Chem. Abstr. 73, 99010v(1971).

119. H.C. Brown, "Boranes in Organic Chemistry", Cornell University Press, Ithaca, New York, 1972.

120. H.I. Schlesinger, R.T. Sanderson and A.B. Burg., J. Am. Chem. Soc., 62, 3421(1940).

121. A.E. Shirk and D.F. Shriver, J. Am. Chem. Soc., 95, 5904(1973).

122. J. Goubeau, R. Epple, D.D. Ulmschieder and H. Lehmann, Angew. Chem., 67, 710(1955).

123. A. Cabana, J. Brault and J.M. Lalantette, Spectro. Chim. Acta., 22, 377(1966).

124. K. Niedenzu and J.W. Dawson, J. Am. Chem. Soc., 81, 5553(1959).

125. B.M. Mikhailov and Yu. N. Bubnov, Izvest. Acad. Nauk SSSS, Otdel. Khim. Nauk., 1378(1962). Chem. Abstr. 58, 5707f(1963).

126. B.M. Mikhailov and T.A. Shchegoleva, Izvest. Acad. Nauk SSSR, Otdel. Khim. Nauk, 1868(1959). Chem. Abstr., 54, 8608a(1960).

127. G.J. Bullen, U.S. Govt. Res. Rept., 39, 23(1964). Chem. Abstr. 62A, 1147d(1965).

128. P.R. Bevington, "Data Reduction and Error Analysis for the Physical Sciences", McGraw-Hill Book Co., New York, 1969.

129. "Tables of Interatomic Distances and Configuration in Molecules and Ions", The Chemical Society, London, 1958.

130. R.C. Weast, Ed., "Handbook of Chemistry and Physics", The Chemical Rubber Co., Cleveland, Ohio, 1968-69.

APPENDIX I

Perfluorovinylbis(triethylphosphine)platinum(II) complexes

SPECTRA

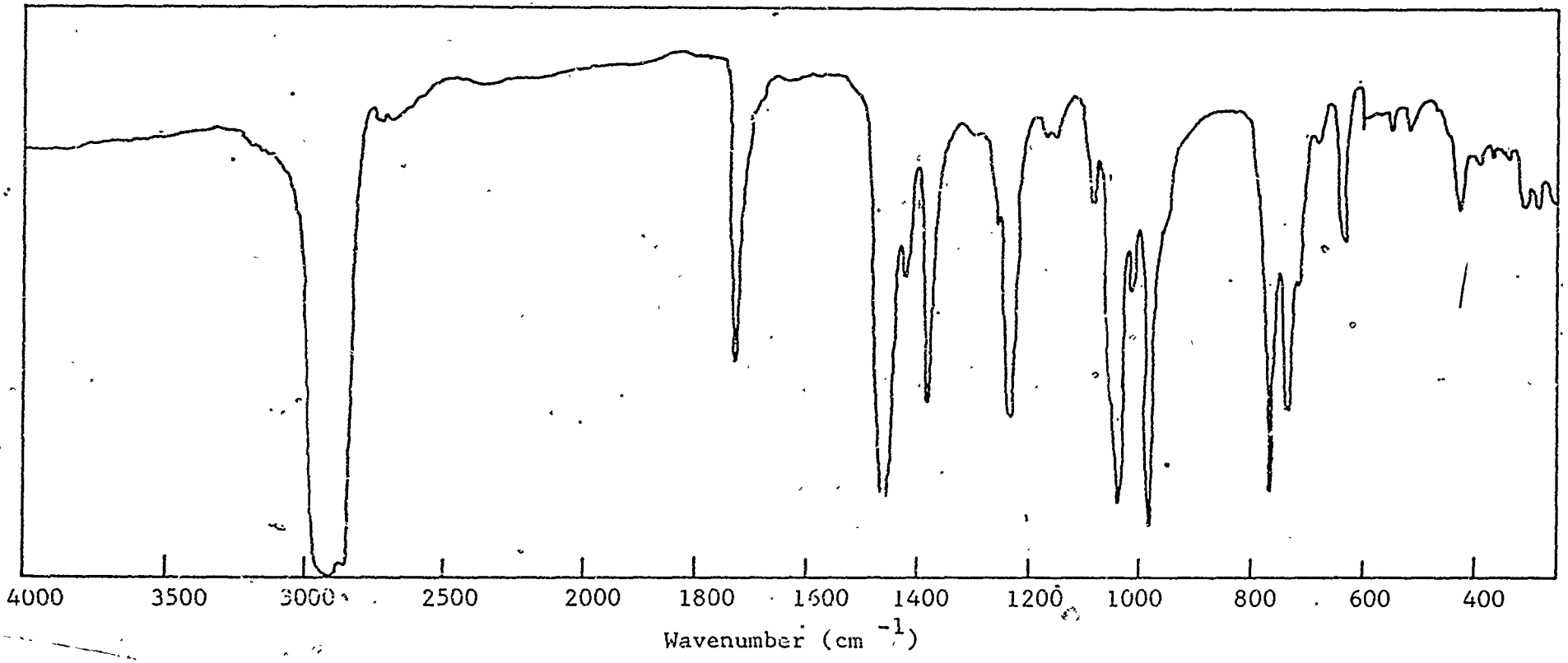

The infrared spectrum of <u>trans</u>-$[PtCl(CF{=}CF_2)(Et_3P)_2]$

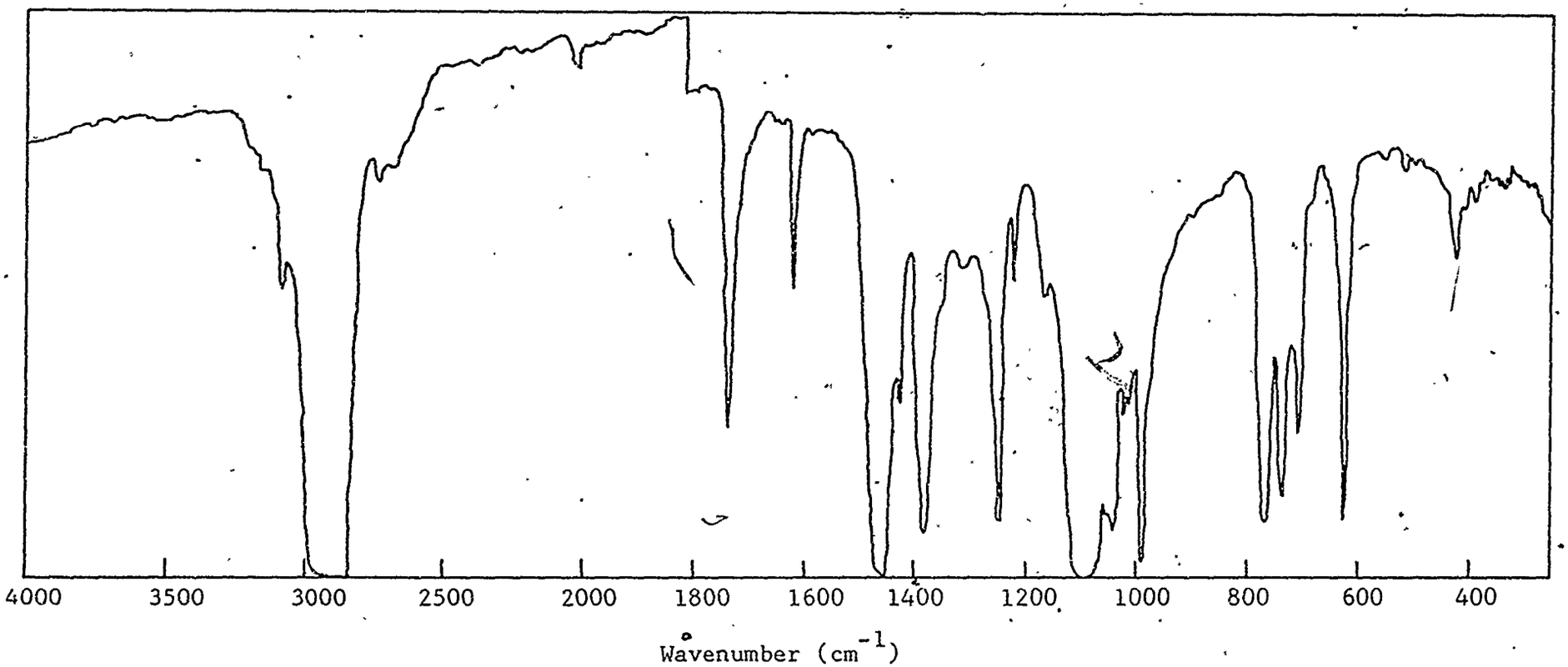

The infrared spectrum of trans-$[Pt(CF=CF_2)(C_5H_5N)(Et_3P)_2][ClO_4]$

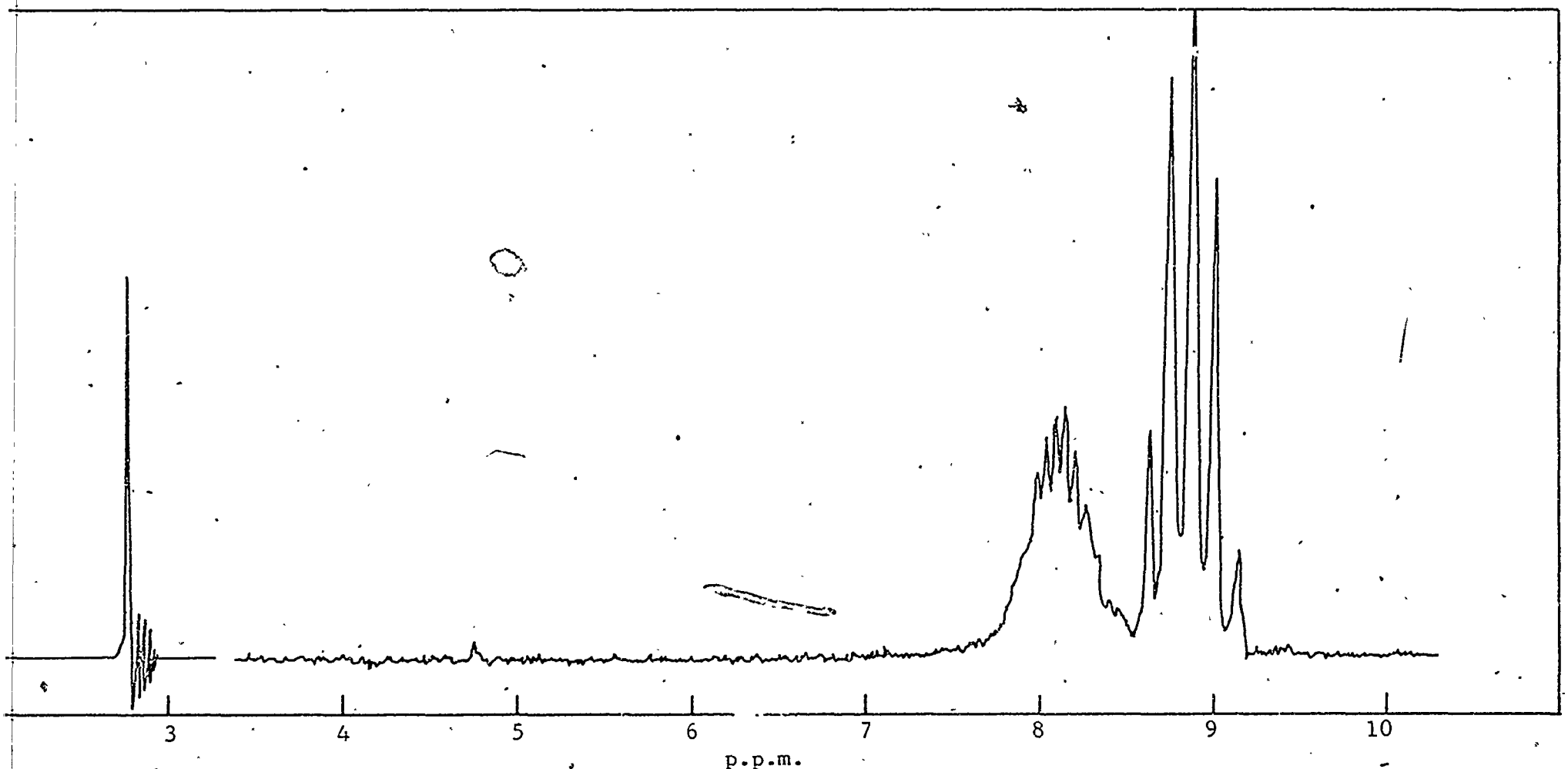

The proton magnetic resonance spectrum of trans-$[PtCl(CF=CF_2)(Et_3P)_2]$

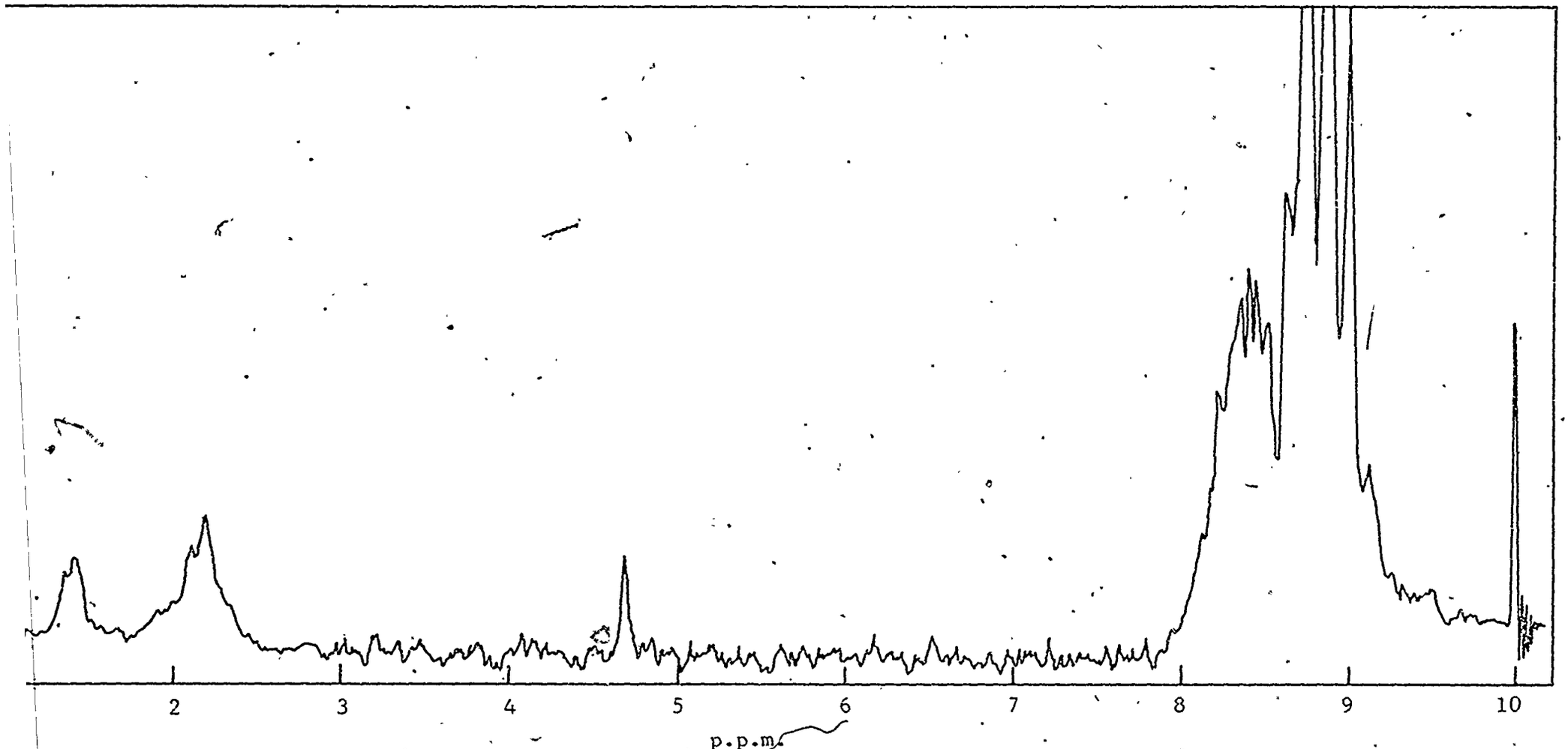

The proton magnetic resonance spectrum of trans-$[Pt(CF{=}CF_2)(C_5H_5N)(Et_3P)_2][ClO_4]$

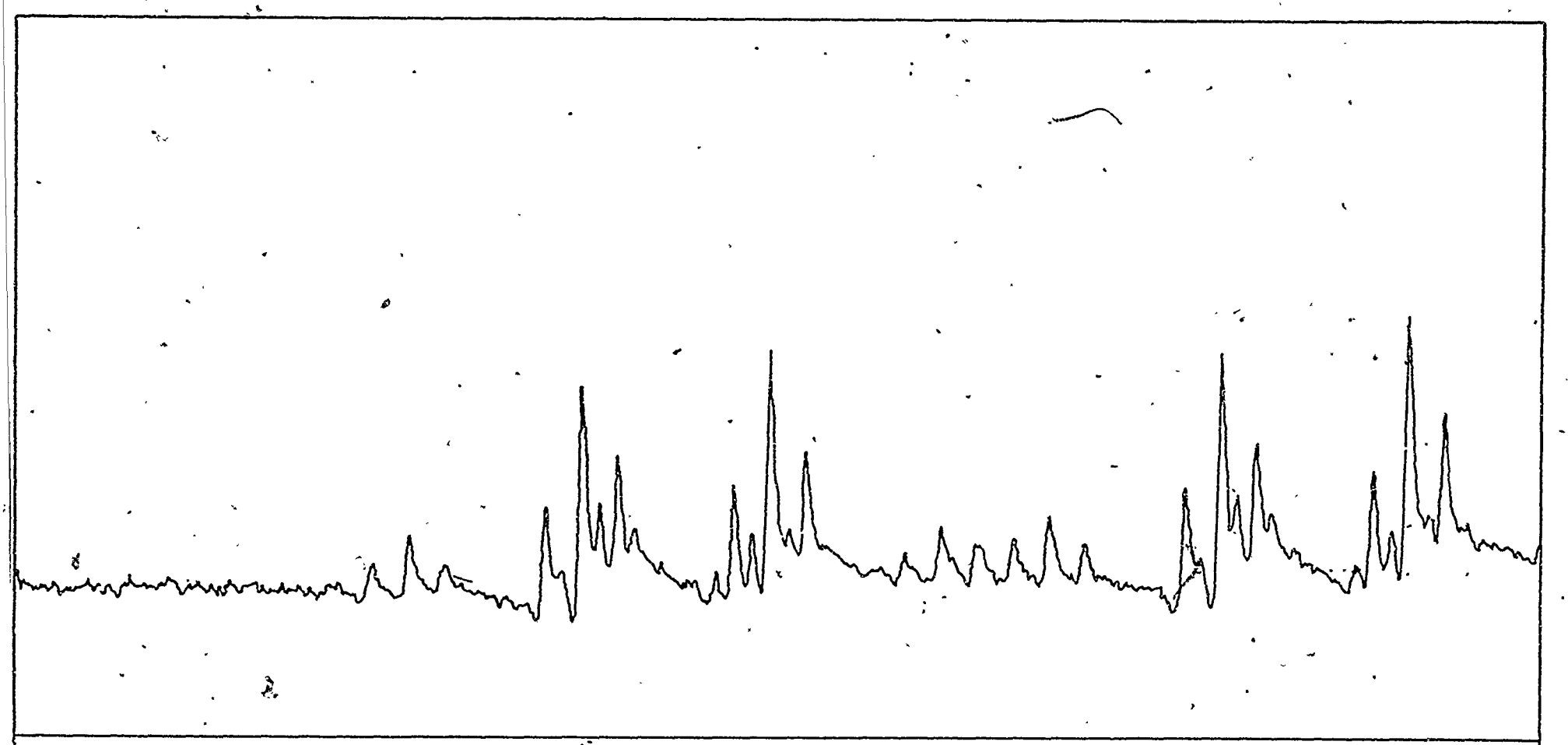

The ^{19}Fluorine magnetic resonance spectrum of trans-$[PtCl(C_2F_3)(Et_3P)_2]$

F_1

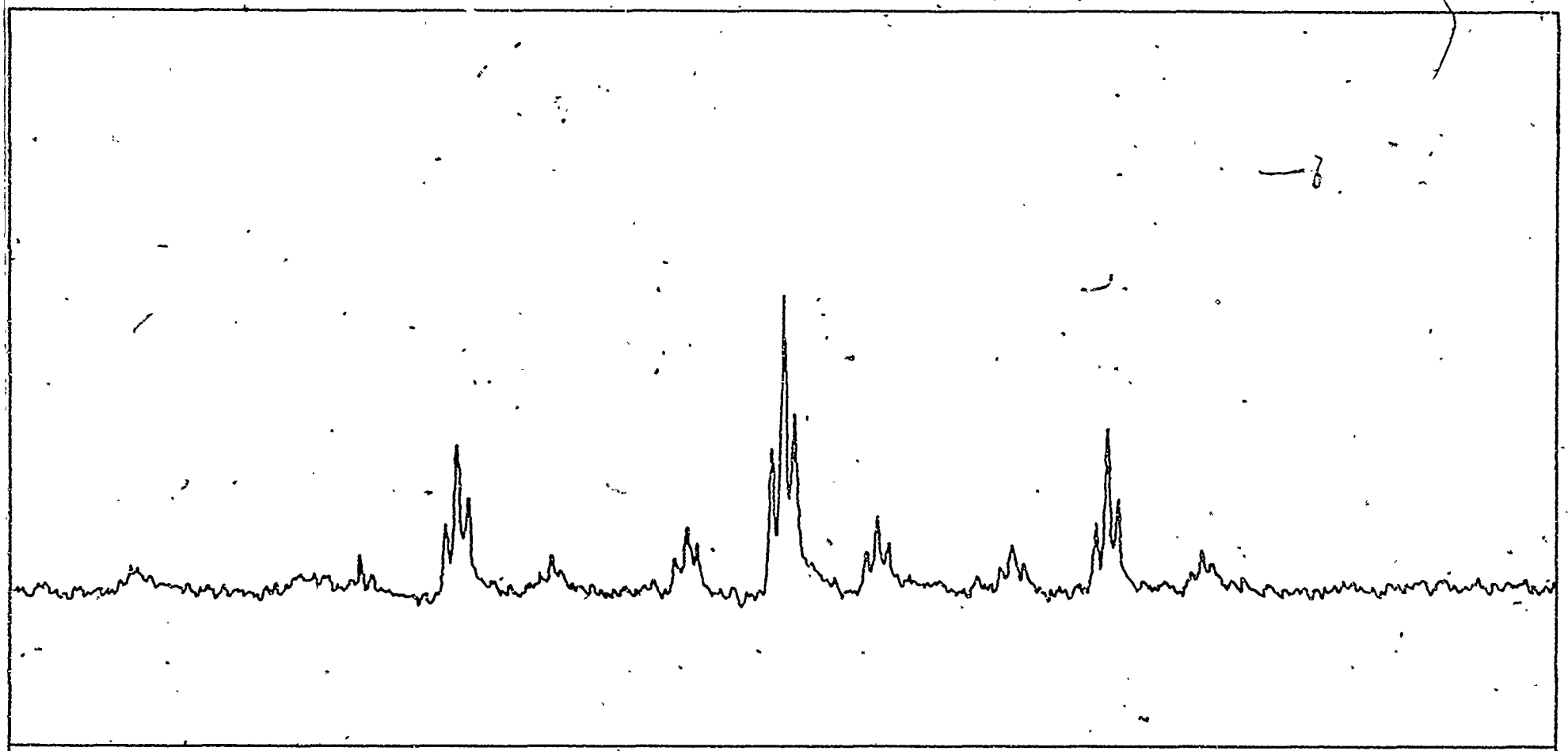

The ^{19}Fluorine magnetic resonance spectrum of trans-$[PtCl(C_2F_3)(Et_3P)_2]$

F_2

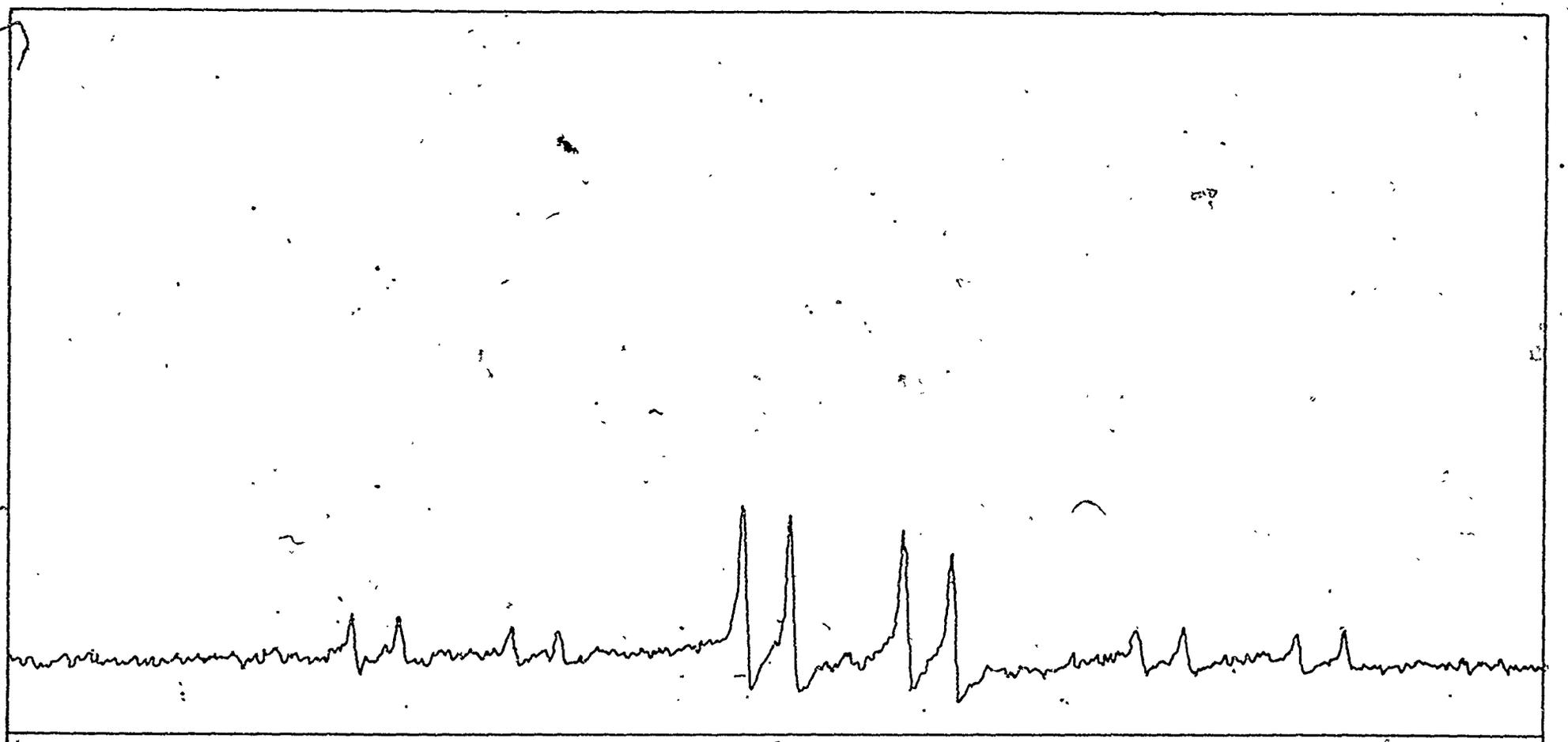

The ^{19}Fluorine magnetic resonance spectrum of trans-$[PtCl(C_2F_3)(Et_3P)_2]$

F_3

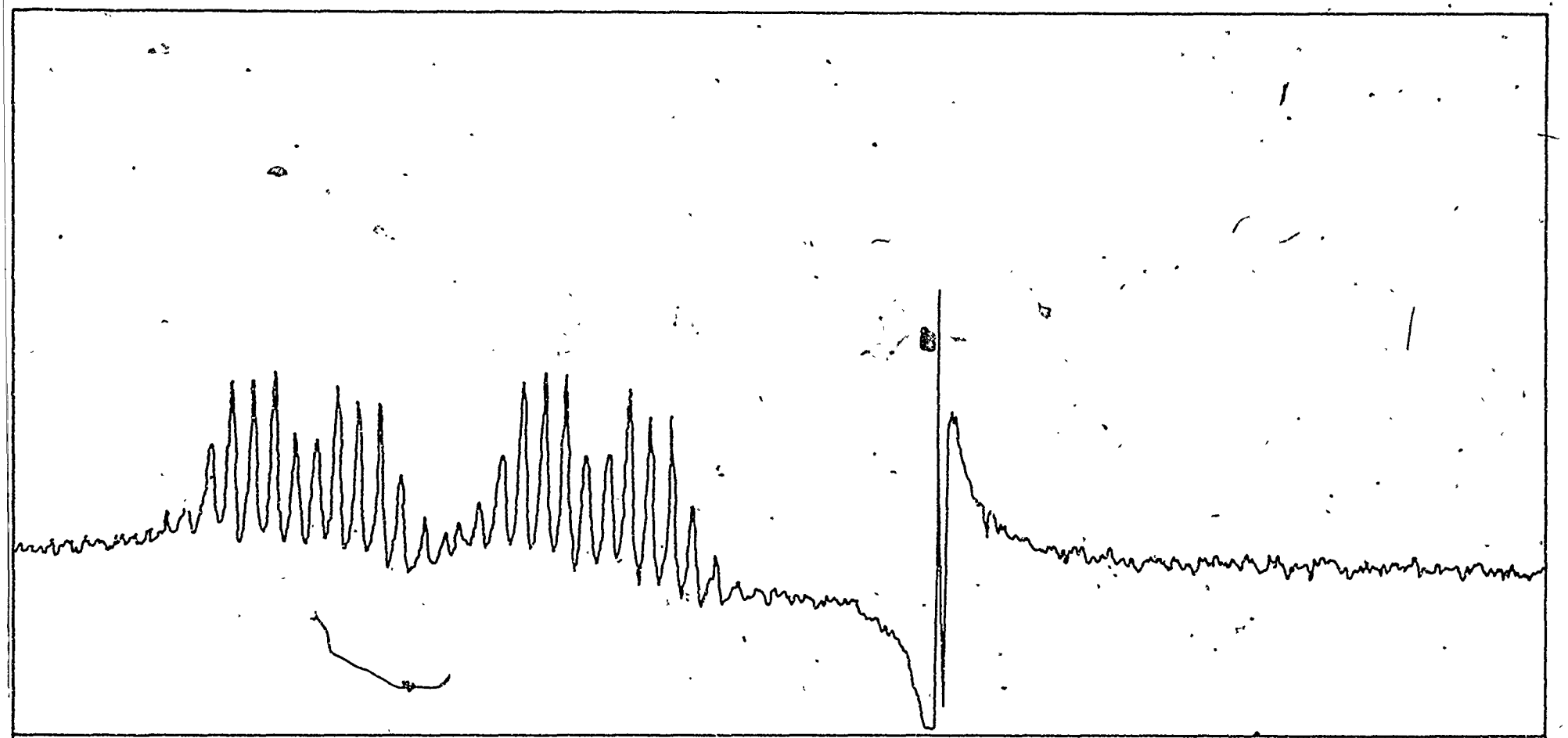

The ^{19}Fluorine magnetic resonance spectrum of trans-$\left[Pt(CF{=}CF_2)(Ph_3P)(Et_3P)_2\right]\left[ClO_4\right]$

F_1

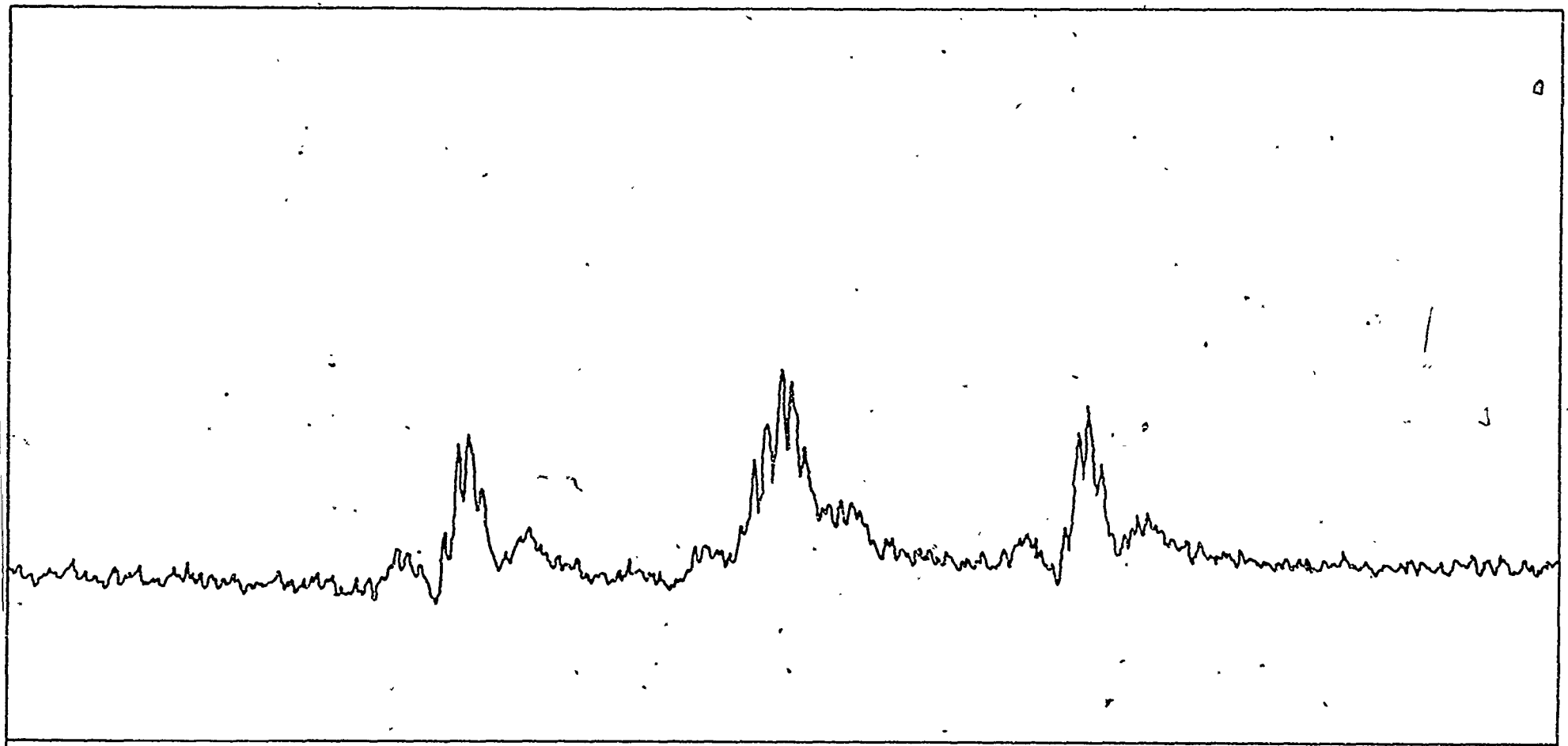

The ^{19}Fluorine magnetic resonance spectrum of <u>trans</u>-$[Pt(CF{=}CF_2)(Ph_3P)(Et_3P)_2][ClO_4]$

$\underline{F_2}$

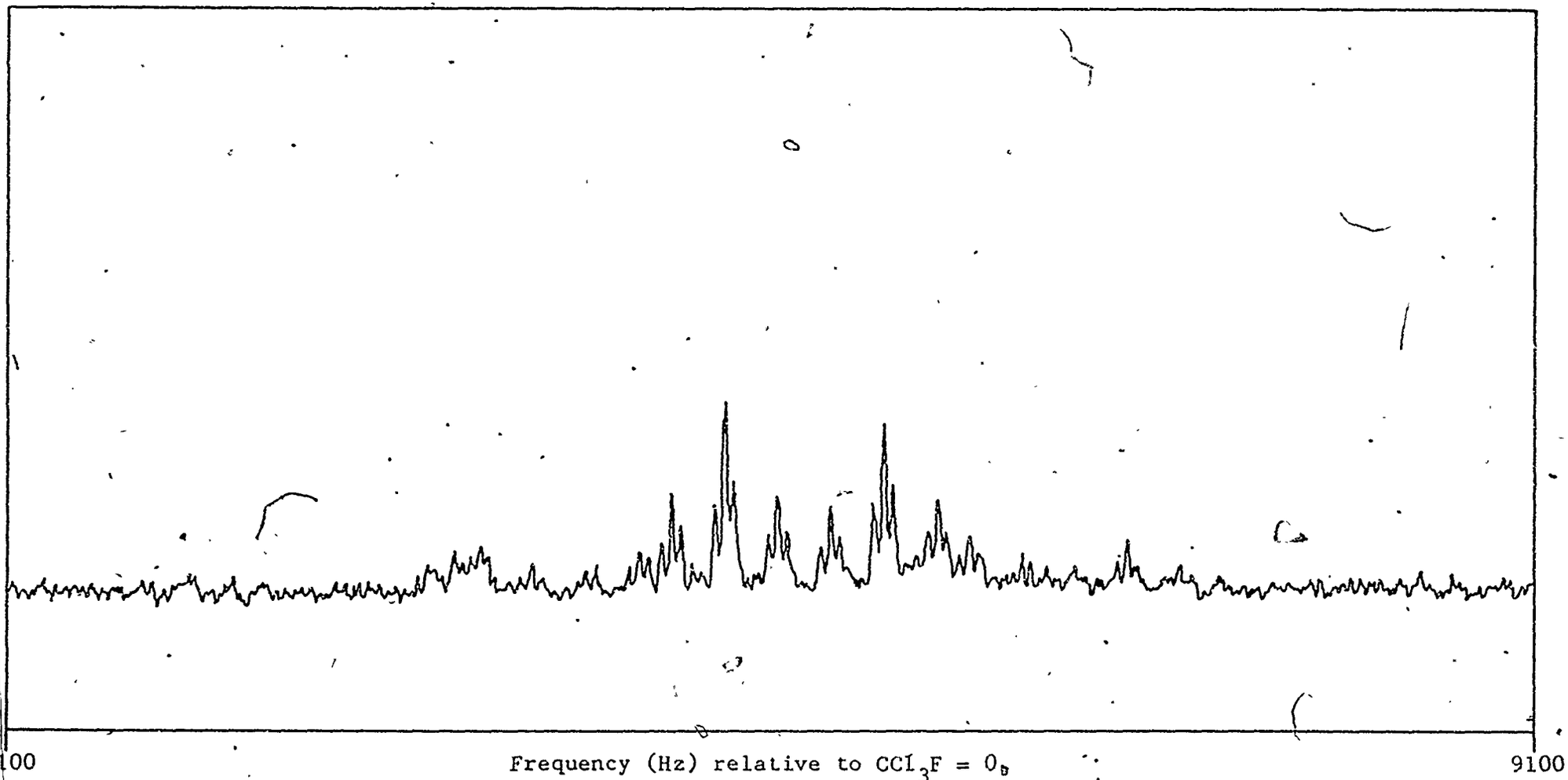

The ^{19}Fluorine magnetic resonance spectrum of <u>trans</u>-$\left[Pt(CF{=}CF_2)(Ph_3P)(Et_3P)_2\right]\left[ClO_4\right]$

<u>F_3</u>

APPENDIX II

Bridge Substitution in Pentaborane(9)

The Crystal Structure of Bis(diethylamino)dithiaboretane

SPECTRA

MASS SPECTRA OF

TRIS(DIETHYLAMINO)TRITHIABORETANE (MS I)

AND

BIS(DIETHYLAMINO)DITHIABORETANE (MS II)

m/e	MS I Intensity (% of m/e 215)	MS II Intensity (% of m/e 215)	m/e	MS I Intensity (% of m/e 215)	MS II Intensity (% of m/e 215)
26	7	8	83	14	3
27	34	33	84	5	4
28	49	62	85	10	6
29	48	50	86	92	18
30	99	34	87	7	3
32	19	14	94	5	3
33	18	12	95	2	1
34	48	35	96	3	1
35	4	2	97	3	1
36	8	17	98	3	2
37	3	1	99	15	19
38	3	6	100	64	83
39	5	5	101	16	8
40	6	10	102	5	6
41	18	19	113	7	5
42	42	43	114	20	20
43	13	6	115	5	4
44	39	16	116	5	3
45	5	5	149	-	9
53	5	2	150	13	2
54	15	15	151	3	-
55	7	5	156	2	1
56	18	11	157	3	1
57	8	5	158	4	2
58	95	37	159	4	-
59	8	5	170	2	3
60	7	7	171	3	4
61	4	4	172	4	-
62	8	6	198	2	-
69	4	3	199	6	-
70	7	5	200	13	-
71	8	10	201	2	-
72	32	34	202	2	-
73	25	10	212	4	-
74	3	3	213	9	6
80	5	1	214	53	48
81	5	2	215	100	100
82	7	4	216	18	14

MASS SPECTRA OF

TRIS(DIETHYLAMINO)TRITHIABORETANE (MS I)

AND

BIS(DIETHYLAMINO)DITHIABORETANE (MS II) Continued

m/e	MS I Intensity (% of m/e 215)	MS II Intensity (% of m/e 215)
217	12	10
218	2	-
228	4	3
229	17	14
230	28	27
231	5	5
232	3	3
240	1	-
241	2	-
242	3	-
279	3	-
280	8	-
281	10	-
282	2	-
296	14	-
297	11	-
298	15	-
299	3	-
300	1	-
311	5	-
312	13	-
313	17	-
314	3	-
315	2	-
326	1	-
327	3	-
328	5	-
329	2	-
330	1	-
343	1	-
344	6	-
345	7	-
346	2	-
347	1	-

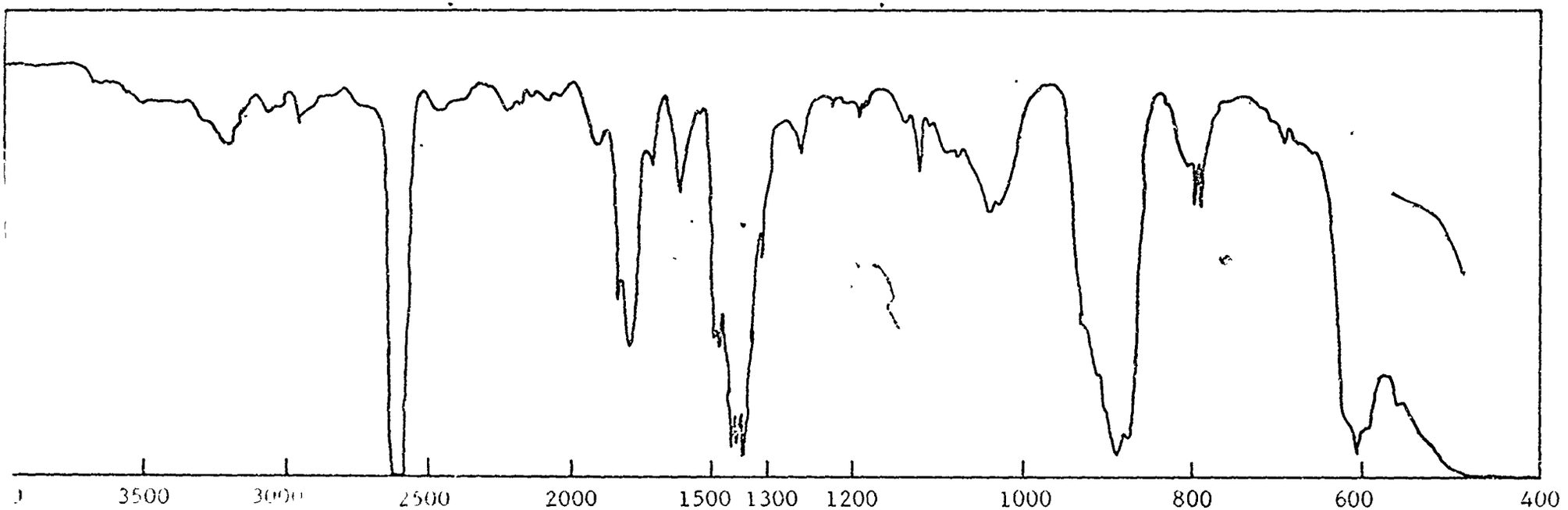

IR I

The Infrared Spectrum of Pentaborane(9)

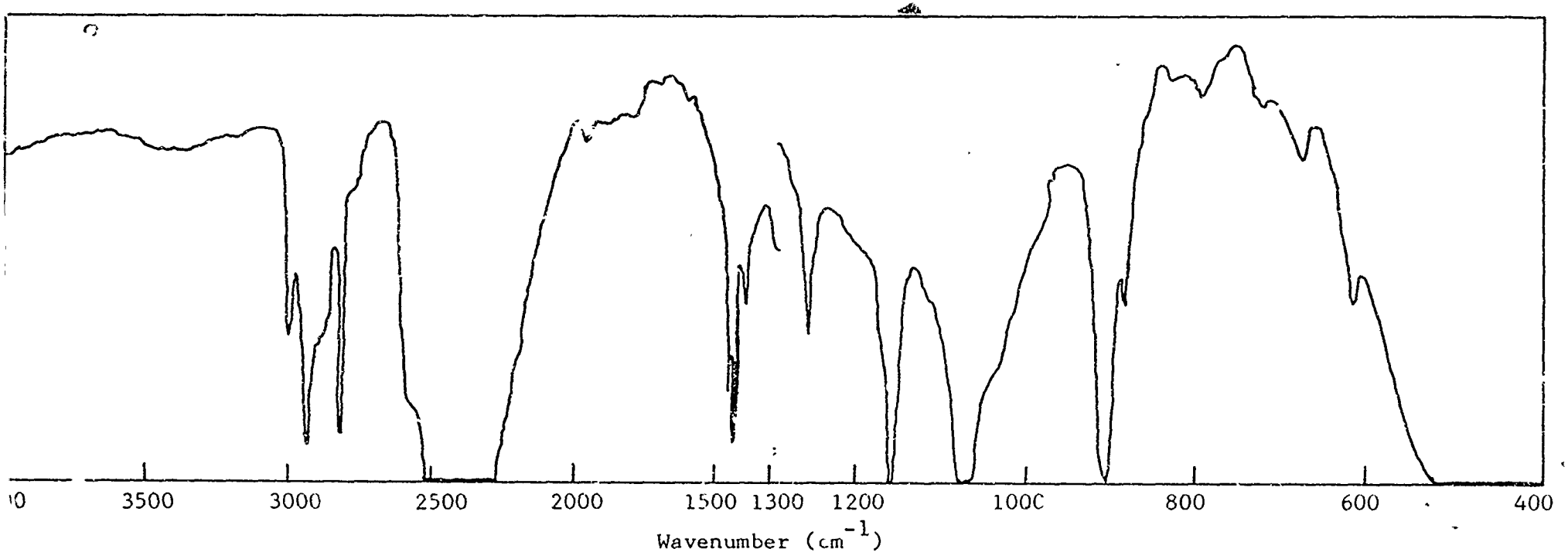

IR IIa

The Infrared Spectrum of the Decomposition Product of Lithium Octahydropentaborate(1-)

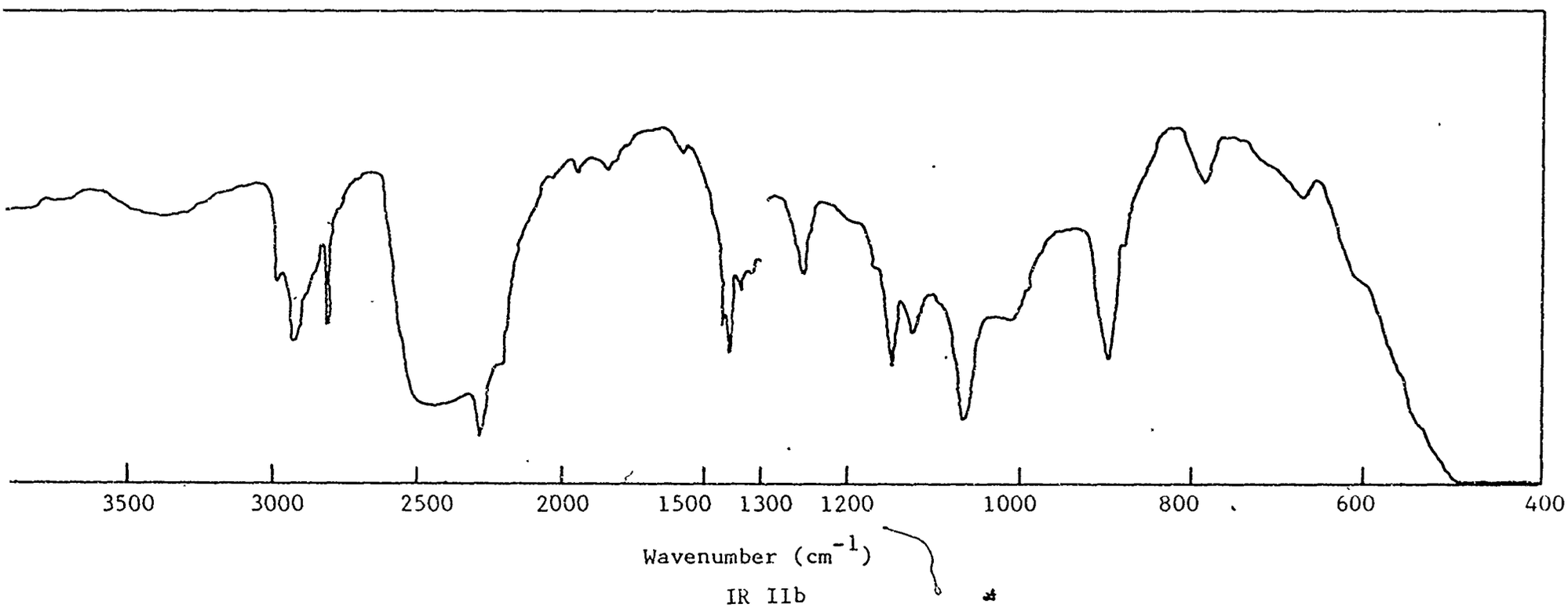

IR IIb

The Infrared Spectrum of the Decomposition Product of Lithium Octahydropentaborate(1-)

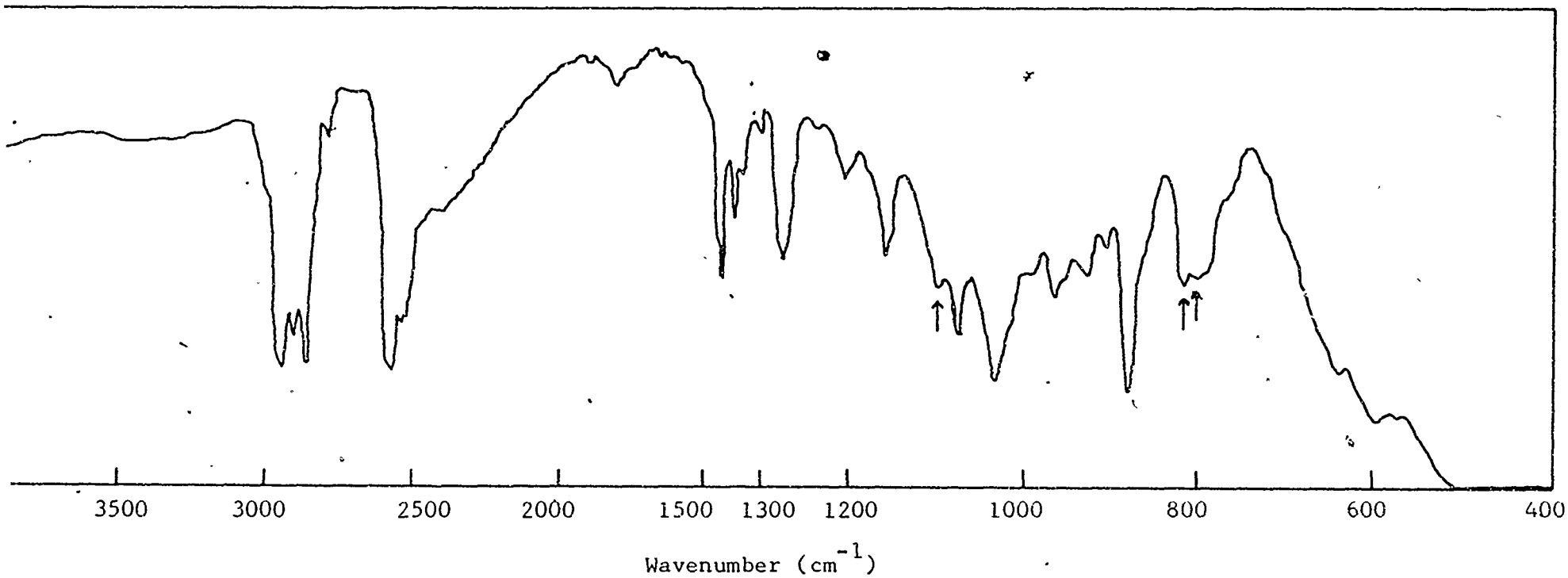

IR III

Infrared Spectrum of the Residue from Reaction of Diethylaluminum Chloride with Lithium Octahydropentaborate(1-)

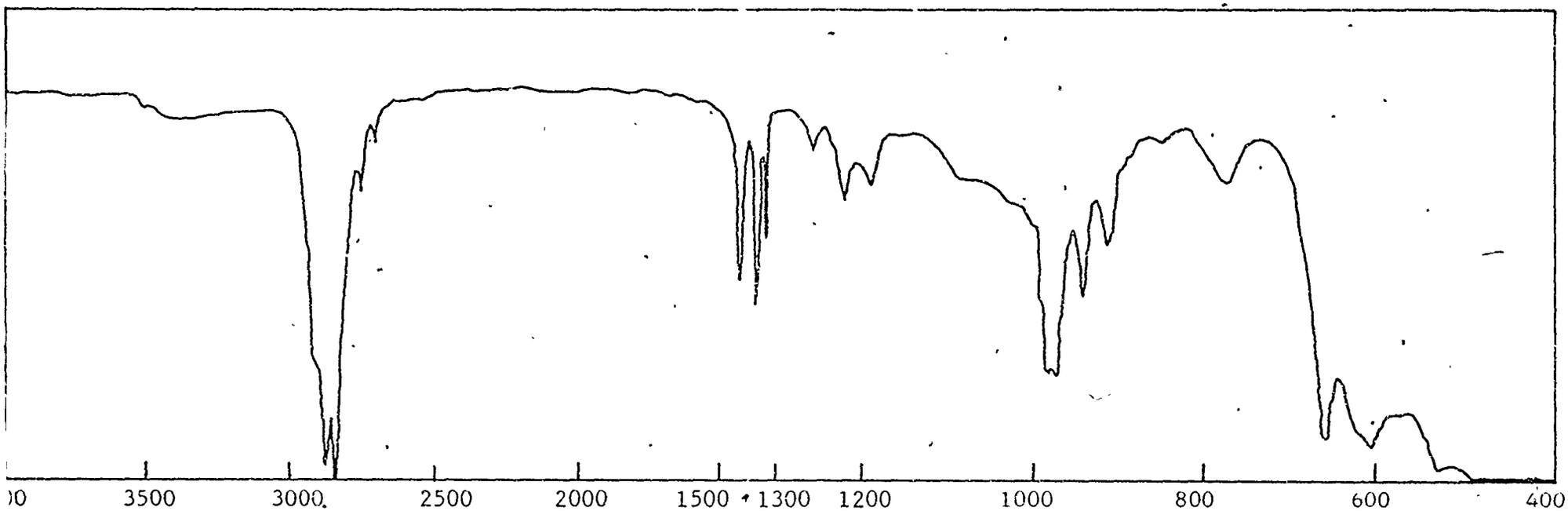

IR IV

The Infrared Spectrum of the Diethylaluminum Chloride Dimer

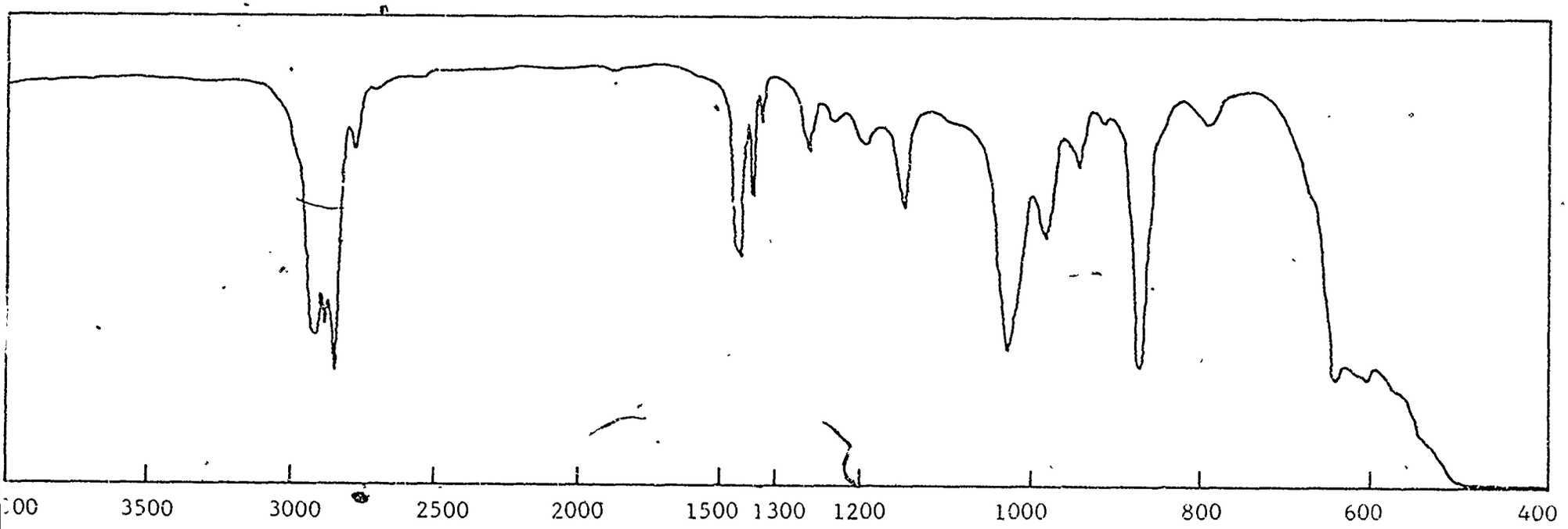

IR V

The Infrared Spectrum of Diethylaluminum Chloride-Dimethyl Etherate

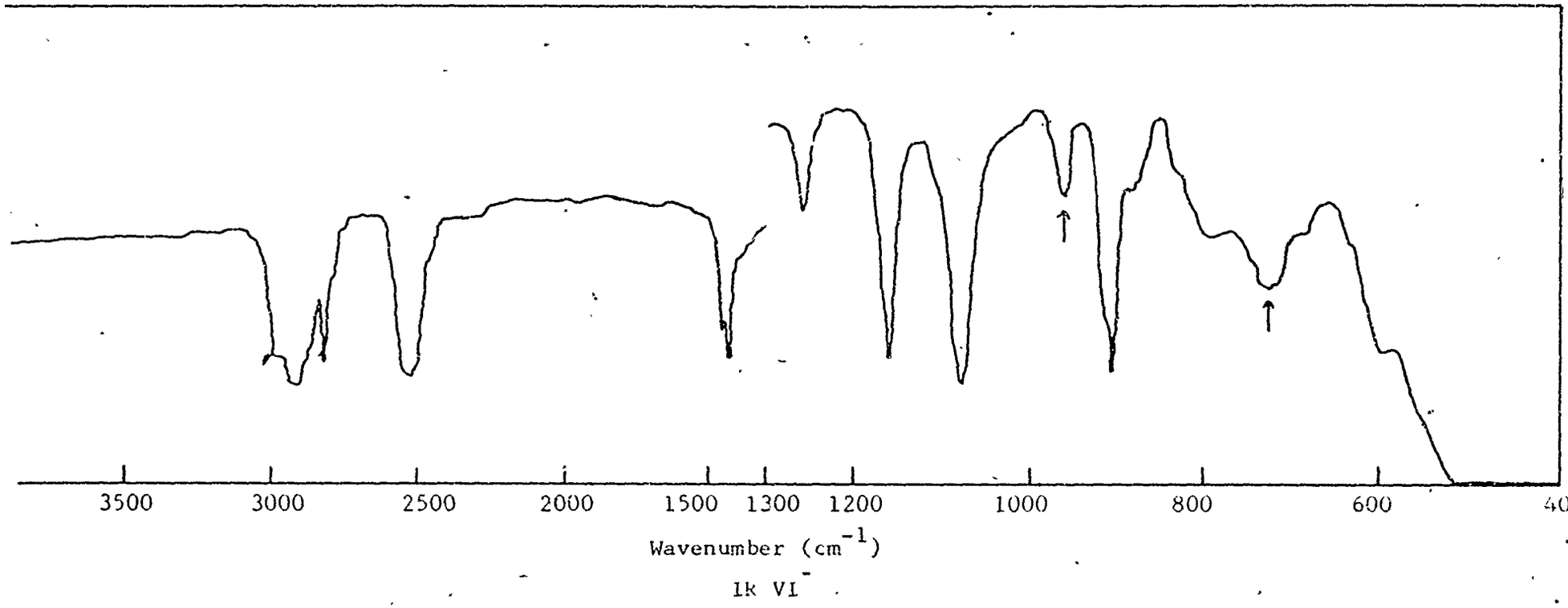

Infrared Spectrum of the Residue from the Reaction of Dimethylthallium Bromide with Lithium Octahydropentaborate(1-)

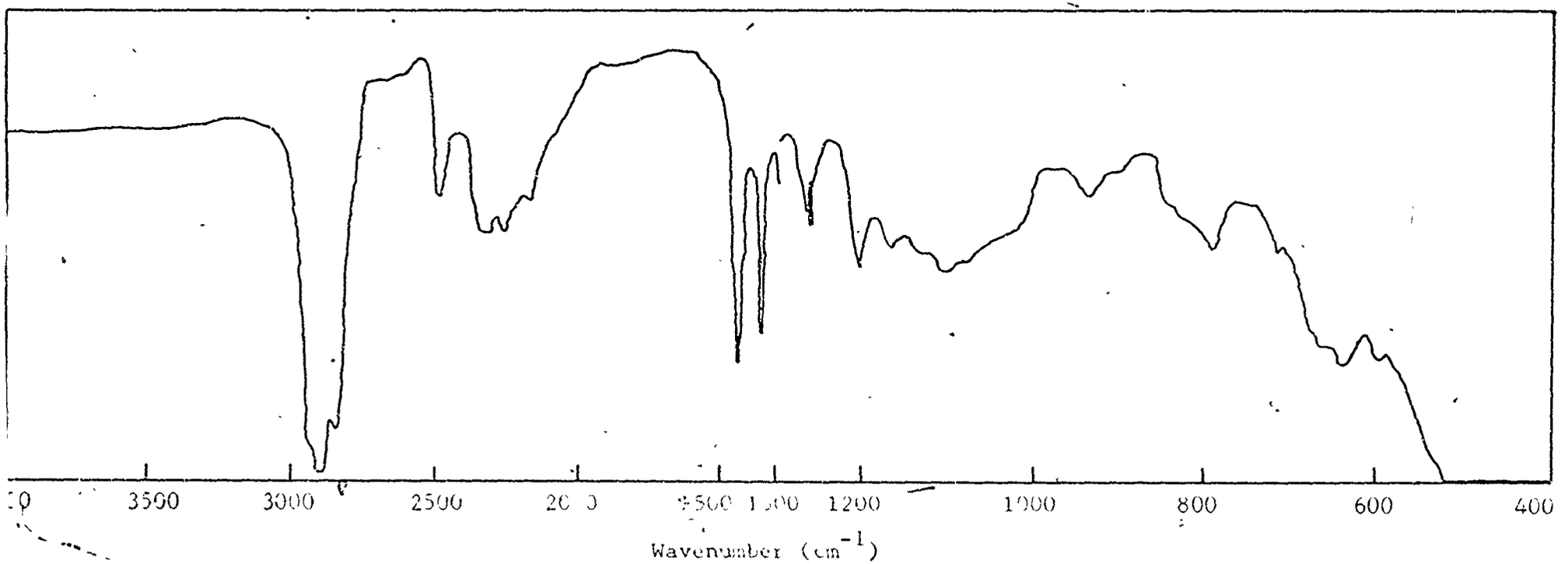

IR VII

The Infrared Spectrum of the Residue from the Reaction of Trimethylaluminum with Pentaborane(9)

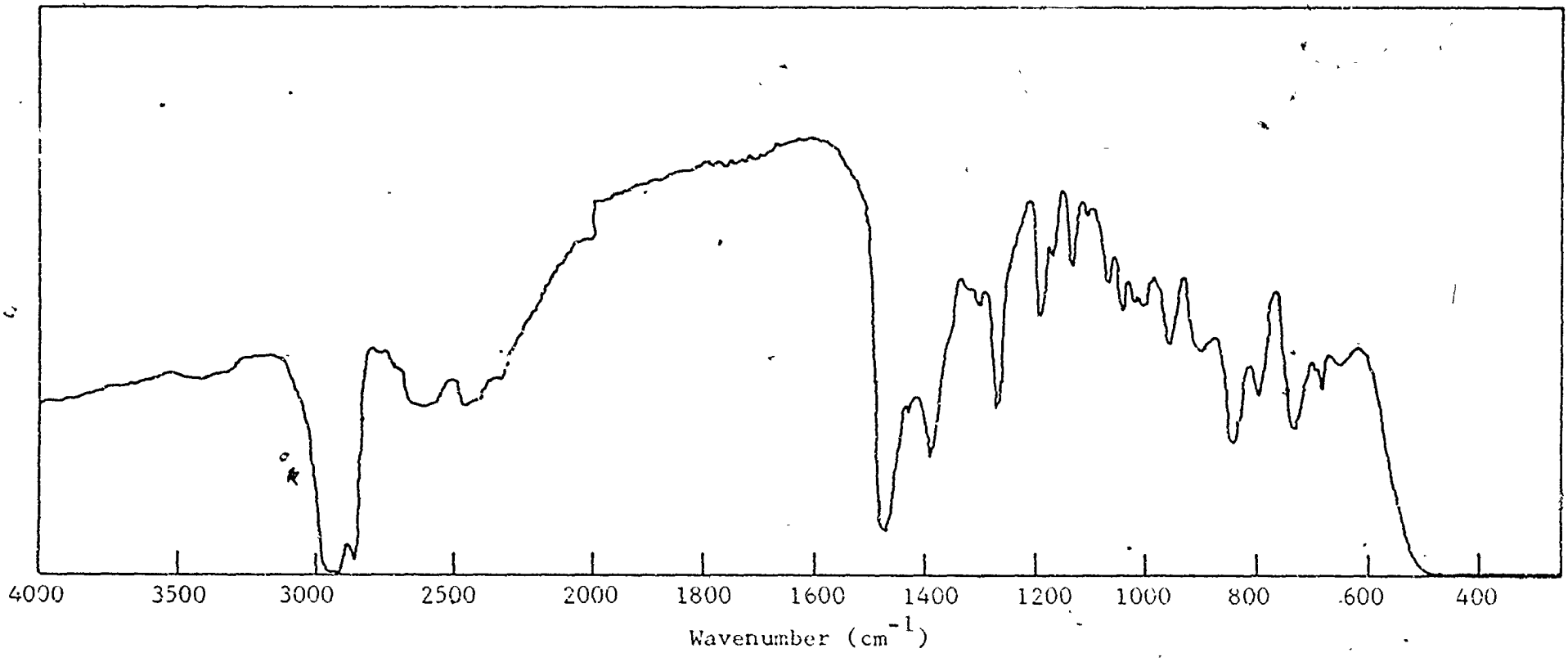

IR VIII

The Infrared Spectrum of Tris(diethylamino)trithiaboretane

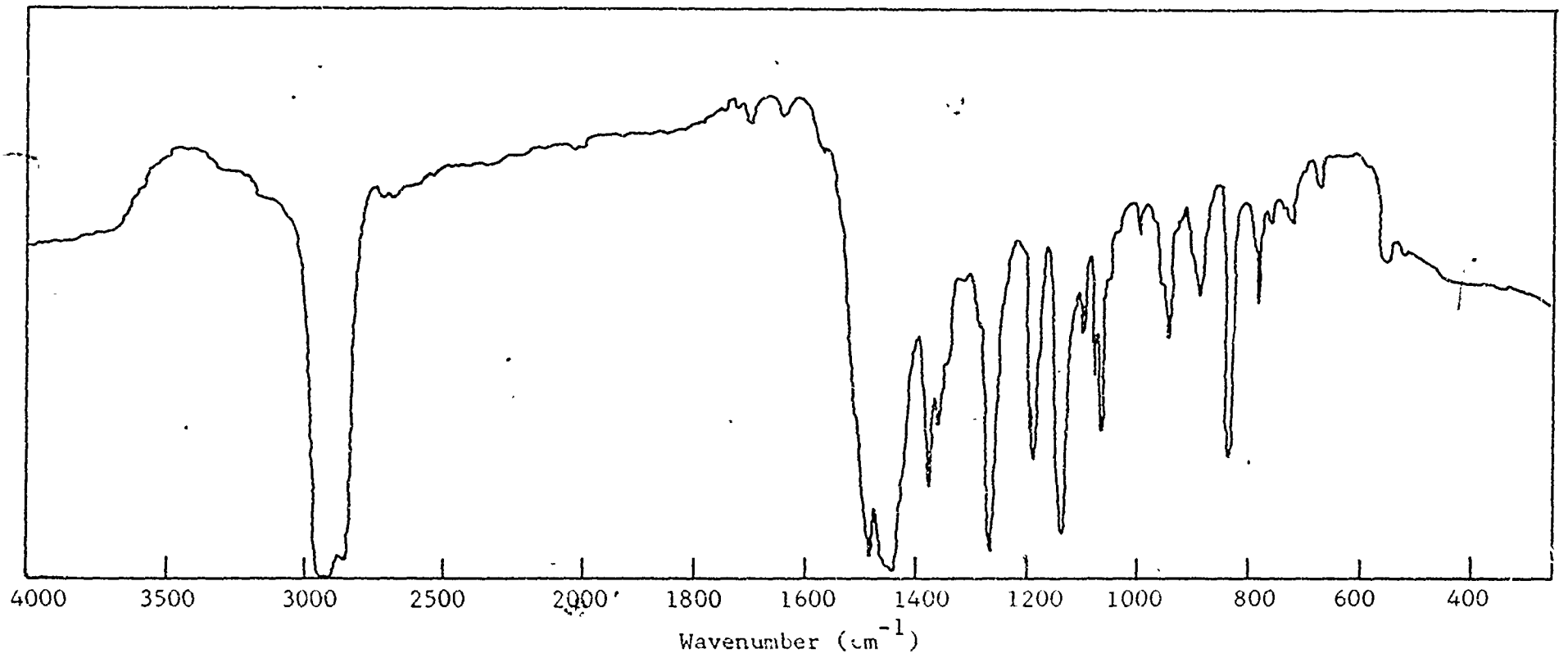

IR IX

The Infrared Spectrum of Bis(diethylamiro)dithiaboretane

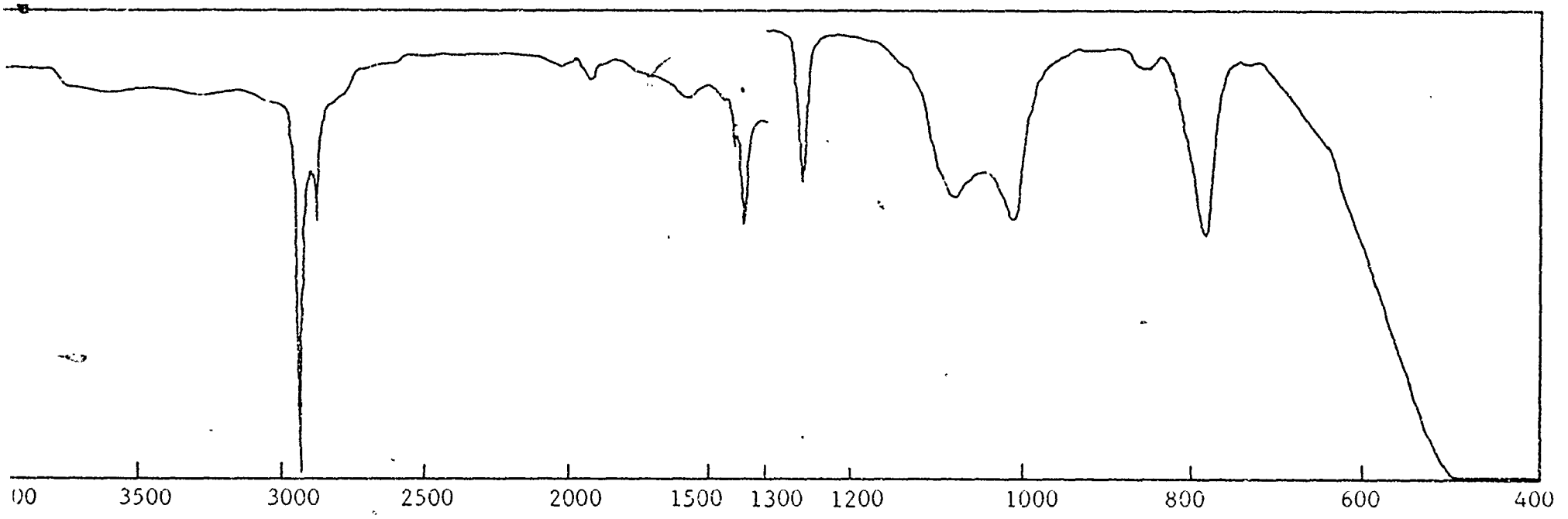

IR X

The Infrared Spectrum of Silicone Grease

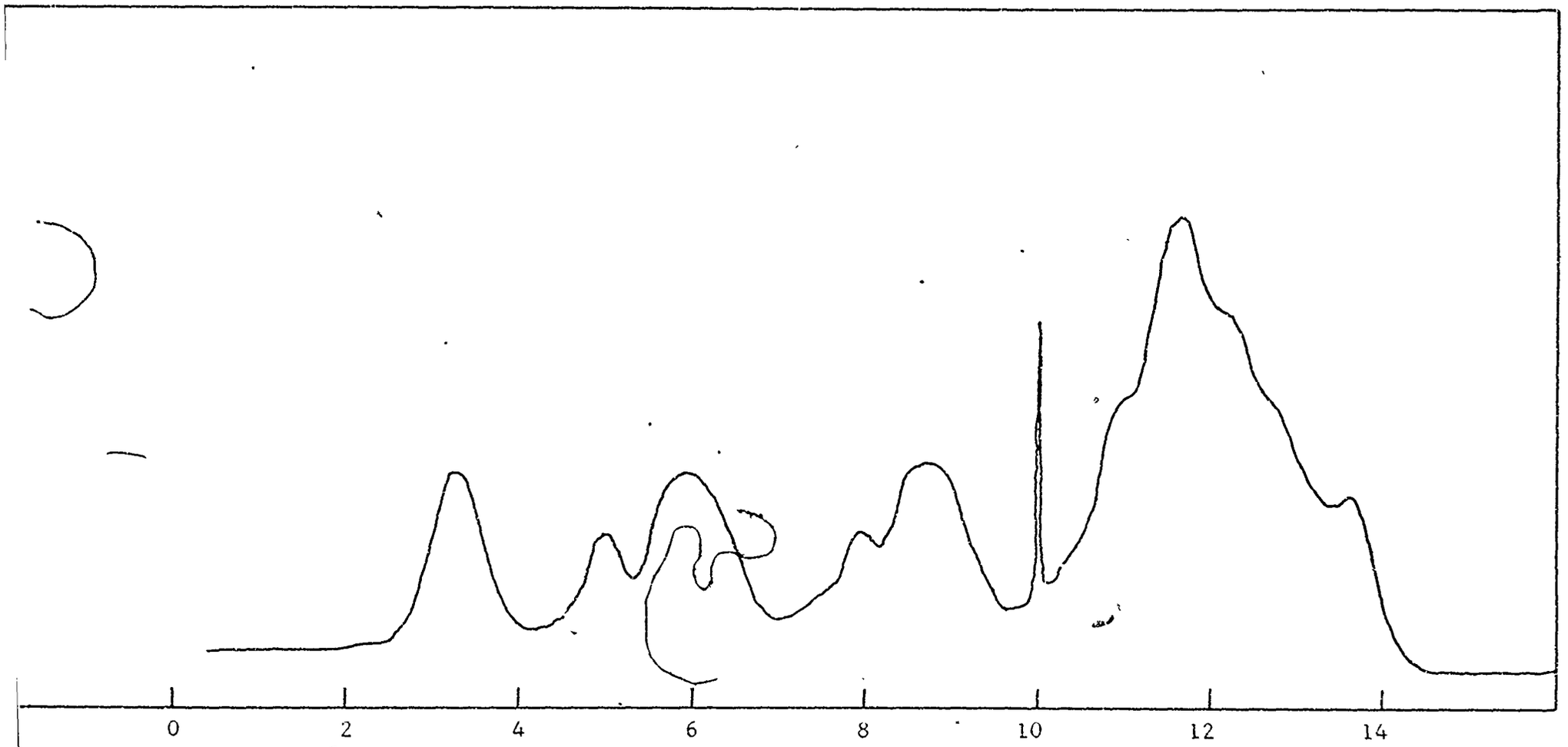

p.p.m. Relative to T.M.S. = 10

NMR I

The Proton Magnetic Resonance Spectrum of Pentaborane(9)

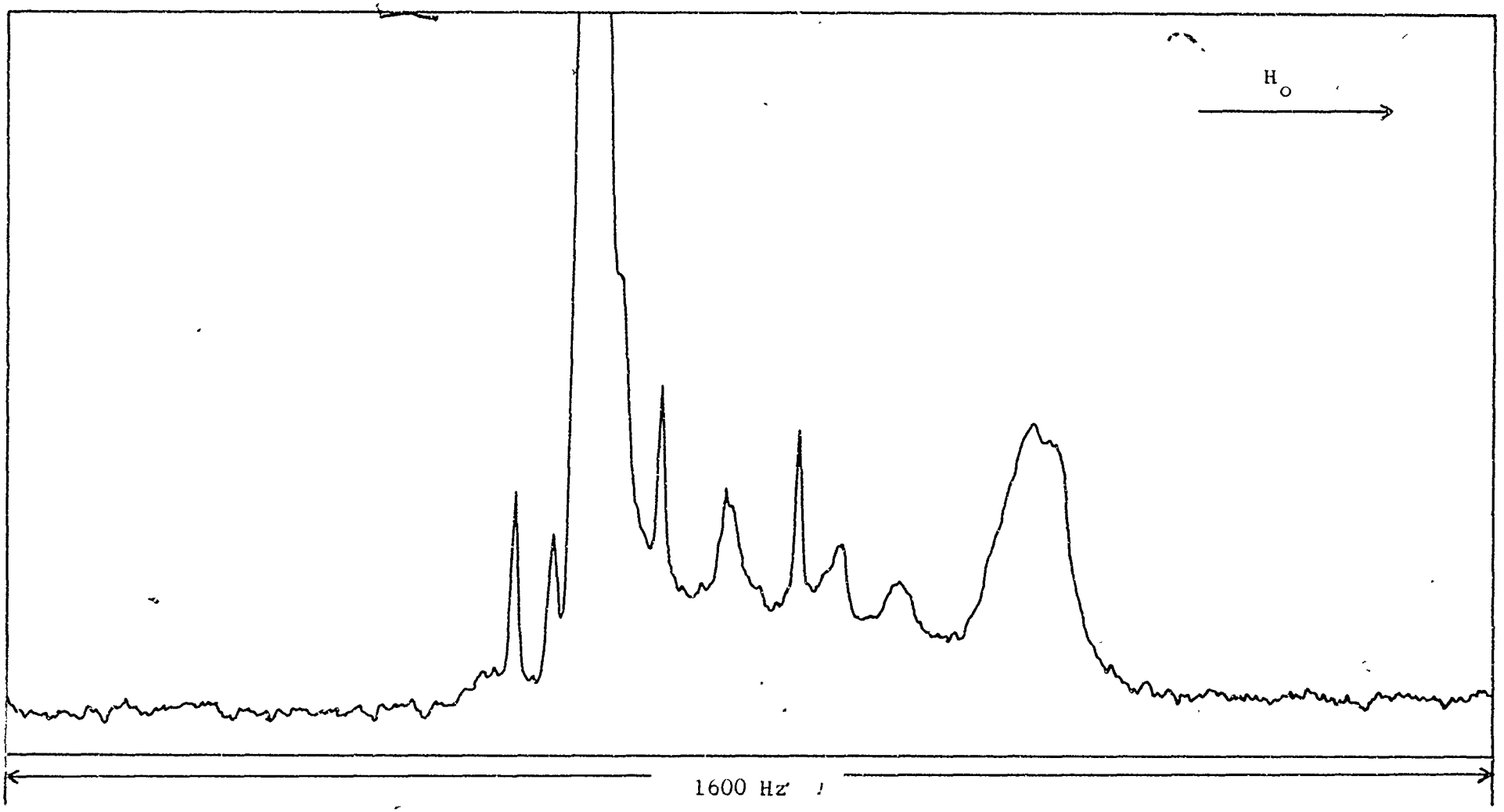

NMR 11

The Proton Magnetic Resonance Spectrum of Lithium Octahydropentaborate(1-)

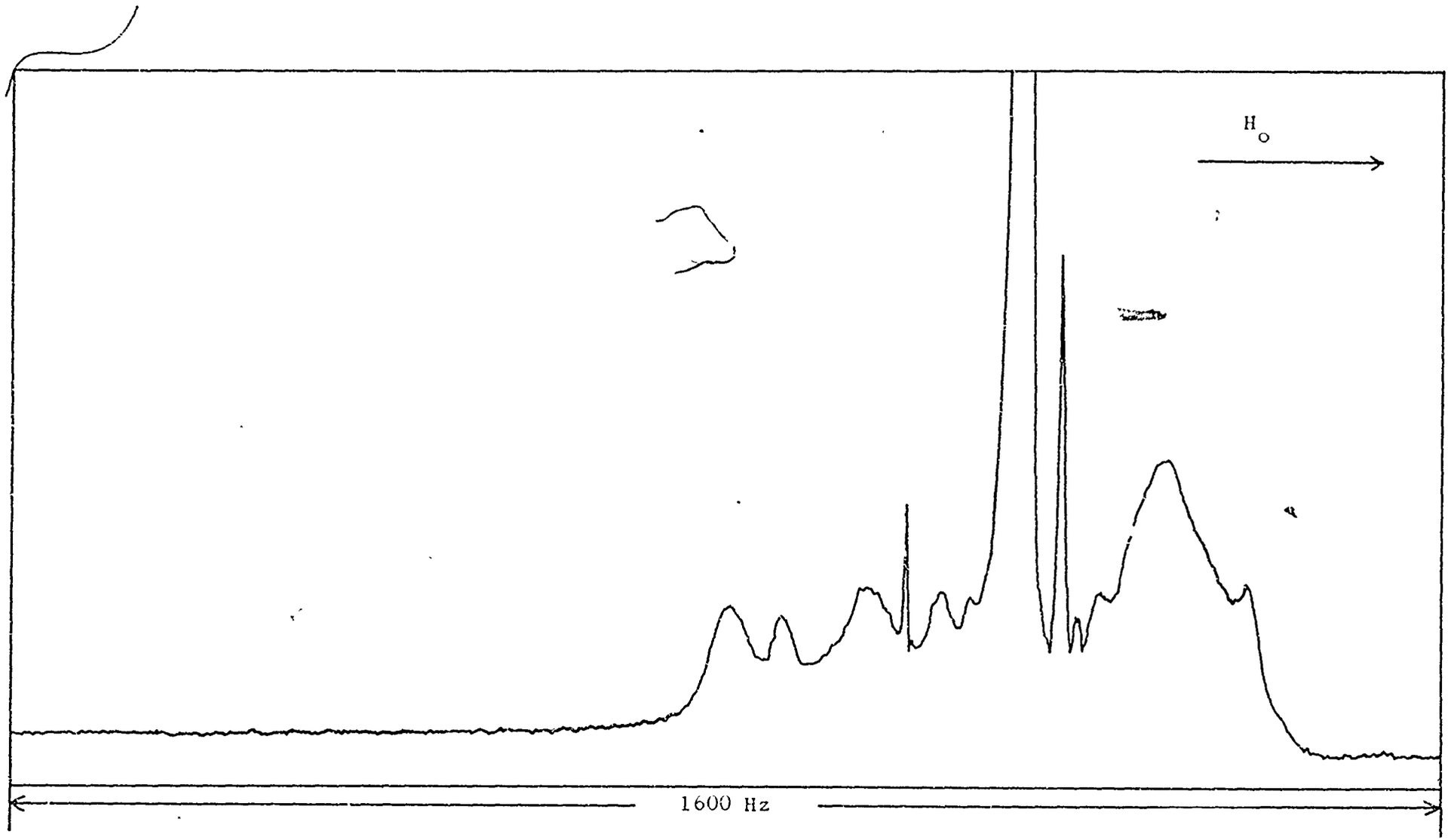

NMR_III

The Proton Magnetic Resonance Spectrum of μ-dimethylborylpentaborane(9)

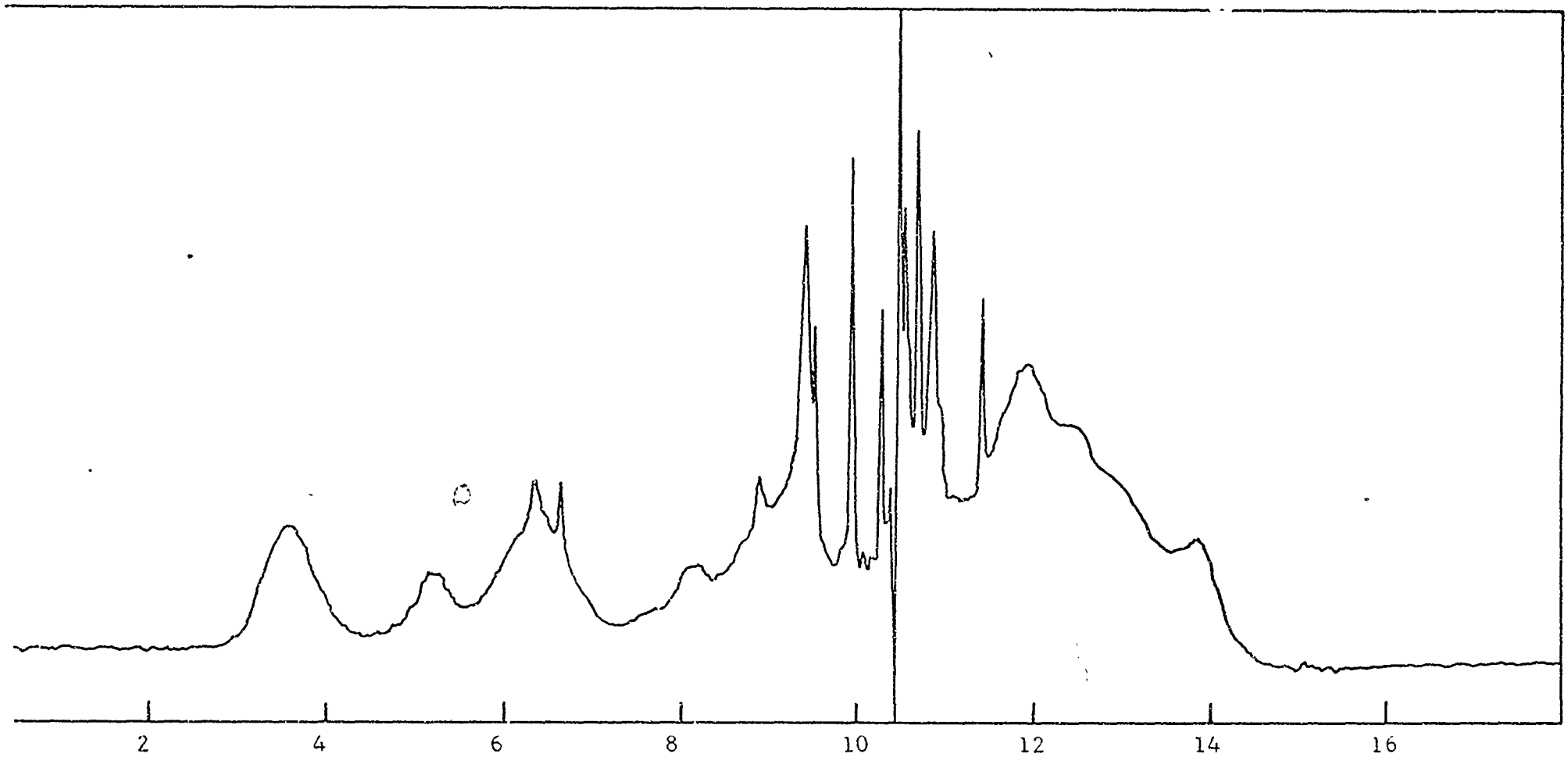

p.p.m. Relative to T.M.S. = 10

NMR IVa

roton Magnetic Resonance Spectrum of the Products of the Reaction of Trimethylaluminum with Pentaborane(9)
One Hour at 60 °C

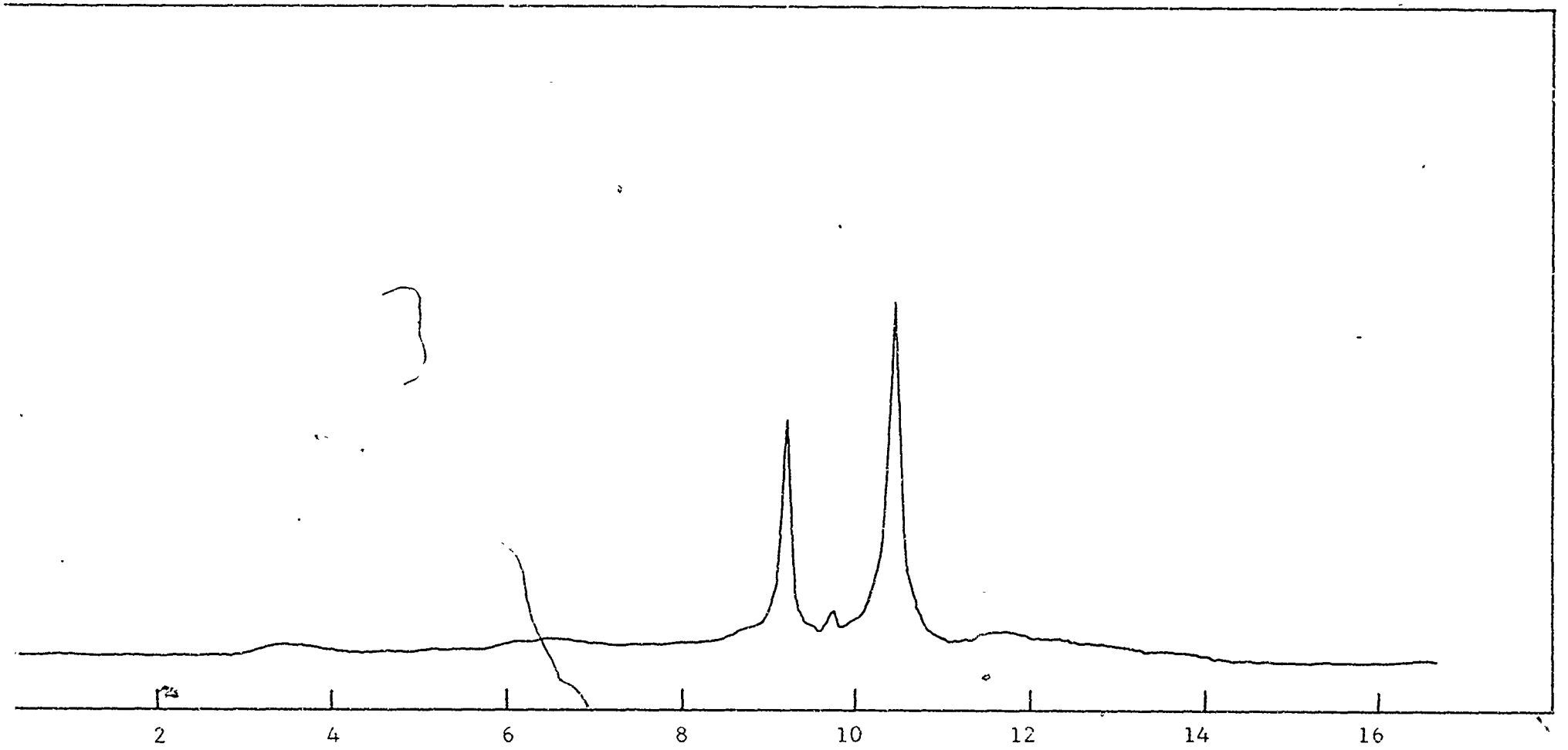

NMR IVb

The Proton Magnetic Resonance Spectrum of the Products of the Reaction of Trimethylaluminum with Pentaborane(9) Twelve Hours at 60 ^{o}C

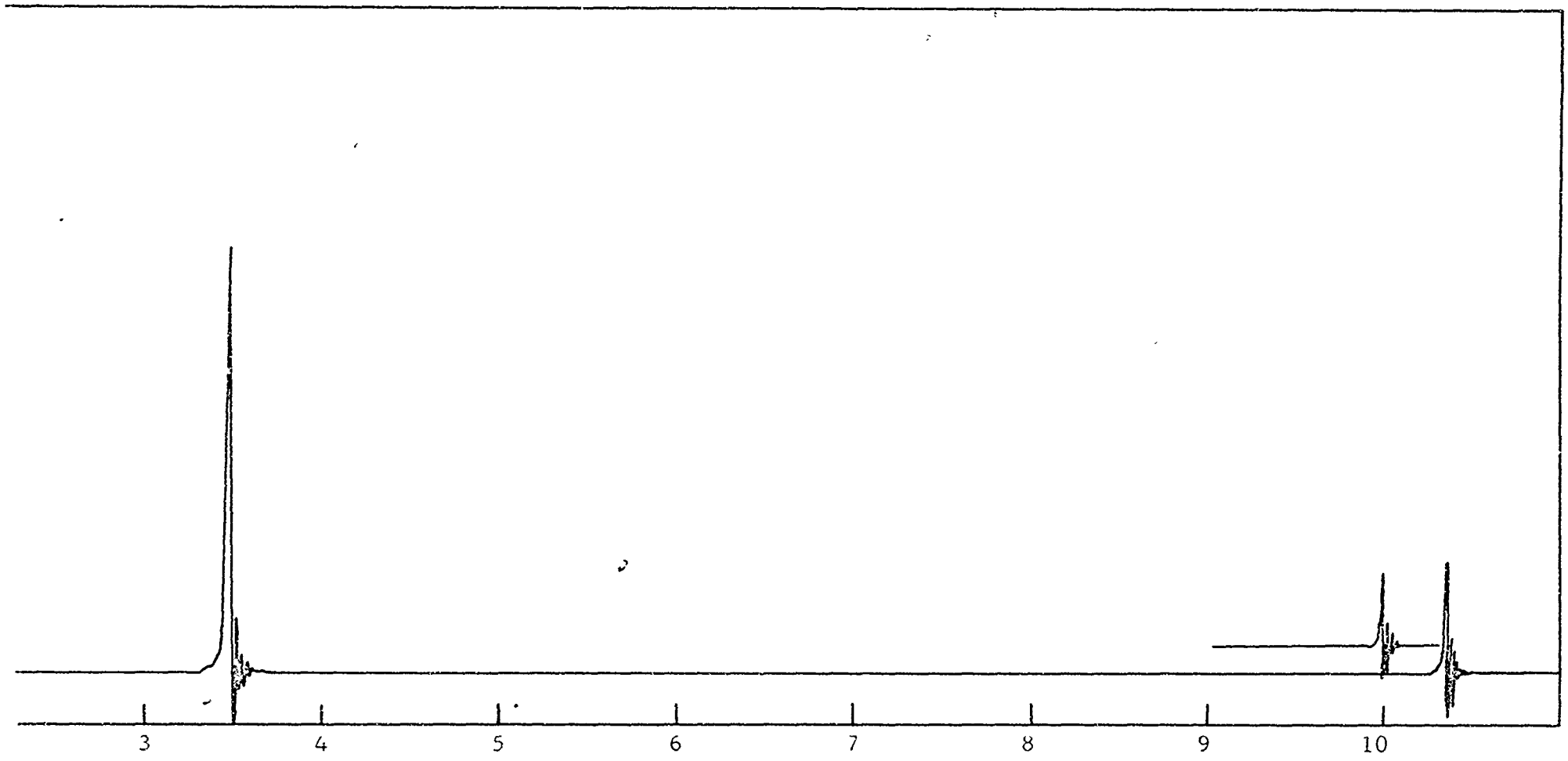

NMR V

The Proton Magnetic Resonance Spectrum of the Benzene Soluble Material in the Residue of the Reaction of Trimethylaluminum with Pentaborane(9)

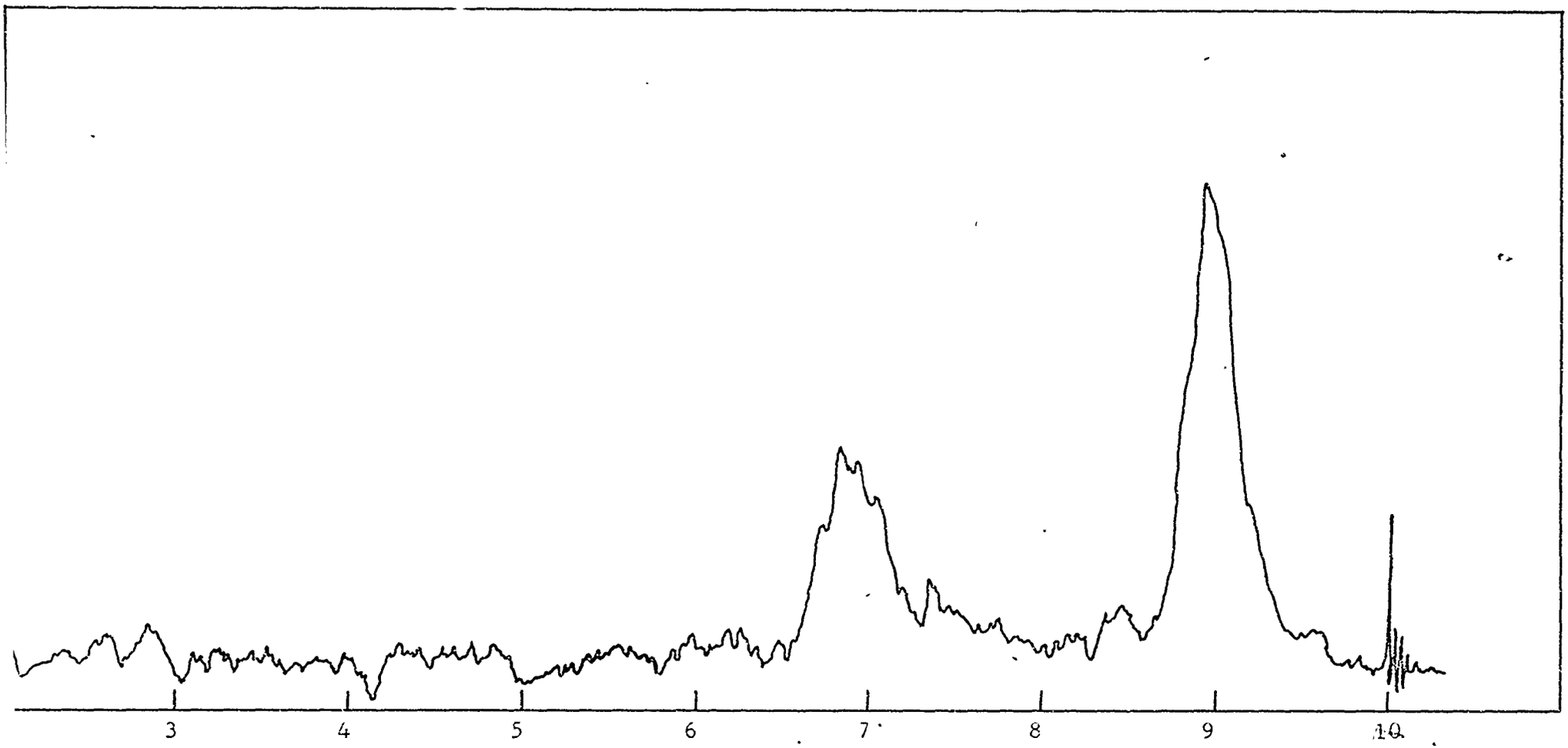

p.p.m. Relative to T.M.S. = 10

NMR VI

The Proton Magnetic Resonance Spectrum of Tris(diethylamino)trithiaboretane

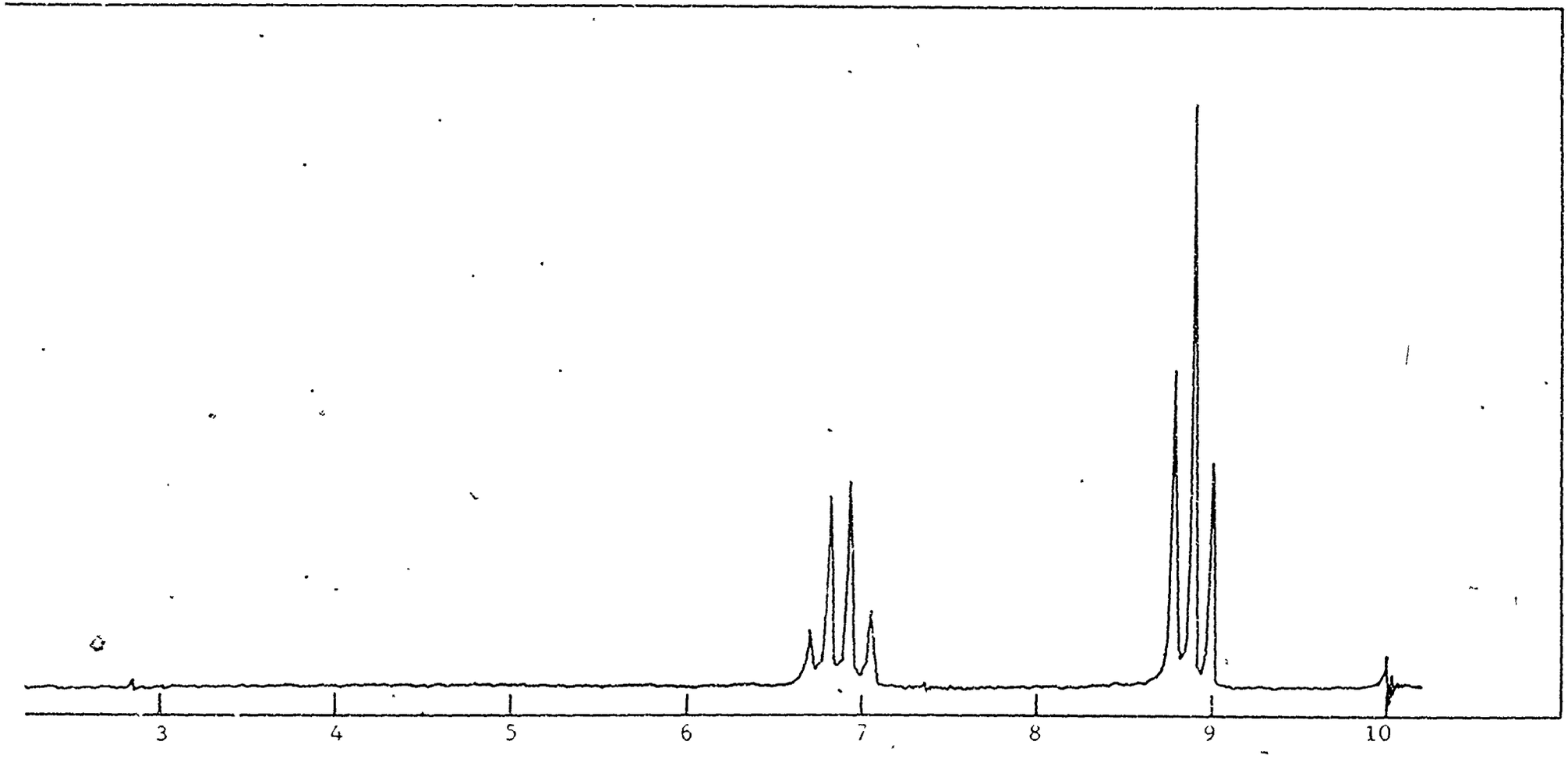

p.p.m. Relative to T.M.S. = 10

NMR VII

The Proton Magnetic Resonance Spectrum of Bis(diethylamino)dithiaboretane

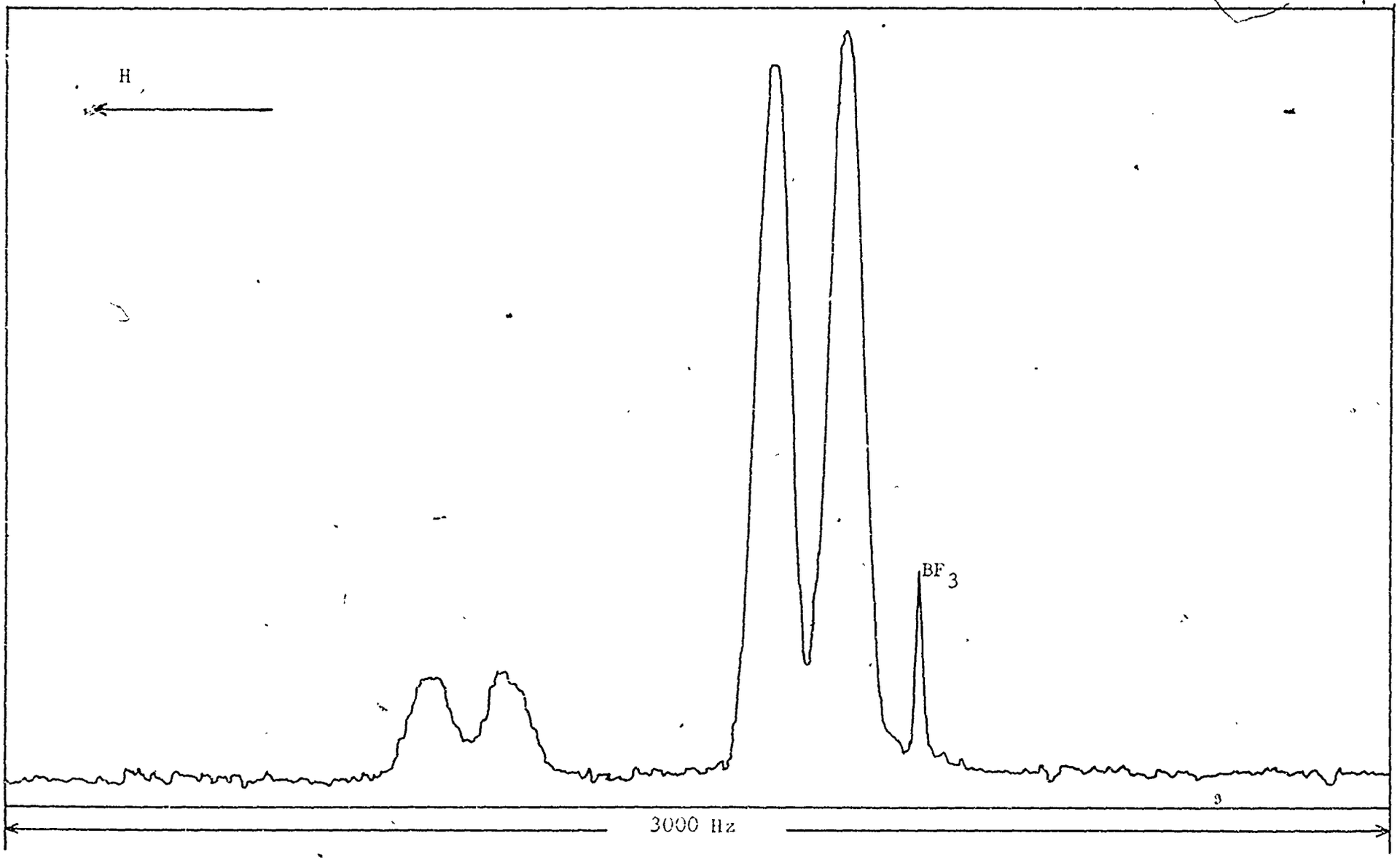

The ^{11}Boron Magnetic Resonance Spectrum of Pentaborane(9).

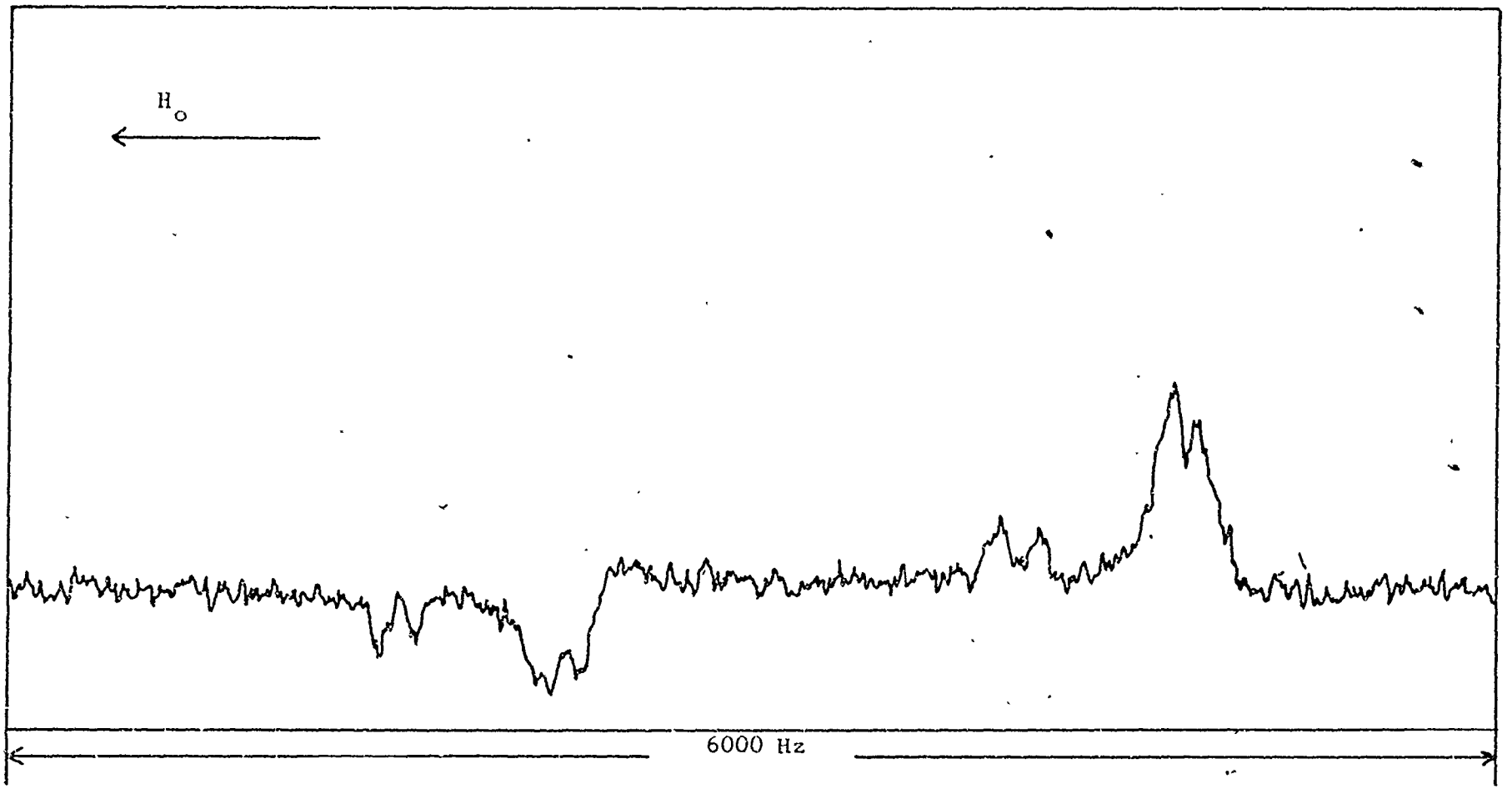

NMR IX

The ^{11}Boron Magnetic Resonance Spectrum of Lithium Octahydropentaborate(1-)

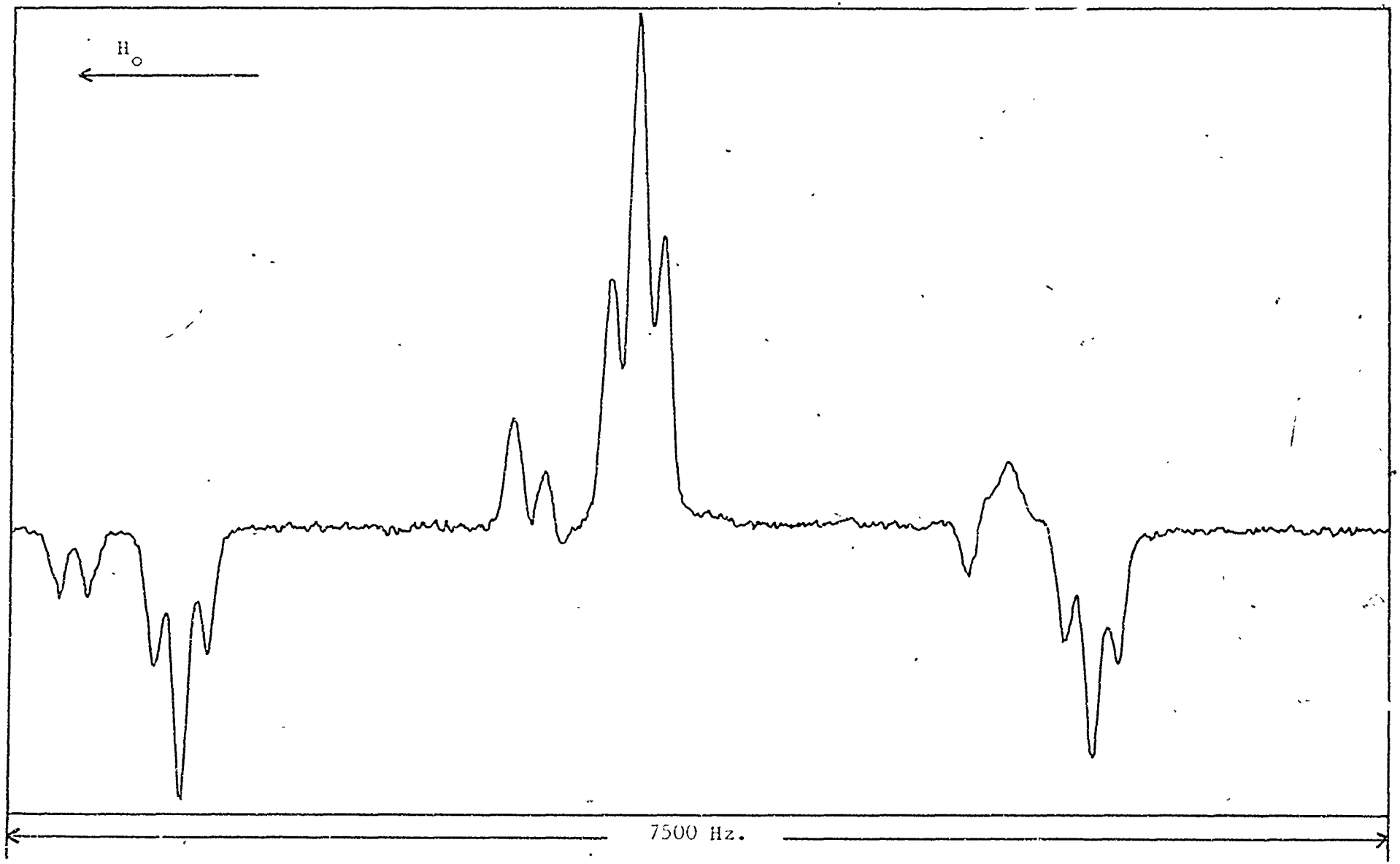

The ^{11}Boron Magnetic Resonance Spectrum of μ-dimethylborylpentaborane(9)

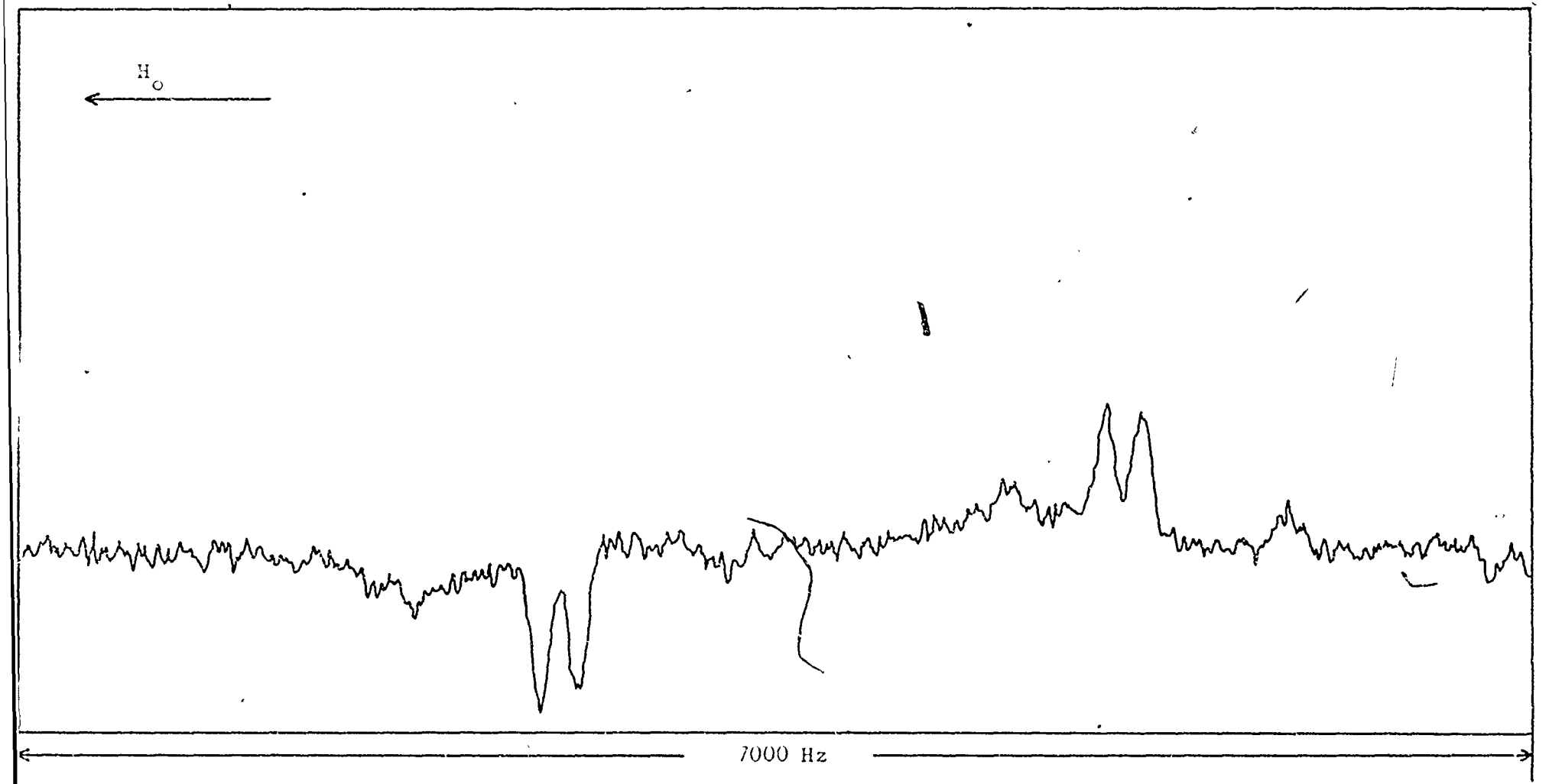

NMR XI

The ^{11}Boron Magnetic Resonance Spectrum of the Products of the Reaction of Trimethylaluminum with Pentaborane(9)

Twelve Hours at 60 °C
and Four Hours at 95 °C

APPENDIX III

Bisdiethylaminodithiaboretane

FINAL VALUES OF 10 F_{obs} AND 10 F_{calc}

K	L	OBS	CALC
****	H = 0	****	
0	4	2406	2502
0	8	2043	2061
0	12	430	432
0	16	1523	1571
1	1	1*	14
1	2	27	24
1	3	18*	85
1	4	44	44
1	5	29	20
1	6	31	22
1	7	108	60
1	8	163	195
1	9	132	86
1	10	14*	54
1	11	3*	58
1	12	12*	47
1	13	24*	31
1	14	65	39
1	15	83	89
1	16	128	202
1	17	117	114
1	18	73	50
2	0	164	128
2	1	190	134
2	2	58	68
2	3	166	40
2	4	189	118
2	5	256	288
2	6	80	45
2	7	368	444
2	8	104	120
2	9	380	444
2	10	3*	15
2	11	307	227
2	12	76	113
2	13	62	57
2	14	122	108
2	15	322	255
2	16	73	55
2	17	391	331
3	1	36	40
3	2	64	93
3	3	66	5
3	4	73	80
3	5	26*	64
3	6	50	27
3	7	29*	86
3	8	53	11
3	9	29*	34
3	10	46	15
3	11	99	96
3	12	149	126
3	13	60	28
3	14	38*	18
3	15	38*	11
3	16	52	58
3	17	4*	9
4	0	991	1017
4	1	182	194
4	2	83	48
4	3	3*	25
4	4	77	49
4	5	51	59
4	6	88	69
4	7	178	138
4	8	1328	1252
4	9	197	198
4	10	30*	3
4	11	147	121
4	12	893	846
4	13	113	93
4	14	44*	37
4	15	77	11
5	1	28*	68
5	2	70	45
5	3	116	110
5	4	112	169
5	5	95	150
5	6	3*	30
5	7	88	49
5	8	52	73
5	9	4*	14
5	10	59	51
5	11	54	14
5	12	46*	30
5	13	67	68
6	0	270	297
6	1	663	693
6	2	54*	8
6	3	439	496
6	4	95	81
6	5	271	230
6	6	128	65

K	L	OBS	CALC
6	11	195	250
7	1	63*	12
7	2	46*	64
7	3	53*	11
7	4	31	7
7	5	5*	21
7	6	6*	5
7	7	91	45
****	H = 1	****	
1	0	1176	1309
1	1	1212	1250
1	2	870	953
1	3	681	733
1	4	571	605
1	5	330	270
1	6	83	99
1	7	300	324
1	9	328	335
1	10	296	314
1	11	281	254
1	12	177	226
1	13	104	89
1	14	235	221
1	15	295	262
1	16	402	426
1	17	402	406
1	18	407	373
2	0	100	109
2	1	440	472
2	2	858	831
2	3	1150	1075
2	4	896	795
2	5	200	134
2	6	384	415
2	7	420	460
2	8	67	50
2	9	232	196
2	10	226	201
2	11	120	72
2	12	327	370
2	13	325	291
2	14	217	171
2	15	163	101
2	16	35*	29
2	17	135	140
3	0	1034	931
3	1	1037	957
3	2	843	751
3	3	426	398
3	4	110	95
3	5	451	456
3	6	730	679
3	7	864	855
3	8	895	839
3	9	975	926
3	10	862	793
3	11	506	482
3	12	263	194
3	13	116	94
3	14	11	95
3	15	272	276
3	16	306	297
4	0	750	643
4	1	494	460
4	2	279	293
4	3	223	181
4	4	300	312
4	5	162	215
4	6	241	307
4	7	39	51
4	8	31	76
4	9	123	117
4	10	114	106
4	11	70	58
4	12	51	41
4	13	21*	30
4	14	147	150
4	15	24*	54
5	0	802	814
5	1	567	571
5	2	345	350
5	3	294	288
5	4	76	68
5	5	131	143
5	6	208	258
5	7	353	405
5	8	646	652
5	9	538	525
5	10	349	365
5	11	285	308
5	12	212	177
5	13	55	68

K	L	OBS	CALC
6	5	124	129
6	6	37*	43
6	7	173	150
6	8	35*	7*
6	9	124	170
6	10	116	103
6	11	97	43
7	0	121	124
7	1	172	196
7	3	65	116
7	4	30*	45
7	5	71	90
7	6	194	217
****	H = 2	****	
2	0	143	74
2	1	219	227
2	2	2684	2729
2	3	258	252
2	4	100	49
2	5	85	64
2	6	829	852
2	7	117	97
2	8	37	30
2	9	162	138
2	10	1584	1515
2	11	164	167
2	12	62	23
2	13	52	15
2	14	218	262
2	15	66	70
2	17	38	59
2	16	54	44
3	0	25*	21
3	1	91	47
3	2	105	115
3	4	229	115
3	5	136	96
3	6	339	283
3	7	359	273
3	8	78	151
3	9	137	152
3	10	256	225
3	11	109	115
3	12	94	101
3	13	130	168
3	14	75	128
3	15	44	55
3	16	47	62
4	0	105	119
4	1	647	642
4	2	137	179
4	3	253	257
4	4	85	83
4	5	191	143
4	6	116	118
4	7	563	508
4	8	80	62
4	9	485	472
4	10	118	121
4	11	191	229
4	12	27	85
4	13	111	73
4	14	63	67
4	15	355	337
5	0	54	80
5	1	109	107
5	2	82	54
5	3	278	257
5	4	280	229
5	5	210	136
5	6	35	112
5	7	160	194
5	8	43	52
5	9	161	213
5	10	141	114
5	11	33	44
5	12	86	112
5	13	161	169
6	0	44	17
6	1	146	140
6	2	466	516
6	3	100	94
6	4	91	78
6	5	87	94
6	6	617	631
6	7	157	187
6	8	29*	44
6	9	174	163
6	10	827	874
7	0	19*	11
7	1	48*	20
7	2	115	115

K	L	OBS	CALC
****	H = 3	****	
3	0	545	585
3	1	641	687
3	2	723	742
3	3	547	551
3	4	343	311
3	5	213	214
3	6	41*	21
3	7	75	49
3	8	95	152
3	9	145	120
3	10	214	262
3	11	136	171
3	12	94	122
3	13	73	38
3	14	192	182
3	15	242	227
4	0	348	340
4	1	300	330
4	2	81	64
4	3	325	282
4	4	228	226
4	5	91	127
4	6	51	32
4	7	74	25
4	8	43	47
4	9	61	43
4	10	34*	28
4	11	88	104
4	12	88	51
4	13	98	53
5	0	264	265
5	1	286	282
5	2	130	138
5	3	80	69
5	4	96	72
5	5	166	159
5	6	305	265
5	7	456	402
5	8	435	403
5	9	416	408
5	10	295	272
5	11	304	315
6	0	65	22
6	1	134	118
6	2	64	148
6	3	86	81
6	4	202	227
6	5	48	28
6	6	148	138
6	7	37	49
6	8	45*	51
****	H = 4	****	
4	0	1742	1800
4	1	252	253
4	2	51	6
4	3	117	95
4	5	45*	75
4	6	32*	33
4	7	185	175
4	8	1051	1155
4	9	200	237
4	10	15*	15
4	11	92	63
4	12	392	370
5	0	152	147
5	1	46	86
5	2	36*	57
5	3	87	32
5	4	254	267
5	5	227	184
5	6	46	75
5	7	169	144
5	8	343	289
5	9	133	116
6	0	173	172
6	1	279	261
6	2	98	90
6	3	142	123
6	4	46	77
6	5	67	102
****	H = 5	****	
5	0	653	681
5	1	435	468
5	2	254	267
5	3	285	304
5	4	173	133
5	5	98	46

VITA FORM

Surname: RIVETT Given Names: GARRY ARTHUR

Place of Birth: SASKATOON, SASK. Date of Birth: OCTOBER 22, 1940

Educational Institutions Attended, with Dates of Entering and Leaving:

UNIVERSITY OF SASKATCHEWAN	1961 to 1969
UNIVERSITY OF VICTORIA	1969 to 1974

Degrees, Diplomas, Etc., Awarded, with Dates and Names of Institutions:

B.A. HONOURS	1967	UNIVERSITY OF SASKATCHEWAN
B. Ed.	1972	UNIVERSITY OF SASKATCHEWAN
M. Sc.	1969	UNIVERSITY OF SASKATCHEWAN

Honours and Awards:

Province of Saskatchewan Bursary in Education, 1965/66

University of Saskatchewan Honours Scholarship, 1966/67

University of Saskatchewan Teaching Fellowship, 1967/68

National Research Council Postgraduate Fellowship, 1968/69, 1970/71, 1971/72, 1972/73

Publications:

J.W. Quail and G.A. Rivett, "Complex Fluorides of Tetravalent Cobalt", Canadian Journal of Chemistry, 50, 2447(1972)

PARTIAL COPYRIGHT LICENSE

I hereby grant to the University of Victoria the right to lend my thesis or dissertation (the title of which is shown below) to users in the University of Victoria Library, and to make single copies only in response to a written request from the library of any other university, or similar institution, on its own behalf or for one of its users. For this service, a fee may be collected by the University of Victoria to cover the bare costs of reproduction. It is expressly understood that there will be no multiple copying, nor will any copies be sold at a profit. This license will continue in effect until further notice from me.

Title of Thesis/Dissertation:

I Diethynyl complexes of Ti (II)

II Iridium Substitution in B_5H_9

III The Crystal Structure of $[(C_2H_5)_2NH_2]_2$

Author: (signature)

Gary Arthur Rice (name)

May 5, 1975 (date)